2019 | Faculty of Sciences

UHASSELT

KNOWLEDGE IN ACTION

Doctoral dissertation submitted to obtain the degree of
Doctor of Sciences: Biology, to be defended by

Rafaela Amaral dos Reis

DOCTORAL DISSERTATION

Two tools, one t(h)ale: Exploring excess Cu- and Cd-induced responses in *Arabidopsis thaliana* using two different genetic resources, natural accessions and mutant lines

D/2019/2451/4

Promoter: Prof. Dr Ann Cuypers

Co-promoter: Prof. Dr Jaco Vangronsveld

PhD thesis presented on the 24th of January 2019 at Hasselt University

Members of the jury

Chair: Prof. Dr Jan Colpaert, Universiteit Hasselt, BELGIUM

Promoter: Prof. Dr Ann Cuypers, Universiteit Hasselt, BELGIUM

Co-promoter: Prof. Dr Jaco Vangronsveld, Universiteit Hasselt, BELGIUM

Prof. Dr Nele Horemans, Universiteit Hasselt, SCK, BELGIUM

Prof. Dr Miguel Mourato, Universidade de Lisboa, PORTUGAL

Prof. Dr Adriano Sofo, Università degli Studi della Basilicata, ITALY

Dr Marijke Jozefczak, Universiteit Hasselt, BELGIUM

ACKNOWLEDGEMENTS

The adventure that started in the summer of 2012, when I applied for a PhD at Hasselt University, ends today. And it was a true adventure. New country, new language, new workplace, new people, no family or friends to rely on, different diet, and unreliable weather. It was a rollercoaster ride with happy and sad moments, filled with good memories, many frustrations, and some disappointments. This PhD was much more than an academic and professional experience. It was a journey of personal discovery and growth. I end this period of my life convinced that if one wants to discover oneself, learn to enjoy the small things in life and appreciate the people around them, one should leave their comfort zone and take on new challenges.

This adventure would not have been possible without the actions of four people. Ann, thank you for the opportunity to come to Hasselt University and learn with you. Thank you for your support and patience. It wasn't an easy road, but we reached the end together. Thank you. Jaco, thank you for welcoming me in the CMK. Your input, comments, and suggestions vastly improved this manuscript. Miguel and Luísa, thank you for believing in me nine years ago. You were the catalysts to this adventure. I will forever be grateful for your support. *Obrigada por tudo.*

I thank all the jury members for taking the time to read and review this manuscript. Your critical comments and suggestions were invaluable.

I also thank all my former and current colleagues for their support and interesting scientific (and non-scientific) discussions. Marijke and Hanne, thank you for the warm welcome in the group. Els, your suggestions were invaluable and your input is visible throughout this manuscript. Thank you for all your help. Ann W. and Carine, thank you for your skillful technical support. You not only keep the lab running, but also all of us organized. Finally, to all the people I've crossed path in the corridors and halls of the university, I wish many successful adventures.

While not looking for one, I was lucky to find a second family in Hasselt. Like a real family, we don't see each other every day and we don't always agree. Nonetheless, we are present when it matters, to share the laughter and the doubts, the happiness and the sadness.

Alejandro, fellow Iberian, you are a great friend, colleague, and scientist. I'm sure that I will witness you achieve great things in the future. You deserve only happiness. Christophe, I haven't forgotten the promised dance; when the moment comes, you will receive an invitation. While you wait for it, please stay happy and keep on having adventures with Tori.

Patrik, you're one of the nicest people I know, always ready to help. How many times have you saved me from a dead battery? Thank you for organizing (and cooking) the 'Monday dinners'; not only do you feed use, but you also make sure that we have a good time and don't lose touch with each other. Ariadna, I wish you only success in your professional career and a lifetime of happiness with Patrik. You both deserve it. Steven, I envy your grasp of the current affairs and your culinary skills. I look forward to visiting you in your 3D holographic virtual reality mansion in Silicon Valley. Greetings to my fellow 'Monday' diners Lode, Kim, and Jeroen and thank you for the often insightful, but always funny, discussions.

Donald, thank you for your support. You are an awesome friend and I miss our conversations. Please don't stay away for too long, ok? Come visit often. You'll always have a room at our place. Jordan, good luck with the final phase of your PhD. I don't often ask you about it, but I'm always ready to listen if you need. I wish you and Donald a fairytale wedding and a happy life together.

Gustavo and Sabine, you were actually two of the first 'family members' I met: Gustavo via other international students that have since moved on, Sabine through Inge. You are both really nice people and you make a great couple. I appreciate our conversations and your insights, and greatly enjoy your company.

Inge, you are my office mate and always will be. I smile every time I remember your reaction when you discovered our age difference. And in spite of that, and some differences in character, we became friends. Thank you for the many 'Jambon'-organized events. The city and shopping trips, the many BBQs, picnics, dinners and drinks, and our amusement park adventures made this journey so much more fun! You are a great friend and deserve only happiness and success. And I hope to be close by to witness it.

Ramon, Daniel, Valeria, Michele, Sofie, and Wouter, thank you for your support and the serious and (much, much, much!) less serious moments together. Wouter and Valeria, good luck with your upcoming defenses!

Iva, thank you for always being present and ready to help me, and anyone who accepts your help. Thank you for your friendship. You have been very supportive of me in

the last two years, now comes the time for me to reciprocate. Good luck with the road ahead. May your curiosity and hard work bring you only success. And please stay happy.

Nikolina, there is a certain serenity about you that is so comforting. It's always a joy to talk to you. Let's do so more often, ok? Promise? Alexander, your enthusiasm is contagious. And your laughter too. You are both good friends and I want only happiness in your lives. Thank you for your support.

Giulia, my twin sister born to other parents, I miss you. I thank Sara for bringing you and Nikolina for lunch some six years ago. Since then, we've built a strong friendship and together we've shared bad moments and celebrated victories. I know we will forever be friends, even with this geographic distance between us: I will come to visit, you will come to visit, and modern technology will bridge the gap. Thank you for your time and patience. Thank you for pushing me when I needed to be pushed. Thank you for being there when I needed you. Thank you for your support. Thank you for being my best friend. You deserve a lifetime full of love and happiness. Lorenzo, thank you for the funny moments and interesting conversations. And for being Giulia's rock. May you both be successful in all your projects and be happy. Truly happy, you both deserve it.

Maarten, 'button-pusher' extraordinaire, thank you for your support, love, and patience these more than four years. They say time flies when you're having fun. It does. I look forward to spending the next four, eight, twelve,… years with you. I love you.

While my character is my own, the principles and ethics I learned from my first family, my blood family. Without their love and full support I would never have accepted this challenge and started this adventure.

Ana and Sónia, my cousins and 'older sisters', thank you for making me feel like I never left home. I miss you and the kids. I regret not seeing them grow but I am very proud of the people they are becoming.

Whenever I return home, I see the changes and it shocks me that life in Portugal dared to continue without me. And it has changed too much lately. Uncle Armando, you were my second father. And like the father you were, you looked out for me (and everyone else) until the very end. Thank you for the memories, stories, and love.

João, my one and only brother, I'm so proud of you! I am so proud of the man you've become. And if I'm honest, I'm also jealous, of your perseverance, your work

ethics, your easiness and friendliness, and your good looks. João, thank you for always supporting me. My life is better because you are in it. I love you.

Mother and Father, thank you for everything. Everything that I am, I am because of you. Thank you for giving me an awesome brother and showing us what love is. Thank you for your steadfast support and your invaluable advice. This manuscript is yours too. Thank you. I love you and I miss you so much.

And because I don't say these things to my family often enough, I will say them again in Portuguese:

Ana e Sónia, vocês não são apenas minhas primas, são as minhas 'irmãs mais velhas'. Obrigada por me fazerem sentir como que nunca deixei Portugal. Tenho muitas saudades vossas e dos miúdos. Tenho pena de não estar presente para vê-los crescer, mas estou muito orgulhosa das pessoas que se estão a tornar.

Cada vez que regresso a casa, deparo-me com todas as mudanças e choca-me que a vida em Portugal tenha continuado na minha ausência. E como mudou nos últimos tempos. Tio Armando, foste um segundo pai para mim. E como pai que eras, estavas sempre preocupado comigo e com todos, até nos últimos momentos. Obrigada pelas memórias e pelas muitas estórias. Tenho saudades suas.

João, só há um, é o meu irmão e mais nenhum! Tenho muito orgulho em ti! Tenho muito orgulho na pessoa que te tornaste. E se for honesta, também tenho alguma inveja de ti, da tua perseverança, do teu espírito trabalhador, da tua boa disposição, e de quanto és giro. João, obrigada por sempre me apoiares. A minha vida é muito melhor porque fazes parte dela. Gosto muito de ti.

Mãe e Pai, obrigada por tudo. Tudo o que sou, deve-o a vocês. Obrigada por me darem um irmão espectacular e por mostrarem-nos o que ser amado. Obrigada pelo vosso apoio inabalável e pelos vossos conselhos preciosos. Esta tese também é vossa. Obrigada. Gosto muito, muito de vocês e tenho imensas saudades vossas.

Obrigada.
Bedankt.
Thank you.

Hasselt, January 24th, 2019
Rafaela

SUMMARY

Commonly known as thale cress, *Arabidopsis thaliana* is the most intensively studied species in fundamental research on plant biology. Although often considered a weed and with little commercial value, its status as a molecular and genetic model plant is maintained by an active cooperative research community. It is further supported by a large collection of mutant lines and genomic resources such as natural accessions, which result from the unique selective pressures associated to the *A. thaliana* subcosmopolitan distribution. Whereas the considerable number of mutant lines makes *Arabidopsis* a unique target for functional identification and analysis of genes and gene products, natural accessions can be important genetic tools in studying adaptation to adverse environmental conditions. Together, these different genetic tools can facilitate the study of plant responses to metal stress.

Toxic metal contamination of soils is a worldwide problem primarily caused by anthropogenic activities. While several metals are fundamental for normal plant development, high bioavailable metal concentrations in the soil often induce toxicity responses that ultimately inhibit plant growth. For example, copper (Cu) is a redox-active micronutrient essential for normal plant development. In excess, it can interfere with cellular and metabolic processes and directly induce oxidative stress. Exposure to non-essential phytotoxic elements, such as cadmium (Cd), also affects several cellular processes, but indirectly induces oxidative stress e.g. by interfering with antioxidative response mechanisms. Moreover, exposure to Cd is also known to disturb the homeostasis of essential elements such as Cu, which in turn enhances the toxic effects of Cd.

The first main objective of the current work was to investigate and compare the plant growth, metal concentration and translocation, metabolic and transcriptomic responses in roots (Chapter 4) and leaves (Chapter 5) of two different natural accessions. More specifically, Columbia (Col-0, the reference

genome) and Wassilewskija (Ws) accessions were exposed to toxic sublethal concentrations of Cu and Cd (respectively 2 μM and 5 μM) for 24 and 72 h. Accession-specific sensitivities to excess Cu and Cd were observed, confirming previous reports that Ws plants are less sensitive to excess Cu and Cd than Col-0 plants. Moreover, our results indicate that, under control conditions, Col-0 and Ws plants favor different life strategies (Chapter 5). Whereas Col-0 plants invest in detoxification responses related to oxidative stress, signaling, and antioxidative defense mechanisms, Ws plants primarily invest in a constitutively efficient metal homeostasis (Chapter 5). We propose that the ability of Ws plants to better counteract alterations to Cu homeostasis culminates in these plants being less sensitive to excess Cu and Cd than Col-0 plants. This is supported by a more efficient modulation of Cu uptake and distribution to minimize Cu toxicity in Ws plants as compared to Col-0 plants (Chapter 4). The Ws accession is also able to rapidly counteract Cd-induced Cu deficiency-like responses characterized by increased Cu uptake and reallocation of intracellular Cu to essential cuproproteins (Chapter 4 and 5). In turn, our results suggest that Col-0 plants favor the activation of detoxification responses after exposure to excess Cu and Cd, which involve antioxidative defense mechanisms (Chapter 4 and 5) and oxidative stress signaling (Chapter 5).

The second main objective of the current work was to investigate oxidative signaling via the OXIDATIVE SIGNAL-INDUCIBLE KINASE 1 (OXI1) downstream targets, functions, and interactions during Cu (Chapter 6) and Cd stress (Chapter 7). Therefore, plant growth, metal translocation, metabolic and transcriptomic responses were analyzed in wild-type (WT) and *oxi1* knockout *A. thaliana* plants after metal exposure (2 μM Cu or 5 μM Cd) for 24 and 72 h. More than just toxic byproducts of aerobic metabolism, reactive oxygen species (ROS) are also important secondary messenger molecules and key regulators of adaptation responses to environmental stimuli. The protein kinase OXI1 plays a central role in the ROS signal transduction pathway by linking ROS production to downstream responses under metal stress. Although Col-0 plants favor the activation of detoxification-related oxidative stress signaling after exposure to excess Cu and Cd (Chapter 5), the loss of OXI1 function resulted, within this experimental timeframe, in Col-0 *oxi1* mutants being less sensitive to both Cu- (Chapter 6) and Cd-induced (Chapter 7) oxidative stress than WT plants. Our

results validate the transcription factor ZAT12 as a downstream target of OXI1 in Cd-exposed roots. Interestingly, these results also allude to the activation of OXI1-independent signaling pathways that eventually bypass the absence of OXI1-regulated *ZAT12* expression. Possible roles for OXI1 in the regulation of Cd-induced SPL7-mediated Cu deficiency-like responses in Col-0 plants and of metal-induced phytohormone signaling in WT plants are discussed.

Considering that plant responses to metal stress are complex and involve diverse cellular and molecular processes, this study focused on investigating aspects and response mechanisms well established in our research group. Therefore, the timeframe and framework of this study provides only a glimpse into the responses of two *A. thaliana* natural accessions and two genotypes to excess Cu and Cd. Ultimately, long-term exposure and a whole genome approach are necessary to fully capture the details underlying the accession- and genotype-specific responses to excess Cu and Cd.

NEDERLANDSTALIGE SAMENVATTING

Arabidopsis thaliana, algemeen gekend als Zandraket, is het best bestudeerde modelorganisme in het fundamenteel onderzoek bij planten. Ondanks het feit dat het als onkruid beschouwd wordt en geen commerciële waarde heeft, is het een moleculaire en genetische modelplant. Dit wordt ondersteund door een grote beschikbaarheid aan mutanten maar ook aan natuurlijke accessies die het resultaat zijn van unieke selectiedruk geassocieerd met de subcosmopolitische distributie van *A. thaliana*. Terwijl het aanzienlijke aantal mutanten ervoor zorgt dat *Arabidopsis* uiterst geschikt is voor functionele identificatie en analyse van genen en genproducten, kunnen natuurlijke accessies belangrijke genetische hulpmiddelen zijn bij het bestuderen van adaptatie aan ongunstige omgevingsomstandigheden. Samen kunnen deze verschillende genetische instrumenten de studie van reacties van planten op metaalstress vergemakkelijken.

Toxische metaalverontreiniging van bodems is een wereldwijd probleem dat hoofdzakelijk wordt veroorzaakt door antropogene activiteiten. Hoewel verschillende metalen van fundamenteel belang zijn voor de normale ontwikkeling van planten, induceren verhoogde biologisch-beschikbare metaalconcentraties in de bodem vaak toxiciteitsreacties die uiteindelijk de groei van planten remmen. Koper (Cu) is bijvoorbeeld een redox-actief micronutriënt dat essentieel is voor de normale ontwikkeling van planten. Bij overmaat kan het echter interfereren met cellulaire en metabole processen en rechtstreeks oxidatieve stress veroorzaken. Blootstelling aan niet-essentiële fytotoxische elementen, zoals cadmium (Cd), beïnvloedt ook verschillende cellulaire processen, maar induceert onrechtstreeks oxidatieve stress, bijvoorbeeld door te interfereren met het antioxidatief verdedigingssysteem. Bovendien is geweten dat blootstelling aan Cd de homeostase van essentiële elementen zoals Cu verstoort, wat op zijn beurt de toxische effecten van Cd versterkt.

De eerste hoofddoelstelling van dit werk was het onderzoeken en vergelijken van de plantengroei, metaalconcentratie en -translocatie, metabole en transcriptionele responsen in wortels (Hoofdstuk 4) en bladeren (Hoofdstuk 5) van twee verschillende natuurlijke accessies. In het bijzonder werden de Columbia (Col-0, het referentiegenoom) en Wassilewskija (Ws) accessies gedurende 24 en 72 uur blootgesteld aan toxische, maar sublethale concentraties van Cu en Cd (respectievelijk 2 µM en 5 µM). Er werden accessie-specifieke gevoeligheden voor deze verhoogde blootstelling aan Cu en Cd waargenomen, die overeenstemden met eerdere rapporten waarbij werd aangetoond dat Ws planten minder gevoelig zijn dan Col-0 planten voor Cu- en Cd-stress. Bovendien geven onze resultaten aan dat, onder normale omstandigheden, Col-0 en Ws planten verschillende overlevingsstrategieën verkiezen (Hoofdstuk 5). Terwijl Col-0 planten investeren in detoxificatiereacties met betrekking tot oxidatieve stress, signalering en antioxidatieve verdedigingsmechanismen, investeren Ws planten voornamelijk in een constitutief efficiënte metaalhomeostase (Hoofdstuk 5). Het vermogen van Ws planten om veranderingen in Cu-homeostase beter te controleren, resulteert bovendien in het feit dat deze planten minder gevoelig zijn voor verhoogde Cu- en Cd-concentraties dan Col-0 planten. Dit wordt ondersteund door een betere regulatie van Cu-opname en -verdeling om Cu-toxiciteit te minimaliseren in Ws planten in vergelijking met Col-0 planten (Hoofdstuk 4). De Ws accessie is ook in staat om Cd-geïnduceerde Cu-deficiëntie-gerelateerde responsen, gekenmerkt door verhoogde Cu-opname en reallocatie van intracellulair Cu naar essentiële cupro-proteïnen, efficiënt te reguleren (Hoofdstuk 4 en 5). Onze resultaten suggereren op hun beurt dat Col-0 planten detoxificatiereacties met daarbij het antioxidatief verdedigingssysteem (Hoofdstuk 4 en 5) alsook oxidatieve stress signalering (Hoofdstuk 5) onmiddellijk activeren na blootstelling aan verhoogde Cu- en Cd-concentraties.

De tweede hoofddoelstelling van dit werk was om meer inzicht te verwerven in deze oxidatieve signalering door gebruik te maken van OXIDATIVE SIGNAL-INDUCIBLE KINASE 1 (OXI1) genmutanten om op die manier specifieke targets, functies en interacties tijdens Cu- (Hoofdstuk 6) en Cd-stress (Hoofdstuk 7) te onderzoeken. Hiervoor werden wild-type (WT) en *oxi1* knock-out *A. thaliana* planten opgekweekt en blootgesteld aan metalen (2 µM Cu of 5

µM Cd) gedurende 24 en 72 uur. Vervolgens werden de plantengroei, metaaltranslocatie, metabole en transcriptionele responsen geanalyseerd. Reactieve zuurstofsoorten (ROS) zijn meer dan alleen toxische bijproducten van het aëroob metabolisme. Ze zijn ook belangrijke secundaire boodschappermoleculen en regulatoren voor organismen om zich aan te passen aan omgevingsstimuli. Het proteïnekinase OXI1 speelt een centrale rol in de ROS-signaaltransductieroute door de ROS-productie te koppelen aan stroomafwaartse responsen onder metaalstress. Hoewel Col-0 planten oxidatieve stress signalering en bijbehorende responsen onmiddellijk activeren na blootstelling aan verhoogde Cu- en Cd-concentraties (Hoofdstuk 5), resulteerde het verlies van OXI1-functionaliteit, binnen het experimentele tijdsbestek, in minder gevoelige Col-0 *oxi1* mutanten dan WT planten voor zowel Cu- (Hoofdstuk 5) als Cd-geïnduceerde (Hoofdstuk 6) oxidatieve stress. Verder valideren onze resultaten de transcriptiefactor ZAT12 als een stroomafwaarts doelwit van OXI1 in aan Cd-blootgestelde wortels. Interessant is dat deze resultaten ook aanwijzingen geven naar de activering van OXI1-onafhankelijke signaalroutes die uiteindelijk de afwezigheid van OXI1-gereguleerde ZAT12-expressie omzeilen. Mogelijke rollen voor OXI1 bij de regulatie van door Cd-geïnduceerde SPL7-gemedieerde Cu-deficiëntie-gerelateerde responsen in Col-0 planten alsook van metaalgeïnduceerde fytohormoonsignalering in WT planten worden in dit kader besproken.

Gezien het feit dat plantenresponsen op metaalstress complex zijn en diverse cellulaire en moleculaire processen omvatten, richtte deze studie zich op het meer in de diepte onderzoeken van plantresponsen die reeds bestudeerd zijn in onze onderzoeksgroep. Daarom geeft het raamwerk van deze studie slechts een beperkte kijk op de responsen van twee *A. thaliana* natuurlijke accessies en twee genotypen na blootstelling aan verhoogde Cu- en Cd-concentraties. In de toekomst zijn een langetermijnblootstelling en een benadering gebaseerd op het volledige genoom noodzakelijk om meer details bloot te leggen die ten grondslag liggen aan de accessie- en genotype-specifieke responsen op Cu- en Cd-blootstelling.

TABLE OF CONTENTS

LIST OF FIGURES

CHAPTER 1: Introduction

CHAPTER 4: Efficient regulation of Cu homeostasis underlies accession-specific sensitivities to excess Cu and Cd in roots of *Arabidopsis thaliana*

CHAPTER 5: Accession-specific life strategies affect responses in leaves of *Arabidopsis thaliana* plants exposed to excess Cu and Cd

LIST OF TABLES

CHAPTER 1

Introduction

1.1 *Arabidopsis thaliana*, the model plant

Arabidopsis thaliana, commonly known as thale cress, is a small flowering plant widely used as a model system for plant genome analysis. Even though *A. thaliana* belongs to the Brassicaceae family that includes important agricultural crops such as cabbages and radish, this species has no economic value and is often considered a weed. Nonetheless, scientific and historical circumstances made *A. thaliana* the most studied plant organism and led to it being the first fully sequenced plant genome (The *Arabidopsis* Genome Initiative, 2000).

1.1.1 *Arabidopsis thaliana*, the plant

Arabidopsis thaliana (L.) Heyhn. is a small annual plant that grows generally up to 40 cm in height (Figure 1.1A). After seed germination, it develops a basal rosette of one to five cm long oblanceolate/spatulate-shaped leaves (Figure 1.1D) covered with simple or branched unicellular trichomes (Figure 1.1F; Nogueira, 1986). The number of leaves in the rosette depends on the genotype and environmental conditions and is strongly correlated with the plant developmental stage (Tsukaya, 2013). During flowering time, a stem is formed with smaller cauline leaves (Figure 1.1E) and small (3-4 mm) white flowers at its terminal (Figure 1.1B, C; Nogueira, 1986). Although the length and structure of its mature roots largely depend on the growth conditions, the cellular organization of primary roots in *Arabidopsis* is very simple and regular, with lateral roots branching and/or root hair differentiating above the elongation area (Petricka *et al*., 2012; Scheres *et al*., 2002; Schiefelbein and Somerville, 1990; Szymanowska-Pułka and Szymanowska-Pulka, 2013).

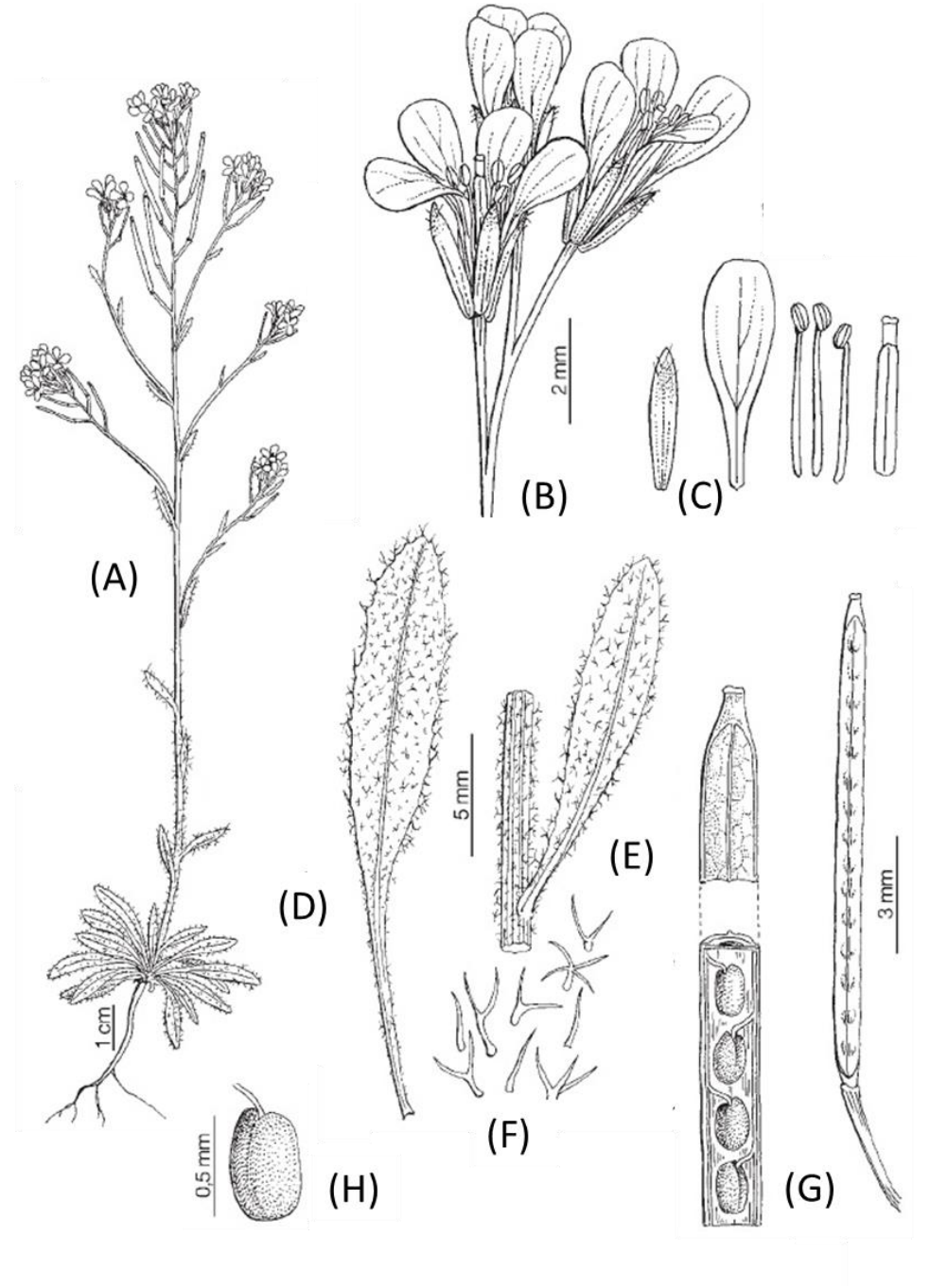

Figure 1.1 – Schematic representation of *A. thaliana* plant structures. (A) Plant habit. **(B)** Flowers. **(C)** Flower parts. **(D)** Basal leaf. **(E)** Stem fragment with cauline leaf. **(F)** Trichomes. **(G)** Silique. **(H)** Seed. Adapted from Nogueira (1986).

A. thaliana plants have a relatively short life cycle. In controlled conditions, only six to eight weeks are needed to go from germination to mature seed (Keunen *et al*., 2011b; Koornneef and Scheres, 2001). Its progeny results almost exclusively from self-pollination, after which 20-30 small (0.5 mm) yellow-brown oval-shaped seeds (Figure 1.1H) develop in a silique (Figure 1.1G) and amount to a few thousand per plant (Koornneef and Scheres, 2001; Nogueira, 1986).

The total size of the genome of *A. thaliana* is approximately 135 Mb and is organized in five chromosomes. After comparing the *Arabidopsis* genome with other fully sequenced eukaryotic genomes at that time, The *Arabidopsis* Genome Initiative (2000) identified 25,498 genes encoding proteins from 11,000 families. This large gene set arises from a high occurrence of tandem gene duplications and segmental duplications, which can result in gene redundancy. These authors also showed that, although numerous families of proteins are common to all eukaryotes, plant genes encode for roughly 150 unique protein families, including transcription factors, structural proteins, and enzymes and proteins of unknown function (The *Arabidopsis* Genome Initiative, 2000).

1.1.2 *Arabidopsis thaliana*, the model organism

Arabidopsis was first suggested as a model organism for plant biological studies by Friedrich Laibach in the 1940s (Koornneef and Meinke, 2010; Meyerowitz, 2001; Somerville and Koornneef, 2002). Interested in natural variation and the effects of light on flowering time and seed dormancy, Laibach enumerated *A. thaliana*'s short generation time and prolific seed production, small size, abundant natural variation, and relatively low chromosome number as advantages to the use of this plant in genetic studies (Koornneef and Scheres, 2001; Laibach, 1943; Meyerowitz, 2001; Somerville and Koornneef, 2002). After inducing mutations using X-ray irradiation, his laboratory also demonstrated its potential as a target for mutagenesis research and started the first collection of *A. thaliana* mutants. In the 1960's, as interest increased and more scientists became involved, an active *Arabidopsis* community was formed which organized diverse international conferences, published an *Arabidopsis* Information Service (AIS) newsletter, and maintained a seed stock center that included Laibach's collection of accessions (Koornneef and Meinke, 2010).

Nevertheless, interest in *Arabidopsis* research waned in the 1970's. In the following decades, the publication of important studies such as the characterization of the size and complexity of its genome (Leutwiler *et al*., 1984) or the first T-DNA-mediated transformation of *A. thaliana* (An *et al*., 1986), together with fortunate support by some funding agencies, invigorated the *Arabidopsis* research and encouraged the use of this plant in molecular and developmental genetics. Nowadays, a fully sequenced genome (The *Arabidopsis* Genome Initiative, 2000), enormous improvements to transformation techniques, shared resources such as seed stock centers (*Arabidopsis* Biological Resource Center, 1991; The Nottingham *Arabidopsis* Stock Centre (NASC), 1991) and information databases (The Arabidopsis information resource, TAIR; Rhee *et al*., 2003), as well as an active cooperative community of more than 35,000 researchers (registered in TAIR) fully established *A. thaliana* as an important model organism for plant biological studies.

It should be kept in mind that model organisms can only be used to study processes that they can perform. Therefore, *A. thaliana* is not suited to investigate the production of root and stem tubers (which develop in major crops like cassava, potatoes, sweet potatoes, and yams) or C4 photosynthesis (which occurs in major crops such as maize, sorghum, and sugarcane). In these situations, it is more efficient to study the crop plant itself, particularly since crop-specific molecular tools are rapidly improving and becoming available. Nevertheless, the extent of genomic information together with the range and versatility of the available genetic, cellular, and biochemical tools makes *Arabidopsis* an exceptionally unique target for functional identification and analysis of genes and gene products.

1.1.3 *Arabidopsis* natural accessions, the product of a broad geographic distribution

Arabidopsis thaliana emerged five million years ago in central Asia and spread throughout Eurasia after the last glaciation (Beck *et al*., 2007; Koch *et al*., 2000; Sharbel *et al*., 2000). It was later introduced in North America, Australia and southern Africa during the European colonialism (Hoffmann, 2002). Nowadays, *A. thaliana* mostly occurs in the temperate regions of the Northern Hemisphere (Figure 1.2). This subcosmopolitan distribution set in

motion unique selective pressures that resulted in genetic and phenotypic diversity in the form of natural accessions, often also referred to as ecotypes (Alonso-Blanco *et al*., 2016; Weigel, 2012).

Figure 1.2 – Subcosmopolitan distribution of *A. thaliana*. Native to Eurasia, *A. thaliana* was introduced in North America, Australia, and southern Africa. Its area of distribution is shown in green. Adapted from Weigel and Mott (2009).

Even though more than 7000 accessions have been collected from the wild and are available in seed stock centers, descriptive and comparative studies on *Arabidopsis* intraspecific variation are limited. For example, Passardi *et al*. (2007) described the morphological and physiological traits of the three most popular accessions in the lab, Columbia (Col-0), Landsberg *erecta* (La*er*), and Wassilewskija (Ws), and attempted to differentiate them at the molecular level by analyzing the expression profiles of all class III *Arabidopsis* peroxidases. In turn, Chevalier *et al*. (2004) investigated the proteome of eight accessions to discriminate and classify natural accessions according to their physiological status. Whereas Pérez-Pérez *et al*. (2002) focused on analyzing variations in the architecture of vegetative leaves of 188 accessions, Beemster *et al*. (2002) studied the primary root growth in 18 *Arabidopsis* accessions. More recently, "The 1001 Genomes Project" was initiated to carry out the whole-genome sequencing of (at least) 1001 accessions (Weigel and Mott, 2009). This research

project quantified genome variation in a larger and more representative sample of accessions (Alonso-Blanco *et al*., 2016; Cao *et al*., 2011; Gan *et al*., 2011; Kawakatsu *et al*., 2016; Long *et al*., 2013; Ossowski *et al*., 2008; Schneeberger *et al*., 2011; Seren *et al*., 2017), investigated *A. thaliana* demographic history (Alonso-Blanco *et al*., 2016; Schmitz *et al*., 2013), identified traits that make specific geographic or genetic subsets particularly well suited for forward genetics (Long *et al*., 2013; Seren *et al*., 2017), and initiated a genome-wide association study (GWAS) platform (Togninalli *et al*., 2018) to facilitate the identification of loci underlying accession-specific responses. Interestingly, these comparative whole-genome studies revealed that over 200 genes found in different accessions are not present in the reference genome Col-0 (Gan *et al*., 2011; Schneeberger *et al*., 2011).

The potential for environmental adaptation, implied by the broad geographic distribution, suggests that *Arabidopsis* natural accessions are excellent targets for environmental stimuli-response experiments. The study of these natural variations can help in unravelling the genes that are key to successfully cope with environmental stress and advance the understanding of the mechanisms involved. Although these resources are still underexploited, several authors have investigated the responses of different accessions to biotic and abiotic environmental factors. For example, Baxter *et al*. (2010) observed that a sodium-transporter gene with reduced function, and linked to elevated salt tolerance, is almost uniquely found in *A. thaliana* populations growing in saline environments. Degenkolbe *et al*. (2012) correlated the relative abundance of some membrane lipid compositions with the freezing tolerance of 15 accessions originating from close to the equator up to Siberia and Scandinavia.

1.2 Metal stress

Toxic metal elements naturally occur in the Earth's crust. However, industrial activities such as mining and smelting, agricultural practices like land application of fertilizers and pesticides, and atmospheric deposition of man-made emissions often result in metal accumulation in soils. In Belgium, historic non-ferrous metal smelting activities in the north-eastern Campine area are responsible for local soil contamination that is still present today. As a target of several remediation studies (Geebelen *et al*., 2006; Vangronsveld *et al*., 1995,

1996, 2009), this extensive contaminated area retains high concentrations of zinc (Zn), lead (Pb), mercury (Hg), arsenic (As), copper (Cu), and cadmium (Cd). This pollution is not only detrimental to human and animal health but also to plant growth. While several metals are fundamental for normal plant development, high bioavailable metal concentrations in the soil often induce metal toxicity responses that ultimately inhibit plant growth (Cuypers *et al*., 2016; DalCorso *et al*., 2013).

Considering that Cu is an essential redox-active micronutrient, whereas Cd is a non-essential non-redox active element, we will focus on plant responses to these two metals.

1.2.1 The metals copper and cadmium

Copper is a micronutrient essential for normal plant growth and development as it is involved in many physiological processes by acting as a functional element of several proteins and enzymes, i.e. cupro-proteins (Festa and Thiele, 2011; Marschner, 2012; Yruela, 2005, 2009). For example, Cu is essential in the last step of respiration as it constitutes the metallic centers of the cytochrome c oxidase, the enzyme in the electron transport chain responsible for the ultimate electron transfer to oxygen (Nelson and Cox, 2008). Moreover, it also plays a major regulatory role in photosynthesis as cofactor to plastocyanin, the last protein in the electron carrier chain between photosystems II and I (Droppa and Horváth, 1990; Gross, 1993). Interestingly, Cu also participates in the first line of defense against reactive oxygen species (ROS), like superoxide radicals ($O_2^{\cdot -}$) deriving from oxygen reduction by photosystem I, as a cofactor to (Cu/Zn) superoxide dismutase (SOD) (Alscher, 2002; Miller, 2004). All of these functions arise from the fact that Cu is able to exist in different oxidation states under normal physiological conditions, and thus take part in redox reactions.

Cadmium is a highly phytotoxic non-essential element that negatively affects normal plant growth and cellular processes, such as photosynthesis, respiration, and transpiration, even when present in low concentrations (Benavides *et al*., 2005; Cuypers *et al*., 2010).

1.2.1.1 Copper deficiency

Factors like alkaline pH, excess Zn, nitrogen (N) or phosphorous (P), and high organic matter content can reduce the bioavailability of Cu in the soil. When this occurs, growth is affected and plants show Cu deficiency symptoms such as chlorosis of young leaves, decreased fruit and seed production, and curling of leaf margins (Marschner, 2012). This last symptom arises from impaired cell wall lignification caused by the decrease in the activities of two cupro-enzymes involved in lignin biosynthesis, polyphenol oxidase and diamine oxidase (Gross, 2008; Vanholme *et al*., 2010). This also results in insufficient water transport due to inadequate lignification of the xylem vessels (Marschner, 2012).

Plants have developed complex mechanisms that allow the tight regulation of cellular Cu concentrations in response to environmental conditions and thus maintain Cu homeostasis (Burkhead *et al*., 2009). In deficiency conditions, an efficient use of intracellular Cu is necessary to preserve essential processes and ensure plant survival. To this purpose, intracellular Cu is remobilized and reallocated to the major cupro-enzymes (Abdel-Ghany *et al*., 2005; Benatti *et al*., 2014; Garcia-Molina *et al*., 2013; Yamasaki *et al*., 2008) and the expression of Cu transporters is regulated to increase Cu uptake (Gayomba *et al*., 2013; Jung *et al*., 2012; Sancenón *et al*., 2003). Both these mechanisms are controlled by the transcription factor *SQUAMOSA* PROMOTOR-BINDING PROTEIN-LIKE 7 (SPL7; Figure 1.3). Mainly expressed in the roots, this central regulator of Cu homeostasis modulates gene expression by way of its SBP domain binding to GTAC motifs within the promoter regions of the target genes (Yamasaki *et al*., 2009). Yamasaki *et al*. (2009) observed that SPL7 activated the transcription of microRNA *miR398* in response to Cu deficiency. In turn, *miR398* post-transcriptionally represses the expression of Cu/Zn-SOD genes *CSD1* and *CSD2* (Yamasaki *et al*., 2007). Together with the SPL7-regulated induction of Fe-SOD *FSD1* expression (Yamasaki *et al*., 2009), this *CSD1/2* repression results in a coordinated substitution of the chloroplastic SODs in favor of Cu allocation to plastocyanin (Abdel-Ghany *et al*., 2005). Members of the Cu transporter (COPT) gene family are also targeted by SPL7. The high-affinity Cu transporters COPT1, and COPT2 are located at the plasma membrane and mediate the transport of Cu to the cytoplasm in response to Cu availability (Puig, 2014; Sancenón *et al*.,

2003). Under Cu deficiency conditions, Yamasaki *et al*. (2009) observed that the transcript levels of *COPT1* and *COPT2* increased in roots of wild-type plants but remained low in roots of *spl7* knockout mutants. Since the Cu concentrations were maintained in both *spl7* mutants and wild-type plants (Yamasaki *et al*., 2009), it appears that SPL7 is only required for the activation of Cu uptake at root level under low Cu, but not for intracellular Cu remobilization. Indeed, the vacuolar Cu exporter COPT5 is known to function in remobilizing Cu from prevacuolar vesicles into the cytosol and interorgan reallocation in Cu deficiency conditions (Garcia-Molina *et al*., 2011; Klaumann *et al*., 2011), but is not reported to be regulated by SPL7.

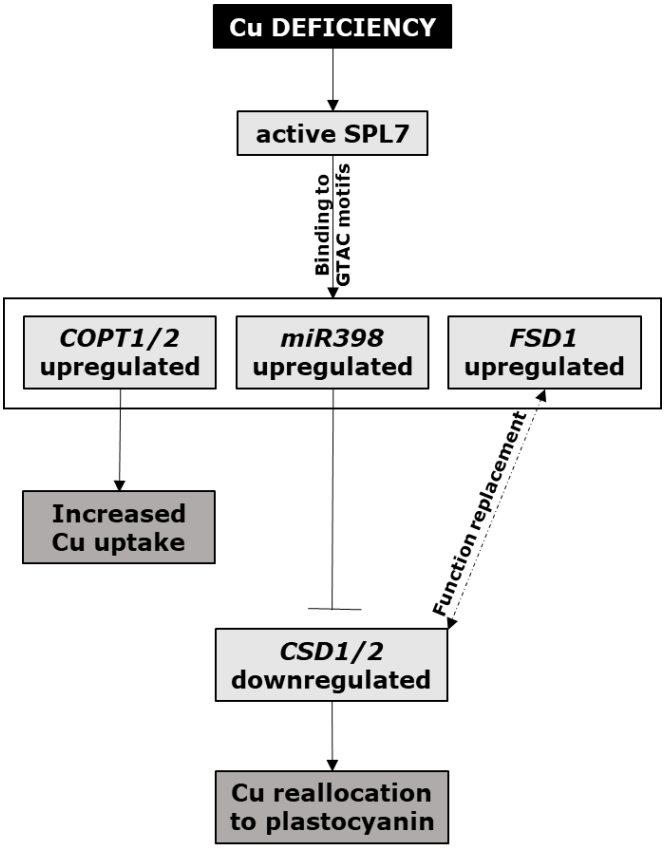

Figure 1.3 – Cu deficiency responses modulated by the central regulator SPL7. In Cu deficiency conditions, the Cu homeostasis central regulator SPL7 modulates gene expression by binding to GTAC motifs within the promoter regions of the target genes. This results in SLP7-regulated substitution of the chloroplastic superoxide dismutases (SODs) in favor of Cu allocation to plastocyanin (via upregulation of Fe-SOD gene *FSD1* and miRNA *miR398* and downregulation of Cu/Zn-SOD genes *CSD1* and *CSD2)* and increased Cu uptake (via upregulation of Cu transporter genes COPT1 and COPT2).

1.2.1.2 Copper toxicity

As a transition metal, Cu can exist in different oxidation states under normal physiological conditions. While this feature underlies its vital role in plants, it also determines its phytotoxicity when Cu is present in excess concentrations. By participating in non-enzymatic Fenton and Haber-Weiss reactions, Cu catalyzes the production of ROS and directly induces oxidative stress (Drążkiewicz *et al*., 2004; Yruela, 2005).

Although several other enzymes and aspects of plant biochemistry are affected, the inhibition of photosynthesis through alterations in pigments, protein and fatty acid composition of thylakoid membranes is one of the most important physiologic consequences of excess Cu (Boucher and Carpentier, 1999; Yruela, 2005; Yruela *et al*., 2000). At whole plant level, these effects result in reduced biomass and chlorotic symptoms (Bernal *et al*., 2006; Fernandes and Henriques, 1991; Lequeux *et al*., 2010; Yruela, 2005).

1.2.1.3 Cadmium toxicity

In addition to a higher bioavailability in acidic soils, Cd solubility is increased by root exudates through interactions with organic acids, particularly carboxylic acids (Nigam *et al*., 2001). Cadmium not only affects plant growth, but it can severely impact soil microbial populations (Fajardo *et al*., 2018).

Cadmium has been shown to interfere with the absorption of nitrate (Hernández *et al*., 1996) and the uptake, transport, and use of several mineral nutrients, such as calcium (Ca), magnesium (Mg), phosphorous (P), potassium (K), and iron (Fe), by competing for the same transmembrane transporters (Connolly, 2002; Hernández *et al*., 1996; Sanità di Toppi and Gabbrielli, 1999; Thomine *et al*., 2000). In fact, one of the main symptoms of Cd toxicity, chlorosis, might result from Cd-induced Fe deficiency (Lešková *et al*., 2017). Other toxicity symptoms are leaf roll and plant stunting.

By interacting with plant water balance and Ca signaling, Cd prevents stomatal opening under light (Chmielowska-Bak *et al*., 2014; Perfus-Barbeoch *et al*., 2002). Moreover, Cd also disturbs photosynthesis through changes to the

chloroplast structure, inhibition of chlorophyll biosynthesis and reduction of the activity of enzymes involved in CO_2 fixation (Parmar *et al*., 2013).

Although Cd is not redox active, and therefore will not participate in Fenton-type reactions, it does interfere with cellular metabolism and antioxidant mechanisms, thereby indirectly inducing oxidative stress (Benavides *et al*., 2005; Cuypers *et al*., 2010, 2011; Sanità di Toppi and Gabbrielli, 1999; Smeets *et al*., 2005). Moreover, Cd is known to induce Cu deficiency-like responses mediated by the Cu homeostasis central regulator SPL7 (Gayomba *et al*., 2013; Gielen *et al*., 2016, 2017), which in turn interferes with Cu uptake and the antioxidant defense responses and enhances its toxicity effects.

1.2.2 Plant defense responses to metal toxicity

In response to excess metal conditions, plants respond among others via the maintenance of metal homeostasis and the activation of antioxidative defense mechanisms (Cuypers *et al*., 2011; Gielen *et al*., 2016; Guo *et al*., 2008, 2003, Jozefczak *et al*., 2014, 2015; Sancenón *et al*., 2003; Smeets *et al*., 2009).

1.2.2.1 Metal homeostasis and chelation mechanisms

Upon exposure to excess Cu, the first strategy relies on controlling intracellular Cu levels by reducing uptake and sequestering free ions. When describing the six-member COPT family, Sancenón *et al*. (2003) observed that, after Cu exposure, *COPT1* and *COPT2* transcript levels were decreased compared to non-exposed conditions, with *COPT2* levels being almost undetectable.

Nevertheless, in excess Cu and Cd conditions, metal cellular content inevitably increases and sequestration mechanisms are activated. Different molecules are involved in the chelation and sequestration of free Cu ions such as heavy metal-binding proteins, like metallothioneins (MTs) and phytochelatins (PCs), and heavy metal-transporting P_{1B}-type ATPases (HMAs).

Arabidopsis has a seven-member gene family encoding four plant MT types (Cobbett and Goldsbrough, 2002). These low molecular weight cysteine-rich proteins bind heavy metals via the thiol groups of their cysteine (Cys)

residues and function cooperatively to protect plants from Cu toxicity (Guo *et al*., 2003, 2008). For example, Guo *et al*. (2003) noticed that the transcript levels of *MT1a* and *MT2b* are inducible by Cu. Later, Guo *et al*. (2008) observed that the roots of the *mt1a-1* and *mt1a-2* knockout mutants accumulated less Cu than the wild-type and *mt2b-1* plants exposed to excess Cu. These authors suggested that only MT1a is essential for Cu sequestration in Cu-exposed root cells. This MT-associated protective effect is furthered by the function of MT2a and MT3 in protecting the root tip from Cu toxicity (Guo *et al*., 2003).

Upon entering the cytosol, metals can induce the synthesis of phytochelatins (PCs) from glutathione (GSH) by PC synthase (Cobbett, 2000; Cobbett and Goldsbrough, 2002; Maitani *et al*., 1996). Then, these Cys-rich peptides can play a role in the detoxification of the same metals by chelating and sequestering these metal-PC complexes in the vacuole (Cobbett, 2000; Cobbett and Goldsbrough, 2002). Both Cu and Cd can increase GSH levels and activate PC production (Cobbett, 2000; Cobbett and Goldsbrough, 2002; Jozefczak *et al*., 2015; Leopold *et al*., 1999; Maitani *et al*., 1996). Afterwards, Cd binds to the thiol group of the Cys residue, whereas free Cu ions are chelated by free electron pairs of the N- and O-atoms of the peptide bound (Leopold *et al*., 1999). Interestingly, Loscos *et al*. (2006) suggested that PC synthesis is relevant to *in vivo* Cd detoxification, but significantly less during Cu stress, after evaluating the substrate specificity in relation to PC synthesis activation and PC accumulation in *A. thaliana*.

The HMA protein family in *A. thaliana* consists of eight members, divided into two groups according to the transported cations. While HMA1-4 are Cd/Zn/cobalt (Co)/Pb transporters, HMA5-8 transport Cu or silver (Ag) (Andrés-Colás *et al*., 2006; Hussain *et al*., 2004; Kobayashi *et al*., 2008; Morel *et al*., 2009; Park *et al*., 2012; Puig *et al*., 2007; Wong and Cobbett, 2009). Among the four Cu-transporting HMAs, only HMA5 has been implicated in Cu detoxification. In particular, Andrés-Colás *et al*. (2006) observed that the expression of *HMA5* is strongly induced by excess Cu and its lack of function resulted in higher Cu accumulation in *hma5* knockout mutants as compared to the wild types. Since this protein is localized in roots and flowers, these authors

hypothesized a role for HMA5 in Cu compartmentalization and detoxification within the roots (Andrés-Colás *et al.*, 2006).

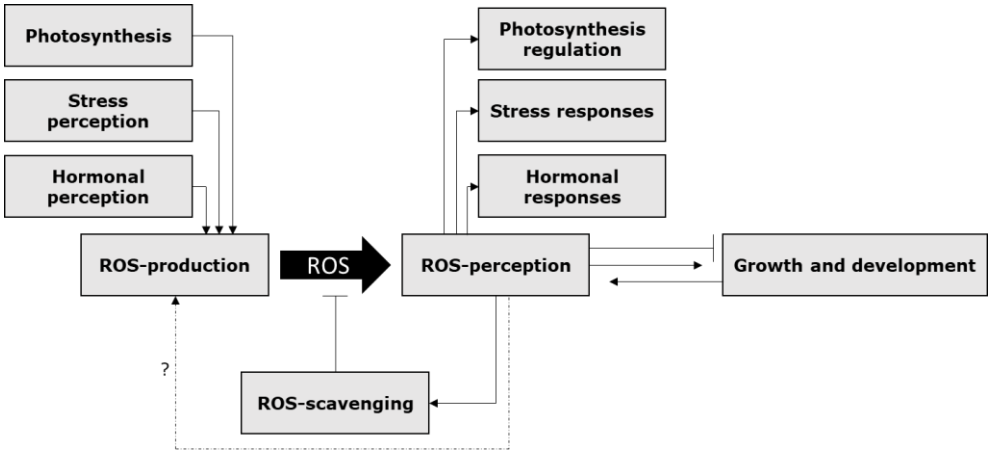

Figure 1.4 – Modulation of ROS signals in plants. Photosynthetic, stress, and hormonal signals induce ROS production which, after signal perception by different ROS sensors, activates different cellular responses. Modulation of the ROS levels by ROS-scavenging pathways is essential to control signal intensity, duration, and localization. This critical modulation might also involve a positive feedback loop between ROS perception and production (dashed line). Adapted from Mittler *et al*. (2004).

1.2.2.2 Antioxidative responses

Exposure to excess Cu or Cd creates an oxidative imbalance that, via signaling pathways, leads to both antioxidative defense responses and/or more oxidative damage (Cuypers *et al*., 2012; Mittler *et al*., 2004). Under normal physiological conditions, ROS are natural by-products of metabolic processes and their levels are tightly controlled and maintained by a complex molecular network of genes encoding for ROS-producing and ROS-scavenging proteins (Figure 1.4; Harir and Mittler, 2009; Mittler *et al*., 2004). This has allowed ROS to evolve as signaling molecules and modulate the activities of downstream components in ROS signaling pathways. Often, these pathways involve mitogen-activated protein kinase (MAPK) cascades (Jalmi and Sinha, 2015; Smékalová *et al*., 2014), which have been shown to be initiated by the H_2O_2-responsive serine/threonine MAPK kinase kinase (MAPKKK) OXIDATIVE SIGNAL-INDUCIBLE KINASE 1 (OXI1). Several authors have investigated the activation of ROS signaling pathways after exposure to excess Cu and Cd. Opdenakker *et al*. (2012a) observed a metal-related time-dependent induction of *OXI1*, *MPK3* and *MPK6* expression in Cu- and Cd-exposed *A. thaliana*. While excess Cu induced

this upregulation as early as 2 h after exposure, Cd-induced upregulation of *OXI1* and *MPK3/6* only occurred after 24 h exposure (Opdenakker *et al*., 2012a). Smeets *et al*. (2013) suggested an essential role for OXI1 in Cu-induced responses in roots. After investigating Cu-induced responses in *oxi1* knockout mutants, these authors proposed H_2O_2, lipoxygenases (LOXes), the transcription factor WRKY25, and miRNA398 as downstream targets of OXI1 under Cu stress (Smeets *et al*., 2013). In turn, Schellingen *et al*. (2015b) proposed a role for OXI1 in the mediation of Cd-induced ethylene responses in *A. thaliana*.

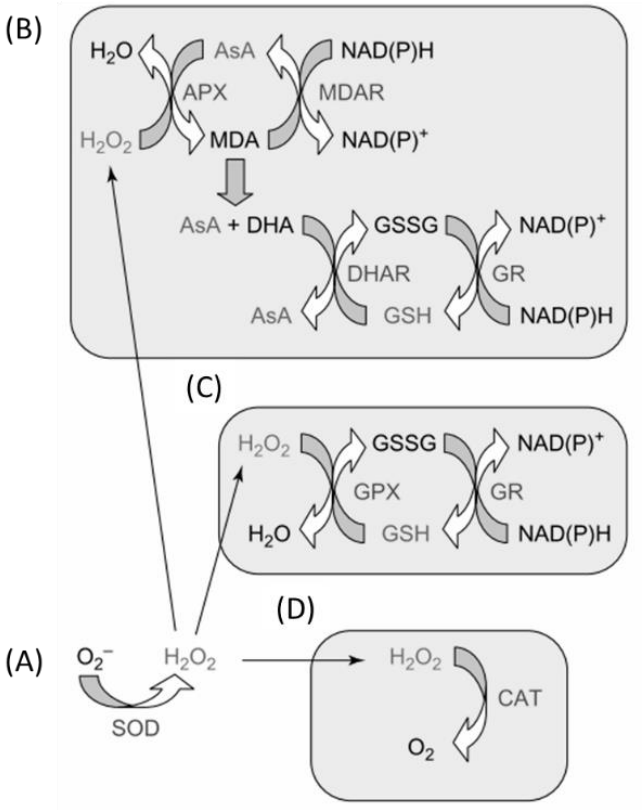

Figure 1.5 – Enzymatic and metabolic ROS-scavenging mechanisms in plants. (A) Superoxide dismutase (SOD) catalyzes the dismutation of superoxide (O_2^-) cations into hydrogen peroxide (H_2O_2). The resulting H_2O_2 is detoxified by: **(B)** the ascorbate-glutathione cycle, which involves the metabolites ascorbate, glutathione, and NADPH, and the enzymes linking them [ascorbate peroxidase (APX), dehydroascorbate reductase (DHAR), monodehydroascorbate reductase (MDHAR), and glutathione reductase (GR)]; **(C)** the glutathione peroxidase cycle, catalyzed by glutathione peroxidase (GPX) and GR; and **(D)** catalase (CAT). Adapted from Mittler (2002).

Antioxidative defense mechanisms involving metabolic antioxidants, such as GSH and ascorbate (AsA), and ROS-scavenging enzymes, such as SODs, catalases (CAT), and peroxidases (PODs or PXs), are initiated in response to excess Cu and Cd (Cuypers *et al*., 2011; Jozefczak *et al*., 2015; Semane *et al*., 2007; Smeets *et al*., 2009). The first line of defense involves SOD converting $O_2^{\cdot -}$ radicals into H_2O_2 (Figure 1.5A), followed by its detoxification by ascorbate and glutathione peroxidases (APX and GPX, respectively; Figure 1.5C) and CAT (Figure 1.5D). Together with the AsA-GSH cycle (Figure 1.5B; Drazkiewicz *et al*., 2003; Foyer and Noctor, 2011; Gupta *et al*., 1999), these mechanisms are essential to maintain the redox balance in the cell and counterbalance the oxidative damage induced by metal stress (Miller *et al*., 2008; Mittler, 2002; Mittler *et al*., 2004; Shulaev *et al*., 2008).

1.2.3 Metal tolerance of natural accessions

A. thaliana natural accessions respond differently to Cu and Cd stress: while some accessions are more sensitive, other are more tolerant to toxic concentrations. Although limited in number, some studies have compared metal sensitivity between different *A. thaliana* accessions. After characterizing the Cu tolerance levels of ten different accessions, Murphy and Taiz (1995) reported significant levels of inducible Cu tolerance in Wassilewskija (Ws) and Enkheim plants, which were later related to higher basal levels of non-protein thiols and GSH (Murphy and Taiz, 1995b). These authors also described the reference genome, the Col-0 accession, as showing the lowest constitutive Cu tolerance (Murphy and Taiz, 1995a). In subsequent studies, this accession-specific Cu sensitivity was associated to a differential regulation of the MT2 gene (Murphy and Taiz, 1995b) and different levels of K-leakage (Murphy and Taiz, 1997). Schiavon *et al.* (2007) evaluated the Cu sensitivity of the three most popular accessions in the lab. Since the less sensitive Ws and La*er* plants accumulated more Cu in both roots and shoots than the more sensitive Col-0 plants, they speculate that Cu exclusion is not the main tolerance mechanism involved. Alternatively, they hypothesized that a higher Cu sensitivity is a manifestation of cation imbalance in the cell, ultimately reflecting Cu-induced nutrient deficiency (Schiavon *et al.*, 2007). Moreover, after studying 103 different accessions, Kobayashi *et al.* (2008) suggested that the variation in Cu tolerance observed in

A. thaliana accessions is partially regulated by their capacity to translocate Cu from the roots to the shoots, associated with the functional integrity of HMA5.

Concerning tolerance to Cd, Park *et al.* (2012) described Col-0 plants to be more sensitive to this metal than Ws plants. These authors correlated the distinct Cd sensitivities to a non-functional HMA3 transporter in Col-0 plants and a differential expression of other *HMA* genes in both accessions (Park *et al*., 2012). Moreover, it was hypothesized that the combined action of vacuolar HMA3 and plasma membrane transporters HMA2 and HMA4 is relevant to detoxify Cd in less sensitive plants. While HMA3 results in Cd sequestration in root vacuoles, HMA2 and HMA4 limit root-to-shoot Cd translocation, thus preventing competition between different elements and nutrient deficiency symptoms in the shoots of Ws plants (Park *et al.*, 2012). In addition, Chao *et al*. (2012) identified HMA3 as the primary cause for the variation in leaf Cd accumulation in the 149 accessions studied, which supports a role for this transporter in limiting the transport of Cd from root to shoot. Fischer *et al*. (2017), however, reported HMA3 to unlikely contribute to the variation in Cd sensitivity observed between the more sensitive Col-0 plants and the less sensitive Burren (Bur-0) plants. Instead, a more efficient activation of transcriptional alterations related to acclimation and reduced Cu accumulation in its organs are suggested as the underlying mechanism for the increased Cd tolerance of Bur-0 plants.

In conclusion, the study of a range of sensitive to tolerant accessions can potentially elucidate plant responses to toxic metals. In turn, this might reveal new tolerance mechanisms that can be explored to improve plant-based strategies to validate contaminated soils and generate metal-tolerant crops. Ultimately, it can help minimize potential toxicity to both plants and humans through environmental and dietary exposure to metals, respectively.

CHAPTER 2

Objectives

Arabidopsis thaliana is the most intensively studied plant species in fundamental research studies on plant biology, particularly in the field of molecular genetics. First suggested as suitable model organism due to its physiological characteristics (Koornneef and Meinke, 2010; Laibach, 1943), its importance was established and advanced by being the first flowering plant (and only the third multicellular organism) to be fully sequenced (The *Arabidopsis* Genome Initiative, 2000). This resulted in a large available collection of mutant lines and genomic resources which encouraged forward genetics approaches. Moreover, the unique selective pressures arising from its subcosmopolitan distribution resulted in different *A. thaliana* natural accessions with specific genetic and phenotypic traits (Alonso-Blanco *et al*., 2016; Cao *et al*., 2011; Weigel and Mott, 2009). Together, these genetic tools facilitate the development of interdisciplinary studies such as stimuli-response experiments to evaluate the diverse plant responses to adverse environmental conditions.

Toxic metal contamination of soils is a worldwide problem caused primarily by anthropogenic activities such as mining, smelting, and agriculture. While several metals are fundamental for normal plant development, high bioavailable metal concentrations in the soil often cause toxicity responses which ultimately inhibit plant growth (Cuypers *et al*., 2016; DalCorso *et al*., 2013). For example, copper (Cu) is a redox-active micronutrient essential to plant growth that in excess interferes with photosynthesis, respiration, pigment synthesis, fatty acid metabolism and plasma membrane permeability (Lequeux *et al*., 2010; Yruela, 2005, 2009). Moreover, Cu directly induces oxidative stress by catalyzing ROS formation through the Fenton and Haber-Weiss reactions (Drążkiewicz *et al*., 2004). Similarly, exposure to non-essential elements, such as cadmium (Cd), also affects several cellular processes such as photosynthesis, respiration and transpiration (Cuypers *et al*., 2010; Lux *et al*., 2011; Park *et al*., 2012; Smeets *et al*., 2008a; Verbruggen *et al*., 2009). While not redox-active,

Cd is a highly phytotoxic element that can hinder normal antioxidative response mechanisms and thus indirectly induce oxidative stress (Cuypers *et al*., 2011; Smeets *et al*., 2005, 2008a). Interestingly, exposure to Cd is also known to disturb the homeostasis of essential elements such as Cu, which in turn enhances its toxicity effects (Cuypers *et al*., 2010; Gayomba *et al*., 2013; Gielen *et al*., 2016, 2017; Lux *et al*., 2011; Park *et al*., 2012; Smeets *et al*., 2008a; Verbruggen *et al*., 2009).

In this study, the **responses of *A. thaliana* plants to excess Cu and Cd were investigated using two different genetic resources, natural accessions and knockout mutants**, and two main objectives were defined:

I. Several authors have described distinct natural accessions to respond differently to environmental stress. Although the commonly used natural accessions Columbia (Col-0) and Wassilewskija (Ws) are known to be respectively more or less sensitive to Cu and Cd (Murphy and Taiz, 1995a; Park *et al*., 2012; Schiavon *et al*., 2007), little is known about the mechanisms underlying these differences in metal sensitivity. Therefore, the first objective of this study was to **compare the responses of roots (Chapter 4) and leaves (Chapter 5) of Col-0 and Ws plants exposed to excess Cu and Cd to reveal accession-specific differences**. To that purpose, Cu- and Cd-induced effects on root and rosette growth, metal concentration and transport, cell wall-related parameters, and their associated oxidative stress signatures were studied. Since both excess Cu and Cd induce alterations to Cu homeostasis (Gayomba *et al*., 2013; Gielen *et al*., 2016, 2017), a special focus was put on investigating accession-specific alterations to Cu homeostasis and establishing a potential link with accession-specific Cu and Cd sensitivities.

II. More than just toxic byproducts of aerobic metabolism, reactive oxygen species (ROS) are also important secondary messenger molecules and key regulators of plant growth and development, adaptation, and responses to environmental stimuli (Bailey-Serres and Mittler, 2006; Harir and Mittler, 2009; Mittler *et al*., 2011). For example, H_2O_2 is known to modulate defense responses during biotic stress by directly inducing protein kinase OXIDATIVE SIGNAL-INDUCIBLE KINASE 1 (OXI1) (Rentel *et al*., 2004; Shoala *et al*., 2018). While

several studies suggest the activation of OXI1 during abiotic stress (Opdenakker *et al*., 2012a; Shumbe *et al*., 2016), its role during Cu- and Cd-induced oxidative stress is mostly unknown. Therefore, the second objective of this study was to **explore and identify possible OXI1 downstream targets, functions, and interactions during Cu (Chapter 6) and Cd stress (Chapter 7)**. To that purpose, growth, metal translocation, and metabolic and transcriptomic responses to excess Cu and Cd were determined in wild types and *oxi1* knockout *A. thaliana* mutants. To allow for the influence of possible accession-specific life strategies (Chapter 4 and 5) on Cu- and Cd-induced OXI1-mediated signaling, wild-type and *oxi1* plants of both Col-0 and Ws background were exposed to excess Cu and Cd and their responses evaluated.

CHAPTER 3

Materials and methods

3.1 Plant material

Arabidopsis thaliana (L.) Heynh, accessions Columbia (Col-0) and Wassilewskija (Ws), wild-type (WT) plants were hydroponically grown on sand (based on the method described by Smeets *et al.* (2008)), during 12 h/12 h light/dark periods at 22 °C/18 °C respectively, light intensity of 170 µmol m^{-2} s^{-1} at the rosette level and 65 % relative humidity. In addition to WT plants, *oxi1* knockout (*oxi1*) plants were also grown for the experiments described in Chapters 6 and 7.

Nineteen-days-old plants of each genotype were exposed to 2 µM (excess) $CuSO_4$ or 5 µM $CdSO_4$ via the roots, representing environmentally realistic sublethal Cu and Cd concentration (Cuypers *et al.*, 2011; Smeets *et al.*, 2008b), or further grown under non-exposed ("control") conditions (32 nM $CuSO_4$). Root and leaf (*i.e.* whole rosette) samples were harvested 24 and 72 h after the start of metal exposure. In addition to corresponding to a circadian cycle (24 h) and representing a more prolonged exposure (72 h), the selection of these time points was based on earlier studies that suggest that the antioxidative defense mechanisms are acutely regulated after 24 h and reach a more equilibrated state after 72 h exposure to 5 µM Cd (Keunen *et al*., 2013; Opdenakker *et al*., 2012a). Depending on the required sample weight for analysis, biological replicates were sampled from one or more individual plants out of one pot at each time point. To avoid within-pot correlation (Smeets *et al.*, 2008b), different biological replicates were sampled from at least two pots containing the same metal concentration. Samples to determine Cu and Cd concentrations were processed as described below, while the remaining samples were snap frozen in liquid nitrogen and stored at – 70 °C for other analyses.

3.2 Determination of metal concentrations

Root samples were first washed for 15 min in 10 mM $Pb(NO_3)_2$ at 4 °C to remove surface-bound metals. Both root and leaf samples were then rinsed in distilled water and subsequently dried at 60 °C for at least one week. Dried root and leaf samples were digested in HNO_3 (65 %) in a microwave oven (CEM MDS-2000 Microwave Digestor Oven, CEM Corporation, NC, USA). After a five-fold dilution in ultrapure water, the Cu and Cd concentrations in the acid-digested samples were determined by atomic absorption spectroscopy (Unicam Solaar M, Thermo Fisher Scientific, Inc., MA, USA), employing a graphite furnace for Cd assessment.

The ratio between metal concentrations in the leaves and in the roots of the same plants was calculated to estimate root-to-shoot translocation factors of Cu and Cd in non-, Cu-, and Cd-exposed plants.

3.3 Enzymatic activity determination

Spectrophotometric (UV-1800 UV-VIS Spectrophotometer, Shimadzu Corporation, Kyoto, Japan) methods were used to estimate the activities of catalase (CAT), glutathione reductase (GR), guaiacol peroxidase (GPOD), syringaldazine peroxidase (SPOD), superoxide dismutase (SOD), malic enzyme (ME), isocitrate dehydrogenase (ICDH), and glucose-6-phospate dehydrogenase (G6PDH) in purified protein extracts. Activities were calculated according to the Lambert-Beer law and defined as the amount of CAT, GR, GPOD, SPOD, ME, ICDH, or G6PDH needed for the conversion of 1 µmol of substrate/product per min and cm^3 at room temperature, or as the amount of SOD necessary to inhibit the reduction of cytochrome c by 50 % per min and cm^3 at room temperature.

To obtain a crude protein extract, root and leaf samples (150 and 200 mg fresh weight, respectively) were first crushed in liquid nitrogen using a mortar and pestle, followed by homogenization in a 0.1 M Tris-HCl (pH 7.8) solution containing 5 mM EDTA, 1 % (w/v) polyvinylpyrrolidone (PVP) K30, 5 mM dithioerythritol (DTE), and 1 % (V/V) Nonidet P-40. After agitation for 30 min, root and leaf homogenates were centrifuged at 50 000 x *g* and 4 °C for 30 min to recover the supernatant (crude protein extract). The proteins were then

fractionated from the crude extract in a two-step ammonium sulfate precipitation method (first by 40 % salt saturation, followed by 80 % salt saturation), each step involving constant stirring for 30 min at 4 °C followed by centrifugation at 50 000 x *g* and 4 °C. Finally, the pelleted proteins were resuspended in a 25 mM Tris-HCl (pH 7.8) buffer. Purified root and leaf protein extracts were desalted using PD-10 Desalting Columns (GE Healthcare, Illinois, USA), snap-frozen in liquid nitrogen, and stored at – 70 °C until the enzyme measurements.

Superoxide dismutase (EC 1.15.1.1) activity was measured at 550 nm in a reaction mixture of 50 mM KH_2PO_4 (pH 7.8) buffer, 0.1 mM EDTA, 10 µmM cytochrome c, 50 µM xanthine, and 7.2 mU xanthine oxidase (EC 1.17.3.2) (McCord and Fridovich, 1969). Catalase (EC 1.11.1.6) activity was assessed at 240 nm ($\varepsilon_{H_2O_2}$ = 40 mM^{-1} cm^{-1}) using 0.1 M KH_2PO_4 (pH 7.0) buffer and 0.85 mM H_2O_2 (Bergmeyer *et al.*, 1974). Guaiacol peroxidase (EC 1.11.1.7) activity was determined at 436 nm ($\varepsilon_{tetraguaiacol}$ = 25.5 mM^{-1} cm^{-1}), in a reaction mixture containing a 0.1 M KH_2PO_4 (pH 7.0) buffer, 0.8 mM H_2O_2, and 1.8 mM guaiacol (Bergmeyer *et al.*, 1974). Syringaldazine peroxidase (EC 1.11.1.7) activity was measured at 530 nm ($\varepsilon_{oxidized\ syringaldazine}$ = 11.6 mM^{-1} cm^{-1}), with the reaction mixture consisting of 0.1 M Tris-HCl (pH 7.5) buffer, 1 mM H_2O_2, 56.6 µM syringaldazine, 0.13 M 1,4-dioxane, and 0.14 M methanol (Imberty *et al.*, 1984). Activities of GR, ME, ICDH, and G6PDH were determined at 340 nm (ε_{NADPH} = 6.22 mM^{-1} cm^{-1}). For glutathione reductase (EC 1.8.1.7), the reaction mixture included 0.1 M Tris and 1 mM EDTA (pH 8.0) buffer, 1.4 mM GSSG, and 0.1 µM NADPH (Bergmeyer *et al.*, 1974). Malic enzyme (EC 1.1.1.39) activity was assessed using 15 mM Tris-HCl (pH 7.3) buffer, 36 mM $MnSO_4$, 10 mM $NADP^+$, and 0.1 M L-malate (Bergmeyer *et al.*, 1974). Isocitrate dehydrogenase (EC 1.1.1.42) activity was measured using 0.1 M Tris (pH 7.5) buffer, 4.6 mM DL-isocitrate, 52 mM NaCl, and 5 mM $NADP^+$ (Bergmeyer *et al.*, 1974). Finally, glucose-6-phosphate dehydrogenase (EC 1.1.1.49) activity was estimated using 50 mM Tris-HCl (pH 7.6) buffer, 1 mM glucose-6-phosphate, 0.2 mM $NADP^+$, and 6.7 mM $MgCl_2$ (Bergmeyer *et al.*, 1974).

3.4 Determination of H_2O_2 concentrations

The concentration of hydrogen peroxide (H_2O_2) in leaves was measured using the Amplex Red Hydrogen Peroxide/Peroxidase Assay Kit (Molecular Probes, Invitrogen, CA, USA). In this one-step fluorometric assay, a highly colored and fluorescent compound (resorufin) is produced after the enzyme horseradish peroxidase catalyzes the oxidation of the Amplex Red reagent (10-acetyl-3,7-dihydroxyphenoxazine) by reducing the H_2O_2 present in the sample. Prior to the measurement, leaf samples (150 mg fresh weight) were shredded twice in liquid nitrogen-cooled adapters for 1 min at 30/s frequency (Retsch Mixer Mill MM400, Verder Scientific GmbH & Co. KG, Haan, Germany), homogenized in 0.2 M $HClO_4$ for 5 min at 4 °C followed by centrifugation at 10 000 x g and 4 °C for 10 min. After adjusting the pH to 8.0-8.5 with 0.2 M NH_4OH, Poly-Prep® Prefilled Chromatography Columns AG 1-X8 Resin (Bio-Rad Laboratories, CA, USA) were used to isolate H_2O_2 from the leaf homogenates. After an eight-fold dilution with the kit's reaction buffer and excitation at 530 nm, the concentrations of H_2O_2 were determined by measuring the fluorescence on a plate reader at 590 nm and calculated using H_2O_2 standard curves ranging from 0 to 10 µM.

3.5 Determination of lipid peroxidation levels

To estimate the levels of lipid peroxidation in root and leaf samples, the concentrations of thiobarbituric acid-reactive metabolites (TBA-rm) were measured using a spectrophotometric method based on the protocol described by Dhindsa *et al.* (1981). Root and leaf samples (30-50 mg fresh weight) were first crushed in liquid nitrogen using a mortar and pestle and then homogenized in 0.1 % (w/v) trichloroacetic acid (TCA). Preceded and followed by centrifugation at 20 000 x *g* and 4 °C for 10 min, the supernatants were incubated in 0.5 % (w/v) TBA [in 20 % (w/v) TCA] at 95 °C for 30 min and then rapidly cooled to 4 °C. The concentrations of TBA-rm in root and leaf samples were assessed by measuring the absorbance at 532 nm (ε = 155 mM^{-1} cm^{-1}), corrected for aspecific absorbance (by measuring absorbance at 600 nm), and calculated according to the Lambert-Beer law.

3.6 Determination of glutathione concentrations

Oxidized (glutathione disulfide, GSSG) and reduced (GSH) forms of glutathione were analyzed using a plate reader system via an enzymatic assay based on the protocol described by Queval and Noctor (2007). Leaf samples (50 mg fresh weight) were first crushed in liquid nitrogen using a mortar and pestle and then homogenized in 200 mM HCl (pH 4.5). Total GSH and GSSG concentrations were determined in leaf samples by a kinetic enzymatic recycling assay, *i.e.* reduction of GSSG to GSH via GR and monitored via the GSH-dependent reduction of 5,5'-dithiobis(2-nitrobenzoic acid) (DTNB). The absorbance at 412 nm was measured in a 200 mM NaH_2PO_4 and 10 mM EDTA (pH 7.5) buffer containing 0.6 mM DTNB (in dimethyl sulfoxide), 0.5 mM NADPH, and 1 U ml^{-1} GR. The rate of change in absorbance over 5 min is proportional to the GSH concentration in the sample, which was calculated using GSH and GSSG standard curves ranging from 0 to 1 or 0.4 nmol, respectively. To determine the concentration of GSSG, the leaf extracts (and GSSG standards) were incubated in 1 % (V/V) 2-vinyl-pyridine (2-VP) at 20 °C for 30 min to derivatize GSH and centrifuged twice for 10 min at 16 100 x *g* and 4 °C (to precipitate 2-VP) prior to absorbance determination.

3.7 Determination of lignin concentrations

Root samples (50 mg fresh weight) were first lyophilized to isolate the cell wall residue (CWR) before lignin solubilization via the acetyl bromide method (Van Acker *et al.*, 2013). The lyophilized material was incubated in ultrapure water for 30 min at 98 °C while shaking at 750 rpm. The supernatant was discarded after centrifugation at 16 000 x *g* for 3 min. To pellet the CWR, the root material was incubated four times for 30 min while shaking at 750 rpm, the first and second time in ethanol at 76 °C, thirdly in chloroform at 59 °C, and the fourth time in acetone at 54 °C. Each of the incubation steps was followed by centrifugation at 16 000 x *g* for 3 min and removal of the supernatant. The final CWR pellet was dried for 24 h before treatment with 25 % (v/v) acetyl bromide/glacial acetic acid and 60 % perchloric acid followed by incubation at 70 °C (while shaking at 850 rpm for 30 min). After centrifugation for 15 min at 16 000 x *g*, the supernatant was transferred to a new tube to which 2 M NaOH and glacial acetic acid were added. The remaining pellet was again washed with

glacial acetic acid and centrifuged for 3 min at 16 000 x *g*. Both supernatant fractions were then combined to constitute the lignin extract, which was additionally 1.5-fold diluted using glacial acetic acid. After vortexing, the lignin mixture was incubated for 20 min at room temperature and the absorbance was measured at 280 nm against a similarly processed blank sample (no CWR) (NanoDrop ND-1000 spectrophotometer, Thermo Fisher Scientific, Inc., MA, USA). Lignin concentrations were calculated using the Lambert-Beer law, considering an extinction coefficient of 23.35 M^{-1} cm^{-1}.

3.8 Gene expression analysis

Frozen root and leaf samples (40-50 mg fresh weight) were shredded twice in liquid nitrogen-cooled adapters for 1 min at 30/s frequency (Retsch Mixer Mill MM400, Verder Scientific GmbH & Co. KG, Haan, Germany). Subsequently, RNA was extracted from the homogenized samples using the Ambion™ RNAqueous® Kit (Life Technologies, Waltham, MA, USA) and eluted in RNase-free water pre-heated at 80 °C. The concentration and quality of the RNA extracts were verified using the NanoDrop ND-1000 spectrophotometer (Thermo Fisher Scientific, Inc., MA, USA). Prior to cDNA synthesis, the TURBO DNA-*free*™ Kit (Life Technologies) was used to clean the RNA samples of genomic DNA. Complementary DNA was synthesized from equal amounts (1.1 µg) of cleaned RNA samples using the PrimeScript™ RT Reagent Kit (Perfect Real Time) (TAKARA BIO Inc., Shiga, Japan) and the thermal cycler Techne TC-5000 (Life Technologies). The cDNA samples were diluted in 1/10 TE (Tris-EDTA) buffer and stored at – 20 °C.

Real-time quantitative PCR (qPCR) analysis was performed using the Applied Biosystems™ Fast SYBR® Master Mix (Thermo Fisher Scientific, Inc.) and 300 (or 600 nM) of gene-specific forward and reverse primers (Supplemental Table 4.1, 5.2, 6.2, and 7.5). The amplification reaction involved 40 cycles of denaturation at 95 °C for 3 s followed by annealing/elongation at 60 °C for 30 s, after an initial denaturation at 95 °C for 20 s, and was performed in the Applied Biosystems™ 7500 Fast Real Time PCR System (Life Technologies). Subsequently, a melting curve was generated to verify amplification specificity. The GrayNorm algorithm (Remans *et al.*, 2014) was used to select reference genes for the normalization of the expression levels of the genes of interest.

After analyzing up to ten candidate reference genes (Remans *et al.*, 2008), reference genes were selected for normalization of root and leaf samples (Supplemental Table 4.2, 5.3, 6.3, and 7.6).

3.9 Hierarchical clustering analysis

Hierarchical clustering analysis was performed (GenEx Pro software, v6.1, MultiD Analyses AB, Sweden) to recognize potential sample-related patterns within leaves of plants of both accessions exposed to excess Cu and Cd. The analysis was based on raw gene expression values (Cq values). The distance between conditions was defined by the "Average linkage" algorithm as the average of distances between all pairs of individuals in all groups, while the distances between the measures were calculated via the Euclidian Distance Measure. Heat maps were constructed to compare expression levels between different genes and samples.

3.10 Statistical analysis

Statistical analysis was performed using R 3.3.1 (R Core Team, 2016) running on RStudio 1.0.143 (RStudio Team, 2015). Data normality was tested using the Shapiro-Wilk test, while homoscedasticity was verified via Bartlett's and Levene's tests, the later resorting to the package "car" (Fox and Weisberg, 2011). For gene expression, and whenever necessary to approximate normality, datasets were log-transformed before the statistical analysis. One- or two-way ANOVA was performed in normally distributed datasets, followed by post hoc analysis via the Tukey's HSD test when significant. Non-normal datasets were analyzed via the Kruskal-Wallis test, followed by post-hoc analysis using the Fisher's LSD method, using the "agricolae" package (de Mendiburu, 2016).

To determine statistical significance of gene expression data, both normalized and non-normalized datasets were statistically analyzed and compared. Expression changes were considered significant only when present in both normalized and non-normalized datasets.

CHAPTER 4

Efficient regulation of Cu homeostasis underlies accession-specific sensitivities to excess Cu and Cd in roots of *Arabidopsis thaliana*

In preparation.

Keywords: *Arabidopsis thaliana*, natural accessions, Columbia, Wassilewskija, roots, copper, cadmium, copper homeostasis.

Abstract

Since diverging from its closest relatives, *Arabidopsis thaliana* has encountered diverse selective evolutionary pressures that resulted in divergent natural accessions. Excessive bioavailable trace element concentrations in the soil constitute a pertinent selective pressure. While several metals such as copper (Cu) are essential for normal plant development, they can also cause toxicity and inhibit plant growth when present in excess. In contrast, non-essential elements like cadmium (Cd) are highly phytotoxic, even when present in low concentrations. Moreover, both Cu and Cd are known to affect Cu homeostasis. The commonly used natural accessions Columbia (Col-0) and Wassilewskija (Ws) are known to be respectively more or less sensitive to Cu and Cd. The mechanisms underlying accession-specific metal sensitivity are further explored in the current study by comparing the responses of Col-0 and Ws plants exposed to excess Cu or Cd (for 24 and 72 h) in the roots. In particular, a potential link between differential regulation of Cu homeostasis and accession-specific Cu and Cd sensitivities is investigated.

Our results indicate that Ws plants are less sensitive to excess Cu and Cd than Col-0 plants, which is in agreement with earlier studies. Exposure to excess Cu resulted in increased Cu concentrations in the roots of both accessions. However, the downregulation of Cu transporter (COPT) genes *COPT1* and *COPT2* in combination with a more pronounced upregulation of metallothionein (MT) gene *MT2b* indicates that Ws plants coped better with the altered Cu homeostasis. Furthermore, roots of both accessions exposed to Cd showed higher concentrations of Cu, indicating that Cd exposure also affects Cu homeostasis. Roots of Ws plants counteract the Cd-induced Cu deficiency responses more efficiently than Col-0 plants. This is evidenced by a higher upregulation of *FSD1* in Ws plants after 24 h, followed by an overall downregulation of *CSD1* and *CSD2* at 72 h. Moreover, the observed expression patterns of *COPT1*, *COPT2,* and *COPT5* in the Ws accession suggest a more effective remobilization of intracellular Cu ions. In conclusion, coping with Cu excess as well as Cd-induced Cu deficiency-like responses in the roots is key to accession-specific differences in Cu and Cd sensitivity.

4.1 Introduction

Arabidopsis thaliana is widely used as a molecular and genetic model plant. Its physiological and genetic characteristics in combination with a fully sequenced genome (The *Arabidopsis* Genome Initiative, 2000) made this plant a common target for transformation techniques. As a result, a large collection of mutant lines and genomic resources is available to the scientific community, facilitating interdisciplinary studies. On the other hand, different geografic and ecological conditions create unique selective pressures, which in turn result in genetic and phenotypic diversity giving rise to natural accessions, often referred to as ecotypes (Alonso-Blanco *et al.*, 2016; Weigel, 2012). More than 7,000 accessions have been collected from the wild and are available in seed stock centers. Columbia (Col-0) is generally considered as the reference accession (Weigel, 2012).

Arabidopsis accessions can vary in thousands of genes, some having fundamental effects on life-history traits. To assess this intraspecies variation, whole-genome sequence variation was reported in "The 1001 Genomes Project" for (at least) 1,001 accessions of *A. thaliana* (Alonso-Blanco *et al.*, 2016). Ultimately, these genetic differences can lead to different phenotypes. Passardi *et al.* (2007) studied the morphological and physiological differences between Columbia (Col-0), Landsberg *erecta* (La*er*) and Wassilewskija (Ws), the three most popular *Arabidopsis* accessions used in laboratory studies. Among these accessions, Ws plants showed the fastest growth rate (Passardi *et al.*, 2007), which was related to larger mature cortical cells and a higher cell production rate in Ws root tissues (Beemster *et al.*, 2002).

Arabidopsis accessions have also been the target of stimuli-response experiments. Since distinctive selective pressures probably result in different life strategies, accessions are perfect tools to evaluate plant responses to adverse environmental conditions of biotic (Kuśnierczyk *et al.*, 2007) or abiotic origin such as metal exposure (Barah *et al*., 2013b, 2013a; Wang *et al*., 2013). While several metals are essential for normal plant development, they can also cause toxicity and inhibit plant growth when present in too high bioavailable concentrations in the soil. They may affect plants at physiological, biochemical,

and molecular levels (DalCorso *et al.*, 2013). Excess metals can also enhance the formation of reactive oxygen species (ROS), leading to a cellular imbalance between pro- and antioxidants in favor of the former and thus inducing oxidative stress (Cuypers *et al.*, 2016).

Copper (Cu) is a redox-active essential micronutrient used as a cofactor in different enzymes crucial within the cellular metabolism. However, excess Cu can inhibit many enzymes and interfere with photosynthesis, respiration, pigment synthesis, fatty acid metabolism, and plasma membrane permeability (Lequeux *et al.*, 2010; Yruela, 2005, 2009). Moreover, Cu catalyzes ROS formation through the Fenton and Haber-Weiss reactions and hence is able to directly induce oxidative stress (Drążkiewicz *et al.*, 2004). As such, the tight regulation of the cellular storage and distribution of Cu is essential to maintain Cu homeostasis and avoid impaired plant growth and development. In *A. thaliana*, the transcription factor *SQUAMOSA* PROMOTER-BINDING PROTEIN-LIKE 7 (SPL7) is a central regulator of Cu homeostasis. Upon Cu deficiency, active SPL7 mediates the induction of several Cu transporters [e.g. Cu TRANSPORTER 2 (COPT2) and ZRT/IRT-like PROTEIN2 (ZIP2)] to increase Cu uptake. In addition, cupro-microRNAs are increased to reallocate Cu to essential proteins such as plastocyanin (Yamasaki *et al.*, 2009).

Cadmium (Cd) is a highly phytotoxic non-essential element that, while not redox-active and therefore not participating in Fenton-type reactions, interferes with cellular metabolism and antioxidative mechanisms, thereby indirectly inducing oxidative stress (Smeets *et al.*, 2005, 2008a). Even in low concentrations, exposure to Cd affects plant growth and cellular processes such as photosynthesis, respiration and transpiration by, for example, disturbing the homeostasis of essential elements (Cuypers *et al.*, 2010; Lux *et al.*, 2011; Park *et al.*, 2012; Smeets *et al.*, 2008a; Verbruggen *et al.*, 2009). Interestingly, recent studies showed that Cd affects Cu homeostasis by inducing SPL7-dependent Cu deficiency-like responses in *A. thaliana* (accession Col-0) (Gayomba *et al.*, 2013; Gielen *et al.*, 2016, 2017). These responses, including Cu uptake and reallocation, were shown to be required for basal Cd tolerance, as seedlings without functional SPL7 are hypersensitive to Cd (Gayomba *et al.*, 2013). Moreover, Cu deficiency responses were diminished in roots and even

disappeared in leaves of Cd-exposed plants that received supplemental Cu (Gielen *et al.*, 2016, 2017). In addition, Cd concentrations were lower in these plants, consequently leading to an improved cellular oxidative state (Gielen *et al.*, 2017).

Although comparative studies are limited, some studies demonstrated *A. thaliana* accessions to respond differently to metal stress. Murphy and Taiz (1995) reported Col-0 plants to be more sensitive to Cd than Ws plants. In addition, they revealed significant levels of inducible Cu tolerance in Ws and a low constitutive tolerance to Cu in Col-0 plants. This accession-specific Cu sensitivity was later associated with a differential regulation of the Cu-chelating *METALLOTHIONEIN 2* (*MT2*) gene (Murphy and Taiz, 1995b) and different levels of potassium leakage (Murphy and Taiz, 1997). Schiavon *et al.* (2007) also described the Ws accession as less sensitive to Cu than Col-0, notwithstanding the higher accumulation of Cu in Ws roots and shoots. These authors hypothesized that the lower sensitivity to higher Cu concentrations in Ws plants was not related to better metal exclusion, but that it could reflect less Cu-induced nutrient deficiency. Finally, Park *et al.* (2012) showed Col-0 to be more sensitive to Cd than Ws, potentially related to differential expression and physiological function of the heavy metal ATPase (HMA) transporter genes, and therefore a different inter-organ transport of elements.

As both excess Cu and Cd affect Cu homeostasis, the current study investigates whether Col-0 and Ws cope differently with these changes. This could then potentially underlie the observed differences in metal sensitivity between the two accessions. As roots are the first plant organ in contact with elements, they are directly affected by excess metal concentrations in the growth medium. As such, this study focuses on comparing the responses of roots of Col-0 and Ws plants to metal stress after 24 and 72 h of exposure. In particular, Cu- and Cd-induced effects on root growth, metal concentration and transport, cell wall-related parameters, and their associated oxidative stress signatures are studied to reveal accession-specific alterations to Cu homeostasis, with special attention to Cd-induced Cu deficiency-like responses.

4.2 Results

4.2.1 Growth and metal concentrations

Hydroponically grown three-week-old *Arabidopsis thaliana* Col-0 and Ws plants were exposed to sublethal concentrations of Cu and Cd (2 µM and 5 µM, respectively). To assess responses after short-term and more prolonged exposure, roots were sampled 24 and 72 h after the start of metal exposure.

Arabidopsis natural accessions Col-0 and Ws are morphologically different plants (Passardi *et al.*, 2007). Under control conditions, at each of the time points, roots of Ws plants were always significantly larger than Col-0 roots (Figure 4.1). Although both Cu and Cd inhibited root growth of Col-0 and Ws, as indicated by a decreased fresh weight, the effects of Cd exposure were only significant after 72 h (Figure 4.1). Similar responses were observed for the dry root weight (Figure 4.2).

Short-term Cu exposure resulted in a higher dry matter content (DMC) in roots, which was also observed after 72 h of exposure, although to a lesser extent (Figure 4.3). As observed for the root weight, only prolonged Cd exposure (72 h) resulted in a significant DMC increase in plants of both accessions (Figure 4.3).

To evaluate the effects on root growth over time, the variations in root weight at 72 h (relative to the average weights at 24 h) were calculated ($\frac{\text{weight 72 h}}{\text{average weight 24 h}} \times 100$), expressed as percentages and generally defined as growth over time (Table 4.1). Considering that 100% corresponds to the average weight at 24 h, root weight of control plants of both Col-0 and Ws plants more than doubled from 24 to 72 h. Root weight was significantly and similarly affected by exposure to Cu and Cd. Although root growth was affected by metal exposure within each accession, Col-0 root growth over time appeared to be more strongly affected than that of Ws plants. Root weights of Cu- and Cd-exposed Col-0 plants increased only about 10 %, while the roots of Ws plants grew about 30 % during that 48 h-period (Table 4.1).

The concentrations of Cu and Cd were determined in roots of control, Cu- and Cd-exposed plants (Table 4.2). The Cu concentration decreased in roots of control plants over time, reflecting plant growth. After 24 and 72 h of exposure to excess Cu, Col-0 roots accumulated more Cu than Ws roots (Table 4.2). Similarly, exposure to Cd increased its concentration in roots of Col-0 and Ws plants. Whereas both accessions presented similar Cd concentrations after 24 h, Col-0 roots accumulated significantly higher Cd concentrations than Ws roots after 72 h (Table 4.2). In addition, when exposed to Cd, root Cu concentrations were significantly higher in both accessions in comparison to control plants (Table 4.2).

4.2.2 Cell wall-related parameters

Since cell wall-associated peroxidases may catalyze the final enzymatic step in lignin biosynthesis (Cuypers *et al.*, 2002), peroxidase activities were determined in roots of control and metal-exposed plants (Figure 4.4 and 4.5). After 72 h of exposure to excess Cu, GPOD and SPOD activities were significantly increased in both Col-0 and Ws roots (Figure 4.4 and 4.5). Although Cd exposure increased GPOD activity in Col-0 and Ws roots after 72 h (Figure 4.4), SPOD activity was only significantly higher in roots of Cd-exposed Ws plants at this time point (Figure 4.5).

Prior to the assessment of lignin concentrations, starch was removed from the cell wall, resulting in lignocellulosic-rich cell wall residue (CWR). The percentage of CWR in Col-0 and Ws roots was significantly enhanced after 72 h of exposure to excess Cu and Cd, with a smaller increase observed for Cd-exposed roots (Figure 4.6). Furthermore, Cu significantly increased the lignin concentration of Col-0 roots after 24 h (Figure 4.7). On the other hand, roots of Col-0 plants exposed to 5 µM Cd for 72 h showed a significantly lower lignin concentration as compared to control plants (Figure 4.7).

4.2.3 Oxidative stress parameters

Activities of the antioxidative enzymes SOD, CAT, and GR, and of the NADPH-producing enzyme G6PDH were determined in roots of Col-0 and Ws (Table 4.3). Whereas Cd exposure induced a significant increase in CAT activity

after 24 h in Col-0 roots, a significant increase in its activity was observed only after 72 h of Cu exposure in Ws roots (Table 4.3). Glutathione reductase activity was particularly enhanced by excess Cu, which was significant in roots of Col-0 (24 and 72 h) and Ws (only 72 h) plants. After 72 h, Cd exposure led to a higher GR activity in Ws roots (Table 4.3). In addition, as compared to the non-exposed controls, G6PDH activities were obviously higher after 72 h of metal exposure but only significantly in roots of Ws plants (Table 4.3).

4.2.4 Gene expression analysis

Expression levels of several genes involved in pro- and antioxidative responses, Cu transport, and Cu chelation (metallothioneins) were determined in roots of Col-0 and Ws plants exposed to 2 µM Cu (Table 4.4) or 5 µM Cd (Table 4.5).

Transcript levels of oxidative stress hallmark genes (Gadjev *et al.*, 2006) were generally upregulated in Col-0 and Ws roots after exposure to excess Cu and Cd. Overall, the levels of these transcripts were higher in roots of plants exposed to Cu (Table 4.4) than in those exposed to Cd (Table 4.5). Similarly, Cu and Cd exposure led to an upregulation of the pro-oxidative gene *LOX1* in Col-0 and Ws roots. The induction of these genes was the highest after 24 h of Cu exposure in both accessions and was lower after 72 h (Table 4.4). A similar expression profile was observed in roots of Cd-exposed Col-0 plants, whereas in Ws the induction still augmented after 72 h of Cd exposure (Table 4.5).

Concerning the genes encoding antioxidative enzymes, a clear metal-induced opposite regulation of the SODs was noticed. Whereas Cu exposure resulted in higher *CSD* transcript levels (Table 4.4), a downregulation was seen after Cd exposure (Table 4.5). An opposite regulation was observed for *FSD1* gene expression. It should be noted that the degree of *FSD1* upregulation was significantly higher in roots of Cd-exposed Ws than Col-0 plants (Table 4.5). Similar to *FSD1* expression, transcript levels of *COPT* genes were predominantly downregulated in roots of Cu-exposed plants (Table 4.4) and upregulated in roots of plants exposed to Cd (Table 4.5).

Both Cu and Cd exposure led to higher *MT1a* and *MT2a* expression in Col-0 and Ws roots, whereas a significant downregulation was observed for *MT1c* gene expression. Concerning *MT2b*, a clear metal- and accession-dependent response was observed (Table 4.4 and 4.5). Excess Cu resulted in an upregulation of *MT2b* transcript levels in both accessions, although this was significantly higher in Ws than in Col-0 roots (Table 4.4). On the other hand, Cd exposure resulted in *MT2b* downregulation in Col-0 after 72 h, while an upregulation was noticed in Ws roots (Table 4.5).

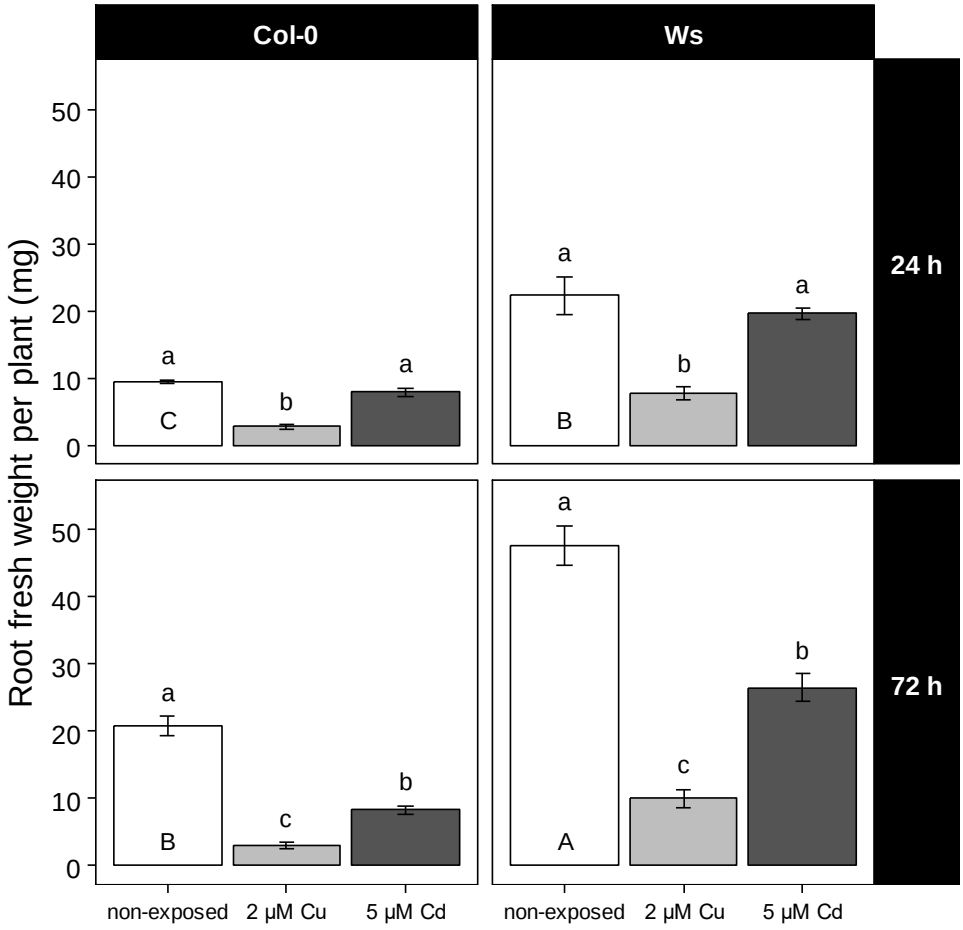

Figure 4.1 – Root fresh weight per plant (in mg) of three-week-old *A. thaliana* plants (accessions Col-0 and Ws) exposed to 2 µM $CuSO_4$, 5 µM $CdSO_4$, or not exposed for 24 and 72 h. Values are the mean ± S.E. of at least three biological replicates, each replicate containing roots of 25 individual plants. □ = non-exposed control. ▒ = exposed to 2 µM $CuSO_4$. ■ = exposed to 5 µM $CdSO_4$. Statistical significance ($P<0.05$) is indicated using lowercase (within accession and time point) and uppercase letters (between controls).

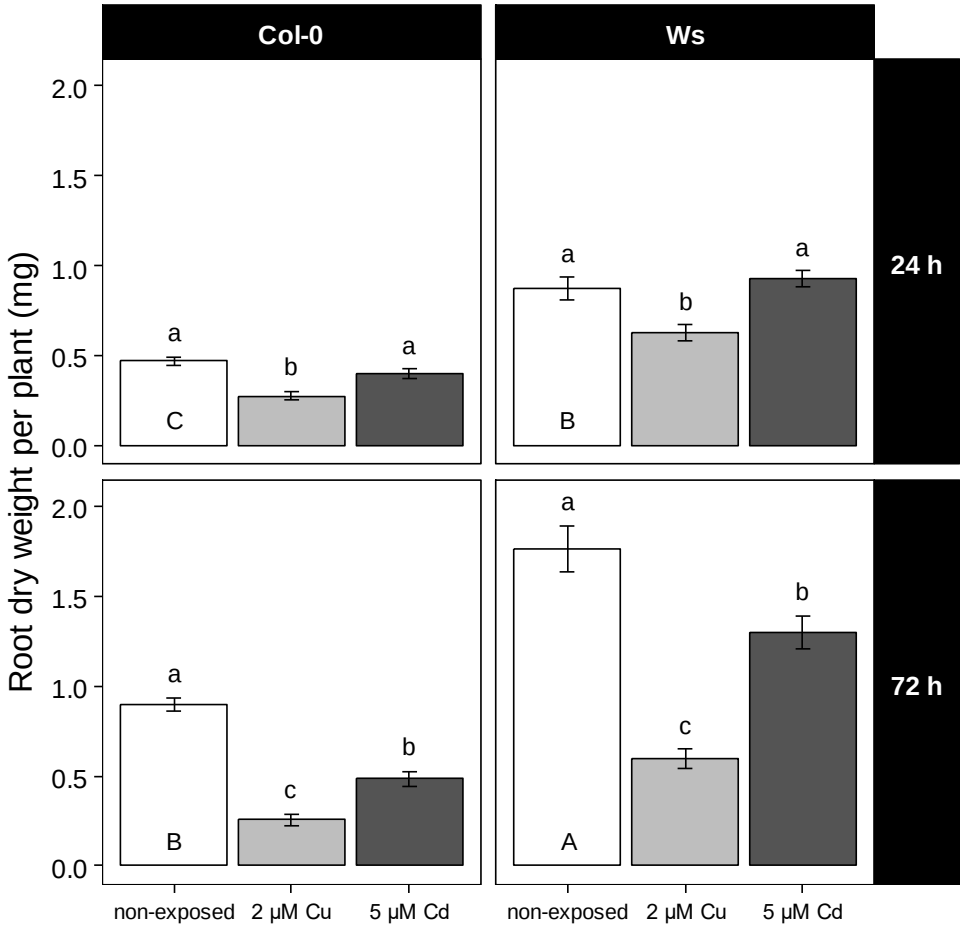

Figure 4.2 – Root dry weight per plant (in mg) of three-week-old *A. thaliana* plants (accessions Col-0 and Ws) exposed to 2 µM $CuSO_4$, 5 µM $CdSO_4$, or not exposed for 24 and 72 h. Values are the mean ± S.E. of at least three biological replicates, each replicate containing roots of 25 individual plants. □ = non-exposed control. ▒ = exposed to 2 µM $CuSO_4$. ■ = exposed to 5 µM $CdSO_4$. Statistical significance ($P<0.05$) is indicated using lowercase (within accession and time point) and uppercase letters (between controls).

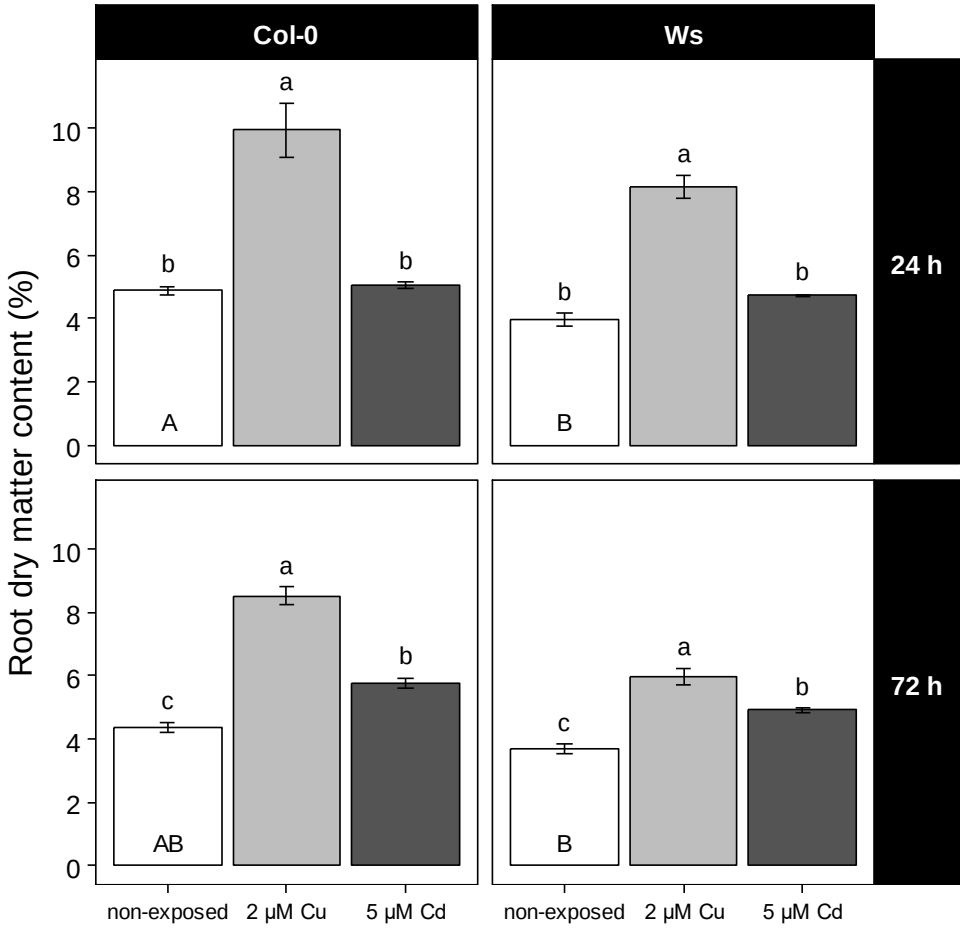

Figure 4.3 – Root dry matter content (%) of three-week-old *A. thaliana* plants (accessions Col-0 and Ws) exposed to 2 µM $CuSO_4$, 5 µM $CdSO_4$, or not exposed for 24 and 72 h. Values are the mean ± S.E. of at least three biological replicates, each replicate containing roots of 25 individual plants. □ = non-exposed control. ▒ = exposed to 2 µM $CuSO_4$. ■ = exposed to 5 µM $CdSO_4$. Statistical significance ($P<0.05$) is indicated using lowercase (within accession and time point) and uppercase letters (between controls).

Table 4.1 – Percentage of root growth over time in three-week-old *A. thaliana* plants (accessions Col-0 and Ws) exposed to 2 µM $CuSO_4$, 5 µM $CdSO_4$, or not exposed for 24 and 72 h. Statistical significance (P<0.05) is indicated using uppercase letters for differences between accessions.

	Col-0			Ws		
	Control	**2 µM Cu**	**5 µM Cd**	**Control**	**2 µM Cu**	**5 µM Cd**
Growth over time (%)	216.90 ± 15.33 A	109.09 ± 17.54 B	105.72 ± 7.61 B	213.80 ± 13.27 A	129.21 ± 17.50 B	135.08 ± 10.85 B

Table 4.2 – Copper and cadmium concentrations (mg kg^{-1} dry weight (DW)) in roots of three-week-old *A. thaliana* plants (accessions Col-0 and Ws) exposed to 2 µM $CuSO_4$, 5 µM $CdSO_4$, or not exposed for 24 and 72 h. Values are the mean ± S.E. of at least three biological replicates, each containing roots of 25 individual plants. Datasets were log-transformed before the statistical analysis to approximate normality. Statistical significance (P<0.05) is indicated using lowercase (within accession and time point), uppercase letters (between controls) or dagger signs (†, within Cd exposure).

	Time	Col-0			Ws		
		Control	**2 µM Cu**	**5 µM Cd**	**Control**	**2 µM Cu**	**5 µM Cd**
Cu	**24 h**	30.35 ± 3.29 c, AB	2288.81 ± 97.20 a	79.58 ± 4.84 b	31.89 ± 3.26 c, A	1757.87 ± 71.83 a	49.59 ± 4.13 b
	72 h	20.80 ± 0.52 c, BC	2719.38 ± 300.14 a	85.26 ± 4.00 b	14.95 ± 1.35 c, C	1684.62 ± 30.88 a	46.42 ± 4.83 b
Cd	**24 h**	—	—	1050.84 ± 61.19 †	—	—	941.78 ± 37.84 †
	72 h	—	—	1943.5 ± 80.10 †††	—	—	1623.91 ± 30.20 ††

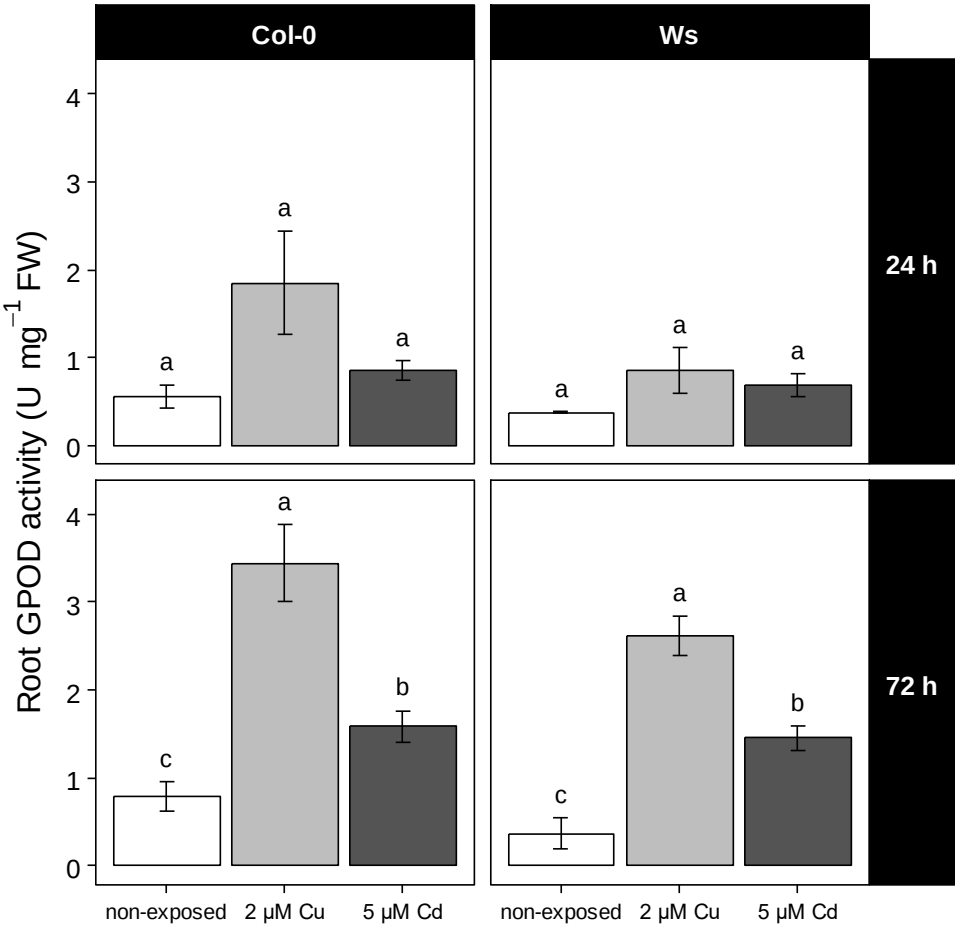

Figure 4.4 – Guaiacol peroxidase (GPOD) activity (U mg^{-1} FW) in roots of three-week-old *A. thaliana* plants (accessions Col-0 and Ws) exposed to 2 µM $CuSO_4$, 5 µM $CdSO_4$, not exposed for 24 and 72 h. Values are the mean ± S.E. of at least three biological replicates, each containing roots of at least four individual plants. □ = non-exposed control. ▒ = exposed to 2 µM $CuSO_4$. ■ = exposed to 5 µM $CdSO_4$. Statistical significance ($P<0.05$) is indicated using different lowercase letters (within accession and time point).

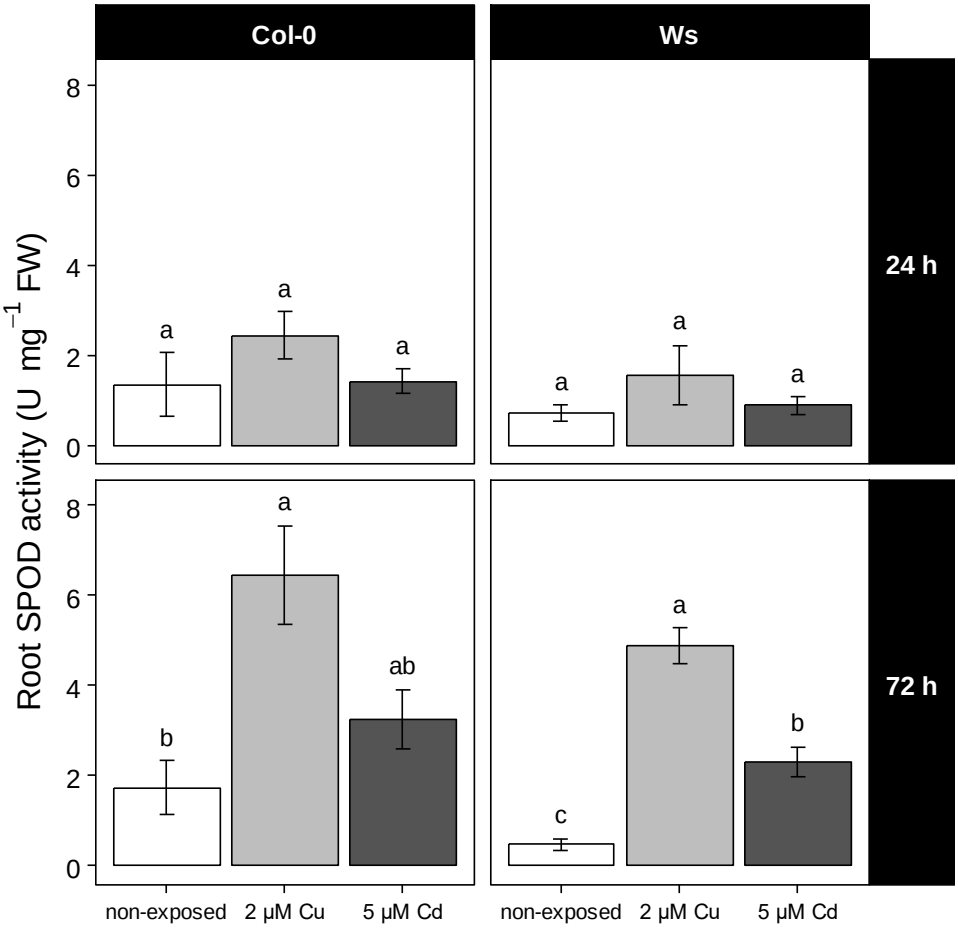

Figure 4.5 – Syringaldazine peroxidase (SPOD) activity (U mg^{-1} FW) in roots of three-week-old *A. thaliana* plants (accessions Col-0 and Ws) exposed to 2 µM $CuSO_4$, 5 µM $CdSO_4$, not exposed for 24 and 72 h. Values are the mean ± S.E. of at least three biological replicates, each containing roots of at least four individual plants. □ = non-exposed control. ▒ = exposed to 2 µM $CuSO_4$. ■ = exposed to 5 µM $CdSO_4$. Statistical significance ($P<0.05$) is indicated using different lowercase letters (within accession and time point).

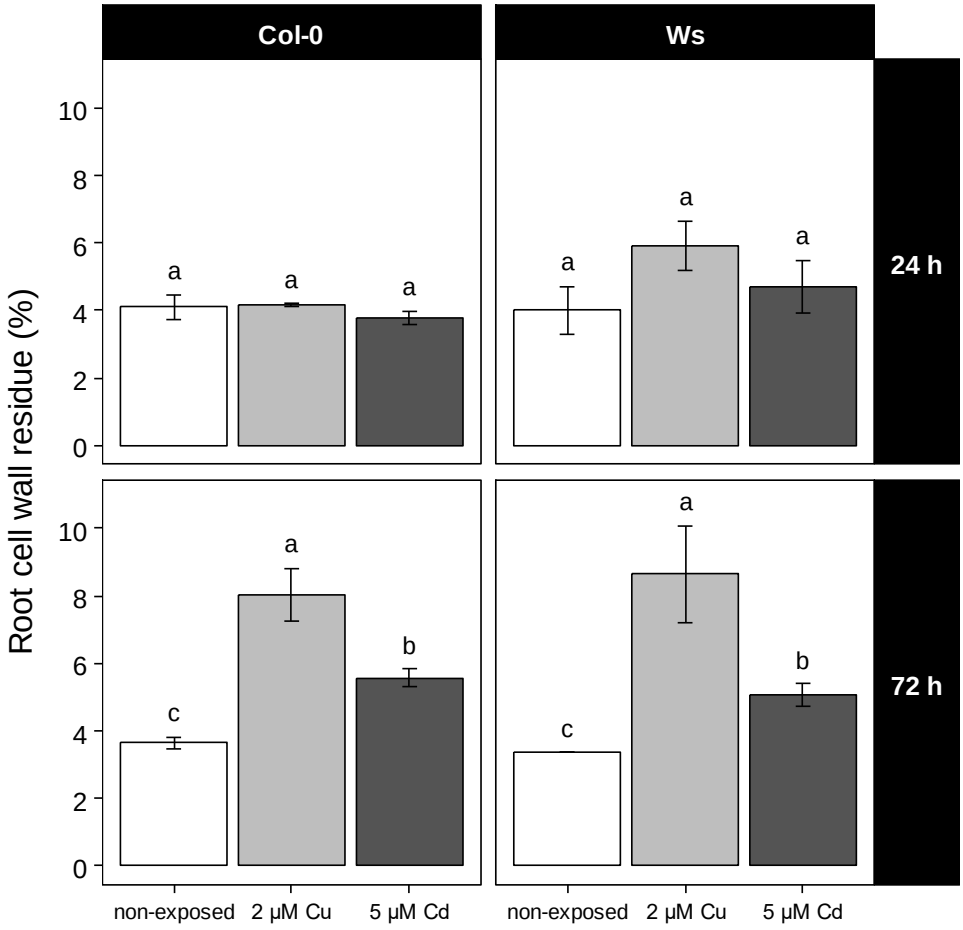

Figure 4.6 – Cell wall residue (CWR) (%) in roots of three-week-old *A. thaliana* plants (accessions Col-0 and Ws) exposed to 2 µM $CuSO_4$, 5 µM $CdSO_4$, or not exposed for 24 and 72 h. Values are the mean ± S.E. of at least four biological replicates, each containing roots of at least four individual plants. □ = non-exposed control. ▒ = exposed to 2 µM $CuSO_4$. ■ = exposed to 5 µM $CdSO_4$. Statistical significance ($P<0.05$) is indicated using different lowercase letters (within accession and time point).

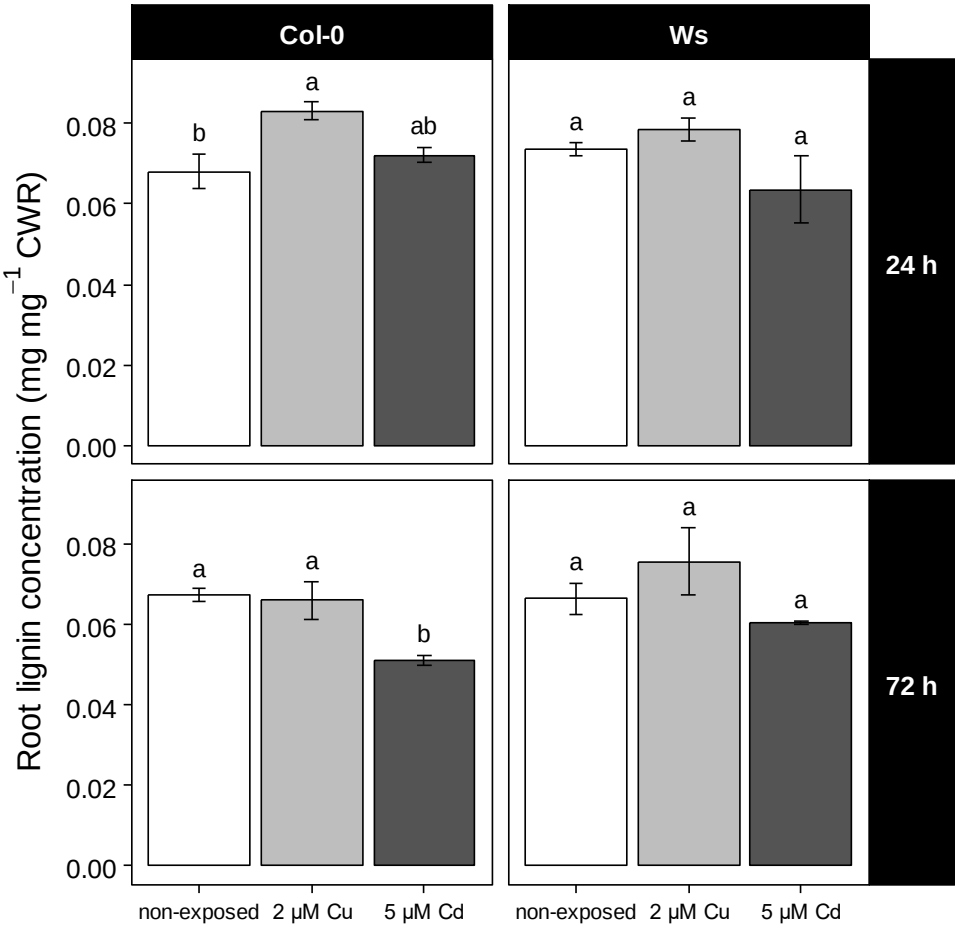

Figure 4.7 – Lignin concentration (mg mg^{-1} CWR) in roots of three-week-old *A. thaliana* plants (accessions Col-0 and Ws) exposed to 2 µM $CuSO_4$, 5 µM $CdSO_4$, or not exposed for 24 and 72 h. Values are the mean ± S.E. of at least four biological replicates, each containing roots of at least four individual plants. □ = non-exposed control. ▒ = exposed to 2 µM $CuSO_4$. ■ = exposed to 5 µM $CdSO_4$. Statistical significance ($P<0.05$) is indicated using different lowercase letters (within accession and time point).

Table 4.3 – Antioxidative and redox-regulating enzymatic activity (mU mg^{-1} fresh weight (FW)) in roots of three-week-old *A. thaliana* plants (accessions Col-0 and Ws) exposed to 2 µM $CuSO_4$, 5 µM $CdSO_4$, or not exposed for 24 and 72 h. Antioxidative enzymes: superoxide dismutase (SOD), catalase (CAT) and glutathione reductase (GR). NADPH-producing enzyme: glucose-6-phosphate dehydrogenase (G6PDH). Values are the mean ± S.E. of at least three biological replicates, each containing roots of at least four individual plants. Statistical significance ($P<0.05$) is indicated using different lowercase letters (within accession and time point) and the conditions in which differences occur are highlighted in grey.

	Time	Col-0			Ws		
		Control	2 µM Cu	5 µM Cd	Control	2 µM Cu	5 µM Cd
SOD	**24 h**	109.79 ± 18.50 a	116.81 ± 24.95 a	68.96 ± 15.00 a	70.31 ± 14.47 a	80.88 ± 23.15 a	67.19 ± 3.82 a
	72 h	101.05 ± 26.00 a	142.45 ± 20.66 a	112.00 ± 16.42 a	118.85 ± 38.54 a	139.73 ± 18.9 a	115.34 ± 20.21 a
CAT	**24 h**	0.45 ± 0.39 a	1.01 ± 0.29 a	3.38 ± 0.94 b	1.58 ± 0.33 a	1.27 ± 0.81 a	3.37 ± 2.14 a
	72 h	1.16 ± 0.64 a	2.43 ± 0.52 a	1.03 ± 0.12 a	1.28 ± 0.72 b	5.27 ± 1.49 a	1.75 ± 0.23 ab
GR	**24 h**	42.86 ± 2.78 b	178.89 ± 42.38 a	88.78 ± 0.02 ab	63.90 ± 16.69 a	123.34 ± 37.40 a	89.22 ± 20.75 a
	72 h	105.89 ± 24.99 b	289.85 ± 32.58 a	169.91 ± 13.02 b	64.67 ± 25.36 b	266.04 ± 18.17 a	243.93 ± 22.17 a
G6PDH	**24 h**	5.04 ± 1.57 a	5.96 ± 2.18 a	21.59 ± 10.80 a	16.53 ± 5.25 a	5.42 ± 1.72 a	9.98 ± 5.01 a
	72 h	5.98 ± 1.90 a	37.02 ± 11.45 a	26.06 ± 1.65 a	9.27 ± 5.00 b	63.75 ± 9.36 a	55.49 ± 9.97 a

Table 4.4 – Relative gene expression levels in roots of three-week-old *A. thaliana* plants (accessions Col-0 and Ws) exposed to 2 µM $CuSO_4$ for 24 and 72 h. Values are mean normalized expression relative to the control at each time point (set at 1.00) ± S.E. of at least three biological replicates, each containing roots of at least one individual plant. Resolution values are mean inverse normalization factors relative to the control at each time point, indicating the stability of the selected reference genes. Statistically significant (P<0.05) metal-induced changes in expression relative to the control at each time point are indicated by color (■ = upregulation; ■ = downregulation) and differences within metal exposure are indicated by different lowercase letters and printed in bold. Abbreviations: *AT1G19020: unknown protein; AT1G05340: unknown protein; TIR-class: Toll-Interleukin-Resistance (TIR) domain family protein; UPOX: upregulated by oxidative stress; Defensin-like: protein member of the defensin-like family; LOX1*: *lipoxygenase 1*; *GSH1*: *glutamate-cysteine ligase*; *GSH2*: *glutathione synthetase 2*; *CSD*: *Cu/Zn superoxide dismutase*; *FSD1*: *Fe superoxide dismutase 1*; *COPT*: *copper transporter*; *MT*: *metallothionein*.

Col-0		2 µM Cu	Ws	
24 h	**72 h**		**24 h**	**72 h**
1.10 ± 0.31	0.96 ± 0.10	Resolution	1.18 ± 0.09	0.99 ± 0.06
Genes encoding oxidative stress hallmark proteins				
5.17 ± 5.17	2.94 ± 0.74	*AT1G05340*	17.39 ± 0.88	5.42 ± 0.17
22.26 ± 4.82	9.66 ± 0.70	*AT1G19020*	24.19 ± 0.92	6.81 ± 0.08
65.58 ± 23.30	23.69 ± 4.34	*TIR-class*	51.20 ± 5.16	16.10 ± 1.17
4.46 ± 1.00	1.49 ± 0.38	*UPOX*	9.07 ± 0.24	0.77 ± 0.05
1841.64 ± 504.33	1057.17 ± 464.11	*Defensin-like*	4759.23 ± 355.97	736.95 ± 37.83
Gene encoding ROS-producing enzyme				
71.85 ± 23.12	11.70 ± 3.61	*LOX1*	56.60 ± 1.88	8.19 ± 0.40
Genes encoding antioxidative enzymes				
1.70 ± 0.28	0.77 ± 0.06	*GSH1*	1.13 ± 0.06	0.66 ± 0.03
2.98 ± 0.77	0.97 ± 0.07	*GSH2*	1.25 ± 0.01	0.77 ± 0.02
1.59 ± 0.24	1.21 ± 0.04	*CSD1*	2.09 ± 0.07	1.71 ± 0.08
1.08 ± 0.02	0.98 ± 0.04	*CSD2*	1.07 ± 0.02	0.90 ± 0.02
0.05 ± 0.01 a	**0.01 ± 0.00 b**	*FSD1*	**0.14 ± 0.04 a**	**0.01 ± 0.01 b**
Genes encoding copper transporter proteins				
0.52 ± 0.03	0.87 ± 0.13	*COPT1*	0.34 ± 0.03	0.42 ± 0.01
0.01 ± 0.01	0.01 ± 0.01	*COPT2*	0.01 ± 0.00	0.01 ± 0.00
1.02 ± 0.03	0.79 ± 0.07	*COPT5*	1.28 ± 0.34	0.83 ± 0.07
Genes encoding metallothionein proteins				
8.43 ± 3.57	4.15 ± 1.4	*MT1a*	4.64 ± 0.45	3.23 ± 0.33
0.13 ± 0.05 ab	**0.25 ± 0.09 ab**	*MT1c*	**0.09 ± 0.00 a**	**0.19 ± 0.00 b**
11.11 ± 0.65	2.68 ± 0.58	*MT2a*	10.21 ± 0.10	2.70 ± 0.37
1.61 ± 0.15 a	**1.62 ± 0.15 a**	*MT2b*	**2.61 ± 0.17 b**	**2.56 ± 0.09 b**

Table 4.5 – Relative gene expression levels in roots of three-week-old *A. thaliana* plants (accessions Col-0 and Ws) exposed to 5 µM $CdSO_4$ for 24 and 72 h. Values are mean normalized expression relative to the control at each time point (set at 1.00) ± S.E. of at least three biological replicates, each containing roots of at least one individual plant. Resolution values are mean inverse normalization factors relative to the control at each time point, indicating the stability of the selected reference genes. Statistically significant (P<0.05) metal-induced changes in expression relative to the control at each time point are indicated by color (■ = upregulation; ■ = downregulation) and differences within metal exposure are indicated by different lowercase letters and printed in bold. Abbreviations: See Table 4.4.

Col-0		5 µM Cd	Ws	
24 h	**72 h**		**24 h**	**72 h**
0.95 ± 0.05	0.80 ± 0.04	Resolution	0.89 ± 0.08	0.87 ± 0.02
Genes encoding oxidative stress hallmark proteins				
1.18 ± 0.12	1.18 ± 0.09	*AT1G05340*	1.35 ± 0.27	3.82 ± 0.63
7.41 ± 0.39	3.87 ± 0.11	*AT1G19020*	5.11 ± 0.49	8.10 ± 1.74
8.70 ± 0.70 a	**7.46 ± 1.59 ab**	*TIR-class*	**3.29 ± 0.25 b**	**9.60 ± 2.60 a**
4.37 ± 0.67	1.18 ± 0.09	*UPOX*	3.87 ± 0.16	3.96 ± 0.74
28.70 ± 15.15	69.01 ± 24.97	*Defensin-like*	12.95 ± 2.80	122.50 ± 29.24
Gene encoding ROS-producing enzyme				
8.81 ± 3.31	4.45 ± 0.79	*LOX1*	2.52 ± 0.36	5.87 ± 1.64
Genes encoding antioxidative enzymes				
1.11 ± 0.09	0.68 ± 0.04	*GSH1*	1.03 ± 0.04	0.81 ± 0.01
1.76 ± 0.26	0.85 ± 0.02	*GSH2*	1.05 ± 0.02	0.91 ± 0.02
0.94 ± 0.07	0.40 ± 0.02	*CSD1*	1.06 ± 0.05	0.80 ± 0.01
0.94 ± 0.03	0.49 ± 0.03	*CSD2*	0.93 ± 0.04	0.62 ± 0.04
6.05 ± 0.10 a	**8.02 ± 0.75 b**	*FSD1*	**92.49 ± 1.32 c**	**7.17 ± 0.32 ab**
Genes encoding copper transporter proteins				
2.23 ± 0.30	1.46 ± 0.13	*COPT1*	1.45 ± 0.08	1.28 ± 0.30
0.90 ± 0.06	1.27 ± 0.08	*COPT2*	1.18 ± 0.13	1.55 ± 0.26
2.09 ± 0.44	1.32 ± 0.22	*COPT5*	2.63 ± 0.46	2.07 ± 0.25
Genes encoding metallothionein proteins				
1.77 ± 0.18	2.09 ± 0.20	*MT1a*	1.61 ± 0.18	2.21 ± 0.54
0.58 ± 0.04	0.62 ± 0.02	*MT1c*	0.64 ± 0.05	0.65 ± 0.02
6.13 ± 0.85	3.81 ± 0.46	*MT2a*	4.30 ± 0.46	3.87 ± 0.74
0.40 ± 0.23	0.67 ± 0.03	*MT2b*	1.17 ± 0.04	1.73 ± 0.32

4.3 Discussion

The species *Arabidopsis thaliana* diverged from its closest relative five million years ago in central Asia (Koch *et al.*, 2000). Since then it spread throughout Eurasia, now naturally occurring in most of the Northern Hemisphere. This geographical expansion implied colonization of new habitats, resulting in selective evolution and divergent natural accessions (Alonso-Blanco *et al.*, 2016). The natural accessions Col-0 and Ws are widely used in molecular and genetic studies. Originally collected from two different geographic locations, Germany and Belarus respectively, Col-0 and Ws plants have been described to have distinct morphological and physiological characteristics (Passardi *et al.*, 2007).

In this study, the most discernable morphological distinction between both accessions is related to root biomass. The root weight of 20- and 22-days-old Ws plants grown in control conditions was significantly higher than that of Col-0 plants at the same time points (Figure 4.1), with generally longer roots in the former accession (data not shown). An earlier study of root growth on vertical agar plates described the primary root length of seven-days-old Col-0 plants to be similar to that of Ws plants, but reported that secondary roots emerged earlier in the latter (Passardi *et al.*, 2007). Beemster *et al.* (2002) studied the root growth rates of 18 different *Arabidopsis* accessions, including Col-0 and Ws, and described Ws as the faster growing accession. This was associated to longer mature cortical cells and higher cell production rates (Beemster *et al.*, 2002). These distinctive physiological characteristics probably explain the observed differences in root growth between the two accessions in the current study (Figure 4.1).

The roots make the first contact with metals in the growth medium. Excess metals greatly impact the root system architecture by inhibiting primary root growth via reduced mitotic activity and cell death, and inducing the formation of lateral roots and lignin accumulation (Bochicchio *et al.*, 2015; Lequeux *et al.*, 2010). Also in the present study, exposure to excess Cu and Cd affected Col-0 and Ws root growth. As evidenced by the average fresh (Figure 4.1) and dry (Figure 4.2) root weights, a Cu-induced stress response is

significant immediately after short-term exposure (24 h), while the Cd-induced stress response is only significant after prolonged exposure (72 h). Whereas absolute fresh root weight values are different within each accession (Figure 4.1), calculated root growth over time shows similar response patterns in both Col-0 and Ws plants (Table 4.1). Root biomass doubled under control conditions between 24 and 72 h, but it was severely affected by metal exposure in both Col-0 and Ws plants. This Cu and Cd-induced growth inhibition appeared less severe in Ws roots, as they grew 20-30% more than Col-0 roots during this period (Table 4.1). These results point towards Ws being less sensitive to these metals than Col-0 plants, which is in agreement with previous reports (Murphy and Taiz, 1995a; Park *et al.*, 2012; Schiavon *et al.*, 2007). Moreover, DMC and CWR levels of Cu-exposed roots complement and support this statement. While Cd effects on DMC (Figure 4.3) can be associated, in both accessions, to changes in the CWR (Figure 4.6) arising from increased lignification (Figure 4.7) and/or other cell wall components, our results suggest distinct Cu-induced responses occurring in Col-0 and Ws roots. Whereas Cu-induced higher DMC is related to increased CWR levels in Ws roots, this is not observed in Col-0 roots (Figure 4.3 and 4.6). The increase in DMC observed after 24 h Cu exposure is not accompanied by similar changes in CWR levels, indicating that Col-0 roots were losing water, probably due to significant membrane damage. Indeed, intracellular free Cu ions interact with several molecules to increase the production of ROS, which in turn cause membrane lipid peroxidation, leading to further (secondary) damage to membrane proteins and, ultimately, cell death (Cuypers *et al.*, 2011; Gielen *et al.*, 2016; Moller *et al.*, 2007; Yruela, 2005, 2009).

The metal-specific responses are a result of the different chemical properties of Cu and Cd. While Cu is a redox-active metal that participates in Fenton-type reactions and directly induces oxidative stress (Drążkiewicz *et al.*, 2004), Cd is not redox-active and only indirectly induces oxidative stress by disrupting normal cellular metabolism (Smeets *et al.*, 2005, 2008a). This metal-related dichotomy is further evident in the intensity of pro-oxidative (Table 4.4 and 4.5) and antioxidative (Table 4.3, 4.4, and 4.5) responses induced upon Cu and Cd exposure. In general, the severity of the responses was stronger in roots of Cu- than in Cd-exposed plants.

Exposure of plants to excess Cu or Cd resulted in elevated metal accumulation in the roots (Table 4.2). Under both metal exposures, metal concentrations were higher in roots of Col-0 than in those of Ws plants, corresponding with the stronger growth reduction observed for Col-0 as compared to Ws plants (Table 4.1). After exposure to Cd, plants of both accessions showed higher concentrations of Cu in the roots (Table 4.2), indicating Cd-induced alterations to Cu homeostasis as described by Gayomba *et al.* (2013) for Col-0 plants. Although excess Cu and Cd are known to affect Cu homeostasis, a potential link between differential regulation of Cu homeostasis and accession-specific sensitivities to Cu and Cd is yet to be established.

Since Cu is an essential micronutrient, plants maintain its homeostasis by tightly regulating the uptake of Cu and its reallocation within the cell to prevent deficiency and avoid toxicity (Burkhead *et al.*, 2009). Within these processes, the SPL7 transcription factor plays a pivotal role by regulating the gene expression of Cu transporters and chaperones, as well as miRNA-dependent reallocation of Cu to proteins with essential functions such as plastocyanin (Gielen *et al.*, 2016; Jung *et al.*, 2012; Yamasaki *et al.*, 2009). Cadmium exposure was shown to induce Cu deficiency-like responses mediated by SPL7 (Gayomba *et al.*, 2013; Gielen *et al.*, 2016). One of the responses to Cd-induced Cu deficiency is the replacement of Cu-containing enzymes by other functionally equivalent enzymes. In accordance with previous studies (Gayomba *et al.*, 2013; Gielen *et al.*, 2016), transcript levels of two Cu/Zn-SOD isozyme genes (*CSD1* and *CSD2*) were downregulated after 72 h exposure to 5 µM Cd, while *FSD1* (iron isozyme) transcript levels were upregulated at both time points (Table 4.5). However, the expression of *FSD1* was significantly more upregulated after 24 h in roots of Cd-exposed Ws than in those of Col-0 plants, suggesting that Ws plants are rapidly able to effectively counteract Cd-induced Cu deficiency-like responses. Interestingly, Gayomba *et al.* (2013) observed that *spl7* mutant plants were hypersensitive to Cd, suggesting these SPL7-mediated pathways to be required for basal Cd tolerance. Therefore, the decreased Cd sensitivity of Ws plants is, among others, likely linked to their ability to better counteract Cd-induced alterations to Cu homeostasis via SPL7-mediated pathways in the roots.

Modulating Cu uptake is essential to maintain Cu homeostasis. The expression of Cu transporter genes is regulated in response to both excess Cu and Cu deficiency to either decrease or enhance Cu uptake, respectively. A six-member CRT-type COPPER TRANSPORT PROTEIN (COPT1-6) family has been described in *A. thaliana* (Jung *et al.*, 2012; Sancenón *et al.*, 2003). Sancenón *et al.* (2003) described *COPT1* and *COPT2* as regulated by Cu availability in Col-0 plants. As expected, transcript levels of these plasma membrane high-affinity Cu transporters were significantly downregulated in Ws roots exposed to excess Cu, whereas this was only observed for *COPT2* in roots of Col-0 plants (Table 4.4). This indicates that the Ws accession rapidly attempts to lower the amounts of Cu transported into the cells to avoid Cu toxicity. This also suggests that roots of Ws plants are able to cope better with excess Cu than Col-0 roots and are therefore less sensitive as observed before (Murphy and Taiz, 1995a; Schiavon *et al.*, 2007). In view of Cd-induced Cu deficiency-like responses, the upregulation of *COPT1* (Table 4.5) emerges as an attempt to enhance Cu uptake in the roots to counteract what is perceived as a micronutrient deficiency. However, while this upregulation was observed at both 24 and 72 h in Col-0 plants, it only occurred after 24 h in Ws plants (Table 4.5). This further suggests that the latter accession rapidly counterbalances Cd-induced alterations to Cu homeostasis, thereby contributing to their reduced Cd sensitivity as compared to that of Col-0 plants.

Transcript levels of the intracellular vacuolar Cu transporter *COPT5* were not altered in roots of plants exposed to excess Cu (Table 4.4), but were significantly upregulated in roots of Cd-exposed plants (Table 4.5). The *COPT5* gene is mostly expressed in roots and is particularly associated with the endodermis and vascular tissues (Garcia-Molina *et al.*, 2011). Earlier studies suggest that this vacuolar Cu exporter plays a role in plant responses to environmental Cu deficiency, probably by remobilizing Cu from prevacuolar vesicles into the cytosol (Garcia-Molina *et al.*, 2011; Klaumann *et al.*, 2011). This is in agreement with the observed Cd-induced Cu deficiency in both accessions. However, roots of Cd-exposed Ws plants showed a continued upregulation of *COPT5* together with restored *COPT1* expression levels at 72 h (Table 4.5). This again suggests that Ws plants react more efficiently and better remobilize the intracellular Cu stores in response to the perceived Cd-induced Cu

deficiency than the Col-0 accession, resulting in Ws plants being less sensitive to Cd.

Once Cu uptake increases, MTs may help to buffer intracellular Cu levels to avoid Cu-induced damage. These small cysteine-rich metal-binding proteins are known to play a role in metal homeostasis and distribution in plants. In particular, MTs have been described as *in vivo* functional chelators of Cu in *Arabidopsis* (Guo *et al.*, 2008) and were shown to be involved in the mobilization of Cu from senescent towards sink organs (Guo *et al.*, 2003). For example, the overall upregulation of *MT2a* (Table 4.4 and 4.5) can be related to the observed increased Cu concentrations after both Cu and Cd exposure, as this gene is highly induced by increasing Cu levels in young tissues such as root tips (Guo *et al.*, 2003). Murphy and Taiz (1995b) reported *MT1* expression to be constant in *Arabidopsis* after Cu exposure, while *MT2* was Cu-inducible. In addition, Ws plants were more tolerant to Cu than Col-0 plants, which was suggested to be strongly positively correlated with *MT2* expression levels (Murphy and Taiz, 1995b). More recently, Guo *et al.* (2003) suggested that MT1a and MT2b play a major role in Cu homeostasis in the phloem, with MT2b functioning as a housekeeping MT and MT1a handling rapid changes in phloem Cu concentrations. These appointed functions, in addition to the involvement of MT1a in the sequestration of excess Cu in roots (Guo *et al.*, 2008), might explain the observed *MT1a* and *MT2b* up-regulation in roots of Cu-exposed plants (Table 4.4). Considering that a higher Cu tolerance is associated with higher *MT2* levels (Murphy and Taiz, 1995b), the significantly higher up-regulation of *MT2b* in Ws than in Col-0 roots (Table 4.4) supports Ws plants to be less sensitive to excess Cu as compared to Col-0 plants. In turn, this further underscores that the regulation of Cu homeostasis underlies accession-specific sensitivities to Cu.

Concerning Cd-induced Cu deficiency responses, a clear accession-specific difference in *MT2b* expression was observed. More specifically, *MT2b* was downregulated in roots of Col-0 plants and upregulated in those of Ws plants (Table 4.5). The MT2b protein could act as a storage mechanism to provide Cu as a cofactor for laccases catalyzing lignification of the cell wall (Guo *et al.*, 2003). The expression differences between both accessions coincide with the

lower amount of lignification in Cd-exposed Col-0 plants and no increased SPOD activity, while this is the opposite in Cd-exposed Ws plants (Figure 4.4 and 4.5). This indicates that lignification can be maintained in Ws plants, suggesting that the binding properties of the cell wall and its role in Cd detoxification are important underlying mechanisms of the improved Cd tolerance in Ws as compared to Col-0 plants. As lignification depends on proper Cu homeostasis (Printz *et al.*, 2016), this again underscores its influence on plant Cd sensitivity.

In conclusion, our results indicate that Ws plants are less sensitive to excess Cu and Cd than Col-0 plants, which is in agreement with earlier studies (Murphy and Taiz, 1995a; Park *et al.*, 2012; Schiavon *et al.*, 2007). Major differences in the response of both accessions to excess Cu and Cd are related to how plants are able to cope with and recover from the alterations to Cu homeostasis induced by both metals. Ultimately, the regulation of Cu homeostasis is put forward as a crucial determinant of the Cu and Cd sensitivities of Col-0 and Ws plants. In particular, the reduced Cd sensitivity of Ws plants seems to be highly related to their ability to effectively counteract Cd-induced Cu deficiency-like responses at different levels, among others via SPL7 mediated pathways.

Supplemental Table 4.1– List of primers used in quantitative real-time PCR. E-E-jn: Exon-Exon-junction. UTR: Untranslated region.

Locus	Annotation	Forward primer (5′ – 3′)	Reverse primer (5′ – 3′)	Exon location	Amplicon length (bp)	Primer Efficiency	
Reference genes							
AT2G28390	*SAND family*	AACTCTATGCAGCATTTGATCCACT	TGATTGCATATCTTTATCGCCATC	Exon 13	61	Col-0	95.56 %
						Ws	97.08 %
AT3G18780	*ACT2*	CTTGCACCAAGCAGCATGAA	CCGATCCAGACACTGTACTTCCTT	Exon 2	68	Col-0	91.68 %
						Ws	94.24 %
AT4G05320	*UBQ10*	GGCCTTGTATAATCCCTGATGAATAAG	AAAGAGATAACAGGAACGGAAACATAGT	3′ UTR	61	Col-0	103.28 %
						Ws	90.94 %
AT4G26410	*RHIP1*	GAGCTGAAGTGGCTTCCATGAC	GGTCCGACATACCCATGATCC	E7-E8-jn	81	Col-0	98.67 %
						Ws	90.85 %
AT4G34270	*TIP41-like*	GTGAAAACTGTTGGAGAGAAGCAA	TCAACTGGATACCCTTTCGCA	E1-E2-jn	61	Col-0	88.47 %
						Ws	80.08 %
AT5G08290	*YLS8*	TTACTGTTTCGGTTGTTCTCCATTT	CACTGAATCATGTTCGAAGCAAGT	Exon 2	61	Col-0	94.93 %
						Ws	93.06 %
AT5G15710	*F-box protein*	TTTCGGCTGAGAGGTTCGAGT	GATTCCAAGACGTAAAGCAGATCAA	Exon 1	63	Col-0	92.07 %
						Ws	82.32 %
AT5G25760	*UBC21*	CTGCGACTCAGGGAATCTTCTAA	TTGTGCCATTGAATTGAACCC	E3-E4-jn	61	Col-0	93.42 %
						Ws	92.78 %
AT5G55840	*PPR gene*	AAGACAGTGAAGGTGCAACCTTACT	AGTTTTTGAGTTGTATTTGTCAGAGAAAG	Intron 2	59	Col-0	93.86 %
						Ws	84.03 %
AT5G60390	*EF1A*	TGAGCACGCTCTTCTTGCTTTCA	GGTGGTGGCATCCATCTTGTTACA	E1-E2-jn	76	Col-0	98.94 %
						Ws	98.09 %

Supplemental Table 4.1– List of primers used in quantitative real-time PCR. Continuation.

Locus	Annotation	Forward primer (5′ – 3′)	Reverse primer (5′ – 3′)	Exon location	Amplicon length (bp)	Primer Efficiency	
Oxidative stress hallmark genes							
AT1G05340	*Unknown*	TCGGTAGCTCAGGGTAAAGTGG	CCAGGGCACAACAGCAACA	E2-E3-jn	91	Col-0	95.55 %
						Ws	90.11 %
AT1G19020	*Unknown*	GAAAATGGGACAAGGGTTAGACAAA	CCCAACGAAAACCAATAGCAGA	Exon 1	92	Col-0	96.64 %
						Ws	96.01 %
AT1G57630	*TIR-class*	ACTCAAACAGGCGATCAAAGGA	CACCAATTCGTCAAGACAACACC	Exon 1	91	Col-0	95.96 %
						Ws	89.74 %
AT2G21640	*UPOX*	GACTTGTTTCAAAAACACCATGGAC	CACTTCCTTAGCCTCAATTTGCTTC	E1-E2-jn	91	Col-0	91.21 %
						Ws	89.23 %
AT2G43510	*Defensin-like*	ATGGCAAAGGCTATCGTTTCC	CGTTACCTTGCGCTTCTATCTCC	E1-E2-jn	91	Col-0	91.16 %
						Ws	92.50 %
Gene encoding ROS-producing enzyme							
AT1G55020	*LOX1*	TTGGCTAAGGCTTTTGTCGG	GTGGCAATCACAAACGGTTC	Exon 6	101	Col-0	99.97 %
						Ws	103.36 %
Genes encoding antioxidative enzymes							
AT4G23100	*GSH1*	CCCTGGTGAACTGCCTTCA	CATCAGCACCTCTCATCTCCA	Exon 5	101	Col-0	99.67 %
						Ws	95.99 %
AT5G27380	*GSH2*	GGACTCGTCGTTGGTGACAA	TCTGGGAATGCAGTTGGTAGC	Exon 11	101	Col-0	91.24 %
						Ws	90.60 %
AT1G08830	*CSD1*	TCCATGCAGACCCTGATGAC	CCTGGAGACCAATGATGCC	Exon 5	102	Col-0	101.93 %
						Ws	95.95 %
AT2G28190	*CSD2*	GAGCCTTTGTGGTTCACGAG	CACACCACATGCCAATCTCC	Exon 6	101	Col-0	99.71 %
						Ws	102.28 %
AT4G25100	*FSD1*	CTCCCAATGCTGTGAATCCC	TGGTCTTCGGTTCTGGAAGTC	Exon 4	101	Col-0	96.82 %
						Ws	91.99 %

Supplemental Table 4.1 – List of primers used in quantitative real-time PCR. Continuation.

Locus	Annotation	Forward primer (5′ – 3′)	Reverse primer (5′ – 3′)	Exon location	Amplicon length (bp)	Primer Efficiency	
Genes encoding copper transporter proteins							
AT5G59030	*COPT1*	GTTAATCCAAACCGCCGTGTATAC	GAGAAACACACCGGCGTTAAAC	Exon 1	91	Col-0	108.48 %
						Ws	83.75 %
AT3G46900	*COPT2*	TCCGGCATGTACGCTCTCTG	CACTGACACGTAGGATCGGTGAA	Exon 1	91	Col-0	94.94 %
						Ws	91.90 %
AT5G20650	*COPT5*	ACCAAACCTCTTCCCAATCC	TGGCTTTGATTCCCCAGTAG	Exon 1	113	Col-0	97.00 %
						Ws	103.30 %
Genes encoding metallothionein proteins							
AT1G07600	*MT1a* *	AACTGTGGATGTGGCTCCTC	CAGTTACAGTTTGACCCACAGC	Exon 1	122	Col-0	110.79 %
						Ws	111.77 %
AT1G07590	*TPR-like* *	AGAGCTAGCGAGAACGTGGA	CCTACTCGAGCAAACGCTTC	Exon 4	93	Col-0	89.85 %
						Ws	89.69 %
AT1G07610	*MT1c*	GCATGGTCTCAAACCAAGGA	TACGCAACACAATGCCAAGT	Intron 2	96	Col-0	97.20 %
						Ws	92.73 %
AT3G09390	*MT2a*	ACCCTGACTTGGGATTCTCC	GCGTTGTTACTCTCCCCTGA	Exon 1	109	Col-0	82.60 %
						Ws	82.56 %
AT5G02380	*MT2b*	ACTCTTGTCCTCGGTGTTGC	TTGCACTTGCAGTCAGATCC	Exon 1	110	Col-0	89.04 %
						Ws	89.66 %

* Since *AT1G07590* overlaps the *MT1a* completely, *AT1G07590*-specific primers were also developed to correct for its contribution to *MT1a* gene expression.

Supplemental Table 4.2 – Quantitative real-time PCR parameters according to the "Minimum Information for publication of Quantitative real-time PCR Experiments" (MIQE) guidelines derived from Bustin *et al.* (2009).

Sample/Template	
Source	Roots of *Arabidopsis thaliana* plants cultivated in hydroponics
Method of preservation	Liquid nitrogen
Storage time	Six weeks at - 70 °C
Handling	Frozen
Extraction method	Phenol-free Total RNA isolation: Ambion™ RNAqueous® Total RNA Isolation Kit * (Life Technologies, Waltham, MA, USA)
RNA: DNA-free	TURBO DNA-*free*™ Kit * (Life Technologies, Waltham, MA, USA) Design of intron-spanning primers whenever possible
Concentration	NanoDrop®: ND-1000 Spectrophotometer (Thermo Fisher Scientific, Inc., MA, USA)
Assay optimization and validation	
Accession number	Supplemental Table 4.1
Amplicon details	Exon location and amplicon size: Supplemental Table 4.1
Primer sequences	Supplemental Table 4.1
In silico	Primers were blasted using the BLAST tool at http://arabidopsis.org/
Empirical	Primer concentration: 300 nM Annealing temperature: 60°C
Priming conditions	Combination of oligo(dT)-primers and random hexamers
PCR efficiency	Dilution series (slope, y-intercept and r^2; Supplemental Table 4.1)
Linear dynamic range	Samples are situated within the range of the efficiency curve
Reverse transcription – PCR	
Protocols	As stated in the Materials and Methods (Section 3.8)
Reagents	As stated in the Materials and Methods (Section 3.8)
No template control (NTC)	Cq and dissociation curve verification
Data analysis	
Specialist software	7500 Fast Real-Time PCR System (Applied Biosystems, Life Technologies, Belgium) Software v2.0.1
Statistical justification	At least three biological replicates Elimination of outliers after statistical validation using the Grubbs' test at significance level 0.05 (R version 3.3.1, package "outliers") Log transformation of the data One- and two-way ANOVA and the Tukey-Kramer post-hoc test to correct for multiple comparisons using R version 3.3.1
Normalization	Four stable reference genes selected using the GrayNorm algorithm (Remans *et al.*, 2014): AT2G28390, AT4G05320, AT4G34270 and AT5G55840

* All procedures were performed according to the manufacturer's protocols.

CHAPTER 5

Accession-specific life strategies affect responses in leaves of *Arabidopsis thaliana* plants exposed to excess Cu and Cd

Rafaela Amaral dos Reis, Els Keunen, Miguel Pedro Mourato, Luísa Louro Martins, Jaco Vangronsveld and Ann Cuypers (2018). Accession-specific life strategies affect responses in leaves of *Arabidopsis thaliana* plants exposed to excess Cu and Cd. Journal of Plant Physiology 223: 37-46.

Keywords: *Arabidopsis thaliana*, natural accessions, leaves, copper, cadmium.

Abstract

The natural accession Columbia (Col-0) is considered the reference genome of the model plant *Arabidopsis thaliana*. Nonetheless, Col-0 plants are more sensitive to excess copper (Cu) and cadmium (Cd) than other widely used accessions such as Wassilewskija (Ws) plants. In the current study, this accession-specific metal sensitivity is further explored by comparing the responses in leaves of Col-0 and Ws plants exposed to excess Cu and Cd.

Our results suggest that different life strategies, favored by both accessions under physiological conditions, affect their response to metal exposure. While Col-0 plants mainly invest in metal detoxification, Ws plants center on nutrient homeostasis. In particular, the higher expression of genes related to Cu homeostasis genes in non-exposed conditions indicates that Ws plants possess a constitutively efficient metal homeostasis. On the other hand, oxidative stress-related MAPK signaling appears to be boosted in leaves of Col-0 plants exposed to excess Cu. Furthermore, the upregulation of the glutathione (GSH) biosynthesis *GSH2* gene and the increased GSH concentration after Cd exposure suggest the activation of detoxification mechanisms, such as phytochelatin production, to counteract the more severe Cd-induced oxidative stress in leaves of Col-0 plants. Exposure to Cd also led to a more pronounced ethylene signaling response in leaves of Col-0 as compared to Ws plants, which could be related to Cd-induced GSH metabolism. In conclusion, accession-specific life strategies clearly affect the way in which leaves of *A. thaliana* plants cope with excess Cu and Cd.

5.1 Introduction

Anthropogenic activities have a worldwide impact on soil elemental composition. In turn, this represents an obstacle to normal plant development. For example, plant survival is commonly affected in metal-enriched environments where excessive concentrations of plant-available metals cause phytotoxicity and inhibit plant growth. However, this toxicity response is highly dependent on the chemical properties of the metal involved. For example, excess copper (Cu) and cadmium (Cd) disturb normal plant metabolism in different ways (Cuypers *et al.*, 2012; Mourato *et al.*, 2012). Copper is a redox-active essential micronutrient that inhibits enzyme functioning and interferes with essential cellular processes when present in excess (Cuypers *et al.*, 2011; Gielen *et al.*, 2016, 2017; Lequeux *et al.*, 2010; Yruela, 2005, 2009). It also directly induces oxidative stress by catalyzing the formation of reactive oxygen species (ROS) through Fenton and Haber-Weiss reactions (Drążkiewicz *et al.*, 2004). Alternatively, Cd is a highly phytotoxic nonessential element affecting plant growth even when available in low concentrations (Jozefczak *et al*., 2014; Keunen *et al*., 2011a, 2013; Park *et al*., 2012; Schellingen *et al*., 2015b; Wong and Cobbett, 2009). It triggers oxidative stress in an indirect way by interfering with the cellular metabolism and antioxidative mechanisms (Cuypers *et al.*, 2011; Jozefczak *et al.*, 2014, 2015; Schellingen *et al.*, 2015a).

Arabidopsis thaliana is a well-established model plant in molecular and genetic studies. Notwithstanding several natural accessions existing, the Columbia (Col-0) accession is generally acknowledged as the reference genome (Weigel, 2012) and is the subject of intensive study. Nonetheless, exploring and comparing the responses of different natural accessions can provide new insights into our current knowledge, for example on stress responses induced by excess soil metal concentrations. Albeit limited, some comparative studies described differences in metal sensitivity between different *A. thaliana* accessions. Indeed, Col-0 plants have been demonstrated to be more sensitive to excess Cu and Cd than plants of other widely used *Arabidopsis* accessions such as Wassilewskija (Ws) or Landsberg *erecta* (L*a*e*r*) (Murphy and Taiz, 1995b, 1995a, 1997; Park *et al*., 2012; Schiavon *et al*., 2007).

In their study using 10 different *A. thaliana* accessions, Murphy and Taiz (1995a) described Col-0 as the accession showing the lowest constitutive Cu tolerance. Furthermore, they reported that Ws plants showed an acclimation response to Cu, resulting in significant levels of inducible Cu tolerance, which was later related to higher basal levels of non-protein thiols and glutathione (GSH) (Murphy and Taiz, 1995b). In subsequent studies, the authors correlated this accession-specific Cu tolerance to a distinctive regulation of the Cu-chelating *METALLOTHIONEIN 2* (*MT2*) gene (Murphy and Taiz, 1995b) and to differences in the ability to reverse Cu-induced potassium leakage (Murphy and Taiz, 1997). Schiavon *et al.* (2007) also explored this accession-specific variation in Cu sensitivity. Since the less sensitive Ws plants accumulated more Cu in the roots and shoots than the more sensitive Col-0 plants, they reasoned that Cu exclusion is not the main tolerance mechanism of the former accession. Alternatively, they hypothesized that a higher Cu sensitivity is a manifestation of cation imbalance in the cell, ultimately reflecting Cu-induced nutrient deficiency (Schiavon *et al.*, 2007). Park *et al.* (2012) described Col-0 plants to be more sensitive to Cd than Ws plants, potentially related to the non-functioning of HEAVY METAL ATPase 3 (HMA3) in Col-0 plants and a differential expression of other *HMA* genes in both accessions. Considering differential localization and expression patterns, it was hypothesized that the combined action of the vacuolar transporter HMA3 and the plasma membrane transporters HMA2 and HMA4 is relevant to detoxify Cd in plants with a lower Cd sensitivity. While HMA3 results in Cd sequestration in root vacuoles, HMA2 and HMA4 limit root-to-shoot Cd translocation, ultimately preventing competition between different elements and nutrient deficiency symptoms in the shoots of Ws plants (Park *et al.*, 2012).

Although roots are the first plant organ coming into contact with metals in the soil and are therefore directly affected, leaves also display metal-induced effects due to root-to-shoot metal translocation and/or inter-organ signaling. In the current study, responses in the leaves of Col-0 and Ws plants exposed to metal excess are compared to reveal accession-specific changes. More specifically, effects of excess Cu and Cd on rosette growth, metal concentrations, and transport, and their associated oxidative stress signatures were determined in both accessions after exposure for 24 and 72 h.

5.2 Results

5.2.1 Rosette growth

Hydroponically grown three-week-old *A. thaliana* plants of Col-0 and Ws background were exposed to excess Cu (2 µM) or Cd (5 µM). To determine responses after short-term and more prolonged metal exposure, leaves were sampled 24 and 72 h after the onset of Cu or Cd exposure.

Arabidopsis natural accessions Col-0 and Ws are morphologically different (Passardi *et al.*, 2007). Under non-exposed conditions, rosettes of Ws plants had a significantly higher fresh weight as compared to those of Col-0 plants (Figure 5.1). Moreover, this was not related to a different number of leaves, but rather to a larger surface area of the leaves of Ws plants versus Col-0 plants (data not shown). Excess Cu and Cd inhibited rosette growth in both accessions as indicated by a lower fresh weight (Figure 5.1). While exposure to excess Cu resulted in an inhibition of Col-0 rosette growth already after 24 h, Ws rosettes were only significantly affected by Cu after 72 h. The effects of Cd exposure were only significant in leaves of both Col-0 and Ws plants after 72 h (Figure 5.1).

5.2.2 Metal translocation factors

To evaluate the ability to translocate Cu and/or Cd, the translocation factors were estimated (Figure 5.2) from the concentrations of Cu and Cd in roots and leaves (Supplemental Table 5.1) of non-exposed, Cu-, and Cd-exposed plants. In non-exposed conditions, the translocation factor of Cu significantly increased in Ws plants over time, with a similar trend in Col-0 plants (Figure 5.2A). Exposure to excess Cu severely impaired relative root-to-shoot Cu translocation as compared to non-exposed conditions (Figure 5.2A). Whereas the Cu translocation factor was significantly higher in Col-0 than Ws plants after 24 h, it decreased to translocation factors similar to those of Ws plants after 72 h. The root-to-shoot Cu translocation factor in Cu-exposed Ws plants decreased as compared to non-exposed conditions but remained constant over time (Figure 5.2A). Although the root-to-shoot Cu translocation factor was reduced by Cd exposure in both accessions (Figure 5.2A), it was significantly higher in Ws than Col-0 plants at each time point (Figure 5.2A). During exposure

to Cd, its translocation factor in Col-0 plants was constant over time (Figure 5.2B). The root-to-shoot Cd translocation factor was significantly higher in Ws than Col-0 plants after 24 h, but decreased to values comparable to those in Col-0 plants after 72 h (Figure 5.2B).

5.2.3 Activities of antioxidative and NAD(P)H-producing enzymes

Activities of antioxidative enzymes (SOD, CAT, GR, GPOD, and SPOD) and of NAD(P)H-producing enzymes (ICDH, ME, and G6PDH) were determined in leaves of Col-0 and Ws plants (Table 5.1). Exposure to excess Cu only affected the enzymatic activities in leaves of Ws plants. Superoxide dismutase activity was significantly higher after exposure to Cu for 72 h, as were GR and ME activities at both time points. Exposure to Cd led to an increased ME activity in leaves of Col-0 and Ws plants at 24 and 72 h. The activities of GR, GPOD, SPOD, ICDH, and G6PDH were only significantly higher in leaves of Col-0 plants after 72 h of Cd exposure (Table 5.1).

5.2.4 Glutathione concentrations

Concentrations of reduced (GSH) and oxidized (glutathione disulfide, GSSG) glutathione were determined in leaves of both accessions (Table 5.2). Total glutathione levels were higher in the leaves of Col-0 plants after exposure to excess Cu for 72 h, which coincided with an increased GSSG concentration. In case of Col-0 plants exposed to Cd for 72 h, higher versus lower concentrations were observed for GSH and GSSG respectively, resulting in a lower GSSG/GSH ratio (Table 5.2). No significant changes in total glutathione concentrations were observed in leaves of Ws plants. However, similar to Col-0 plants, a higher GSSG concentration was observed in leaves of Cu-exposed Ws plants after 72 h, resulting in a higher GSSG/GSH ratio. Exposure to Cd significantly lowered the GSSG concentration in leaves of both genotypes (Table 5.2).

5.2.5 Gene expression analysis

Expression levels of several genes involved in Cu transport and chelation (MTs), pro- and antioxidative responses, secondary metabolism, ethylene/MAPK signaling pathways, and genes encoding transcription factors were determined in

leaves of Col-0 and Ws plants either not exposed (Table 5.3) or exposed to excess Cu (Table 5.4) or Cd (Table 5.5).

Representation of the gene expression data of leaves from plants grown under non-exposed conditions using a heat map revealed an accession-related clustering, with Ws samples mostly clustering separated from Col-0 samples (Figure 5.3). In addition, hierarchical clustering revealed two gene clusters responding differently in the leaves of both accessions. One cluster included Cu homeostasis-related genes such as the iron superoxide dismutase gene *FSD1*, primary microRNAs *pri-miR398a* and *pri-miR398b*, MT genes *MT1a* and *MT1c* and the Cu transporter gene *COPT2*, and the lipoxygenase gene *LOX2* with higher expression levels in leaves of Ws (green-shaded rectangles) than Col-0 plants (red-shaded rectangles). Opposite expression patterns were observed within the other gene cluster grouping three oxidative stress hallmark genes (Gadjev *et al.*, 2006), MAPK/ethylene signaling-related genes (mitogen-activated kinase gene *MPK3*, WRKY DNA-binding protein gene *WRKY33*, and ethylene response factor gene *ERF1*), the pro-oxidative gene *LOX1*, as well as *COPT5* and *MT2a* (Figure 5.3). Transcript level analysis of both gene clusters confirmed accession-specific expression levels in leaves of non-exposed Col-0 and Ws plants (Table 5.3).

Comparing non-exposed to Cu- or Cd-exposed samples revealed a separate clustering between the metal-exposed and non-exposed groups (Figure 5.4 and 5.5). After including only non-exposed and Cu-exposed samples in the heat map, two groups of genes emerged (Figure 5.4): (1) as indicated by the red-shaded rectangles, genes that were less expressed after Cu exposure, including those involved in Cu homeostasis, such as *FSD1*, *pri-miR398b*, *COPT1*, *COPT2*, and *MT1c* (Cluster Cu-I); (2) as indicated by the green-shaded rectangles, genes that were more expressed under excess Cu conditions, including those involved in MAPK/ethylene signaling such as *OXI1*, *MPK3*, *WRKY33*, and *ERF1*, four oxidative stress hallmark genes, *pri-miR398a*, *LOX1* and *LOX2*, *GSH2*, and *MT2a* (Cluster Cu-II). Moreover, gene expression data revealed some accession-specific changes in the expression of these genes upon exposure to excess Cu (Table 5.4). Concerning the genes in cluster Cu-I, transcript levels of *FSD1*, *pri-miR398b*, and *COPT2* were significantly lower only

in leaves of Cu-exposed Ws plants after 72 h (Table 5.4). Expression of *MT1c* was significantly lower in leaves of Ws plants exposed to excess Cu at both time points (Table 5.4). Regarding the genes in cluster Cu-II, transcript levels of *GSH2* and *OXI1* were significantly higher only in leaves of Cu-exposed Col-0 plants (at 72 and 24 h respectively) (Table 5.4). Moreover, while *pri-miR398a* transcript levels were higher after 24 h of Cu exposure in leaves of both accessions, its upregulation was significantly higher in Col-0 as compared to Ws plants (Table 5.4). Transcript levels of *MPK3* and *WRKY33* were higher in leaves of Cu-exposed Ws plants at both time points. In Col-0 plants, *MPK3* was only upregulated after 24 h, whereas *WRKY33* was significantly upregulated after 72 h of exposure to excess Cu (Table 5.4). The ethylene signaling-related gene *ERF1* was significantly upregulated after Cu exposure and its transcript levels were significantly higher in leaves of Ws as compared to Col-0 plants (Table 5.4).

Leaves of Cd-exposed Col-0 and Ws plants generally clustered away from leaves of plants grown under non-exposed conditions (Figure 5.5). Several genes grouped together due to their higher expression upon Cd exposure (green-shaded rectangles). This cluster included oxidative stress-related genes such as all five oxidative stress hallmark genes, *GSH2*, *LOX1,* and *LOX2*, the MAPK/ethylene signaling-related genes (*OXI1*, *MPK3*, *WRKY33,* and *ERF1*), *COPT5*, *FSD1*, *MT2a,* and *pri-miR398a/b* (Figure 5.5). Moreover, gene expression analysis revealed some accession-specific differences in their expression upon Cd exposure (Table 5.5). Transcript levels of oxidative stress hallmark genes (Gadjev *et al.*, 2006) and ethylene signaling-related gene *ERF1* were generally more upregulated in leaves of Col-0 than Ws plants after Cd exposure (Table 5.5). Transcript levels of *LOX1* were significantly higher in leaves of Col-0 plants after 72 h exposure to Cd. While *LOX2* and *pri-miR398a* were upregulated in the leaves of both accessions after 24 h, their transcript levels were significantly higher in Col-0 than in Ws plants and remained upregulated after 72 h in the former accession (Table 5.5). Cadmium-induced upregulation of the *GSH2* gene occurred in leaves of Col-0 plants only. Exposure to Cd led to significantly increased expression levels of *MT2a* in leaves of both accessions. Although *OXI1* expression increased in leaves of both accessions

exposed to Cd, its transcript levels were significantly higher in leaves of Col-0 than Ws plants after 24 h (Table 5.5).

Although not included in one of the above-mentioned gene clusters (Figure 5.3 and 5.5), *CSD1*, *MT2b*, *MT3*, and *WRKY29* were differentially expressed in leaves of Col-0 and Ws plants exposed to excess Cu (Table 5.4) or Cd (Table 5.5). On the one hand, exposure to Cu increased *CSD1* expression in leaves of Ws plants after 24 h (Table 5.4). Furthermore, *MT2b* and *MT3* were upregulated in leaves of Ws plants after 72 h (Table 5.4). On the other hand, exposure to Cd alone caused upregulation of *WRKY29* in leaves of Col-0 plants after 72 h (Table 5.5).

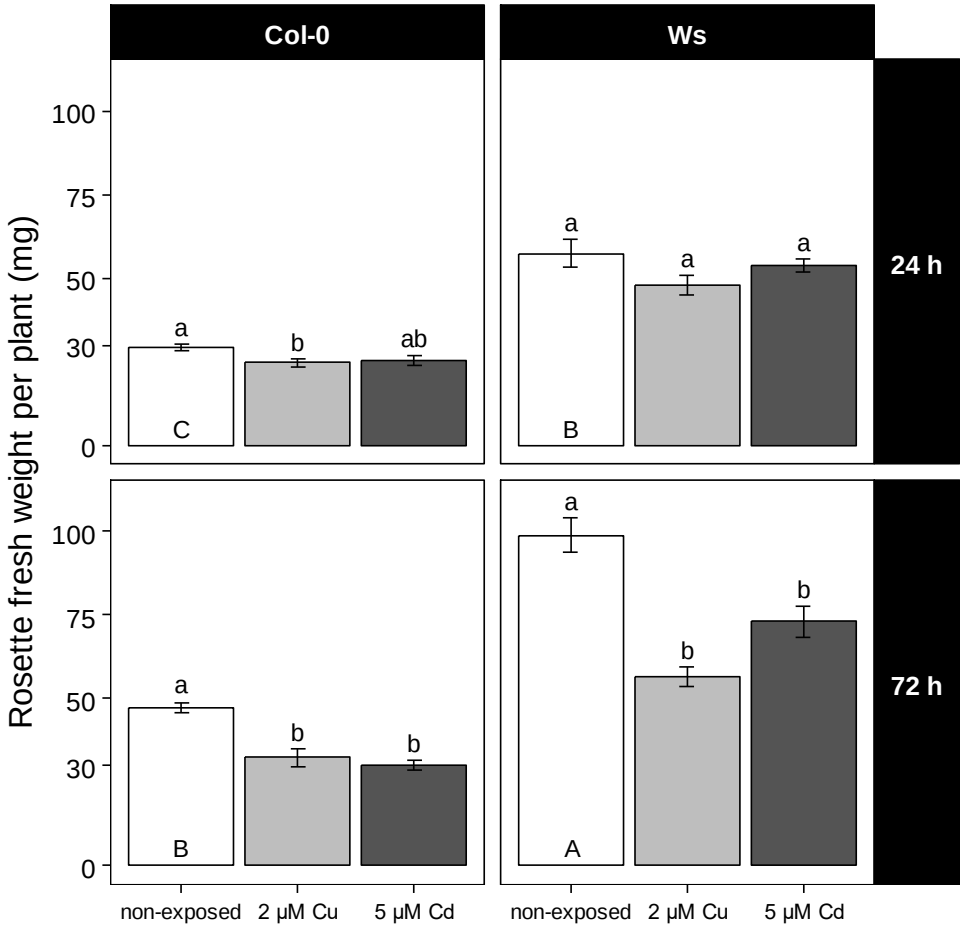

Figure 5.1 – **Rosette fresh weight per plant (in mg) of three-week-old *A. thaliana* plants (accessions Col-0 and Ws) exposed to 2 µM $CuSO_4$, 5 µM $CdSO_4$, or not exposed for 24 and 72 h.** Values are the mean ± S.E. of at least three biological replicates, each containing rosettes of 25 individual plants. □ = non-exposed. ▒ = exposed to 2 µM $CuSO_4$. ■ = exposed to 5 µM $CdSO_4$. Statistical significance ($P<0.05$) is indicated using lowercase (within accession and time point) or uppercase letters (between non-exposed accessions at both time points).

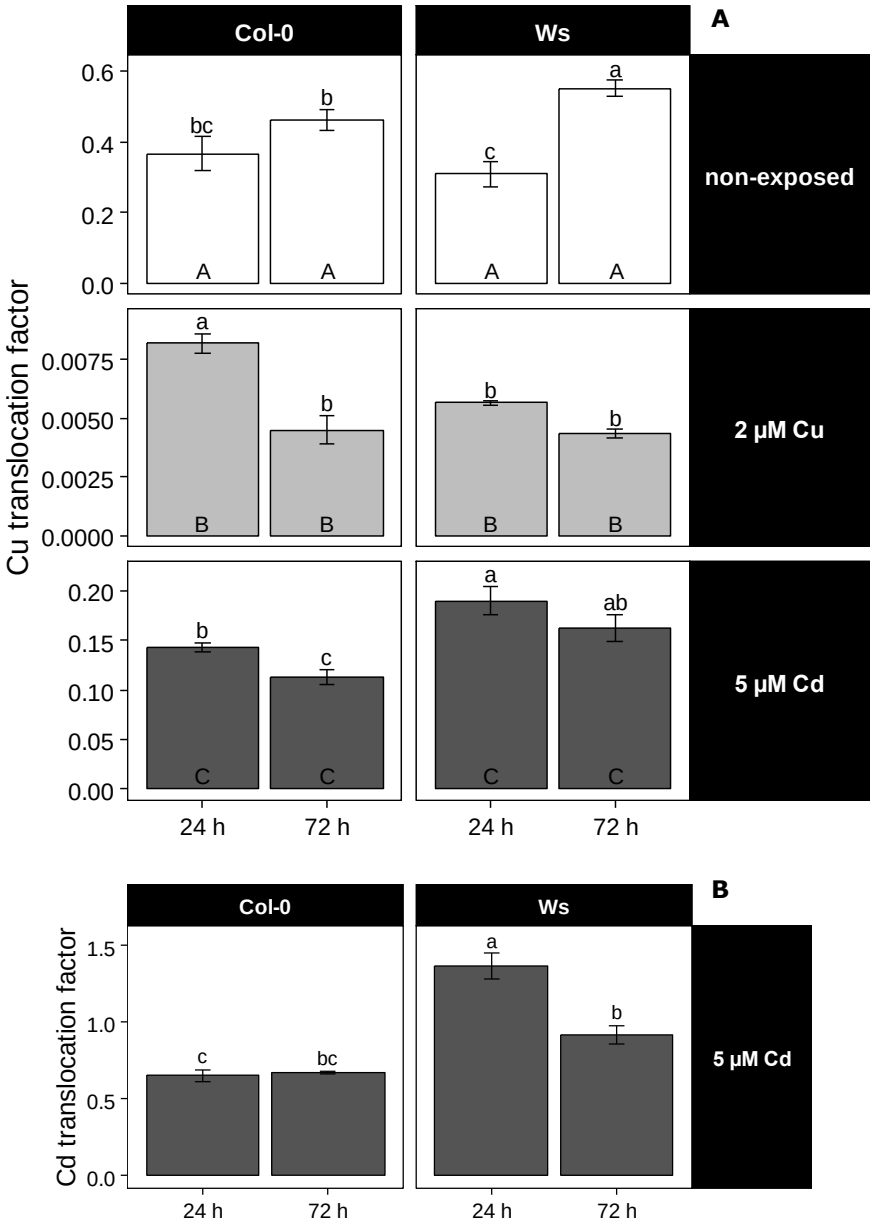

Figure 5.2 – Root-to-shoot translocation factors of Cu and Cd in three-week-old *A. thaliana* plants (accessions Col-0 and Ws) exposed to 2 µM $CuSO_4$, 5 µM $CdSO_4$, or not exposed for 24 and 72 h. (A) Cu translocation factors in non-exposed, Cu- and Cd-exposed plants. **(B)** Cd translocation factors in Cd-exposed plants. Values are the mean ± S.E. of at least three biological replicates. □ = non-exposed. ▒ = exposed to 2 µM $CuSO_4$. ■ = exposed to 5 µM $CdSO_4$. Statistical significance ($P<0.05$) is indicated using different lowercase (within exposure condition, between accessions and time points) or uppercase letters (across exposure conditions, within accession and time point).

Table 5.1 – Activities of antioxidative and NAD(P)H-producing enzymes (mU mg^{-1} fresh weight) in leaves of three-week-old *A. thaliana* plants (accessions Col-0 and Ws) exposed to 2 µM $CuSO_4$, 5 µM $CdSO_4$, or not exposed for 24 and 72 h. Antioxidative enzymes: superoxide dismutase (SOD), catalase (CAT), glutathione reductase (GR), guaiacol peroxidase (GPOD) and syringaldazine peroxidase (SPOD). NAD(P)H-producing enzymes: isocitrate dehydrogenase (ICDH), malic enzyme (ME) and glucose-6-phosphate dehydrogenase (G6PDH). Values are mean ± S.E. of at least three biological replicates, each containing rosettes of at least two individual plants. Statistical significance ($P<0.05$) is indicated using different lowercase letters (for differences within each accession and time point) and the conditions in which differences occur are highlighted in grey.

		Col-0			Ws		
		non-exposed	2 µM Cu	5 µM Cd	non-exposed	2 µM Cu	5 µM Cd
SOD	24 h	367.76 ± 40.50 a	360.55 ± 18.92 a	317.46 ± 3.74 a	301.20 ± 33.15 a	361.16 ± 31.59 a	299.82 ± 7.10 a
	72 h	249.82 ± 70.80 a	251.60 ± 15.27 a	254.87 ± 18.20 a	188.26 ± 43.72 b	362.51 ± 14.07 a	257.89 ± 28.82 ab
CAT	24 h	1.24 ± 0.40 a	0.71 ± 0.20 a	3.71 ± 1.37 a	1.03 ± 0.57 a	13.80 ± 7.55 a	2.51 ± 0.99 a
	72 h	1.98 ± 1.13 a	3.59 ± 2.01 a	6.32 ± 1.66 a	2.72 ± 0.98 a	1.34 ± 0.39 a	2.64 ± 1.10 a
GR	24 h	872.14 ± 47.96 a	1073.43 ± 97.31 a	1133.84 ± 0.05 a	851.58 ± 122.55 b	1283.30 ± 70.17 a	1055.06 ± 67.42 ab
	72 h	828.67 ± 39.95 b	850.93 ± 36.70 b	1075.80 ± 47.91 a	634.20 ± 176.64 b	1168.64 ± 46.39 a	953.59 ± 31.51 ab
GPOD	24 h	23.64 ± 4.06 a	52.00 ± 14.12 a	42.06 ± 8.66 a	17.88 ± 7.06 a	47.98 ± 10.97 a	36.66 ± 7.82 a
	72 h	15.82 ± 3.94 a	19.62 ± 2.31 a	243.45 ± 16.19 b	6.93 ± 3.26 a	37.34 ± 9.04 a	36.75 ± 8.68 a
SPOD	24 h	57.08 ± 23.18 a	115.99 ± 49.15 a	219.87 ± 63.35 a	102.93 ± 43.91 a	172.16 ± 40.75 a	207.41 ± 45.11 a
	72 h	89.49 ± 18.23 a	102.54 ± 11.86 a	1421.37 ± 127.49 b	110.81 ± 22.40 a	258.37 ± 56.62 a	189.89 ± 56.43 a
ICDH	24 h	559.68 ± 25.79 a	588.77 ± 55.00 a	647.77 ± 24.68 a	618.51 ± 218.03 a	549.57 ± 17.21 a	492.95 ± 25.93 a
	72 h	450.08 ± 38.11 b	483.27 ± 20.55 b	615.23 ± 19.18 a	330.77 ± 59.84 a	446.75 ± 20.71 a	402.64 ± 8.68 a
ME	24 h	242.72 ± 6.70 b	285.70 ± 76.98 b	501.06 ± 49.35 a	154.88 ± 23.55 c	293.80 ± 8.03 a	230.86 ± 9.90 b
	72 h	220.22 ± 10.33 b	357.39 ± 18.44 b	771.33 ± 132.53 a	169.89 ± 22.83 b	349.42 ± 28.93 a	397.00 ± 1.77 a
G6PDH	24 h	105.96 ± 7.61 a	138.12 ± 13.80 a	136.36 ± 10.97 a	60.76 ± 16.62 a	140.10 ± 46.75 a	115.95 ± 11.28 a
	72 h	95.06 ± 6.34 b	109.37 ± 0.87 b	168.55 ± 18.84 a	73.75 ± 27.27 a	150.68 ± 14.85 a	118.88 ± 3.88 a

Table 5.2 – Concentrations of total (GSH + GSSG), reduced (GSH), oxidized (GSSG) glutathione (nmoles g^{-1} fresh weight), and GSSG/GSH ratio in leaves of three-week-old *A. thaliana* plants (accessions Col-0 and Ws), exposed to 2 µM $CuSO_4$, 5 µM $CdSO_4$, or not exposed for 24 and 72 h. Values are the mean ± S.E. of at least three biological replicates, each containing rosettes of at least one individual plant. Statistical significance ($P<0.05$) is indicated using different lowercase letters (for differences within each accession and time point) and the conditions in which differences occur are highlighted in grey.

		Col-0			Ws		
		non-exposed	**2 µM Cu**	**5 µM Cd**	**non-exposed**	**2 µM Cu**	**5 µM Cd**
Total (GSH+GSSG)	**24 h**	266.27 ± 55.68 a	266.50 ± 43.31 a	216.64 ± 44.62 a	212.71 ± 37.42 a	272.60 ± 87.22 a	208.77 ± 37.20 a
	72 h	229.71 ± 10.34 b	361.00 ± 37.53 a	419.32 ± 13.45 a	290.43 ± 35.95 a	301.74 ± 24.88 a	335.00 ± 66.45 a
GSH	**24 h**	250.93 ± 51.43 a	256.67 ± 39.82 a	213.58 ± 44.77 a	205.20 ± 37.58 a	261.07 ± 85.92 a	205.66 ± 37.37 a
	72 h	212.67 ± 11.15 b	328.90 ± 37.55 b	416.37 ± 13.03 a	280.44 ± 35.78 a	246.21 ± 5.74 a	330.05 ± 66.15 a
GSSG	**24 h**	15.34 ± 4.77 a	9.83 ± 3.91 a	3.06 ± 0.42 a	7.51 ± 0.86 ab	11.53 ± 2.16 a	3.11 ± 0.45 b
	72 h	15.84 ± 1.74 b	31.68 ± 0.58 a	6.25 ± 0.63 c	9.99 ± 0.83 b	55.54 ± 20.91 a	4.95 ± 0.43 c
GSSG/GSH	**24 h**	0.059 ± 0.011 a	0.035 ± 0.009 ab	0.011 ± 0.000 b	0.040 ± 0.011 a	0.068 ± 0.028 a	0.017 ± 0.005 a
	72 h	0.062 ± 0.004 a	0.075 ± 0.010 a	0.018 ± 0.002 b	0.037 ± 0.005 b	0.223 ± 0.080 a	0.016 ± 0.002 b

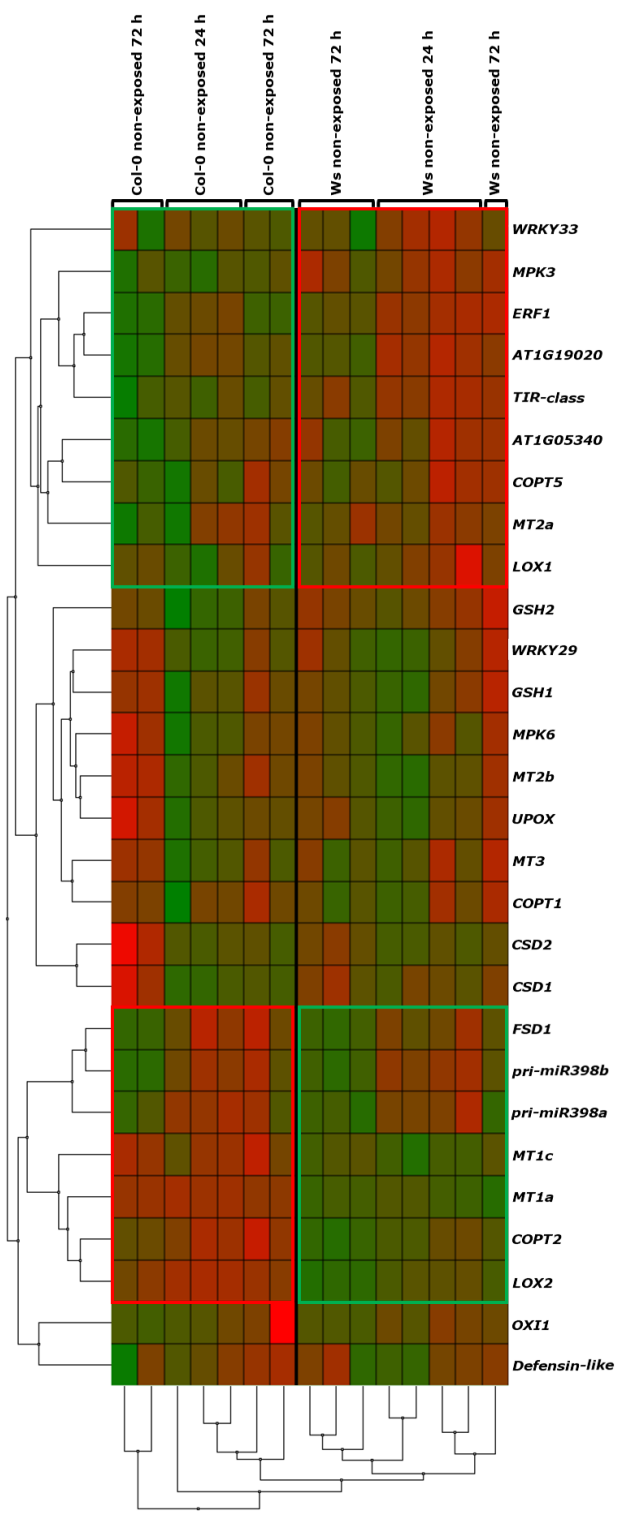

Figure 5.3 – Heat map representation of gene expression data obtained in leaves of three-week-old *A. thaliana* plants (accessions Col-0 and Ws) grown in non-exposed conditions for 24 and 72 h. Hierarchical clustering of genes is shown at the top (gene names at the bottom); genotype clustering is displayed on the left (conditions at the right). Green-shaded rectangles indicate increased, while red-shaded rectangles indicate decreased gene expression. Abbreviations: *UPOX: upregulated by oxidative stress; Defensin-like: protein member of the defensin-like (DEFL) family; AT1G19020: unknown protein; AT1G05340: unknown protein; TIR-class: Toll-Interleukin-Resistance (TIR) domain family protein; LOX1: lipoxygenase 1; GSH1: glutamate-cysteine ligase; GSH2: glutathione synthetase 2; CSD: Cu/Zn superoxide dismutase; FSD1: Fe superoxide dismutase 1; pri-miR398a: primary microRNA 398a; pri-miR398b: primary microRNA 398b; COPT: copper transporter; MT: metallothionein; OXI1: Oxidative signal inducible 1; MPK: mitogen-activated protein kinase; WRKY: WRKY DNA-binding protein; ERF1: ethylene response factor 1.*

Table 5.3 – Transcript levels of genes within clusters identified in leaves of three-week-old *A. thaliana* plants (accessions Col-0 and Ws) grown under non-exposed conditions for 24 and 72 h. Values are the mean normalized expression of Col-0 samples at 24 h ± S.E. (abundance, within gene family) or relative to Col-0 samples at 24 h (set at 1.00) ± S.E (fold-change) of at least three biological replicates, each containing rosettes of at least one individual plant. Resolution values are mean inverse normalization factors relative to the non-exposed at each time point, indicating the stability of the selected reference genes. Statistical significance ($P<0.05$) is indicated by asterisks and printed in bold (for differences within each time point, between accessions). Abbreviations: see Figure 5.3.

Col-0		**Non-exposed**	**Ws**	
24 h	**72 h**		**24 h**	**72 h**
1.00 ± 0.18	1.48 ± 0.17	Resolution	1.08 ± 0.10	1.40 ± 0.19
Genes encoding oxidative stress hallmark proteins				
1.00 ± 0.13	3.77 ± 1.28	*AT1G19020*	**0.51 ± 0.04 ***	1.86 ± 0.22
1.00 ± 0.13	1.73 ± 0.38	*AT1G05340*	0.86 ± 0.06	1.29 ± 0.09
1.00 ± 0.38	3.88 ± 2.41	*TIR-class*	**0.18 ± 0.03 ***	0.66 ± 0.21
Genes encoding ROS-producing enzymes				
1.00 ± 0.22	1.22 ± 0.15	*LOX1*	0.70 ± 0.09	1.14 ± 0.11
1.00 ± 0.17	**2.14 ± 0.43**	*LOX2*	**2.47 ± 0.20 ***	**4.85 ± 0.38 ***
Gene encoding antioxidative enzyme				
1.00 ± 0.48	15.09 ± 8.20	*FSD1*	2.24 ± 0.82	15.21 ± 3.04
Primary microRNA transcripts				
1.00 ± 0.22	46.45 ± 28.43	*pri-miR398a*	**3.97 ± 0.17 ***	94.66 ± 25.62
1.00 ± 0.22	15.31 ± 7.69	*pri-miR398b*	0.92 ± 0.21	11.75 ± 2.25
Genes encoding copper transporters				
1.00 ± 0.08	**2.58 ± 0.98**	*COPT2*	**3.16 ± 0.37 ***	**7.09 ± 0.48 ***
1.00 ± 0.10	1.28 ± 0.27	*COPT5*	0.74 ± 0.06	1.09 ± 0.05
Genes encoding metallothioneins				
1.00 ± 0.21	**1.81 ± 0.13**	*MT1a*	**5.46 ± 0.82 ***	**9.94 ± 2.87 ***
1.00 ± 0.02	**1.38 ± 0.01**	*MT1c*	**2.13 ± 0.24 ***	**2.36 ± 0.30 ***
1.00 ± 0.08	1.65 ± 0.32	*MT2a*	1.01 ± 0.07	1.37 ± 0.19
Gene encoding protein kinase				
1.00 ± 0.22	1.41 ± 0.35	*MPK3*	**0.53 ± 0.02 ***	0.75 ± 0.10
Gene encoding transcription factor				
1.00 ± 0.25	1.94 ± 0.62	*WRKY33*	0.55 ± 0.04	1.48 ± 0.21
Gene encoding protein involved in ethylene signaling				
1.00 ± 0.13	**4.38 ± 1.03**	*ERF1*	**0.49 ± 0.05 ***	**1.68 ± 0.19 ***

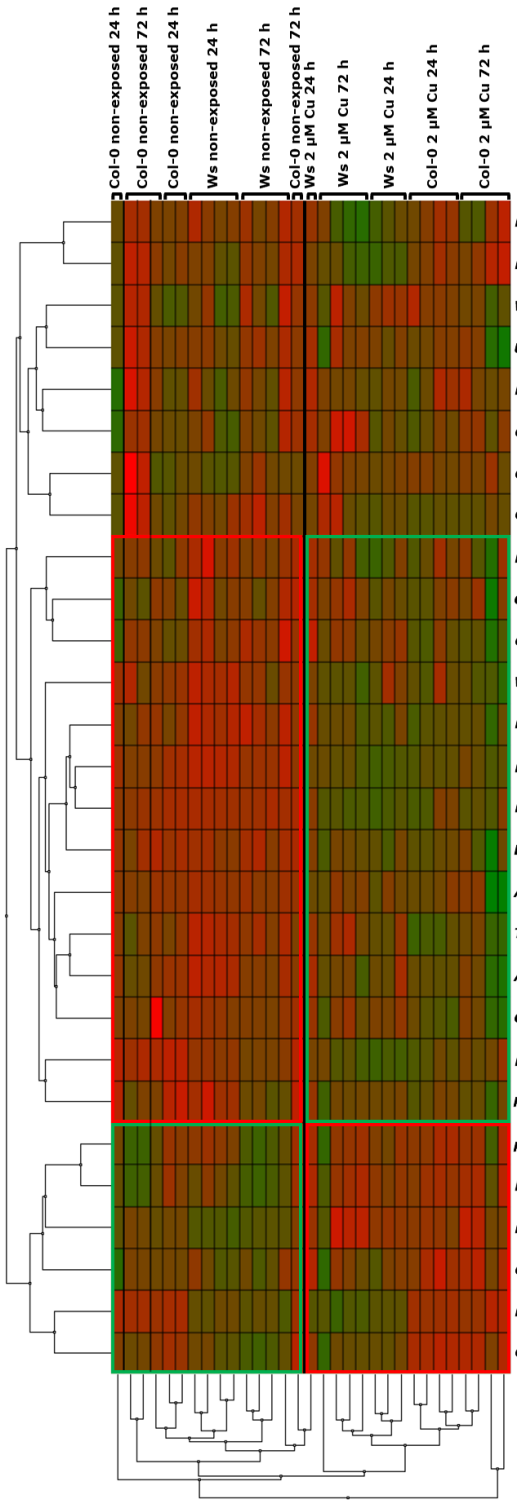

Figure 5.4 – Heat map representation of gene expression data obtained in leaves of three-week-old *A. thaliana* plants (accessions Col-0 and Ws) exposed to 2 µM $CuSO_4$ or not exposed for 24 and 72 h. Hierarchical clustering of genes is shown at the top (gene names at the bottom); genotype clustering is displayed on the left (conditions at the right). Green-shaded rectangles indicate increased, while red-shaded rectangles indicate decreased gene expression. Abbreviations: See Figure 5.3.

Table 5.4 – Relative gene expression levels in leaves of three-week-old *A. thaliana* plants (accessions Col-0 and Ws) exposed to 2 µM $CuSO_4$ for 24 and 72 h. Values are the mean normalized expression relative to the non-exposed accession at each time point (set at 1.00) ± S.E. of at least three biological replicates, each containing rosettes of at least one individual plant. Resolution values are mean inverse normalization factors relative to the non-exposed accession at each time point, indicating the stability of the selected reference genes. Statistically significant (P<0.05) metal-induced changes in expression relative to the non-exposed accession at each time point are indicated by color (■ = upregulation; ■ = downregulation). Statistically significant (P<0.05) differences between accessions and within metal exposure are indicated by asterisks and printed in black and bold. Abbreviations: see Figure 5.3.

Col-0		**2 µM Cu**	**Ws**	
24 h	**72 h**		**24 h**	**72 h**
1.49 ± 0.35	0.95 ± 0.21	Resolution	1.40 ± 0.39	1.11 ± 0.29
Genes encoding oxidative stress hallmark proteins				
1.38 ± 0.09	3.98 ± 1.49	*UPOX*	1.06 ± 0.00	2.02 ± 0.64
5.31 ± 0.53	7.86 ± 5.90	*Defensin-like*	3.99 ± 0.90	4.03 ± 0.52
6.07 ± 1.14	3.90 ± 1.77	*AT1G19020*	5.29 ± 1.77	3.40 ± 1.10
2.94 ± 0.48	8.97 ± 4.54	*AT1G05340*	3.95 ± 0.88	1.98 ± 0.24
16.6 ± 3.71	4.35 ± 2.04	*TIR-class*	16.03 ± 6.58	2.92 ± 1.27
Genes encoding ROS-producing enzymes				
1.42 ± 0.06	1.29 ± 0.23	*LOX1*	2.22 ± 0.24	1.41 ± 0.30
9.89 ± 0.45	2.70 ± 0.60	*LOX2*	5.33 ± 0.65	2.44 ± 0.55
Genes encoding antioxidative enzymes				
1.32 ± 0.10	**1.06 ± 0.05**	*GSH1*	1.24 ± 0.05	**0.80 ± 0.05 ***
1.39 ± 0.12	1.65 ± 0.11	*GSH2*	1.37 ± 0.06	1.62 ± 0.11
1.73 ± 0.18	2.28 ± 0.35	*CSD1*	2.34 ± 0.21	1.81 ± 0.60
0.96 ± 0.19	1.37 ± 0.05	*CSD2*	0.88 ± 0.09	1.04 ± 0.03
0.36 ± 0.07	0.07 ± 0.06	*FSD1*	0.21 ± 0.07	0.17 ± 0.15
Primary microRNA transcripts				
85.67 ± 23.78	5.40 ± 3.50	*pri-miR398a*	**12.1 ± 2.84 ***	1.82 ± 1.15
0.68 ± 0.13	0.25 ± 0.21	*pri-miR398b*	1.48 ± 0.50	0.08 ± 0.02
Genes encoding copper transporters				
0.90 ± 0.06	0.73 ± 0.05	*COPT1*	1.15 ± 0.08	1.13 ± 0.07
0.90 ± 0.01	0.32 ± 0.03	*COPT2*	1.04 ± 0.11	0.66 ± 0.02
1.38 ± 0.13	1.11 ± 0.19	*COPT5*	1.77 ± 0.08	1.08 ± 0.11

Table 5.4 – Relative gene expression levels in leaves of three-week-old *A. thaliana* plants (accessions Col-0 and Ws) exposed to 2 µM $CuSO_4$ for 24 and 72 h. Continuation.

Col-0		2 µM Cu	Ws	
24 h	**72 h**		**24 h**	**72 h**
1.49 ± 0.35	0.95 ± 0.21	Resolution	1.40 ± 0.39	1.11 ± 0.29
Genes encoding metallothioneins				
1.91 ± 0.27	0.93 ± 0.26	*MT1a*	1.55 ± 0.03	1.67 ± 0.46
0.70 ± 0.14	0.45 ± 0.15	*MT1c*	0.25 ± 0.03	0.09 ± 0.01
3.56 ± 0.43	2.19 ± 0.37	*MT2a*	4.14 ± 0.45	3.7 ± 0.36
1.22 ± 0.08	1.17 ± 0.29	*MT2b*	**1.76 ± 0.07 ***	2.00 ± 0.25
1.23 ± 0.06	1.41 ± 0.41	*MT3*	**1.93 ± 0.12 ***	2.79 ± 0.05
Genes encoding protein kinases				
10.65 ± 3.20	12.83 ± 6.78	*OXI1*	2.22 ± 0.42	3.12 ± 1.54
2.77 ± 0.23	1.68 ± 0.18	*MPK3*	3.92 ± 0.58	3.37 ± 0.46
1.07 ± 0.04	1.24 ± 0.07	*MPK6*	1.26 ± 0.04	1.18 ± 0.13
Genes encoding transcription factors				
0.60 ± 0.14	2.12 ± 0.25	*WRKY29*	0.64 ± 0.13	1.28 ± 0.25
4.14 ± 1.21	4.32 ± 1.08	*WRKY33*	5.48 ± 1.62	3.10 ± 0.54
Gene encoding protein involved in ethylene signaling				
24.71 ± 2.85	**4.76 ± 1.20**	*ERF1*	**86.51 ± 20.55 ***	**18.85 ± 5.43 ***

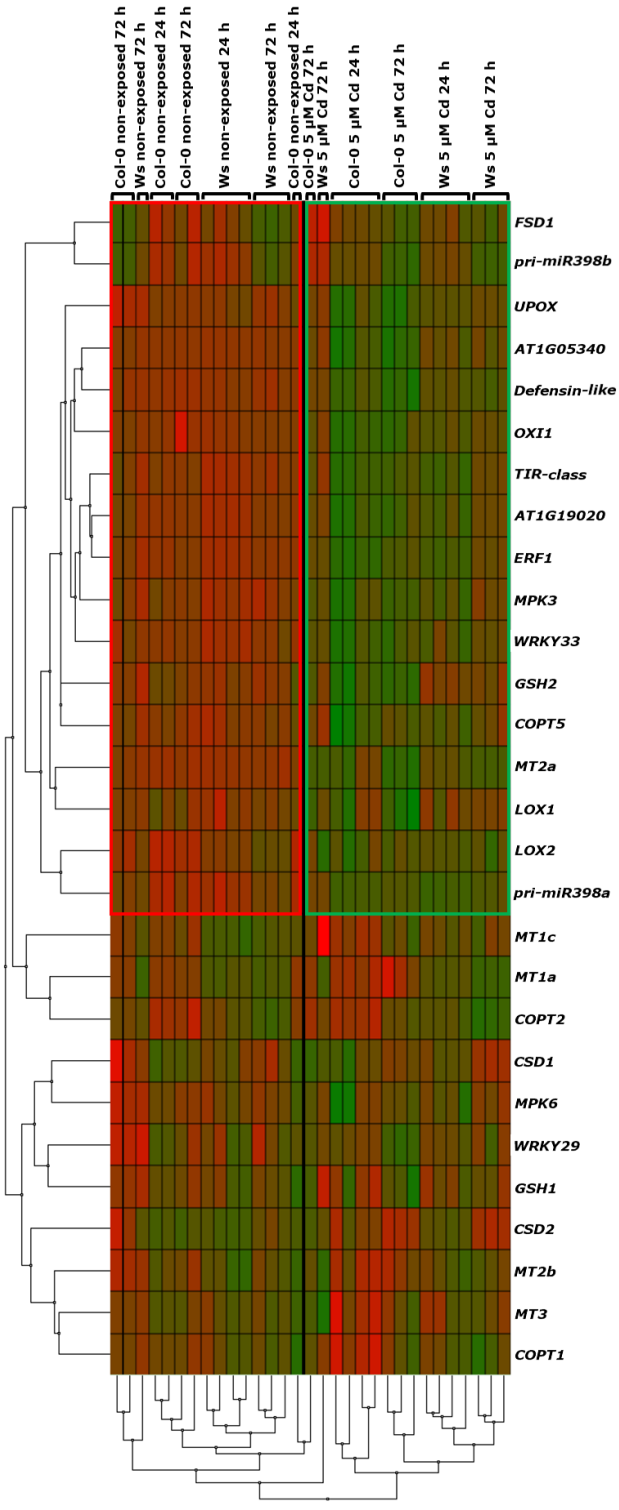

Figure 5.5 – Heat map representation of gene expression data obtained in leaves of three-week-old *A. thaliana* plants (accessions Col-0 and Ws) exposed to 5 µM $CdSO_4$ or not exposed for 24 and 72 h. Hierarchical clustering of genes is shown at the top (gene names at the bottom); genotype clustering is displayed on the left (conditions at the right). Green-shaded rectangles indicate increased, while red-shaded rectangles indicate decreased gene expression. Abbreviations: See Figure 5.3.

Table 5.5 – Relative gene expression levels in leaves of three-week-old *A. thaliana* plants (accessions Col-0 and Ws) exposed to 5 µM $CdSO_4$ for 24 and 72 h. Values are the mean normalized expression relative to the non-exposed accession at each time point (set at 1.00) ± S.E. of at least three biological replicates, each containing rosettes of at least one individual plant. Resolution values are mean inverse normalization factors relative to the non-exposed accession at each time point, indicating the stability of the selected reference genes. Statistically significant (P<0.05) metal-induced changes in expression relative to the non-exposed accession at each time point are indicated by color (= upregulation; = downregulation). Statistically significant (P<0.05) differences between accessions and within metal exposure are indicated by asterisks and printed in black and bold. Abbreviations: see Figure 5.3.

Col-0		5 µM Cd	Ws	
24 h	**72 h**		**24 h**	**72 h**
1.61 ± 0.22	0.74 ± 0.15	Resolution	1.07 ± 0.16	1.01 ± 0.16
Genes encoding oxidative stress hallmark proteins				
5.93 ± 1.16	6.27 ± 2.19	*UPOX*	2.21 ± 0.19	2.21 ± 0.32
27.80 ± 4.70	46.09 ± 17.38	*Defensin-like*	**6.81 ± 0.60 ***	8.93 ± 2.33
129.71 ± 43.01	9.28 ± 4.87	*AT1G19020*	56.87 ± 15.44	3.58 ± 0.06
77.41 ± 36.40	30.25 ± 15.94	*AT1G05340*	7.82 ± 2.30	4.14 ± 1.55
231.62 ± 80.13	9.90 ± 4.53	*TIR-class*	422.48 ± 106.43	8.84 ± 1.00
Genes encoding ROS-producing enzymes				
1.99 ± 0.37	1.90 ± 0.18	*LOX1*	1.27 ± 0.04	1.11 ± 0.11
9.42 ± 2.21	2.30 ± 0.50	*LOX2*	**2.24 ± 0.08 ***	1.95 ± 0.51
Genes encoding antioxidative enzymes				
1.19 ± 0.19	**1.27 ± 0.07**	*GSH1*	0.92 ± 0.05	**0.94 ± 0.09 ***
3.31 ± 0.35	2.05 ± 0.27	*GSH2*	1.25 ± 0.07	1.46 ± 0.10
1.40 ± 0.23	0.85 ± 0.02	*CSD1*	1.25 ± 0.14	0.67 ± 0.06
0.61 ± 0.17	0.22 ± 0.01	*CSD2*	0.80 ± 0.08	0.45 ± 0.22
4.83 ± 1.14	0.85 ± 0.15	*FSD1*	1.92 ± 0.60	0.55 ± 0.28
Primary microRNA transcripts				
2330.58 ± 267.36	13.67 ± 0.86	*pri-miR398a*	**831.04 ± 180.57 ***	5.22 ± 2.00
7.51 ± 0.39	1.72 ± 0.15	*pri-miR398b*	5.00 ± 0.48	2.05 ± 0.10
Genes encoding copper transporters				
0.88 ± 0.09	0.88 ± 0.02	*COPT1*	1.12 ± 0.08	1.16 ± 0.10
1.41 ± 0.19	1.15 ± 0.27	*COPT2*	1.47 ± 0.05	1.38 ± 0.30
5.40 ± 1.06	1.28 ± 0.10	*COPT5*	2.76 ± 0.17	1.24 ± 0.16

Table 5.5– Relative gene expression levels in leaves of three-week-old *A. thaliana* plants (accessions Col-0 and Ws) exposed to 5 µM $CdSO_4$ for 24 and 72 h. Continuation.

Col-0		5 µM Cd	Ws	
24 h	**72 h**		**24 h**	**72 h**
1.61 ± 0.22	0.74 ± 0.15	Resolution	1.07 ± 0.16	1.01 ± 0.16
Genes encoding metallothioneins				
1.07 ± 0.27	0.45 ± 0.16	*MT1a*	0.93 ± 0.11	1.22 ± 0.08
1.03 ± 0.06	1.70 ± 0.25	*MT1c*	0.65 ± 0.09	0.61 ± 0.22
3.30 ± 0.44	2.22 ± 0.22	*MT2a*	2.21 ± 0.06	2.63 ± 0.17
0.93 ± 0.09	0.88 ± 0.08	*MT2b*	0.94 ± 0.05	1.32 ± 0.21
0.74 ± 0.12	0.88 ± 0.07	*MT3*	0.94 ± 0.14	1.30 ± 0.34
Genes encoding protein kinases				
272.11 ± 75.02	62.59 ± 36.07	*OXI1*	**38.74 ± 1.32 ***	5.94 ± 1.96
5.83 ± 1.49	2.24 ± 0.34	*MPK3*	5.35 ± 0.61	2.34 ± 0.38
2.28 ± 0.51	1.40 ± 0.06	*MPK6*	1.48 ± 0.12	1.11 ± 0.09
Genes encoding transcription factors				
1.02 ± 0.07	2.80 ± 0.33	*WRKY29*	0.93 ± 0.03	1.53 ± 0.32
41.42 ± 13.28	7.69 ± 3.75	*WRKY33*	18.64 ± 5.94	2.82 ± 0.29
Gene encoding protein involved in ethylene signaling				
759.48 ± 165.90	13.11 ± 4.95	*ERF1*	289.41 ± 46.10	12.64 ± 2.50

5.3 Discussion

Arabidopsis thaliana is a well-established model plant with several resources and tools available for molecular and genetic studies. Natural phenotypic variation, manifested by different natural accessions, is one such important resource. Therefore, morphological and physiological differences among the most popular *Arabidopsis* accessions have been well described and, to a more limited extent, their genetic variability is studied (Alonso-Blanco *et al.*, 2016; Passardi *et al.*, 2007). In this study on accession-specific responses, morphological differences between both accessions were evident from leaf growth data of non-exposed plants (Figure 5.1). In addition to the biometrical parameters, genetic differences between the two accessions were highlighted in a heat map presenting gene expression data of non-exposed plants (Figure 5.3). Hierarchical clustering revealed two clusters of genes with differential expression patterns in leaves of Col-0 and Ws plants. The higher expressed genes in Col-0 as compared to Ws plants were hallmark genes for oxidative stress or associated to the MAPK and ethylene signaling pathways, while the lower expressed genes were related to Cu homeostasis (Figure 5.3, Table 5.3). These results suggest that Col-0 and Ws plants employ different life strategies. While Ws plants appear to constitutively invest in nutrient homeostasis, Col-0 plants invest more in detoxification responses, related to oxidative stress signaling and antioxidative defense mechanisms. In particular, the constitutively higher expressed Cu homeostasis-related genes in leaves of Ws plants (Figure 5.3) encode for proteins that are either involved in the mobilization or sequestration of Cu, such as *COPT2*, *MT1a* and *MT1c* (Table 5.3; Guo *et al.*, 2008; Sancenón *et al.*, 2003), or are part of the trademark strategy to redirect Cu, from dispensable to essential cupro-proteins, under Cu deficiency conditions, such as *FSD1*, *pri-miR398a*, and *pri-miR398b* (Gielen *et al.*, 2016; Yamasaki *et al.*, 2007, 2008, 2009). As nutrient homeostasis is important in metal sensitivity, this supports our results obtained in roots (Chapter 4) suggesting that Ws plants are less sensitive to excess Cu and Cd than Col-0 plants due their ability to better counteract alterations to Cu homeostasis, including a perceived Cd-induced Cu deficiency (Gielen *et al.*, 2016).

Exposure for 72 h, but not for 24 h, to Cd significantly inhibited rosette growth in both accessions. A similar response was observed for Ws plants after exposure to excess Cu (Figure 5.1). This delayed effect is not surprising since leaves are not in direct contact with the metals in the growth medium and, as such, metal-induced responses depend on root-to-shoot translocation of the metals and/or inter-organ signaling. Exposure to excess Cu, however, significantly inhibited rosette growth of Col-0 plants already after 24 h (Figure 5.1), coinciding with a significantly higher Cu concentration (Supplemental Table 5.1) and higher root-to-shoot Cu translocation factor at this time point (Figure 5.2A). These observations suggest that growth is more severely affected in Col-0 than Ws plants after exposure to excess Cu, agreeing with an enhanced constitutive Cu homeostasis in Ws plants (Figure 5.3 and Table 5.3). In addition to the COPT family members (Sancenón *et al.*, 2003), several other transporters are involved in plant nutrient distribution (Puig *et al*., 2007). Among these, HMA proteins are implicated in the transport of essential and non-essential heavy metals (Andrés-Colás *et al*., 2006; Hussain *et al*., 2004; Kobayashi *et al*., 2008; Morel *et al*., 2009; Park *et al*., 2012; Puig *et al*., 2007; Wong and Cobbett, 2009). In *Arabidopsis*, this P1B-ATPase family consists of eight members, divided into two groups according to metal-substrate specificity associated to the valence of the transported cations. Whereas HMA1-4 are transporters of the divalent cations Cd/zinc/cobalt/lead, HMA5-8 transport monovalent Cu or silver. Therefore, the mobilization of essential Cu in the plant does not involve the same HMA proteins as the mobilization of non-essential Cd. Furthermore, different HMA transporters have specific subcellular locations and functions. For example, the plasma membrane HMA5 protein is involved in Cu translocation from roots to shoots (Kobayashi *et al.*, 2008), and Cu compartmentalization and detoxification within roots (Andrés-Colás *et al.*, 2006). After studying 103 different accessions, Kobayashi *et al.* (2008) suggested that the variation in Cu tolerance observed in *A. thaliana* is partially regulated by the root-to-shoot Cu translocation capacity associated with the functional integrity of HMA5. However, the Ws accession was not included in that study and should be investigated in future research.

The root-to-shoot translocation factor of Cu significantly decreased in plants exposed to Cd (Figure 5.2A) as compared to those not exposed, pointing

towards a Cd-induced decreased ability to translocate Cu, which leads to Cd-induced Cu deficiency-like responses (Gayomba *et al.*, 2013; Gielen *et al.*, 2016, 2017). Nonetheless, at each time point, the Cu translocation factor was significantly higher in Cd-exposed Ws versus Col-0 plants (Figure 5.2A). Gielen *et al.* (2016) observed that Cd-induced Cu deficiency-like responses could be alleviated by supplying extra Cu to Cd-exposed *Arabidopsis* plants, resulting in a lower *HMA5* upregulation in Cu-supplemented plants as compared to non-supplemented plants (Gielen *et al.*, 2017). Therefore, the significantly lower *HMA5* upregulation in leaves of Cd-exposed Ws after 72 h (Supplemental Table 5.1) indicates that these Cu deficiency-like responses were less pronounced in Ws plants than in Col-0 plants. This again supports our statement that Cu homeostasis mechanisms are less disturbed in leaves of Cd-exposed Ws plants.

After 24 h of exposure, the root-to-shoot Cd translocation factor was significantly higher in Ws than in Col-0 plants (Figure 5.2B). Both HMA2 and HMA4 are known to mediate Cd translocation in *A. thaliana* (Wong and Cobbett, 2009), whereas HMA3 is involved in Cd sequestration in the vacuole (Morel *et al.*, 2009). In addition, it was shown that the *HMA3* gene bears a point mutation in the Col-0 accession, consequently encoding for a truncated protein differing from the protein in Ws plants (Hussain *et al.*, 2004; Morel *et al.*, 2009). Although an obvious candidate gene, Fischer *et al.* (2017) observed that *HMA3* is unlikely determining the variation in Cd tolerance observed in different *Arabidopsis* accessions. However, the Ws accession was not included in that study and therefore this difference in HMA3 function may still account for some of the differences in the Cd translocation factor observed between both these accessions (Figure 5.2B). Moreover, Park *et al.* (2012) hypothesized that the non-functional HMA3 results in a preference for the expression of *HMA4* over *HMA2* in Col-0 plants, suggesting that the cooperation between HMA3 and HMA4 is relevant for Cd detoxification. These authors also reported that whereas short-term exposure to Cd did not alter HMA4 expression in Ws plants, it induced *HMA4* overexpression in Col-0 plants (Park *et al.*, 2012). This can explain the time-associated alterations to the Cd concentrations in leaves of both accessions (Supplemental Table 5.1) and the apparent arrest in the Cd transport observed in Ws plants as indicated by the decreased translocation factor (Figure 5.2B). Since metal sequestration and transport are important mechanisms in metal

tolerance, future research on the root-to-shoot Cd translocation and *HMA2-4* expression patterns after long-term exposure to Cd are required to further elucidate how Col-0 and Ws plants cope with this toxic metal.

Exposure to excess Cu and Cd affected transcript levels of different genes in the leaves of both accessions as evidenced by their representation in heat maps (Figure 5.4 and 5.5). Regardless of the time point or accession, samples obtained from Cu- or Cd-exposed plants generally clustered away from samples of non-exposed plants, allowing the identification of genes affected by each metal. The heat map representation revealed that excess Cu affected genes involved in Cu homeostasis mechanisms (Figure 5.4). These mechanisms are known to be mediated by the central regulator *SQUAMOSA* PROMOTER-BINDING PROTEIN-LIKE 7 (SPL7) by way of its binding to GTAC motifs within the promoter regions of the target genes (Gayomba *et al.*, 2013; Gielen *et al.*, 2016; Yamasaki *et al.*, 2009). Although more research is needed, Dąbrowska *et al.* (2012) identified GTAC motif-containing Cu response elements located in the promoter regions of *A. thaliana MT1a* and *MT1c* genes, suggesting that these cysteine-rich proteins are also targeted by the SPL7 transcription factor (Yamasaki *et al.*, 2009). Therefore, the significant downregulation of *MT1c* after 24 h and 72 h of exposure and the upregulation of *MT2b* and *MT3* after 72 h suggest yet again that Ws plants are more efficient at counteracting the altered Cu homeostasis. The same heat map revealed another gene cluster including oxidative stress and MAPK/ethylene signaling-related genes, with a higher expression after exposure to excess Cu than under non-exposed conditions (Figure 5.4). In particular, excess Cu appeared to induce different signaling mechanisms in leaves of Col-0 and Ws plants (Table 5.4). The upregulation of *OXI1* and *MPK3* suggests that MAPK signaling pathways were activated in leaves of Cu-exposed Col-0 plants. The OXI1 kinase is essential to ROS sensing and MAPK signaling (Rentel *et al.*, 2004), linking oxidative burst signals to downstream responses such as the activation of detoxification mechanisms following Cu exposure (Smeets *et al.*, 2013). On the other hand, the upregulation of *MPK3*, *WRKY33,* and *ERF1* indicates that excess Cu stimulated ethylene signaling in leaves of Ws plants (Table 5.4). The phytohormone ethylene regulates several developmental and physiological processes such as seed germination, growth, flowering, and senescence (Iqbal *et al.*, 2017).

Ethylene is also a known "stress hormone", modulating hormone and redox signaling processes under several biotic and abiotic stress conditions, including metal stress (Keunen *et al*., 2016b; Schellingen *et al*., 2015a, 2015b), via a signaling cascade that, among others, induces the expression of *ERF1* (Huang *et al.*, 2016). Both MPK3 and MPK6 are known to play a role in controlling the rate-limiting step in ethylene biosynthesis via the transcription factor WRKY33 (Li *et al.*, 2012). Although ethylene signaling is clearly favored in Cu-exposed Ws plants, the upregulation of *ERF1* in combination with the upregulation of *OXI1* suggests that these two signaling-related molecules interact in leaves of Col-0 plants in response to excess Cu. This interaction needs to be further investigated to not only clarify the crosstalk between ethylene and ROS signaling, but also to explore the activation of these signaling pathways in both accessions, particularly their time-related patterns.

Exposure to Cd increased the transcript levels of oxidative stress hallmark genes (Gadjev *et al.*, 2006), LOX genes, and genes related to MAPK/ethylene signaling compared to non-exposed plants (Figure 5.5). The overall higher upregulation of the oxidative stress hallmark genes and the expression patterns of *LOX1* and *LOX2* in leaves of Cd-exposed Col-0 plants (Table 5.5) suggest that these plants respond more strongly to Cd-induced oxidative stress than Ws plants. The observed alterations in the GSH metabolism in leaves of Cd-exposed Col-0 plants, such as the significant upregulation of *GSH2* (Table 5.5) and the increased GSH concentration (Table 5.2), point towards the activation of detoxification mechanisms, by means of phytochelatin production, to counteract the more severe Cd-induced oxidative stress response (Table 5.5). This is in agreement with the proposed strategy favored by Col-0 plants. Several studies suggest an association between GSH metabolism and ethylene signaling in metal stress conditions (Keunen *et al*., 2016b; Schellingen *et al*., 2015a, 2015b), which appears to be supported by the concurrent induction of both processes in the leaves of Cd-exposed Col-0 plants (Table 5.5). Recently, Schellingen *et al*. (2015b) proposed a model linking ethylene biosynthesis, signal transduction and oxidative stress in leaves of Cd-exposed *A. thaliana* leaves. In this model, it is hypothesized that Cd induces an oxidative burst that leads to ethylene signaling via a MAPK cascade initiated by OXI1. In turn, the ethylene signal cascade induces the expression of downstream transcription factors such as *ERF1*. The

expression of *ERF1* is known to increase in response to ethylene signaling during Cd exposure (Schellingen *et al*., 2015a, 2015b). Moreover, Schellingen *et al.* (2015a) also described ethylene to be involved in regulating GSH levels during the early Cd-induced oxidative challenge. Indeed, several MAPK/ethylene signaling-related genes were upregulated in leaves of Cd-exposed Col-0 plants, particularly after 24 h (Table 5.5), suggesting a stronger ethylene signaling response in Col-0 than in Ws plants, which in turn might have determined the GSH metabolism response observed in leaves of Col-0 plants (Table 5.2 and 5.5).

In conclusion, our results suggest that Col-0 and Ws plants developed different life strategies. While Ws plants have enhanced nutrient homeostatic capacities, particularly related to Cu homeostasis mechanisms, Col-0 plants have boosted oxidative stress-related responses, mainly related to MAPK/ethylene signaling and GSH detoxification mechanisms. This is evident not only under non-exposed conditions, but also determines how both accessions respond to excess Cu and Cd.

Supplemental Table 5.1 – Concentrations of Cu and Cd (mg kg^{-1} dry weight) in leaves of three-week-old *A. thaliana* plants (accessions Col-0 and Ws) exposed to 2 µM $CuSO_4$, 5 µM $CdSO_4$, or not exposed for 24 and 72 h. Values are the mean ± S.E. of at least three biological replicates, each containing rosettes of 25 individual plants. Statistical significance ($P<0.05$) is indicated using lowercase letters (for differences within accession and time point), uppercase letters (between non-exposed Col-0 and Ws) or dagger signs (†, for Cd exposure).

	Time	Col-0			Ws		
		non-exposed	2 µM Cu	5 µM Cd	non-exposed	2 µM Cu	5 µM Cd
Cu	24 h	10.75 ± 0.40 a, A	18.58 ± 0.27 b	11.39 ± 0.70 a	9.62 ± 0.52 a, AB	9.89 ± 0.30 a	9.29 ± 0.07 a
	72 h	9.57 ± 0.44 a, AB	11.87 ± 0.46 a	9.68 ± 0.98 a	8.20 ± 0.61 a, B	7.27 ± 0.20 a	7.39 ± 0.18 a
Cd	24 h	–	–	686.57 ± 39.82 †	–	–	1281.59 ± 42.83 ††
	72 h	–	–	1309.36 ± 68.96 ††	–	–	1489.77 ± 80.86 ††

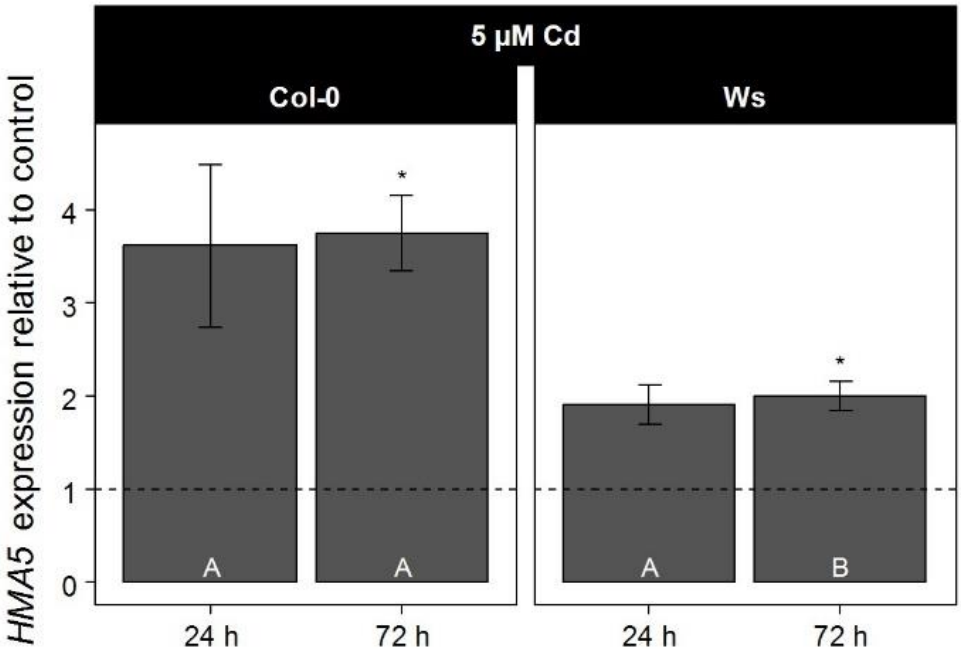

Supplemental Figure 5.1 – *HMA5* expression in leaves of three-week-old *A. thaliana* plants (accessions Col-0 and Ws) exposed to 5 µM $CdSO_4$ for 24 and 72 h. Values are the mean normalized expression relative to the non-exposed at each time point (set at 1.00, indicated by the dotted line) ± S.E. of at least three biological replicates, each containing rosettes of at least one individual plant. Statistical significance ($P<0.05$) is indicated using asterisks (relative to the non-exposed accession at each time point) or uppercase letters (across accessions, within time point).

Supplemental Table 5.2 – List of primers used in quantitative real-time PCR. E-E-jn: Exon-Exon-junction. UTR: Untranslated region.

Locus	Annotation	Forward primer (5′ – 3′)	Reverse primer (5′ – 3′)	Exon location	Amplicon length (bp)	Primer Efficiency	
Reference genes							
AT2G28390	*SAND family*	AACTCTATGCAGCATTTGATCCACT	TGATTGCATATCTTTATCGCCATC	Exon 13	61	Col-0	100.95 %
						Ws	99.73 %
AT3G18780	*ACT2*	CTTGCACCAAGCAGCATGAA	CCGATCCAGACACTGTACTTCCTT	Exon 2	68	Col-0	96.05 %
						Ws	97.33 %
AT4G05320	*UBQ10*	GGCCTTGTATAATCCCTGATGAATAAG	AAAGAGATAACAGGAACGGAAACATAGT	3′ UTR	61	Col-0	103.37 %
						Ws	103.14 %
AT5G15710	*F-box protein*	TTTCGGCTGAGAGGTTCGAGT	GATTCCAAGACGTAAAGCAGATCAA	Exon 1	63	Col-0	99.48 %
						Ws	91.03 %
AT5G60390	*EF1A*	TGAGCACGCTCTTCTTGCTTTCA	GGTGGTGGCATCCATCTTGTTACA	E1-E2-jn	76	Col-0	97.49 %
						Ws	101.62 %
Genes encoding oxidative stress hallmark proteins							
AT1G05340	Unknown	TCGGTAGCTCAGGGTAAAGTGG	CCAGGGCACAACAGCAACA	E2-E3-jn	91	Col-0	96.63 %
						Ws	101.14 %
AT1G19020	Unknown	GAAAATGGGACAAGGGTTAGACAAA	CCCAACGAAAACCAATAGCAGA	Exon 1	92	Col-0	96.35 %
						Ws	100.40 %
AT1G57630	*TIR-class*	ACTCAAACAGGCGATCAAAGGA	CACCAATTCGTCAAGACAACACC	Exon 1	91	Col-0	95.60 %
						Ws	102.66 %
AT2G21640	*UPOX*	GACTTGTTTCAAAAACACCATGGAC	CACTTCCTTAGCCTCAATTTGCTTC	E1-E2-jn	91	Col-0	94.41 %
						Ws	102.10 %
AT2G43510	*Defensin-like*	ATGGCAAAGGCTATCGTTTCC	CGTTACCTTGCGCTTCTATCTCC	E1-E2-jn	91	Col-0	95.19 %
						Ws	98.75 %

Supplemental Table 5.2 – List of primers used in quantitative real-time PCR. Continuation.

Locus	Annotation	Forward primer (5′ – 3′)	Reverse primer (5′ – 3′)	Exon location	Amplicon length (bp)	Primer Efficiency	
Genes encoding ROS-producing enzymes							
AT1G55020	*LOX1*	TTGGCTAAGGCTTTTGTCGG	GTGGCAATCACAAACGGTTC	Exon 6	101	Col-0	93.40 %
						Ws	95.17 %
AT3G45140	*LOX2*	TTTGCTCGCCAGACACTTG	GGGATCACCATAAACGGCC	E3-E4-jn	102	Col-0	91.07 %
						Ws	95.51 %
Genes encoding antioxidative enzymes							
AT4G23100	*GSH1*	CCCTGGTGAACTGCCTTCA	CATCAGCACCTCTCATCTCCA	Exon 5	101	Col-0	81.01 %
						Ws	101.29 %
AT5G27380	*GSH2*	GGACTCGTCGTTGGTGACAA	TCTGGGAATGCAGTTGGTAGC	Exon 11	101	Col-0	95.30 %
						Ws	98.02 %
AT1G08830	*CSD1*	TCCATGCAGACCCTGATGAC	CCTGGAGACCAATGATGCC	Exon 5	102	Col-0	95.03%
						Ws	96.55 %
AT2G28190	*CSD2*	GAGCCTTTGTGGTTCACGAG	CACACCACATGCCAATCTCC	Exon 6	101	Col-0	98.37 %
						Ws	105.29 %
AT4G25100	*FSD1*	CTCCCAATGCTGTGAATCCC	TGGTCTTCGGTTCTGGAAGTC	Exon 4	101	Col-0	94.81 %
						Ws	94.90 %
Primary microRNA transcripts							
AT2G03445	*pri-miRNA398a*	AGAAGAAGAGAAGAACAACAGGAGGTG	ATTAGTAAGGTGAAAAAATGG		156	Col-0	88.14 %
						Ws	102.96 %
AT5G14545	*pri-miRNA398b*	AGTAATCAACGGCTGTAATGACGCTAC	TGACCTGAGAACACATGAAAACGAGAG		67	Col-0	90.36 %
						Ws	83.82 %

Supplemental Table 5.2 – List of primers used in quantitative real-time PCR. Continuation.

Locus	Annotation	Forward primer (5′ – 3′)	Reverse primer (5′ – 3′)	Exon location	Amplicon length (bp)	Primer Efficiency	
Gene encoding heavy metal ATPase transporter							
AT1G63440	*HMA5*	CAGAAGTTGGCTGATCGGATTT	TCCCAGCTAAGAACCAGGCAA	E2-E3-jn	91	Col-0	84.95 %
						Ws	115.02 %
Genes encoding copper transporters							
AT5G59030	*COPT1*	GTTAATCCAAACCGCCGTGTATAC	GAGAAACACACCGGCGTTAAAC	Exon 1	91	Col-0	93.79 %
						Ws	95.56 %
AT3G46900	*COPT2*	TCCGGCATGTACGCTCTCTG	CACTGACACGTAGGATCGGTGAA	Exon 1	91	Col-0	99.23 %
						Ws	99.54 %
AT5G20650	*COPT5*	ACCAAACCTCTTCCCAATCC	TGGCTTTGATTCCCCAGTAG	Exon 1	113	Col-0	107.90 %
						Ws	94.60 %
Genes encoding metallothioneins							
AT1G07600	*MT1a* *	AACTGTGGATGTGGCTCCTC	CAGTTACAGTTTGACCCACAGC	Exon 1	122	Col-0	104.91 %
						Ws	112.02%
AT1G07590	TPR-like *	AGAGCTAGCGAGAACGTGGA	CCTACTCGAGCAAACGCTTC	Exon 4	93	Col-0	87.88 %
						Ws	90.37 %
AT1G07610	*MT1c*	GCATGGTCTCAAACCAAGGA	TACGCAACACAATGCCAAGT	Intron 2	96	Col-0	95.44 %
						Ws	96.09 %
AT3G09390	*MT2a*	ACCCTGACTTGGGATTCTCC	GCGTTGTTACTCTCCCCTGA	Exon 1	109	Col-0	97.01 %
						Ws	97.48 %
AT5G02380	*MT2b*	ACTCTTGTCCTCGGTGTTGC	TTGCACTTGCAGTCAGATCC	Exon 1	110	Col-0	87.74 %
						Ws	100.66 %
AT3G15353	*MT3*	TCGACATCGTCGAGACTCAG	CACTTGCAATTTGCGTTGTT	E2-E3-jn	85	Col-0	94.71 %
						Ws	97.63 %

Supplemental Table 5.2 – List of primers used in quantitative real-time PCR. Continuation.

Locus	Annotation	Forward primer (5′ – 3′)	Reverse primer (5′ – 3′)	Exon location	Amplicon length (bp)	Primer Efficiency	
Genes encoding protein kinases							
AT3G25250	*OXI1*	TAGAGGATCGAACCGGAAAG	GACCCTTGATTTCCTCAACG	Exon 2	149	Col-0	95.76 %
		TTCAATCGACTCGAGGTTTTG	AGCAAGCAATTTAGCGTCGT	Exon 1	90	Ws	100.35 %
AT3G45640	*MPK3*	GACGTTTGACCCCAACAGAA	TGGCTTTTGACAGATTGGCTC	E5-E6-jn	103	Col-0	95.50 %
						Ws	97.04 %
AT2G43790	*MPK6*	TAAGTTCCCGACAGTGCATCC	GATGGGCCAATGCGTCTAA	E5-E6-jn	100	Col-0	94.05 %
						Ws	100.87 %
Genes encoding transcription factors							
AT4G23550	*WRKY29*	CATGGGCGTGGCGTAAATA	TTGTTTTCTTGCCAAACACCC	E2-E3-jn	104	Col-0	103.48 %
						Ws	94.72 %
AT2G38470	*WRKY33*	TCATCGATTGTCAGCAGAGACG	CCATTCCCACCATTTGTTTCAT	E3-E4-jn	92	Col-0	95.78 %
						Ws	102.46 %
Gene encoding protein involved in ethylene signaling							
AT3G23240	*ERF1*	TCCTCGGCGATTCTCAATTTT	CAACCGGAGAACAACCATCCT	Exon 1	91	Col-0	98.47 %
						Ws	98.59 %

* Since *AT1G07590* overlaps the *MT1a* completely, *AT1G07590*-specific primers were also developed to correct for its contribution to *MT1a* gene expression.

Supplemental Table 5.3 – Quantitative real-time PCR parameters according to the "Minimum Information for publication of Quantitative real-time PCR Experiments" (MIQE) guidelines derived from Bustin *et al.* (2009).

Sample/Template	
Source	Rosettes of *Arabidopsis thaliana* plants cultivated in hydroponics
Method of preservation	Liquid nitrogen
Storage time	Six weeks at - 70 °C
Handling	Frozen
Extraction method	Phenol-free Total RNA isolation: Ambion™ RNAqueous® Total RNA Isolation Kit * (Thermo Fisher Scientific, Inc., Massachusetts, USA)
RNA: DNA-free	TURBO DNA-*free*™ Kit * (Thermo Fisher Scientific, Inc., Massachusetts, USA) Design of intron-spanning primers whenever possible
Concentration	NanoDrop®: ND-1000 Spectrophotometer (Thermo Fisher Scientific, Inc., Massachusetts, USA)
Assay optimization and validation	
Accession number	Supplemental Table 5.2
Amplicon details	Exon location and amplicon size: Supplemental Table 5.2
Primer sequences	Supplemental Table 5.2
In silico	Primers were blasted using the BLAST tool at http://arabidopsis.org/
Empirical	Primer concentration: 300 nM (600 nM for *ERF1* measurements) Annealing temperature: 60°C
Priming conditions	Combination of oligo(dT)-primers and random hexamers
PCR efficiency	Dilution series (slope, y-intercept and r^2; Supplemental Table 5.2)
Linear dynamic range	Samples are situated within the range of the efficiency curve
Reverse transcription – PCR	
Protocols	As stated in the Materials and Methods (Section 3.8)
Reagents	As stated in the Materials and Methods (Section 3.8)
No template control (NTC)	Cq and dissociation curve verification
Data analysis	
Specialist software	7500 Fast Real-Time PCR System (Applied Biosystems, Life Technologies, Belgium) Software v2.0.1
Statistical justification	At least three biological replicates Elimination of outliers after statistical validation using the Grubbs' test at significance level 0.05 (R version 3.3.1, package "outliers") Log transformation of the data Two-way ANOVA and the Tukey-Kramer post-hoc test to correct for multiple comparisons using R version 3.3.1
Normalization	Three stable reference genes selected using the GrayNorm algorithm (Remans *et al.*, 2014): *AT2G28390*, *AT4G05320* and *AT5G15710*

* All procedures were performed according to the manufacturer's protocols.

CHAPTER 6

The OXI1 kinase is functionally relevant in the initial response phase to excess Cu in *Arabidopsis thaliana* plants

In preparation.

Keywords: *Arabidopsis thaliana*, Columbia, OXI1, knockout mutant, copper, copper homeostasis.

Abstract

Copper (Cu) is a redox-active metal essential to normal plant growth and development which directly induces oxidative stress when present in excessive bioavailable concentrations. Under normal physiological conditions, reactive oxygen species (ROS) act as signaling molecules, activating diverse signal transduction pathways. The OXIDATIVE SIGNAL-INDUCIBLE KINASE 1 (OXI1) protein kinase is essential to oxidative burst-mediated signaling pathways in *Arabidopsis thaliana*. Since excess Cu induces ROS production, we investigated Cu-induced responses in wild-type (WT) and *oxi1* knockout *A. thaliana* (accession Columbia, Col-0) plants exposed to excess Cu for a maximum of 72 h to explore its role in Cu-induced oxidative stress responses.

Diminished growth inhibition and increased antioxidant and NAD(P)H-producing enzyme activities, together with lower levels of lipid peroxidation (in roots) and ROS (in leaves) suggest that, within the experimental timeframe, Col-0 *oxi1* mutants are less sensitive to Cu-induced oxidative stress than WT plants. In addition, our results establish OXI1 as functionally relevant in the initial phase of responses after exposure to excess Cu via ROS and in relation to phytohormone signaling. The interchanged expression of the ethylene/jasmonic acid-responsive genes ERF1 and PDF1.2 in leaves of Cu-exposed *oxi1* mutants as compared to WT plants indicates that crosstalk between and circumvention by different signaling pathways is omnipresent, and that OXI1 is involved in Cu-induced phytohormone signaling in WT plants.

6.1 Introduction

Copper (Cu) is a redox-active metal essential to normal plant growth and development as a cofactor to diverse metalloproteins and enzymes such as plastocyanin (Yruela, 2005, 2009). While its deficiency leads to inhibition of photosynthetic reactions and severely limits other metabolic processes, exposure to excess of this micronutrient can inhibit plant growth and interfere with diverse physiological responses (Cuypers *et al*., 2011; Drążkiewicz *et al*., 2004; Lequeux *et al*., 2010; Yruela, 2005). In fact, the ability to exist in different oxidation states under normal physiological conditions, which underlies the essential role of Cu in plants, is also a determinant to its phytotoxicity when present in excess. By participating in Fenton and Haber-Weiss reactions, Cu catalyzes the formation of reactive oxygen species (ROS) and directly induces oxidative stress (Drążkiewicz *et al*., 2004). In combination with a Cu-mediated inhibition of antioxidant defense mechanisms, this Cu-induced increase in ROS production causes an oxidative imbalance that, via signaling pathways, leads to both defense responses and/or more oxidative damage (Cuypers *et al*., 2012; Mittler *et al*., 2004).

Under normal physiological conditions, ROS are natural by-products of metabolic processes such as photosynthesis and respiration, and their levels are tightly controlled and maintained by a complex molecular network of genes encoding for ROS-producing and ROS-scavenging proteins (Harir and Mittler, 2009; Mittler *et al*., 2004). The resulting ROS balance allowed these molecules to evolve into key regulators of plant growth and development, adaptation, and responses to environmental stimuli as well as programmed cell death (Bailey-Serres and Mittler, 2006; Harir and Mittler, 2009; Mittler *et al*., 2004, 2011). As signaling molecules, ROS modulate the activities of downstream components of the signal transduction pathway, generally by the activation of mitogen-activated protein kinase (MAPK) cascades (Jalmi and Sinha, 2015; Smékalová *et al*., 2014). Also important in the transduction of second messenger and hormone signals, MAPK phosphorylation cascades are highly conserved signaling modules consisting minimally of a MAPK kinase kinase (MAPKKK/MEKK), a MAPK kinase (MAPKK/MKK), and a MAPK (Keunen *et al*., 2016b; Nakagami *et al*., 2005; Opdenakker *et al*., 2012b; Pitzschke *et al*., 2009; Schellingen *et al*., 2015b;

Smékalová *et al*., 2014). For example, Rentel *et al*. (2004) observed the direct induction of the activity of a serine/threonine MAPKKK, OXIDATIVE SIGNAL-INDUCIBLE KINASE 1 (OXI1), by H_2O_2, which in turn activated a signaling cascade involving the MAPKs MPK3 and MPK6 and ultimately resulted into pathogen resistance and root hair growth responses. Interestingly, these authors hypothesized that the activation of OXI1 is essential to the oxidative burst-mediated signaling pathway in *A. thaliana* (Rentel *et al*., 2004). Since excess Cu induces ROS production, several authors have investigated the activation of OXI1 and MAPK signaling cascades in Cu-exposed plants. Opdenakker *et al*. (2012a) observed an early, time-dependent induction of *OXI1* and *MPK3* expression in *A. thaliana* (accession Columbia, Col-0) exposed to sublethal Cu concentrations. After exposing *A. thaliana oxi1* knockout plants (accession Wassilewskija) to excess Cu, Smeets *et al*. (2013) proposed H_2O_2, lipoxygenases (LOXes), and miRNA398 as downstream targets of OXI1 under Cu stress. These authors also suggested an essential role for OXI1 in Cu-induced responses in roots, hypothesizing that it regulates downstream transcription factors such as WRKY25 via the MEKK1-MKK2 cascade (Smeets *et al*., 2013). Nonetheless, further investigation is required to identify more downstream targets of OXI1 and fully understand Cu-induced OXI1-mediated responses.

In this study, we investigated Cu-induced responses in *A. thaliana* plants (accession Col-0) to identify possible new targets and functions for OXI1 in Cu-induced oxidative stress conditions. To this purpose, growth, metal translocation, and metabolic and transcriptomic responses were determined in wild-type (WT) and *oxi1* plants exposed to excess Cu (2 µM) for a maximum of 72 h.

6.2 Results

6.2.1 Plant growth

Hydroponically grown three-week-old *A. thaliana* WT and *oxi1* knockout plants (accession Columbia, Col-0) were exposed to an excess sublethal Cu concentration (2 µM). Roots and rosettes were sampled 24 and 72 h after the start of metal exposure to evaluate plant growth after one circadian cycle or a more prolonged exposure to excess Cu.

In non-exposed conditions, *oxi1* mutants were significantly larger than WT plants at each time point. As indicated by a decreased fresh weight, excess Cu inhibited root and rosette growth in plants of both genotypes (Figure 6.1). In spite of the observed differences between root and rosette fresh weight in non-exposed WT and *oxi1* plants, only rosette fresh weight remained significantly higher in *oxi1* plants than in WT plants after exposure to Cu for 24 h. To further assess the effects of 2 µM Cu on plant growth, the inhibition of growth relative to non-exposed plants was calculated $[(1-\frac{\text{weight Cu-exposed}}{\text{average weight non-exposed}}) \times 100]$ and expressed as percentages (Table 6.1) at each time point. Exposure to excess Cu inhibited root growth (60-85 %) more than rosette growth (5-40 %). Comparing both genotypes, the percentage of rosette growth inhibition was significantly lower in *oxi1* plants than in the wild types only after short-term Cu exposure (24 h).

6.2.2 Copper concentrations and translocation factors

Concentrations of Cu were determined in roots and leaves of non-exposed and Cu-exposed Col-0 WT and *oxi1* knockout plants to evaluate Cu uptake (Table 6.2). Exposure to excess Cu resulted in significantly higher root Cu concentrations in both genotypes. In particular, higher Cu concentrations were observed in roots of WT as compared to *oxi1* mutant plants after exposure to Cu for 24 and 72 h (Table 6.2). Exposure to excess Cu for 24 h also resulted in increased leaf Cu concentrations, with leaves of *oxi1* mutants accumulating significantly higher Cu concentrations than those of WT plants (Table 6.2). In addition, after 72 h, the concentration of Cu significantly increased only in

leaves of Cu-exposed *oxi1* plants as compared to non-exposed plants (Table 6.2).

Considering the plant's ability to translocate Cu from roots to shoots, translocation factors were estimated in non-exposed and Cu-exposed plants (Figure 6.2). The Cu translocation factors were similar in WT and *oxi1* plants in non-exposed conditions during the experimental timeframe (Figure 6.2). Exposure to excess Cu severely impaired relative root-to-shoot Cu translocation (Figure 6.2). Whereas the root-to-shoot Cu translocation factor overall decreased, it remained significantly higher in *oxi1* mutants than in WT plants after exposure to excess Cu for 24 h, but was similar in both genotypes after 72 h (Figure 6.2).

6.2.3 Activities of antioxidative and NAD(P)H-producing enzymes

Since Cu is redox-active, activities of antioxidative (SOD, CAT, GR, GPOD, and SPOD; Table 6.3 and 6.5) as well as NAD(P)H-producing enzymes (ICDH, ME, and G6PDH; Table 6.4 and 6.6) were determined in roots and leaves of non-exposed and Cu-exposed Col-0 WT and *oxi1* plants to evaluate the metabolic responses to excess Cu. In both genotypes, exposure to excess Cu did not affect SOD activities (Table 6.3 and 6.5). For the other enzymes, the activities were more affected in roots (Table 6.3) than in leaves (Table 6.5) of Cu-exposed plants and also more strongly in *oxi1* than in WT plants. Whereas GR, GPOD, SPOD, and ME activities were already significantly higher in roots of *oxi1* plants after 24 h exposure to excess Cu, their activities were only significantly increased in roots of WT plants after 72 h (Table 6.3 and 6.4). Moreover, ME activity was significantly more elevated in roots of *oxi1* than WT plants after Cu exposure for 72 h (Table 6.4). In addition, increased enzyme activities were only observed in roots of *oxi1* mutants after exposure to Cu for CAT (24 h; Table 6.3) and for ICDH and G6PDH (72 h; Table 6.4). In leaves, the activities of GR, GPOD, ME, and G6PDH were also increased in Cu-exposed plants, but only in *oxi1* plants except for ME (Table 6.5 and 6.6). After 72 h, GR and GPOD activities were significantly higher in leaves of Cu-exposed *oxi1* mutants as compared to non-exposed plants, which was also observed for G6PDH and ME activities after both time points. For WT plants, only the activity of ME was

elevated in the leaves after 72 h of excess Cu exposure. In addition, at this time point, ME activity was higher in leaves of Cu-exposed *oxi1* mutants than WT plants (Table 6.6).

6.2.4 Thiobarbituric acid-reactive metabolites concentrations

The determination of the activities of antioxidative enzymes revealed major differences in the antioxidant defense response in roots and leaves of Col-0 WT and *oxi1* mutant plants exposed to excess Cu for 24 h (Table 6.3 and 6.5). Therefore, lipid peroxidation levels were assessed to investigate possible oxidative damage occurring within this timeframe. Since TBA-rm are end-products of lipid peroxidation reactions, their concentrations were determined in roots and leaves of non-exposed and Cu-exposed WT and *oxi1* mutant plants before (0 h) and after 2, 4, 6, and 24 h exposure to excess Cu (Figure 6.3). Concentrations of TBA-rm were only significantly increased in roots of Cu-exposed WT and *oxi1* plants. Whereas excess Cu increased concentrations of TBA-rm in roots of WT plants already 4 h after the exposure started, an increase in roots of *oxi1* plants only occurred from 6 h onwards (Figure 6.3). Moreover, TBA-rm concentrations were significantly higher in roots of Cu-exposed WT than *oxi1* plants after 6 and 24 h (Figure 6.3).

6.2.5 Gene expression in leaves

Although no Cu-induced oxidative damage was observed in leaves of both genotypes (Figure 6.3), root-to-shoot translocation factors, and biometric and metabolic results suggested different Cu-induced responses in leaves of WT and *oxi1* plants after 24 h exposure. To strengthen and further examine these observations, expression levels of several genes involved in pro- and antioxidative responses, Cu transport, Cu chelation (metallothioneins), and signaling were determined in leaves of Col-0 WT and *oxi1* plants exposed to excess Cu for 24 h (Table 6.7).

Transcript levels of oxidative stress hallmark genes (Gadjev *et al*., 2006) were generally upregulated after exposure to excess Cu. Overall, the levels of these transcripts were higher in leaves of WT than *oxi1* mutant plants (Table 6.7). Similarly, excess Cu induced the upregulation of the pro-oxidative gene

LOX2 in leaves of both genotypes, but its induction was significantly higher in WT plants. On the other hand, whereas no significant Cu-induced effects were observed in the expression of *RBOH* genes, *RBOHC* expression was significantly higher in leaves of Cu-exposed *oxi1* mutants than in Cu-exposed WT plants (Table 6.7).

Although clear differences were observed between both genotypes for the expression of genes related to ROS production, this was not apparent for genes related to antioxidative defense and chelating molecules. Concerning the genes encoding antioxidative enzymes, exposure to Cu induced a downregulation of *FSD1* and *CAT2* and an upregulation of *CAT3* in leaves of WT and *oxi1* plants (Table 6.7). In addition, excess Cu led to higher *MT2a* and *MT3* expressions and downregulation of *MT1c* transcription in both genotypes (Table 6.7).

The protein kinase OXI1 plays an important role in ROS signal transduction by sensing ROS and initiating downstream responses via MAPK-mediated signaling pathways (Opdenakker *et al*., 2012a, 2012b). Accordingly, *OXI1* expression was significantly upregulated in leaves of Cu-exposed WT plants. Although the MAPK *MPK3* was upregulated in both genotypes, its expression levels were significantly higher in leaves of WT as compared to *oxi1* plants after 24 h exposure to Cu (Table 6.7). In turn, transcript levels of downstream targets such as the *WRKY22* and *WRKY25* transcription factors were upregulated in leaves of genotypes exposed to Cu, while *ZAT12* and *WRKY33* were only significantly upregulated in Cu-exposed *oxi1* plants (Table 6.7).

Several authors established a link between OXI1-activated MAPK-mediated signaling and stress hormone signaling pathways such as those mediated by ethylene (Keunen *et al*., 2016b; Schellingen *et al*., 2015b) or jasmonic acid (JA) (Shumbe *et al*., 2016; Smékalová *et al*., 2014). Therefore, transcript levels of ethylene and JA signaling marker genes, *ERF1* and *PDF1.2* respectively, were also measured. Both marker genes were upregulated after excess Cu exposure in both genotypes, but the relative fold changes were significantly different in leaves of WT and *oxi1* mutant plants (Table 6.7). The upregulation of *ERF1* was significantly higher in leaves of WT than in leaves of *oxi1* plants, whereas the opposite was observed for *PDF1.2* transcript levels.

6.2.6 Biochemical oxidative stress signature in leaves

To investigate the genotype-specific oxidative stress signature suggested by significantly less upregulation of oxidative stress hallmark genes in leaves of *oxi1* mutants as compared to WT plants (Table 6.7), concentrations of H_2O_2 were determined in leaves of non-exposed and Cu-exposed Col-0 WT and *oxi1* mutant plants after 24 h of exposure (Figure 6.4). The H_2O_2 concentration was significantly lower in leaves of *oxi1* mutant plants exposed to excess Cu as compared to non-exposed mutant plants (Figure 6.4).

Although the level of oxidative stress was lower in leaves of *oxi1* mutant as compared to those of WT plants (Table 6.7, Figure 6.4), activities of antioxidative enzymes were not altered after 24 h exposure to excess Cu (Table 6.3 and 6.5). Therefore, the possible role of glutathione in the antioxidative defense was investigated in leaves of both genotypes, but no significant differences were observed (Table 6.8).

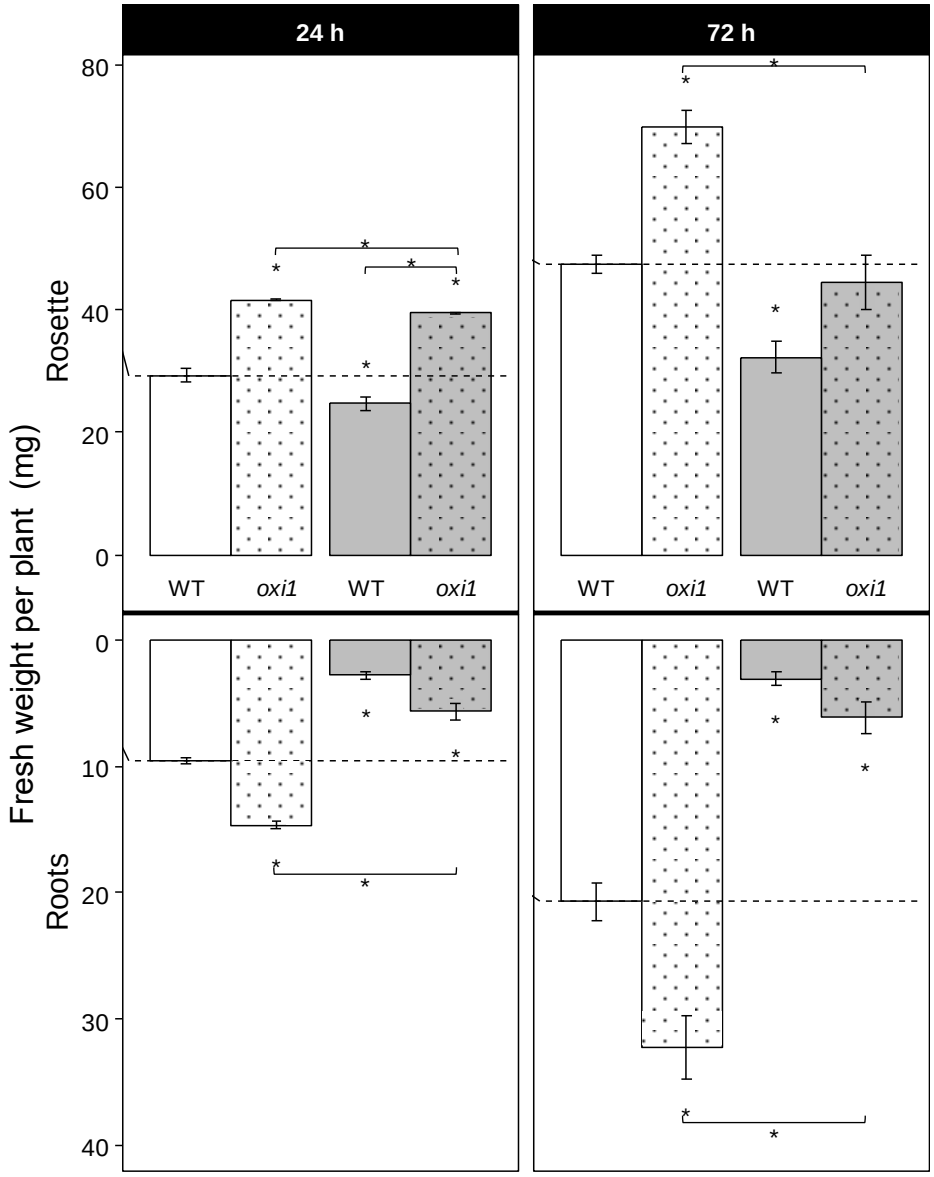

Figure 6.1 – Root and rosette fresh weight per plant (in mg) of three-week-old *A. thaliana* wild-type (WT) and *oxi1* knockout (*oxi1*) plants (accession Col-0) exposed to 2 µM $CuSO_4$ or not exposed for 24 and 72 h. Values are the mean ± S.E. of at least three biological replicates, each containing roots or rosettes of 25 individual plants. □ = non-exposed WT plant. ⁘ = non-exposed *oxi1* mutant. ■ = WT plant exposed to 2 µM $CuSO_4$. ⁘ = *oxi1* mutant exposed to 2 µM $CuSO_4$. Statistical significance ($P<0.05$) is indicated using asterisks for differences relative to WT non-exposed plants (within organ and time point) or between conditions connected by brackets.

Table 6.1 – Percentages of growth inhibition of roots and leaves of three-week-old *A. thaliana* wild-type (WT) and *oxi1* knockout (*oxi1*) plants (accession Col-0) exposed to 2 μM $CuSO_4$ for 24 and 72 h. Values are the mean ± S.E. of at least three biological replicates, each containing roots or rosettes of 25 individual plants. Statistical significance (P<0.05) is indicated using asterisks for differences relative to the non-exposed genotype (at each time point) or by dagger signs and printed in bold between genotypes (within organ and time point).

			2 μM Cu	
			Roots	**Leaves**
% inhibition	**24 h**	**WT**	70.81 ± 3.22 *	**15.80 ± 4.14 *,†**
		oxi1	61.58 ± 4.61 *	**5.16 ± 0.12 *,†**
	72 h	**WT**	85.32 ± 2.36 *	31.86 ± 5.68 *
		oxi1	80.98 ± 3.87 *	36.24 ± 6.45 *

Table 6.2 – Concentrations of Cu (mg kg^{-1} dry weight) in roots and leaves of three-week-old *A. thaliana* wild-type (WT) and *oxi1* knockout (*oxi1*) plants (accession Col-0) exposed to 2 μM $CuSO_4$ or not exposed for 24 and 72 h. Values are the mean ± S.E. of at least three biological replicates, each containing roots or rosettes of 25 individual plants. Statistical significance (P<0.05) is indicated using different lowercase letters (for differences within organ and time point).

				non-exposed	2 μM Cu
Cu	**Leaves**	**24 h**	**WT**	10.75 ± 0.40 c	18.58 ± 0.27 b
			oxi1	9.60 ± 0.37 c	21.72 ± 0.58 a
		72 h	**WT**	9.57 ± 0.44 bc	11.87 ± 0.46 ab
			oxi1	8.87 ± 0.51 c	12.21 ± 0.58 a
	Roots	**24 h**	**WT**	30.35 ± 3.29 c	2288.81 ± 97.20 a
			oxi1	34.26 ± 4.86 c	1856.42 ± 38.65 b
		72 h	**WT**	20.80 ± 0.52 c	2719.38 ± 300.14 a
			oxi1	19.79 ± 3.50 c	1899.48 ± 38.65 b

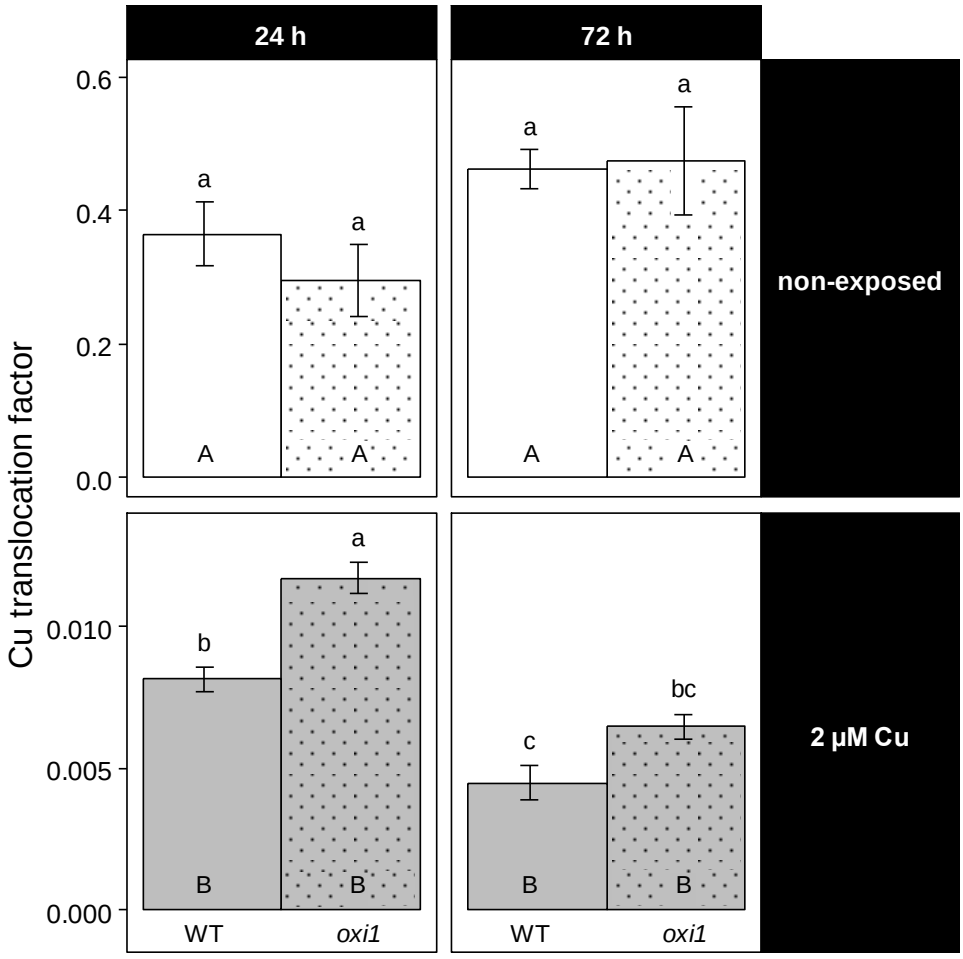

Figure 6.2 – Root-to-shoot translocation factors of Cu in three-week-old *A. thaliana* wild-type (WT) and *oxi1* knockout (*oxi1*) plants (accession Col-0) exposed to 2 µM $CuSO_4$ or not exposed for 24 and 72 h. Values are the mean ± S.E. of at least three biological replicates. □ = non-exposed WT plant. ⁘ = non-exposed *oxi1* mutant. ■ = WT plant exposed to 2 µM $CuSO_4$. ▦ = *oxi1* mutant exposed to 2 µM $CuSO_4$. Statistical significance ($P<0.05$) is indicated using different lowercase (for differences within exposure condition) or uppercase letters (for differences across exposure conditions, within genotype and time point).

Table 6.3 – Activities of antioxidative enzymes (mU mg^{-1} fresh weight) in roots of three-week-old *A. thaliana* wild-type (WT) and *oxi1* knockout (*oxi1*) plants (accession Col-0) exposed to 2 µM $CuSO_4$ or not exposed for 24 and 72 h. Values are the mean ± S.E. of at least three biological replicates, each containing roots of at least two individual plants. Statistical significance ($P<0.05$) is indicated using different lowercase letters (for differences within time point); the conditions in which differences occur are highlighted in grey. Abbreviations: CAT: catalase; GR: glutathione reductase; SOD: superoxide dismutase; GPOD: guaiacol peroxidase; SPOD: syringaldazine peroxidase.

				non-exposed	2 µM Cu
Roots	CAT	24 h	WT	0.45 ± 0.39 b	1.01 ± 0.29 ab
			oxi1	0.20 ± 0.05 b	2.05 ± 0.86 a
		72 h	WT	1.16 ± 0.64 a	2.43 ± 0.52 a
			oxi1	4.12 ± 2.37 a	1.18 ± 0.33 a
	GR	24 h	WT	42.86 ± 2.78 b	178.89 ± 42.38 ab
			oxi1	118.71 ± 36.95 b	288.23 ± 34.96 a
		72 h	WT	105.89 ± 24.99 b	289.85 ± 32.58 a
			oxi1	108.77 ± 29.16 b	326.27 ± 27.23 a
	SOD	24 h	WT	109.79 ± 18.50 a	116.81 ± 24.95 a
			oxi1	161.50 ± 28.05 a	152.79 ± 5.07 a
		72 h	WT	101.05 ± 26.00 a	142.45 ± 20.66 a
			oxi1	190.22 ± 128.46 a	159.83 ± 28.37 a
	GPOD	24 h	WT	553.30 ± 134.43 b	1843.09 ± 585.90 ab
			oxi1	557.76 ± 331.65 b	3088.99 ± 585.98 a
		72 h	WT	797.58 ± 166.91 b	3446.04 ± 432.85 a
			oxi1	708.14 ± 243.05 b	3404.74 ± 321.91 a
	SPOD	24 h	WT	1343.20 ± 703.79 b	2435.07 ± 522.55 ab
			oxi1	1398.73 ± 748.66 b	4480.40 ± 687.08 a
		72 h	WT	1737.52 ± 591.75 b	6446.80 ± 1103.20 a
			oxi1	2227.00 ± 29.73 b	7835.05 ± 1108.88 a

Table 6.4 – **Activities of NAD(P)H-producing enzymes (mU mg^{-1} fresh weight) in roots of three-week-old *A. thaliana* wild-type (WT) and *oxi1* knockout (*oxi1*) plants (accession Col-0) exposed to 2 µM $CuSO_4$ or not exposed for 24 and 72 h.** Values are the mean ± S.E. of at least three biological replicates, each containing roots of at least two individual plants. Statistical significance ($P<0.05$) is indicated using different lowercase letters (for differences within time point); the conditions in which differences occur are highlighted in grey. Abbreviations: ICDH: isocitrate dehydrogenase; ME: malic enzyme; G6PDH: glucose-6-phosphate dehydrogenase.

				non-exposed	2 µM Cu
Roots	**ICDH**	**24 h**	**WT**	101.74 ± 30.01 a	207.24 ± 65.97 a
			oxi1	157.79 ± 101.53 a	333.38 ± 36.05 a
		72 h	**WT**	137.29 ± 41.35 b	280.49 ± 16.55 ab
			oxi1	146.59 ± 53.93 b	361.26 ± 21.04 a
	ME	**24 h**	**WT**	76.97 ± 19.88 b	185.59 ± 72.57 ab
			oxi1	125.23 ± 47.36 b	272.04 ± 18.37 a
		72 h	**WT**	111.53 ± 28.23 c	245.82 ± 19.58 b
			oxi1	115.23 ± 41.46 c	382.06 ± 20.02 a
	G6PDH	**24 h**	**WT**	5.04 ± 1.57 c	5.96 ± 2.18 bc
			oxi1	45.41 ± 14.87 ab	49.68 ± 14.66 a
		72 h	**WT**	5.98 ± 1.90 b	37.02 ± 11.45 ab
			oxi1	13.89 ± 2.94 b	61.07 ± 11.65 a

Table 6.5 – Activities of antioxidative enzymes (mU mg^{-1} fresh weight) in leaves of three-week-old *A. thaliana* wild-type (WT) and *oxi1* knockout (*oxi1*) plants (accession Col-0) exposed to 2 µM $CuSO_4$ or not exposed for 24 and 72 h. Values are the mean ± S.E. of at least three biological replicates, each containing rosettes of at least two individual plants. Statistical significance ($P<0.05$) is indicated using different lowercase letters (for differences within time point); the conditions in which differences occur are highlighted in grey. Abbreviations: see Table 6.3.

				non-exposed	2 µM Cu
Leaves	CAT	24 h	WT	1.24 ± 0.40 a	0.71 ± 0.20 a
			oxi1	11.00 ± 5.96 a	1.37 ± 0.23 a
		72 h	WT	1.98 ± 1.13 a	3.59 ± 2.01 a
			oxi1	1.97 ± 0.89 a	1.64 ± 0.42 a
	GR	24 h	WT	872.14 ± 47.96 a	1073.43 ± 97.31 a
			oxi1	794.07 ± 211.22 a	1254.01 ± 51.97 a
		72 h	WT	828.67 ± 39.95 b	850.93 ± 36.7 b
			oxi1	850.25 ± 47.03 b	1053.64 ± 17.67 a
	SOD	24 h	WT	367.76 ± 40.50 a	360.55 ± 18.92 a
			oxi1	372.46 ± 60.06 a	405.37 ± 46.92 a
		72 h	WT	249.82 ± 70.80 a	251.60 ± 15.27 a
			oxi1	341.38 ± 7.98 a	379.38 ± 9.30 a
	GPOD	24 h	WT	23.64 ± 4.06 ab	52.00 ± 14.12 a
			oxi1	7.63 ± 5.44 b	29.47 ± 3.07 ab
		72 h	WT	15.82 ± 3.94 b	19.62 ± 2.31 b
			oxi1	12.03 ± 2.05 b	38.76 ± 3.56 a
	SPOD	24 h	WT	57.08 ± 23.18 a	115.99 ± 49.15 a
			oxi1	33.46 ± 9.12 a	115.02 ± 35.27 a
		72 h	WT	89.49 ± 18.23 a	102.54 ± 11.86 a
			oxi1	83.35 ± 8.62 a	166.8 ± 37.56 a

Table 6.6 – Activities of NAD(P)H-producing enzymes (mU mg^{-1} fresh weight) in leaves of three-week-old *A. thaliana* wild-type (WT) and *oxi1* knockout (*oxi1*) plants (accession Col-0) exposed to 2 µM $CuSO_4$ or not exposed for 24 and 72 h. Values are the mean ± S.E. of at least three biological replicates, each containing rosettes of at least two individual plants. Statistical significance ($P<0.05$) is indicated using different lowercase letters (for differences within time point); the conditions in which differences occur are highlighted in grey. Abbreviations: see Table 6.4.

				non-exposed	2 µM Cu
Leaves	ICDH	24 h	WT	559.68 ± 25.79 a	588.77 ± 55.00 a
			oxi1	471.41 ± 89.16 a	640.92 ± 42.95 a
		72 h	WT	450.08 ± 38.11 a	483.27 ± 20.55 ab
			oxi1	530.17 ± 26.67 ab	584.02 ± 14.38 b
	ME	24 h	WT	242.72 ± 6.70 ab	285.7 ± 76.98 ab
			oxi1	126.45 ± 70.81 b	388.28 ± 33.20 a
		72 h	WT	220.22 ± 10.33 c	357.39 ± 18.44 b
			oxi1	285.36 ± 11.87 bc	486.46 ± 41.06 a
	G6PDH	24 h	WT	105.96 ± 7.61 ab	138.12 ± 13.80 ab
			oxi1	71.49 ± 31.76 b	163.43 ± 10.65 a
		72 h	WT	95.06 ± 6.34 b	109.37 ± 0.87 b
			oxi1	111.51 ± 12.88 b	149.18 ± 8.99 a

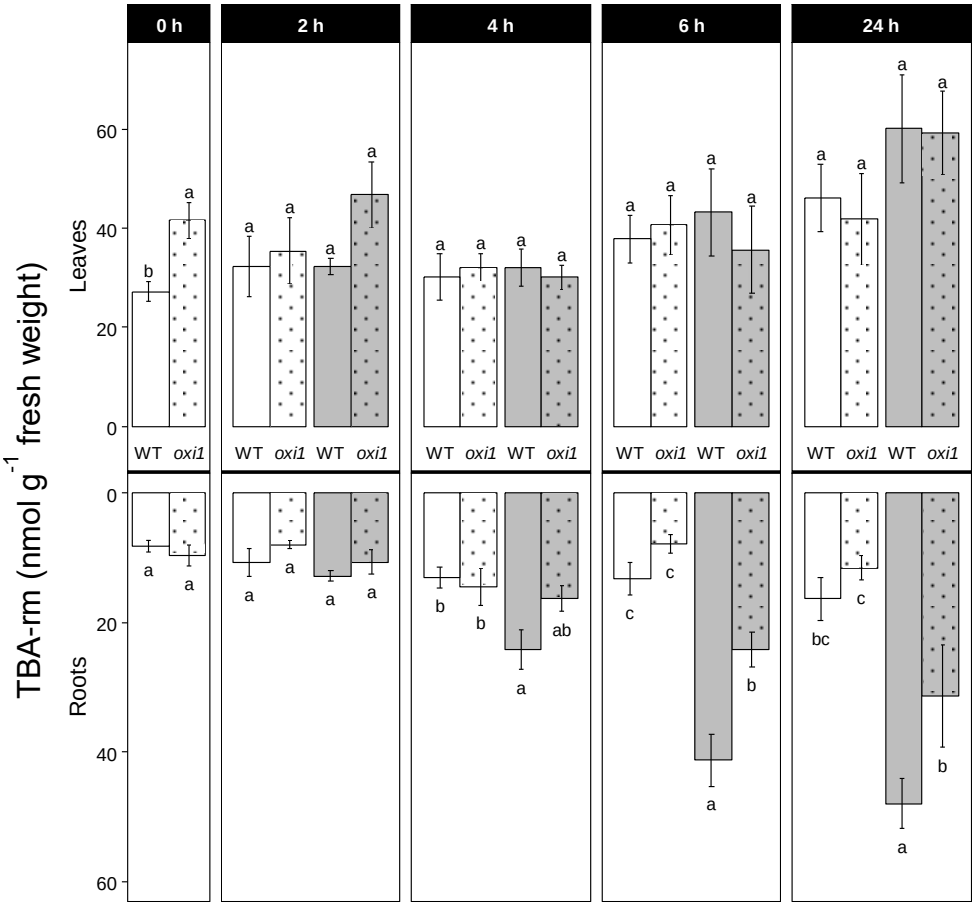

Figure 6.3 – Lipid peroxidation levels based on the concentration of thiobarbituric acid-reactive metabolites (TBA-rm; nmol g^{-1} fresh weight) in roots and leaves of three-week-old *A. thaliana* wild-type (WT) and *oxi1* knockout (*oxi1*) plants (accession Col-0) exposed to 2 µM $CuSO_4$ or not exposed for 0, 2, 4, 6, and 24 h. Values are the mean ± S.E. of at least six biological replicates, each containing roots or rosettes of at least three individual plants. □ = non-exposed WT plant. ⁙ = non-exposed *oxi1* mutant. ■ = WT plant exposed to 2 µM $CuSO_4$. ▩ = *oxi1* mutant exposed to 2 µM $CuSO_4$. Statistical significance ($P<0.05$) is indicated using different lowercase letters (for differences within organ and time point).

Table 6.7 – Transcript levels in leaves of three-week-old *A. thaliana* wild-type (WT) and *oxi1* knockout (*oxi1*) plants (accession Col-0) exposed to 2 µM $CuSO_4$ for 24 h. Values are the mean normalized expression relative to the non-exposed genotype (set at 1.00) ± S.E. of at least three biological replicates, each containing rosettes of at least one individual plant. Resolution values are the mean inverse normalization factors relative to the non-exposed genotype, indicating the stability of the selected reference genes. Statistically significant (P<0.05) Cu-induced changes in expression relative to the non-exposed genotype are indicated by color (■ = upregulation; ■ = downregulation). Statistically significant (P<0.05) differences between genotypes are indicated by asterisks and printed in bold. Abbreviations: *UPOX: upregulated by oxidative stress; Defensin-like: protein member of the defensin-like (DEFL) family; AT1G19020: unknown protein; AT1G05340: unknown protein; TIR-class: Toll-Interleukin-Resistance (TIR) domain family protein; LOX: lipoxygenase; RBOH (C/D): respiratory burst oxidase homolog protein (C/D); FSD1: Fe superoxide dismutase 1; CSD: Cu/Zn superoxide dismutase; CAT: catalase; MT: metallothionein; OXI1: oxidative signal inducible 1; MPK: mitogen-activated protein kinase; ZAT12: zinc finger of Arabidopsis thaliana 12; WRKY: WRKY DNA-binding protein; ERF1: ethylene response factor 1; PDF1.2: plant defensin 1.2.*

	2 µM Cu	
	WT	***oxi1***
Resolution	1.49 ± 0.21	1.42 ± 0.03
Genes encoding oxidative stress hallmark proteins		
UPOX	1.38 ± 0.09	1.12 ± 0.06
Defensin-like	**5.31 ± 0.53**	**2.58 ± 0.25 ***
AT1G19020	**6.07 ± 0.19**	**2.75 ± 0.23 ***
AT1G05340	**2.94 ± 0.48**	**1.42 ± 0.10 ***
TIR-class	**16.60 ± 3.71**	**3.49 ± 0.74 ***
Genes encoding ROS-producing enzymes		
LOX1	1.42 ± 0.06	1.23 ± 0.05
LOX2	**9.89 ± 0.45**	**5.61 ± 0.55 ***
RBOHC	**0.45 ± 0.15**	**2.42 ± 1.05 ***
RBOHD	1.56 ± 0.53	2.64 ± 1.15
Genes encoding antioxidative enzymes		
FSD1	0.09 ± 0.02	0.06 ± 0.01
CSD1	**1.73 ± 0.18**	**1.21 ± 0.05 ***
CSD2	0.96 ± 0.19	0.92 ± 0.04
CAT1	0.89 ± 0.04	0.81 ± 0.04
CAT2	0.56 ± 0.06	0.64 ± 0.04
CAT3	3.13 ± 0.32	2.35 ± 0.41

Table 6.7 – Transcript levels in leaves of three-week-old *A. thaliana* wild-type (WT) and *oxi1* knockout (*oxi1*) plants (accession Col-0) exposed to 2 µM $CuSO_4$ for 24 h. Continuation.

	2 µM Cu	
	WT	***oxi1***
Resolution	1.49 ± 0.21	1.42 ± 0.03
Genes encoding metallothionein proteins		
MT1a	**0.65 ± 0.04**	**1.10 ± 0.05 ***
MT1c	0.18 ± 0.03	0.27 ± 0.03
MT2a	2.33 ± 0.11	2.59 ± 0.13
MT2b	0.95 ± 0.04	1.11 ± 0.10
MT3	1.59 ± 0.10	1.53 ± 0.12
Genes encoding protein kinases		
OXI1	10.65 ± 3.20	ND
MPK3	**2.77 ± 0.23**	**2.11 ± 0.07 ***
MPK6	1.07 ± 0.04	1.10 ± 0.05
Genes encoding transcription factors		
ZAT12	**0.97 ± 0.13**	**1.95 ± 0.36 ***
WRKY22	3.13 ± 0.72	5.54 ± 0.83
WRKY25	2.80 ± 0.60	4.81 ± 1.02
WRKY29	0.60 ± 0.14	1.23 ± 0.14
WRKY33	4.14 ± 1.21	3.20 ± 0.69
Genes encoding proteins involved in hormone signaling		
ERF1	**23.34 ± 3.28**	**3.74 ± 0.55 ***
PDF1.2	**13.91 ± 3.83**	**27.07 ± 8.21 ***

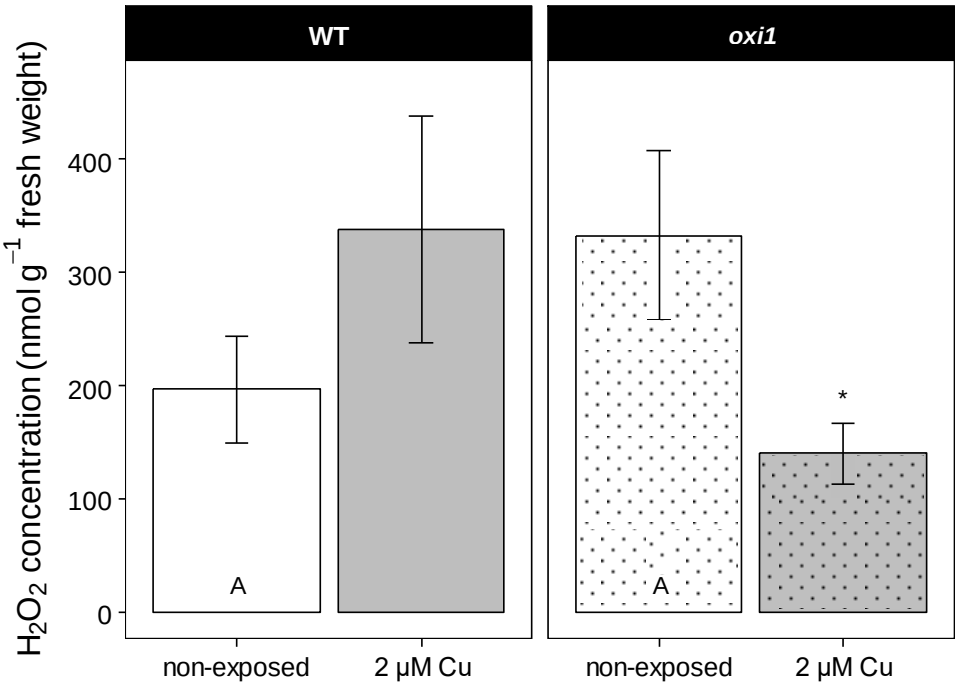

Figure 6.4 – Concentrations of H_2O_2 (nmol g^{-1} fresh weight) in leaves of three-week-old *A. thaliana* wild-type (WT) and *oxi1* knockout (*oxi1*) plants (accession Col-0) exposed to 2 µM $CuSO_4$ or not exposed for 24 h. Values are the mean ± S.E. of at least five biological replicates, each containing rosettes of at least one individual plant. □ = non-exposed WT plant. ⁘ = non-exposed *oxi1* mutant. ■ = WT plant exposed to 2 µM $CuSO_4$. ⁘ = *oxi1* mutant exposed to 2 µM $CuSO_4$. Statistical significance ($P<0.05$) is indicated using uppercase letters (between non-exposed genotypes) or asterisks (within genotype, between conditions).

Table 6.8 – Concentrations (nmol g^{-1} fresh weight) of total (GSH + GSSG), reduced (GSH), oxidized (GSSG) glutathione, and GSSG/GSH ratio in leaves of three-week-old *A. thaliana* wild-type (WT) and *oxi1* knockout (*oxi1*) plants (accession Col-0) exposed to 2 μM $CuSO_4$ or not exposed for 24 h. Values are the mean ± S.E. of at least three biological replicates, each containing rosettes of at least one individual plant. Statistical significance ($P<0.05$) is indicated using different lowercase letters (for differences within each genotype and time point).

			Leaves	
			non-exposed	**2 μM Cu**
24 h	**Total (GSH+GSSG)**	**WT**	266.27 ± 55.68 a	266.50 ± 43.31 a
		oxi1	230.01 ± 23.94 a	256.49 ± 43.17 a
	GSH	**WT**	250.93 ± 51.43 a	256.67 ± 39.82 a
		oxi1	219.26 ± 24.15 a	249.48 ± 44.54 a
	GSSG	**WT**	15.34 ± 4.77 a	9.83 ± 3.91 a
		oxi1	10.75 ± 2.67 a	7.01 ± 1.55 a
	GSSG/GSH	**WT**	0.06 ± 0.01 a	0.04 ± 0.01 a
		oxi1	0.05 ± 0.01 a	0.04 ± 0.01 a

6.3 Discussion

While essential to normal plant development, excess bioavailable concentrations of Cu induce phytotoxicity and inhibit plant growth (Cuypers *et al*., 2011; Drążkiewicz *et al*., 2004; Lequeux *et al*., 2010; Yruela, 2005). In fact, Cu is a redox-active micronutrient and can directly induce oxidative stress by catalyzing ROS formation via Fenton and Haber-Weiss reactions (Drążkiewicz *et al*., 2004). Interestingly, ROS are not only toxic metabolic byproducts but also important signaling molecules (Cuypers *et al*., 2016; Mittler *et al*., 2011). In healthy cells, a complex molecular network tightly controls and maintains ROS levels, allowing ROS signaling to be involved in the regulation of plant growth and development, adaptation to abiotic stress factors and responses to pathogen infections (Mittler *et al*., 2004, 2011; Opdenakker *et al*., 2012b; Suzuki *et al*., 2012; Tena *et al*., 2011). The protein kinase OXI1 plays a central role in the ROS signal transduction pathway by linking ROS production to downstream responses under metal stress (Opdenakker *et al*., 2012b). In particular, Opdenakker *et al*. (2012a) observed a strong induction of *OXI1* expression in both roots and leaves of *Arabidopsis thaliana* plants exposed to excess Cu. Since a reverse genetics approach might provide new insights into the function of the OXI1 kinase in Cu-induced oxidative stress responses, we investigated growth, and metabolic and transcriptomic responses in Col-0 WT and *oxi1* knockout plants exposed to excess Cu during 72 h.

In non-exposed conditions, average root and rosette fresh weights were always significantly higher for *oxi1* knockout mutants than for WT plants (Figure 6.1). Similar growth trends were observed by Smeets *et al*. (2013) for both *A. thaliana* genotypes in a Wassilewskija (Ws) background. Exposure to excess Cu inhibited root and rosette growth in both genotypes (Figure 6.1 and Table 6.1), but the percentage of Cu-induced growth inhibition was lower in *oxi1* than in WT plants, which was significant for the leaves of Cu-exposed plants after 24 h (Table 6.1). This suggests that a lack of functional OXI1 not only affects plant growth under control conditions (Figure 6.1) but also the plant's response to excess Cu (Table 6.1). In fact, after short-term exposure, leaves of *oxi1* plants appear to be less sensitive to excess Cu as compared to those of WT plants.

Exposure to excess Cu resulted in significantly increased Cu concentrations in roots of both genotypes (Table 6.2). However, roots of WT plants accumulated higher Cu concentrations as compared to those of *oxi1* plants. Rentel *et al*. (2004) observed that average root hair length was significantly lower in Ws *oxi1* knockout than in Ws WT plants, concluding that OXI1 activity is required for normal root hair development. Since root hairs increase the surface area for the absorption of water and nutrients, their impaired growth in *oxi1* plants can underlie the observed differences in Cu concentrations between both genotypes. Exposure to excess Cu for 24 h resulted in higher Cu concentrations in leaves of *oxi1* mutants than those of WT plants (Table 6.2). These results point to potential genotype-specific Cu translocation. To investigate this, root-to-shoot Cu translocation factors were estimated (Figure 6.2). Whereas no significant differences were observed between non-exposed genotypes (Figure 6.2), exposure to excess Cu severely impaired the Cu translocation factor in both genotypes. Moreover, the root-to-shoot Cu translocation factor was significantly higher in *oxi1* mutant as compared to WT plants after 24 h (Figure 6.2). This indicates that OXI1 has no direct function in Cu translocation under normal conditions, but is temporarily involved in its regulation when plants are grown under excess Cu conditions. Interestingly, rosette growth inhibition was significantly lower in *oxi1* plants as compared to WT plants at this time point. Due to its role in ROS sensing, OXI1 activates diverse signaling pathways leading to various oxidative stress responses. Since Cu is a redox-active element, investigating alterations to pro- and antioxidative processes in Cu-exposed WT and *oxi1* plants is relevant to assess genotype-specific sensitivities to excess Cu and identify new functions for OXI1.

The analysis of enzyme activities in roots revealed that exposure to Cu resulted in (1) increased activities in *oxi1* plants alone (ICDH and G6PDH) or (2) an accelerated rise in activities (GR, GPOD, SPOD, and ME) in *oxi1* plants at 24 h, whereas this was only observed after 72 h in WT plants (Table 6.3 and 6.4). This indicates that the lack of a functional OXI1 protein interferes with Cu-induced stress mechanisms, resulting in overall earlier and more intense antioxidative and NAD(P)H-producing responses. This in its turn resulted in delayed and diminished Cu-induced ROS-mediated damage, *i.e.* lipid peroxidation, in roots of *oxi1* mutant as compared to WT plants (Figure 6.3). In

leaves of Cu-exposed plants, similar responses of enzyme activities were noticed, *i.e.* a single increase in GPOD (72 h), GR (72 h) and G6PDH (24-72 h) activities or an accelerated response of ME activities in *oxi1* plants (Table 6.5 and 6.6). Whereas no significant differences were observed for lipid peroxidation (Figure 6.3) or for GSH concentrations (Table 6.8) in leaves of both genotypes at 24 h, WT plants displayed a higher H_2O_2 concentration (Figure 6.4) and higher expression of oxidative stress hallmark genes (Table 6.7) as compared to *oxi1* mutants. Taken together, results obtained for growth and enzymatic activities, lipid peroxidation levels (in roots), and ROS levels (in leaves) suggest that *oxi1* mutant plants are less sensitive to Cu-induced oxidative stress as compared to WT plants within the current experimental timeframe.

The hitherto discussed results highlight the important role of OXI1 in the early onset of responses to Cu exposure. This is in line with the reports of other authors observing a rapid induction of OXI1 kinase activity by H_2O_2 (Anthony *et al*., 2006; Rentel *et al*., 2004) and of *OXI1* expression by excess Cu exposure (Opdenakker *et al*., 2012a). In fact, Rentel *et al*. (2004) suggested that OXI1 is essential for H_2O_2-mediated signaling in *A. thaliana*. In turn, ROS signaling is involved in the modulation of plant stress responses, with the outcome depending on the interaction with other signaling pathways (Cuypers *et al*., 2016; Opdenakker *et al*., 2012b; Smékalová *et al*., 2014). As such, investigating the early effects on gene regulation caused by a non-functional OXI1 protein kinase might reveal potential downstream targets and interactions with other mechanisms. In the present study, this is of particular interest at the leaf level since Cu-induced growth inhibition is significantly lower in leaves of *oxi1* mutant than WT plants, but only after a short exposure of 24 h (Table 6.1).

Following ROS sensing by OXI1, a MAPK signaling cascade is initiated, which then mediates phosphorylation of a wide range of substrates (Colcombet and Hirt, 2008; Pitzschke and Hirt, 2006; Rodriguez *et al*., 2010). Rentel *et al*. (2004) identified the MAPKs MPK3 and MPK6 as downstream elements of the signal transduction pathway initiated by OXI1 and induced by H_2O_2. Interestingly, Opdenakker *et al*. (2012a) observed the induction of *OXI1* and *MPK3* expression in *A. thaliana* plants exposed to excess Cu. Our results show a similar upregulation of *OXI1* and *MPK3* in leaves of WT plants exposed to Cu, but

MPK3 expression was significantly less increased in Cu-exposed *oxi1* knockout plants (Table 6.7). This confirms that MPK3 is involved in Cu-induced oxidative stress signaling and is modulated upstream by OXI1. Moving further downstream, MAPK cascades are able to regulate gene transcription by activating or repressing different transcription factors (Opdenakker *et al*., 2012b; Pitzschke *et al*., 2009). Several proteins of the WRKY superfamily are known to be involved in diverse abiotic and biotic stress responses (Opdenakker *et al*., 2012b; Phukan *et al*., 2016; Rodriguez *et al*., 2010), often upon their activation by MAPK phosphorylation (Asai *et al*., 2002; Smeets *et al*., 2013). Whereas the transcript levels of several *WRKYs* were upregulated in leaves after short-term exposure to excess Cu, we did not observe genotype-specific *WRKY* expression patterns (Table 6.7). In addition to WRKY proteins, the zinc-finger protein ZAT12 also plays an important role in oxidative stress signaling in *Arabidopsis* (Davletova *et al*., 2005; Phukan *et al*., 2016). In fact, it has been suggested that ZAT12 activity is essential to the induction of *ASCORBATE PEROXIDASE 1* expression during oxidative stress (Rizhsky *et al*., 2004). In Cu stress conditions, Opdenakker *et al*. (2012a) observed an early increase in *ZAT12* transcript levels in roots of *Arabidopsis* plants. After gene clustering analysis, these authors proposed a link between *RBOHD*, *OXI1,* and *ZAT12* regulation in *Arabidopsis* roots exposed to excess Cu. In our study, Cu-induced *ZAT12* upregulation was only observed in leaves of *oxi1* mutants, which indicates that alternative signaling routes next to OXI1 are present and essential in the modulation of *ZAT12* expression in leaves of Cu-exposed plants.

In metal-induced oxidative stress conditions, the interaction and crosstalk between ROS and hormone signaling networks, particularly via MAPK cascades, is well known (Cho and Yoo, 2009; Keunen *et al*., 2016b; Lequeux *et al*., 2010; Li *et al*., 2012; Opdenakker *et al*., 2012b; Rodriguez *et al*., 2010; Schellingen *et al*., 2015b; Smékalová *et al*., 2014; Takahashi *et al*., 2007). For example, MPK3 and MPK6 are not only well-known downstream targets of OXI1 in ROS signaling (Rentel *et al*., 2004), but are also regulators of ethylene biosynthesis and thus determinant to ethylene production (Li *et al*., 2012). Schellingen *et al*. (2015b) proposed a regulatory model linking cadmium (Cd)-induced ROS production to an ethylene response via OXI1 sensing and MPK3/6 signaling. Ethylene is a stress-inducible phytohormone that mediates defense responses to diverse

abiotic and biotic stresses. Through signaling cascades, ethylene activates the transcription of diverse target genes such as the highly ethylene-responsive *ETHYLENE RESPONSE FACTOR 1 (ERF1)* (Keunen *et al*., 2016b; Müller and Munné-Bosch, 2015). Therefore, *ERF1* upregulation after exposure to excess Cu (Table 6.7) hints at early ethylene-mediated responses occurring in leaves of both genotypes. However, this upregulation was significantly lower in the *oxi1* mutants than in WT plants (Table 6.7). This suggests that OXI1 is an upstream regulator of *ERF1*, implying that ethylene signaling is impaired in *oxi1* mutant plants exposed to excess Cu. Future research is needed to validate, complement, and translate the proposed model for ethylene-mediated early responses to Cd-induced oxidative stress (Schellingen *et al*., 2015b) into a Cu-induced oxidative stress context. As such, it is known that ERF1 is also a regulator of JA-mediated responses and a key element in the integration of both hormonal signals to activate ethylene/JA-dependent defense responses (Lorenzo *et al*., 2003). Jasmonic acid regulates a wide variety of physiological processes such as senescence and is involved in defense responses to pathogen and herbivore attacks (Kim *et al*., 2015; Rehrig *et al*., 2014). Although *PLANT DEFENSIN 1.2 (PDF1.2)* is generally regarded as a JA target, Penninckx *et al*. (1998) suggested that the concomitant triggering of ethylene and JA pathways is required for *PDF1.2* induction after pathogen infection. Exposure to excess Cu induced the upregulation of *PDF1.2* in leaves of both genotypes (Table 6.7), but contrary to the *ERF1* expression patterns, *PDF1.2* transcript levels were significantly higher in leaves of *oxi1* mutant as compared to WT plants (Table 6.7). These results point towards a bypass mechanism to circumvent an impaired ERF1-mediated phytohormone signaling caused by the non-functional OXI1 kinase.

In conclusion, a non-functional OXI1 not only affects plant growth under control conditions, but also plant responses to excess Cu. Our results suggest that, within the experimental timeframe, Col-0 *oxi1* mutant plants are less sensitive to Cu-induced oxidative stress than Col-0 WT plants. This is particularly relevant in the early phase of leaf responses to excess Cu, when OXI1 plays a role in the modulation of *ERF1* expression. Therefore, the Cu-induced ethylene-mediated signaling model in WT plants might be affected in leaves of *oxi1* plants. However, our results also suggest that a PDF1.2-mediated mechanism is

induced in leaves of *oxi1* mutants to bypass the impaired phytohormone signaling via ERF1. As such, several transcription factors downstream of OXI1 were at least similarly or even more induced in leaves of Cu-exposed *oxi1* mutants as compared to WT plants. This suggests that the early decrease in sensitivity to Cu-induced oxidative stress in *oxi1* mutant plants is the result of a bypass of the OXI1 signaling route with an efficient alternative signal transduction pathway. Taken together, the interplay between ROS production, OXI1 signaling and hormone signaling should be the subject of future research focusing on plant responses to excess Cu.

Supplemental Table 6.1 – Transcript levels in leaves of three-week-old *A. thaliana* non-exposed wild-type (WT) and *oxi1* knockout (*oxi1*) plants (accession Col-0). Values are the mean normalized expression values relative to the non-exposed WT plant (set at 1.00) ± S.E. of at least three biological replicates, each containing rosettes of at least one individual plant. Resolution values are mean inverse normalization factors relative to the non-exposed WT plant, indicating the stability of the selected reference genes. Statistically significant ($P<0.05$) differences between genotypes are indicated by asterisks and printed in bold. Abbreviations: see Table 6.7.

	Non-exposed	
	WT	***oxi1***
Resolution	1.00 ± 0.18	1.14 ± 0.20
Genes encoding oxidative stress hallmark proteins		
UPOX	1.00 ± 0.06	1.05 ± 0.07
Defensin-like	1.00 ± 0.13	1.53 ± 0.28
AT1G19020	1.00 ± 0.13	1.84 ± 0.34
AT1G05340	1.00 ± 0.14	1.28 ± 0.14
TIR-class	1.00 ± 0.38	1.89 ± 0.59
Genes encoding ROS-producing enzymes		
LOX1	1.00 ± 0.22	1.18 ± 0.10
LOX2	1.00 ± 0.17	1.21 ± 0.10
RBOHC	1.00 ± 0.47	0.14 ± 0.02
RBOHD	1.00 ± 0.38	0.43 ± 0.02
Genes encoding antioxidative enzymes		
FSD1	1.00 ± 0.26	1.84 ± 0.65
CSD1	1.00 ± 0.16	1.01 ± 0.11
CSD2	1.00 ± 0.20	1.01 ± 0.13
CAT1	1.00 ± 0.11	1.13 ± 0.03
CAT2	1.00 ± 0.08	1.00 ± 0.08
CAT3	1.00 ± 0.10	0.99 ± 0.11
Genes encoding metallothionein proteins		
MT1a	1.00 ± 0.06	0.84 ± 0.04
MT1c	1.00 ± 0.08	1.06 ± 0.10
MT2a	1.00 ± 0.04	0.85 ± 0.06
MT2b	1.00 ± 0.13	0.97 ± 0.07
MT3	1.00 ± 0.07	1.04 ± 0.06

Supplemental Table 6.1 – Transcript levels in leaves of three-week-old *A. thaliana* non-exposed wild-type (WT) and *oxi1* knockout (*oxi1*) plants (accession Col-0). Continuation.

	Non-exposed	
	WT	***oxi1***
Resolution	1.00 ± 0.18	1.14 ± 0.20
Genes encoding protein kinases		
OXI1	1.00 ± 0.19	ND
MPK3	1.00 ± 0.22	1.11 ± 0.05
MPK6	1.00 ± 0.08	0.96 ± 0.03
Genes encoding transcription factors		
ZAT12	1.00 ± 0.22	0.52 ± 0.06
WRKY22	1.00 ± 0.20	0.63 ± 0.06
WRKY25	1.00 ± 0.15	0.74 ± 0.07
WRKY29	1.00 ± 0.23	0.89 ± 0.07
WRKY33	1.00 ± 0.25	1.51 ± 0.24
Genes encoding proteins involved in hormone signaling		
ERF1	**1.00 ± 0.22**	**4.53 ± 1.36 ***
PDF1.2	1.00 ± 0.45	0.15 ± 0.04

Supplemental Table 6.2 – List of primers used in quantitative real-time PCR. E-E-jn: Exon-Exon-junction. UTR: Untranslated region.

Locus	Annotation	Forward primer (5′ – 3′)	Reverse primer (5′ – 3′)	Exon location	Amplicon length (bp)	Primer Efficiency
Reference genes						
AT2G28390	*SAND family*	AACTCTATGCAGCATTTGATCCACT	TGATTGCATATCTTTATCGCCATC	Exon 13	61	107.80 %
AT3G18780	*ACT2*	CTTGCACCAAGCAGCATGAA	CCGATCCAGACACTGTACTTCCTT	Exon 2	68	88.10 %
AT4G05320	*UBQ10*	GGCCTTGTATAATCCCTGATGAATAAG	AAAGAGATAACAGGAACGGAAACATAGT	3′ UTR	61	87.18 %
AT5G15710	*F-box protein*	TTTCGGCTGAGAGGTTCGAGT	GATTCCAAGACGTAAAGCAGATCAA	Exon 1	63	99.89 %
AT5G60390	*EF1A*	TGAGCACGCTCTTCTTGCTTTCA	GGTGGTGGCATCCATCTTGTTACA	E1-E2-jn	76	97.04 %
Oxidative stress hallmark genes						
AT1G05340	*Unknown*	TCGGTAGCTCAGGGTAAAGTGG	CCAGGGCACAACAGCAACA	E2-E3-jn	91	97.07 %
AT1G19020	*Unknown*	GAAAATGGGACAAGGGTTAGACAAA	CCCAACGAAAACCAATAGCAGA	Exon 1	92	93.25 %
AT1G57630	*TIR-class*	ACTCAAACAGGCGATCAAAGGA	CACCAATTCGTCAAGACAACACC	Exon 1	91	96.51 %
AT2G21640	*UPOX*	GACTTGTTTCAAAAACACCATGGAC	CACTTCCTTAGCCTCAATTTGCTTC	E1-E2-jn	91	96.04 %
AT2G43510	*Defensin-like*	ATGGCAAAGGCTATCGTTTCC	CGTTACCTTGCGCTTCTATCTCC	E1-E2-jn	91	99.55%
Genes encoding ROS-producing enzymes						
AT1G55020	*LOX1*	TTGGCTAAGGCTTTTGTCGG	GTGGCAATCACAAACGGTTC	Exon 6	101	94.40 %
AT3G45140	*LOX2*	TTTGCTCGCCAGACACTTG	GGGATCACCATAAACGGCC	E3-E4-jn	102	86.65 %
AT5G51060	*RBOHC*	TCACCAGAGACTGGCACAATAAA	GATGCTCGACCTGAATGCTC	E6-E7-jn	101	92.31 %
AT5G47910	*RBOHD*	AACTCTCCGCTGATTCCAACG	TGGTCAGCGAAGTCTTTAGATTCCT	E1-E2-jn	91	104.23 %
Genes encoding antioxidative enzymes						
AT4G25100	*FSD1*	CTCCCAATGCTGTGAATCCC	TGGTCTTCGGTTCTGGAAGTC	Exon 4	101	88.80 %
AT1G08830	*CSD1*	TCCATGCAGACCCTGATGAC	CCTGGAGACCAATGATGCC	Exon 5	102	93.80 %
AT2G28190	*CSD2*	GAGCCTTTGTGGTTCACGAG	CACACCACATGCCAATCTCC	Exon 6	101	93.90 %
AT1G20630	*CAT1*	AAGTGCTTCATCGGGAAGGA	CTTCAACAAAACGCTTCACGA	E5-E6-jn	103	97.60 %
AT4G35090	*CAT2*	AACTCCTCCATGACCGTTGGA	TCCGTTCCCTGTCGAAATTG	E2-E3-jn	76	98.30 %
AT1G20620	*CAT3*	TCTCCAACAACATCTCTTCCCTCA	GTGAAATTAGCAACCTTCTCGATCA	E2-E3-jn	91	95.60 %

Supplemental Table 6.2 – List of primers used in quantitative real-time PCR. Continuation

Locus	Annotation	Forward primer (5′ – 3′)	Reverse primer (5′ – 3′)	Exon location	Amplicon length (bp)	Primer Efficiency
Genes encoding metallothionein proteins						
AT1G07600	*MT1a* *	AACTGTGGATGTGGCTCCTC	CAGTTACAGTTTGACCCACAGC	Exon 1	122	90.43 %
AT1G07590	TPR-like *	AGAGCTAGCGAGAACGTGGA	CCTACTCGAGCAAACGCTTC	Exon 4	93	87.04 %
AT1G07610	*MT1c*	GCATGGTCTCAAACCAAGGA	TACGCAACACAATGCCAAGT	Intron 2	96	86.37 %
AT3G09390	*MT2a*	ACCCTGACTTGGGATTCTCC	GCGTTGTTACTCTCCCCTGA	Exon 1	109	90.17 %
AT5G02380	*MT2b*	ACTCTTGTCCTCGGTGTTGC	TTGCACTTGCAGTCAGATCC	Exon 1	110	81.17 %
AT3G15353	*MT3*	TCGACATCGTCGAGACTCAG	CACTTGCAATTTGCGTTGTT	E2-E3-jn	85	88.03 %
Genes encoding protein kinases						
AT3G25250	*OXI1*	TAGAGGATCGAACCGGAAAG	GACCCTTGATTTCCTCAACG	Exon 2	149	85.67 %
AT3G45640	*MPK3*	GACGTTTGACCCCAACAGAA	GACGTTTGACCCCAACAGAA	E5-E6-jn	103	100.37 %
AT2G43790	*MPK6*	TAAGTTCCCGACAGTGCATCC	GATGGGCCAATGCGTCTAA	E5-E6-jn	100	107.68 %
Genes encoding transcription factors						
AT5G59820	*ZAT12*	GTGCGAGTCACAAGAAGCCTAACA	GCGACGACGTTTTCACCTTCTTCA	Exon 1	72	92.05 %
AT4G01250	*WRKY22*	AAACCCATCAAAGGTTCACCA	GGGTCGGATCTATTTCGCTC	E2-E3-jn	101	101.59 %
AT2G30250	*WRKY25*	GAAAGATCCGCAGCAGACG	TCCCAATAATTTCACGAGCG	Exon 5	101	98.35 %
AT4G23550	*WRKY29*	CATGGGCGTGGCGTAAATA	TTGTTTTCTTGCCAAACACCC	E2-E3-jn	104	103.08 %
AT2G38470	*WRKY33*	TCATCGATTGTCAGCAGAGACG	CCATTCCCACCATTTGTTTCAT	E3-E4-jn	92	89.92 %
Genes encoding proteins involved in hormone signaling						
AT3G23240	*ERF1*	TCCTCGGCGATTCTCAATTTT	TCCTCGGCGATTCTCAATTTT	Exon 1	91	98.40 %
AT5G44420	*PDF1.2*	TTTGCTGCTTTCGACGCAC	GCATGCATTACTGTTTCCGCA	Exon 1	99	94.45 %

* Since *AT1G07590* overlaps the *MT1a* completely, *AT1G07590*-specific primers were also developed to correct for its contribution to *MT1a* gene expression.

Supplemental Table 6.3 – Quantitative real-time PCR parameters according to the "Minimum Information for publication of Quantitative real-time PCR Experiments" (MIQE) guidelines derived from Bustin *et al*. (2009).

Sample/Template	
Source	Leaves of *Arabidopsis thaliana* plants (accession Col-0) cultivated in hydroponics
Method of preservation	Liquid nitrogen
Storage time	Six weeks at - 70 °C
Handling	Frozen
Extraction method	Phenol-free Total RNA isolation: Ambion™ RNAqueous® Total RNA Isolation Kit * (Life Technologies, Waltham, MA, USA)
RNA: DNA-free	TURBO DNA-*free*™ Kit * (Life Technologies, Waltham, MA, USA) Design of intron-spanning primers whenever possible
Concentration	NanoDrop®: ND-1000 Spectrophotometer (Thermo Fisher Scientific, Inc., MA, USA)
Assay optimization and validation	
Accession number	Supplemental Table 6.2
Amplicon details	Exon location and amplicon size: Supplemental Table 6.2
Primer sequences	Supplemental Table 6.2
In silico	Primers were blasted using the BLAST tool at http://arabidopsis.org/
Empirical	Primer concentration: 300 nM Annealing temperature: 60°C
Priming conditions	Combination of oligo(dT)-primers and random hexamers
PCR efficiency	Dilution series (slope, y-intercept and r^2; Supplemental Table 6.2)
Linear dynamic range	Samples are situated within the range of the efficiency curve
Reverse transcription – PCR	
Protocols	As stated in the Materials and Methods (Section 3.8)
Reagents	As stated in the Materials and Methods (Section 3.8)
No template control (NTC)	Cq and dissociation curve verification
Data analysis	
Specialist software	7500 Fast Real-Time PCR System (Applied Biosystems, Life Technologies, Belgium) Software v2.0.1
Statistical justification	At least three biological replicates Elimination of outliers after statistical validation using the Grubbs' test at significance level 0.05 (R version 3.3.1, package "outliers") Log transformation of the data One- and two-way ANOVA and the Tukey-Kramer post-hoc test to correct for multiple comparisons using R version 3.3.1
Normalization	Three stable reference genes selected using the GrayNorm algorithm (Remans *et al*., 2014): *AT2G28390, AT4G05320,* and *AT5G15710.*

* All procedures were performed according to the manufacturer's protocols.

CHAPTER 7

Loss of OXI1 function affects Cd-induced responses in *Arabidopsis thaliana* Col-0 and Ws plants

In preparation.

Keywords: *Arabidopsis thaliana*, Columbia, Wassilewskija, OXI1, knockout mutant, cadmium.

Abstract

Reactive oxygen species (ROS) not only induce cellular oxidative damage but also serve as important signaling molecules during normal plant development or in response to environmental stimuli. These responses often depend on the integration of ROS signaling pathways with other signaling components and pathways. For example, the H_2O_2-responsive protein kinase OXI1 is essential in relaying the oxidative signal downstream by activating MAPK cascades. Although non-redox active, cadmium (Cd) is able to induce oxidative stress and OXI1 activity. Since information on OXI1 downstream targets, functions and interactions during Cd stress is limited, we examined its role in Cd-induced oxidative stress responses by investigating Cd-induced responses in wild-type (WT) and *oxi1* knockout *A. thaliana* (accessions Col-0 and Ws) plants exposed to Cd for 24 and 72 h.

Our results indicate that OXI1 is essential for normal plant growth and its absence leads to disturbed responses of Col-0 and Ws plants to Cd. In particular, growth inhibition and transcriptome data indicate that Col-0 *oxi1* mutant plants are less sensitive to Cd-induced oxidative stress than their WT counterparts. This arises from a possible role of OXI1 in the regulation of Cd and Cu transportation, as evidenced by the alterations in Cd root-to-shoot translocation factors and total Cu concentrations in these plants, and Cu remobilization, as indicated by other genotype-specific Cu deficiency-like responses. Our results indicated that *MPK3/6* upregulation is not dependent on OXI1 activity during Cd stress and confirmed the transcription factor ZAT12 as a downstream target of OXI1 in Cd-exposed roots. Although the loss of function affected early OXI1-mediated ethylene signaling, our results hint at the activation of OXI1-independent signaling pathways to mediate later Cd-induced phytohormonal responses. Therefore, further research should define the links between OXI1 and phytohormonal signaling pathways and elucidate the signaling networks involved in plant responses to Cd stress.

7.1 Introduction

More than just harmful byproducts of aerobic metabolism, reactive oxygen species (ROS) also function as important signaling molecules in plants. The dynamic and precise control of the cellular ROS levels allows ROS signaling networks to interact with other signaling pathways and regulate diverse cellular processes such as normal plant development, responses to environmental stimuli (Cheeseman, 2007; Cuypers *et al*., 2016; Neill *et al*., 2002), and programmed cell death (Gechev *et al*., 2006; Van Breusegem and Dat, 2006). One of the most stable ROS, hydrogen peroxide (H_2O_2) is a dynamic signaling molecule due to its relatively low toxicity, long lifespan, and ability to cross cellular membranes. Generally, H_2O_2 acts as a secondary messenger by relaying the initial signal to downstream components via the activation of mitogen-activated protein kinase (MAPK) cascades (Jalmi and Sinha, 2015; Rentel *et al*., 2004; Smékalová *et al*., 2014). This signal transduction is dependent on H_2O_2-responsive components such as the serine/threonine MAPKKK OXIDATIVE SIGNAL-INDUCIBLE KINASE 1 (OXI1). In particular, H_2O_2-induced OXI1 activity initiates a signaling cascade involving the MAPKs MPK3 and MPK6 which ultimately regulates pathogen resistance and root hair growth responses (Rentel *et al*., 2004).

Considering Rentel *et al*. (2004) hypothesized that the activation of OXI1 is essential to the oxidative burst-mediated signaling pathway in *Arabidopsis thaliana*, it is important to identify possible roles for OXI1-mediated responses in other oxidative stress-inducing conditions such as phytotoxic trace metal concentrations. Although non-redox active, cadmium (Cd) is able to induce oxidative stress by either indirectly inducing the production of ROS, or inhibiting enzymatic and non-enzymatic antioxidative mechanisms (Cho and Seo, 2005; Cuypers *et al*., 2011; Opdenakker *et al*., 2012a; Smeets *et al*., 2008a, 2009). It is widely reported that Cd exposure induces oxidative stress-mediated MAPK activity and/or transcript levels (Jin *et al*., 2013; Liu *et al*., 2010; Opdenakker *et al*., 2012a; Smeets *et al*., 2013). Interestingly, Jin *et al*. (2013) observed that *A. thaliana mpk6* knockout mutants were less sensitive to Cd and connected it a mitigation of the Cd-induced ROS burst. Although Cd exposure induces a concurrent increase of *OXI1* and *MPK3/6* transcript levels (accession Columbia,

Col-0; Opdenakker *et al*., 2012a), Smeets *et al*. (2013) observed that downstream responses of MAPK-related signaling pathways are still occurring in Cd-exposed *A. thaliana oxi1* knockout plants (accession Wassilewskija, Ws). These authors hypothesized that in these mutants the absence of OXI1-mediated signal transduction is circumvented by OXI1-independent MAPK signaling pathways responsive to the Cd-induced ROS signal (Smeets *et al*., 2013).

Notwithstanding, Smeets *et al*. (2013) identified lipoxygenases as OXI1 downstream targets during Cd stress, which supports the possible role for OXI1 in lipid signaling suggested by Anthony *et al*. (2006). Alike a lipid phosphatidic acid signal, H_2O_2 induces the activation of the protein kinase 3'-PHOSPHOINOSITIDE-DEPENDENT PROTEIN KINASE 1 (PDK1)-OXI1 signaling module, which in turn regulates lipid signaling via OXI1-targeted PTI1-LIKE TYROSINE-PROTEIN KINASE 2 (PTI1-2) activity (Anthony *et al*., 2006). Additionally, Schellingen *et al*. (2015b) proposed a role for OXI1 as catalyst for ROS-induced MAPK-mediated ethylene signaling during Cd stress. Although the data is limited, these results hint at metal stress responses requiring crosstalk between ROS and other signaling pathways.

To identify possible OXI1 downstream targets, functions, and interactions, we investigated Cd-induced oxidative stress responses in wild-type (WT) and *oxi1* knockout *A. thaliana* plants. Our previous studies (Chapters 4 and 5) revealed accession-specific life strategies regarding oxidative stress signaling in response to Cd exposure. Therefore, growth, metal translocation, metabolic, and transcriptomic responses were investigated in wild types and mutants of two different *A. thaliana* accessions (Col-0 and Ws) after exposure to sublethal concentrations of Cd (5 µM) for 24 and 72 h.

7.2 Results

7.2.1 Plant growth

Hydroponically grown three-week-old *Arabidopsis thaliana* wild-type (WT) and *oxi1* knockout plants of accessions Columbia (Col-0) and Wassilewskija (Ws) were exposed to 5 µM Cd. To assess Cd-induced plant growth effects, roots and rosettes were sampled after exposure to Cd for one circadian cycle (24 h) and three days (72 h).

In non-exposed conditions, the knockout of the *oxi1* gene affected the growth of plants of accessions Col-0 and Ws differently (Figure 7.1). Whereas Col-0 *oxi1* mutants were significantly larger than the WT plants at each time point, Ws *oxi1* plants mostly grew similar (24 h) or even a bit less (72 h) as compared to their respective wild types. After exposure to Cd, the rosettes of Col-0 WT plants were significantly smaller than those of non-exposed plants at both time points; this was not observed for Col-0 *oxi1* plants. Exposure to Cd for 72 h negatively affected root growth in both Col-0 genotypes as compared to their non-exposed counterparts (Figure 7.1). Although exposure to Cd for 24 h did not affect the growth of Ws plants, both Cd-exposed Ws genotypes were significantly smaller than non-exposed plants after 72 h (Figure 7.1). To further explore the effects of Cd exposure on root and rosette growth, the growth inhibition relative to non-exposed plants was calculated $[(1-\frac{\text{weight Cd-exposed}}{\text{average weight non-exposed}})\times 100]$ and expressed as percentages (Table 7.1) for each accession and at each time point. Overall, for both accessions, significant growth inhibition in WT plants was only observed after 72 h exposure to Cd. Whereas no significant difference was observed in the percentage of growth inhibition between Ws *oxi1* mutants and WT plants, *oxi1* mutants in the Col-0 accession performed better than WT plants after Cd exposure (Table 7.1).

7.2.2 Concentrations and translocation factors of Cu and Cd

To evaluate the effects of Cd exposure on Cd and Cu uptake, the concentrations of these elements were determined in roots and leaves of non- and Cd-exposed WT and *oxi1* plants of both Col-0 and Ws accessions (Table 7.2 and 7.3). Exposure to Cd increased the concentrations of Cd in all plants (Table

7.2). No genotype effect was observed except in Col-0 plants, in which the Cd concentrations were higher in leaves of WT plants than in *oxi1* mutants after 72 h exposure. In general, Cd concentrations were higher in leaves of both Ws genotypes as compared to the Col-0 plants (both time points), whereas the opposite was observed in roots of Cd-exposed plants at 72 h (Table 7.2). Although exposure to Cd did not significantly affect the Cu concentration in leaves of Col-0 plants as compared to non-exposed plants, higher concentrations of Cu were observed in leaves of Col-0 WT plants than in *oxi1* mutants after 24 h Cd exposure (Table 7.3). Overall, the concentrations of Cu increased in roots of Cd-exposed plants. However, whereas the *oxi1* mutation had no effect in Ws plants, the Cu concentration increased significantly less in the roots of Cd-exposed Col-0 mutant plants than in their wild types (Table 7.3).

Both the translocation factors of Cd (Figure 7.2) and Cu (Figure 7.3) were calculated in Cd-exposed plants. After exposure to Cd for 24 h, the translocation factor of Cd was significantly higher in Col-0 *oxi1* mutants than in WT plants (Figure 7.2). On the contrary, the root-to-shoot Cd translocation factor was higher in Ws WT plants than in Ws *oxi1* mutants after 24 h exposure (Figure 7.2). Overall, when compared to non-exposed plants, exposure to Cd impaired root-to-shoot translocation of Cu in Col-0 and Ws plants, except in Col-0 *oxi1* plants exposed for 24 h (Figure 7.3). Whereas the Cu translocation factor was similarly affected in both Ws genotypes at both time points, the translocation factor of Cu was always higher in Cd-exposed *oxi1* mutants than in the wild types of the Col-0 accession. Moreover, the root-to-shoot Cu translocation factor significantly decreased throughout time in Cd-exposed Col-0 WT plants but not in the *oxi1* mutants (Figure 7.3).

7.2.3 Activities of antioxidative and NAD(P)H-producing enzymes

In order to evaluate the metabolic responses to Cd, the activities of antioxidative enzymes (SOD, GR, GPOD, and SPOD) and of NAD(P)H-producing enzymes (ICDH, ME and G6PDH) were determined in roots (Table 7.4 and 7.5) and leaves (Table 7.6 and 7.7) of non-exposed and Cd-exposed WT and *oxi1* plants (accessions Col-0 and Ws). In general, exposure to Cd resulted in increased activities of these enzymes in both roots and leaves. Only a few major

differences were observed between both accessions, as well as between the WT and *oxi1* genotypes. Comparing the results of the roots, no major accession- or genotype-dependent responses were observed. Significant increases of the activities of GR, GPOD (Table 7.4), and ME (Table 7.5) were observed at 72h for both accessions and genotypes. Similar observations were made for SPOD (Table 7.4) and ICDH (Table 7.5), but only in Col-0 or Ws respectively. Although significantly higher activities were detected for ME at 24 h (Table 7.5) and for G6PDH at 72 h (Table 7.4) in Ws plants after Cd exposure, an increasing trend was also observed for Col-0. Comparing WT and *oxi1* mutants within an accession revealed a significant increase in GR activity in roots of Col-0 plants after 72 h exposure, which was more pronounced in *oxi1* mutants than in WT plants (Table 7.4). In the leaves, a clear Cd-induced accession-specific effect was noticed for the activities of GPOD and SPOD after 72 h exposure to Cd, which was higher in Col-0 plants than in Ws plants (Table 7.6). In the leaves of Ws accession, minor genotype-related differences were observed for SOD, ME, and G6PDH activities (24 h: increased activity in *oxi1*, but not in WT), and GPOD (72 h: increased activity in WT, but not in *oxi1*) (Table 7.6 and 7.7).

7.2.4 Gene expression

The expression levels of several genes involved in pro- and antioxidative responses, and signaling were determined in roots and leaves of WT and *oxi1* plants of the accessions Col-0 (Table 7.8 and 7.10) and Ws (Table 7.9 and 7.11) exposed to Cd for 24 and 72 h.

Transcript levels of oxidative stress hallmark genes (Gadjev *et al*., 2006) were largely upregulated in roots of Col-0 and Ws plants (Table 7.8 and 7.9). These were generally more increased in roots of Col-0 WT plants than in *oxi1* mutants at both time points, which was only apparent in Ws plants at 72 h. Exposure to Cd induced the upregulation of the pro-oxidative gene *LOX1* in roots of Col-0 (Table 7.8) and Ws (Table 7.9) plants, but transcript levels were similar between genotypes. Concerning genes encoding antioxidative enzymes, exposure to Cd led to an upregulation of *FSD1* and a downregulation of the *CSD* genes in roots of Col-0 and Ws plants (Table 7.8 and 7.9). In particular, *FSD1* transcript levels were significantly more increased in roots of Col-0 *oxi1* mutants than Col-0 WT plants after 24 h and vice versa after 72 h. Concomitantly, *CSD1*

was downregulated after 24 h in roots of Col-0 *oxi1* mutants, but both *CSD* genes were downregulated in roots of Col-0 *oxi1* and WT plants exposed to Cd for 72 h (Table 7.8). In roots of Ws plants, *FSD1* was more upregulated in *oxi1* mutants than in the wild types after 72 h, just as a stronger and significant downregulation of *CSD* genes was observed (Table 7.9). Exposure to Cd caused the overall upregulation of primary microRNA transcripts *pri-miRNA398b* in roots of Col-0 WT plants (Table 7.8). Accession and genotype-dependent differences were observed in the expression levels of *pri-miRNA398a*: (1) genotype-specific inductions were noticed in Col-0 plants, *i.e.* an increased induction after 24 h in *oxi1* mutants as compared to the wild types and vice versa at 72 h after Cd exposure (Table 7.8); (2) between both accessions, an overall induction was seen in Col-0 plants, whereas an upregulation after 24 h and a downregulation after 72 h Cd exposure were observed in the Ws plants with no difference between the genotypes (Table 7.9).

Genes involved in signaling were affected in roots of both accessions and genotypes exposed to Cd. Transcript levels of protein kinase *OXI1* were significantly increased in Col-0 and Ws WT plants after exposure to Cd (Table 7.8 and 7.9). The majority of the downstream signaling MAPKs and transcription factors were also upregulated in both accessions (Table 7.8 and 7.9), with no clear differences between the genotypes except for *ZAT12* transcript levels, which were upregulated in WT plants but not in the *oxi1* mutants. A marker for ethylene signaling, *ERF1* gene expression was induced in both accessions. Whereas it reached a maximum in roots of Col-0 plants at 24 h, *ERF1* remained strongly upregulated in the roots of Ws plants after Cd exposure (Table 7.8 and 7.9).

In leaves, oxidative stress hallmark genes were strongly upregulated in both accessions and genotypes exposed to Cd (Table 7.10 and 7.11). This was also observed for the pro-oxidative *LOX1* and *LOX2* transcript levels in Col-0 but not in Ws plants. Whereas the gene expression of antioxidative enzymes was not altered in WT plants after Cd exposure (regardless of the accession), it was more strongly affected in leaves of Col-0 *oxi1* plants than in the Ws *oxi1* mutants (Table 7.10 and 7.11). In particular, a Cd-induced upregulation of the transcript levels of *GSH2* at both time points and *FSD1* after 72 h, as well as a

prior downregulation of *CSD2* at 24 h, was observed in Col-0 *oxi1* plants (Table 7.10). Furthermore, exposure to Cd led to an upregulation of *pri-miRNA398b* in leaves of both Col-0 genotypes after 24 h, and only in leaves of Col-0 *oxi1* plants after 72 h (Table 7.10). The transcript levels of *pri-miRNA398b* were also upregulated in leaves of both Ws genotypes, but significantly more in leaves of *oxi1* mutants than of WT plants (Table 7.11). Similar to the roots, a genotype-specific induction was observed for the gene expression of *pri-miRNA398a* in Col-0 exposed plants (Table 7.10). An accession-specific difference was also noticed for its transcript levels, more specifically an upregulation at both time points for Col-0 (Table 7.10) that was not observed at 72 h for Ws plants (Table 7.11).

Concerning the signaling genes, and in contrast to the roots, *ZAT12* was more prominently expressed after 72 h Cd exposure in leaves of *oxi1* mutants than in wild types (regardless of the accession; Table 7.10 and 7.11). Overall, exposure to Cd induced the upregulation of the ethylene responsive gene *ERF1* in leaves of both accessions, with the highest induction at 24 h. Nevertheless, these transcript levels were significantly more increased in leaves of Col-0 WT plants than in Col-0 *oxi1* mutants after exposure to Cd for 24 h, whereas after 72 h the opposite genotype-related upregulation pattern was observed (Table 7.10).

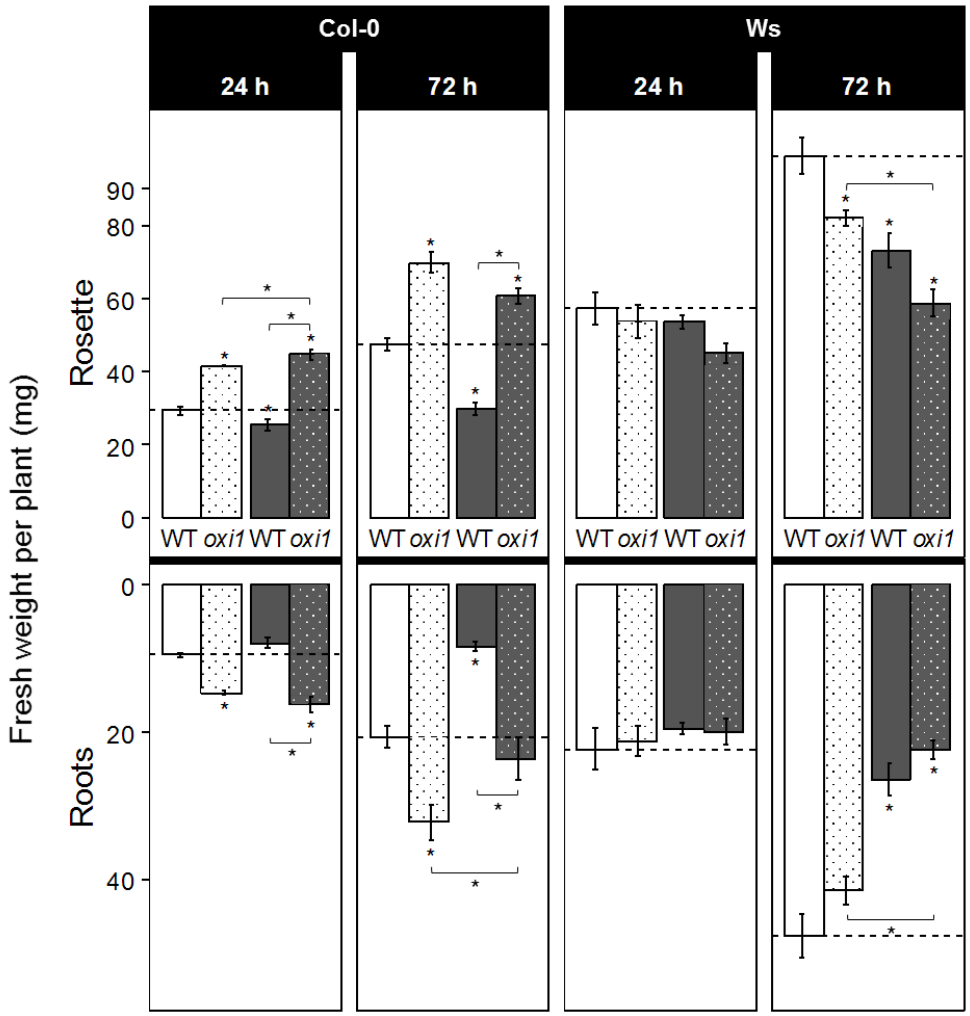

Figure 7.1 – Root and rosette fresh weight per plant (in mg) of three-week-old *A. thaliana* wild-type (WT) and *oxi1* knockout (*oxi1*) plants (accessions Col-0 and Ws) exposed to 5 µM $CdSO_4$ or not exposed for 24 and 72 h. Values are the mean ± S.E. of at least three biological replicates, each containing rosettes or roots of 25 individual plants. □ = non-exposed WT plant. ⁘ = non-exposed *oxi1* mutant. ■ = WT plant exposed to 5 µM $CdSO_4$. ⁘ = *oxi1* mutant exposed to 5 µM $CdSO_4$. Statistical significance ($P<0.05$) is indicated using asterisks for differences relative to WT non-exposed plants (within organ and time point) or between conditions connected by brackets.

Table 7.1 – Percentage of growth inhibition of roots and leaves of three-week-old *A. thaliana* plants wild-type (WT) and *oxi1* knockout (*oxi1*) plants (accessions Col-0 and Ws) exposed to 5 µM $CdSO_4$ for 24 and 72 h. Values are the mean ± S.E. of at least three biological replicates, each containing roots or rosettes of 25 individual plants. Statistical significance (P<0.05) is indicated using asterisks for differences relative to the non-exposed genotype (at each time point) or by dagger signs and printed in bold between genotypes (within organ, accession and time point).

		5 µM Cd			
		Col-0		Ws	
		Roots	Leaves	Roots	Leaves
24 h	WT	**17.04 ± 6.97 †**	**13.16 ±5.22 †**	12.13 ± 3.45	6.30 ± 3.32
	oxi1	**-11.26 ± 7.26 †**	**-7.56 ± 3.64 †**	6.01 ± 8.72	15.61 ± 5.17
72 h	WT	**59.56 ± 2.91 *,†**	**36.69 ± 3.40 *,†**	44.48 ± 4.46 *	26.12 ± 4.73 *
	oxi1	**26.66 ± 8.90 †**	**13.22 ± 3.06 †**	46.10 ± 2.96 *	28.48 ± 4.23 *

Table 7.2 – Concentrations of Cd (mg kg^{-1} dry weight) in roots and leaves of three-week-old *A. thaliana* wild-type (WT) and *oxi1* knockout (*oxi1*) plants (accessions Col-0 and Ws) exposed to 5 µM $CdSO_4$ for 24 and 72 h. Values are the mean ± S.E. of at least three biological replicates, each containing roots or rosettes of 25 individual plants. Statistical significance (P<0.05) is indicated using different uppercase letters (for differences within organ, across accessions, genotypes, and time points).

				5 µM Cd	
				Col-0	Ws
Cd	LEAVES	24 h	WT	686.57 ± 39.82 E	1281.59 ± 42.83 B
			oxi1	883.10 ± 38.70 DE	1134.59 ± 60.48 BC
		72 h	WT	1309.36 ± 68.96 B	1489.77 ± 80.86 A
			oxi1	1065.23 ± 34.63 CD	1489.37 ± 64.03 A
	ROOTS	24 h	WT	1050.84 ± 61.19 C	941.78 ± 37.84 C
			oxi1	1016.27 ± 46.35 C	1064.52 ± 40.95 C
		72 h	WT	1943.50 ± 80.10 A	1623.91 ± 30.20 B
			oxi1	1722.27 ± 66.17 AB	1490.76 ± 57.92 B

Table 7.3 – Concentrations of Cu (mg kg^{-1} dry weight) in roots and leaves of three-week-old *A. thaliana* wild-type (WT) and *oxi1* knockout (*oxi1*) plants (accessions Col-0 and Ws) exposed to 5 µM $CdSO_4$ or not exposed for 24 and 72 h. Values are the mean ± S.E. of at least three biological replicates, each containing roots or rosettes of 25 individual plants. Statistical significance (P<0.05) is indicated using different lowercase letters (for differences within accession, organ, and time point).

				Col-0		Ws	
				Control	5 µM Cd	Control	5 µM Cd
Cu	LEAVES	24 h	WT	10.75 ± 0.40 a	11.39 ± 0.70 a	9.62 ± 0.52 a	9.29 ± 0.07 a
			oxi1	9.60 ± 0.37 ab	7.74 ± 0.53 b	9.42 ± 0.64 a	9.26 ± 0.13 a
		72 h	WT	9.57 ± 0.44 a	9.68 ± 0.98 a	8.20 ± 0.61 a	7.39 ± 0.18 a
			oxi1	8.87 ± 0.51 a	7.64 ± 0.18 a	6.92 ± 0.34 a	7.55 ± 0.58 a
	ROOTS	24 h	WT	30.35 ± 3.29 b	79.58 ± 4.84 a	31.89 ± 3.26 b	49.59 ± 4.13 a
			oxi1	34.26 ± 4.86 b	45.66 ± 2.98 b	34.82 ± 1.30 b	50.10 ± 2.66 a
		72 h	WT	20.80 ± 0.52 c	85.26 ± 4.00 a	14.95 ± 1.35 b	46.42 ± 4.83 a
			oxi1	19.79 ± 3.50 c	36.31 ± 3.33 b	16.12 ± 0.94 b	50.67 ± 1.64 a

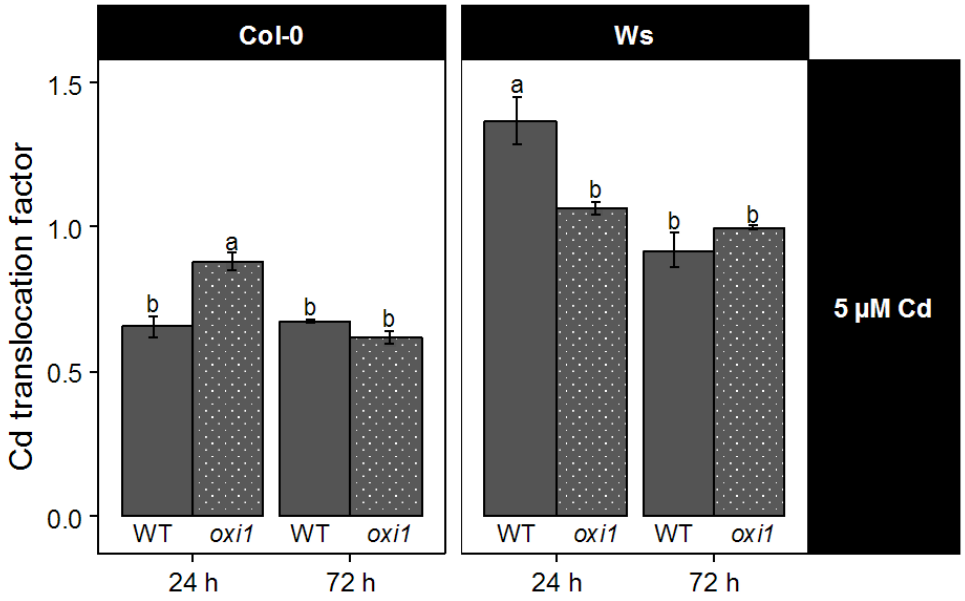

Figure 7.2 – Root-to-shoot translocation factors of Cd in three-week-old *A. thaliana* wild-type (WT) and *oxi1* knockout (*oxi1*) plants (accessions Col-0 and Ws) exposed to 5 µM $CdSO_4$ or not exposed for 24 and 72 h. Values are the mean ± S.E. of at least three biological replicates. ■ = WT plant exposed to 5 µM $CdSO_4$. ▩ = *oxi1* mutant exposed to 5 µM $CdSO_4$. Statistical significance ($P<0.05$) is indicated using different lowercase (for differences within accession).

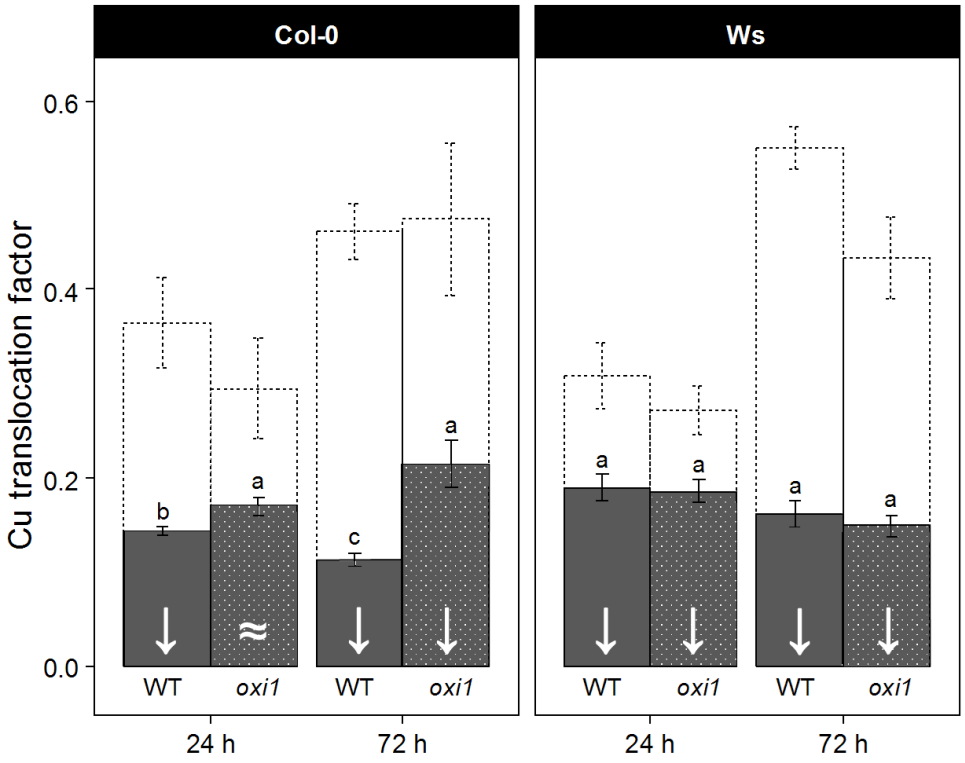

Figure 7.3 – Root-to-shoot translocation factors of Cu in three-week-old *A. thaliana* wild-type (WT) and *oxi1* knockout (*oxi1*) plants (accessions Col-0 and Ws) exposed to 5 µM $CdSO_4$ for 24 and 72 h. Values are the mean ± S.E. of at least three biological replicates. ■ = WT plant exposed to 5 µM $CdSO_4$. ▩ = *oxi1* mutant exposed to 5 µM $CdSO_4$. Statistical significance ($P<0.05$) is indicated by arrows (to illustrate differences relative to non-exposed genotype shown as dashed bars) and using different lowercase (for differences within accession).

Table 7.4 – Activities of antioxidative enzymes (mU mg^{-1} fresh weight) in roots of three-week-old *A. thaliana* wild-type (WT) and *oxi1* knockout (*oxi1*) plants (accessions Col-0 and Ws) exposed to 5 µM $CdSO_4$ or not exposed for 24 and 72 h. Values are the mean ± S.E. of at least three biological replicates, each containing roots of at least two individual plants. Statistical significance ($P<0.05$) is indicated using different lowercase letters (for differences within organ and time point) and the conditions in which differences occur are highlighted in grey. Abbreviations: GR: glutathione reductase; SOD: superoxide dismutase; GPOD: guaiacol peroxidase; SPOD: syringaldazine peroxidase.

			Col-0		Ws	
			Control	5 µM Cd	Control	5 µM Cd
GR	24 h	WT	42.86 ± 2.78 a	88.78 ± 15.9 a	63.90 ± 16.69 a	89.22 ± 20.75 a
		oxi1	118.71 ± 36.95 a	173.11 ± 55.68 a	67.96 ± 11.93 a	160.33 ± 37.13 a
	72 h	WT	105.89 ± 24.99 c	169.91 ± 13.02 b	64.67 ± 25.36 b	243.93 ± 22.17 a
		oxi1	108.77 ± 29.16 bc	237.96 ± 21.07 a	70.85 ± 24.41 b	252.98 ± 15.14 a
SOD	24 h	WT	109.79 ± 18.50 ab	68.96 ± 15.00 b	70.31 ± 14.47 b	67.19 ± 3.82 b
		oxi1	161.50 ± 28.05 a	119.70 ± 16.57 ab	86.62 ± 13.02 ab	123.07 ± 1.89 a
	72 h	WT	101.05 ± 26.00 a	112.00 ± 16.42 a	118.85 ± 38.54 a	115.34 ± 20.21 a
		oxi1	190.22 ± 128.46 a	123.30 ± 21.50 a	93.20 ± 7.34 a	128.21 ± 9.92 a
GPOD	24 h	WT	553.30 ± 134.43 a	855.91 ± 109.72 a	377.04 ± 4.86 a	691.33 ± 132.17 a
		oxi1	557.76 ± 331.65 a	1264.92 ± 407.85 a	447.61 ± 85.80 a	818.14 ± 189.41 a
	72 h	WT	797.58 ± 166.91 b	1585.97 ± 181.99 a	369.16 ± 184.64 b	1452.94 ± 141.60 a
		oxi1	708.14 ± 243.05 b	1933.53 ± 19.13 a	495.56 ± 170.69 b	1487.09 ± 70.54 a
SPOD	24 h	WT	1343.20 ± 703.79 a	1425.64 ± 273.25 a	707.16 ± 180.39 a	885.24 ± 195.28 a
		oxi1	1398.73 ± 748.66 a	2543.08 ± 938.04 a	812.86 ± 168.18 a	1768.53 ± 586.27 a
	72 h	WT	1737.52 ± 591.75 a	3253.69 ± 666.05 a	479.36 ± 127.38 c	2308.62 ± 323.62 ab
		oxi1	2227.00 ± 29.73 a	3597.32 ± 571.78 a	1096.56 ± 495.21 bc	2509.09 ± 171.48 a

Table 7.5 – Activities of NAD(P)H-producing enzymes (mU mg^{-1} fresh weight) in roots of three-week-old *A. thaliana* wild-type (WT) and *oxi1* knockout (*oxi1*) plants (accessions Col-0 and Ws) exposed to 5 µM $CdSO_4$ or not exposed for 24 and 72 h. Values are the mean ± S.E. of at least three biological replicates, each containing roots of at least two individual plants. Statistical significance (P<0.05) is indicated using different lowercase letters (for differences within organ and time point) and the conditions in which differences occur are highlighted in grey. Abbreviations: ICDH: isocitrate dehydrogenase; ME: malic enzyme; G6PDH: glucose-6-phosphate dehydrogenase.

			Col-0		Ws	
			Control	5 µM Cd	Control	5 µM Cd
ICDH	24 h	WT	101.74 ± 30.01 a	131.39 ± 44.47 a	37.99 ± 15.97 b	116.68 ± 31.08 ab
		oxi1	157.79 ± 101.53 a	231.32 ± 87.29 a	82.37 ± 23.01 ab	200.25 ± 54.05 b
	72 h	WT	137.29 ± 41.35 b	331.52 ± 23.03 a	193.93 ± 118.91 ab	369.33 ± 30.20 a
		oxi1	146.59 ± 53.93 b	353.18 ± 24.80 a	88.57 ± 40.46 b	338.22 ± 19.36 ab
ME	24 h	WT	76.97 ± 19.88 a	126.76 ± 29.78 a	35.41 ± 6.98 b	93.22 ± 15.38 ab
		oxi1	125.23 ± 47.36 a	210.99 ± 69.73 a	53.39 ± 15.30 b	175.55 ± 38.24 a
	72 h	WT	111.53 ± 28.23 b	421.91 ± 31.31 a	102.47 ± 51.27 b	366.34 ± 24.13 a
		oxi1	115.23 ± 41.46 b	480.85 ± 25.06 a	53.94 ± 24.12 b	350.43 ± 17.44 a
G6PDH	24 h	WT	5.04 ± 1.57 a	21.59 ± 10.80 a	16.53 ± 5.25 a	9.98 ± 5.01 a
		oxi1	45.41 ± 14.87 a	38.94 ± 21.11 a	19.24 ± 4.66 a	8.70 ± 0.72 a
	72 h	WT	5.98 ± 1.90 b	26.06 ± 1.65 ab	9.27 ± 5.00 b	55.49 ± 9.97 a
		oxi1	13.89 ± 2.94 ab	38.55 ± 10.28 a	6.94 ± 2.91 b	74.94 ± 12.32 a

Table 7.6 – Activities of antioxidative (mU mg^{-1} fresh weight) in leaves of three-week-old *A. thaliana* wild-type (WT) and *oxi1* knockout (*oxi1*) plants (accessions Col-0 and Ws) exposed to 5 µM $CdSO_4$ or not exposed for 24 and 72 h. Values are the mean ± S.E. of at least three biological replicates, each containing rosettes of at least two individual plants. Statistical significance ($P<0.05$) is indicated using different lowercase letters (for differences within organ and time point) and the conditions in which differences occur are highlighted in grey. Abbreviations: see Table 7.4.

			Col-0		Ws	
			Control	5 µM Cd	Control	5 µM Cd
GR	24 h	WT	872.14 ± 47.96 a	1133.84 ± 0.05 a	851.58 ± 122.55 a	1055.06 ± 67.42 a
		oxi1	794.07 ± 211.22 a	1067.70 ± 42.05 a	1030.00 ± 32.03 a	1100.04 ± 39.28 a
	72 h	WT	828.67 ± 39.95 b	1075.80 ± 47.91 a	634.20 ± 176.64 a	953.59 ± 31.51 a
		oxi1	850.25 ± 47.03 b	1127.54 ± 27.31 a	760.78 ± 10.31 a	905.54 ± 89.28 a
SOD	24 h	WT	367.76 ± 40.50 a	317.46 ± 3.74 a	301.20 ± 33.15 b	299.82 ± 7.10 b
		oxi1	372.46 ± 60.06 a	354.36 ± 32.84 a	323.62 ± 18.12 b	403.52 ± 1.85 a
	72 h	WT	249.82 ± 70.80 a	254.87 ± 18.20 a	188.26 ± 43.72 a	257.89 ± 28.82 a
		oxi1	341.38 ± 7.98 a	357.35 ± 24.59 a	212.52 ± 56.52 a	232.45 ± 9.79 a
GPOD	24 h	WT	23.64 ± 4.06 ab	42.06 ± 8.66 a	17.88 ± 7.06 a	36.66 ± 7.82 a
		oxi1	7.63 ± 5.44 b	22.36 ± 5.25 ab	22.44 ± 9.39 a	23.31 ± 1.87 a
	72 h	WT	15.82 ± 3.94 b	243.45 ± 16.19 a	6.93 ± 3.26 b	36.75 ± 8.68 a
		oxi1	12.03 ± 2.05 b	185.76 ± 22.67 a	15.09 ± 7.53 ab	20.48 ± 1.68 ab
SPOD	24 h	WT	57.08 ± 23.18 a	219.87 ± 63.35 a	102.93 ± 43.91 a	207.41 ± 45.11 a
		oxi1	33.46 ± 9.12 a	188.15 ± 43.27 a	118.97 ± 36.32 a	223.17 ± 15.42 a
	72 h	WT	89.49 ± 18.23 b	1421.37 ± 127.49 a	110.81 ± 22.40 a	189.89 ± 56.43 a
		oxi1	83.35 ± 8.62 b	1051.10 ± 96.61 a	45.19 ± 19.99 a	197.37 ± 9.70 a

Table 7.7 – Activities of NAD(P)H-producing enzymes (mU mg^{-1} fresh weight) in leaves of three-week-old *A. thaliana* wild-type (WT) and *oxi1* knockout (*oxi1*) plants (accessions Col-0 and Ws) exposed to 5 µM $CdSO_4$ or not exposed for 24 and 72 h. Values are the mean ± S.E. of at least three biological replicates, each containing rosettes of at least two individual plants. Statistical significance (P<0.05) is indicated using different lowercase letters (for differences within organ and time point) and the conditions in which differences occur are highlighted in grey. Abbreviations: see Table 7.5.

			Col-0		Ws	
			Control	5 µM Cd	Control	5 µM Cd
ICDH	24 h	WT	559.68 ± 25.79 a	647.77 ± 24.68 a	618.51 ± 218.03 a	492.95 ± 25.93 a
		oxi1	471.41 ± 89.16 a	605.55 ± 40.57 a	457.36 ± 19.35 a	454.54 ± 22.09 a
	72 h	WT	450.08 ± 38.11 c	615.23 ± 19.18 ab	330.77 ± 59.84 a	402.64 ± 8.68 a
		oxi1	530.17 ± 26.67 bc	663.35 ± 28.14 a	341.47 ± 26.08 a	355.05 ± 29.20 a
ME	24 h	WT	242.72 ± 6.70 b	501.06 ± 49.35 a	154.88 ± 23.55 b	230.86 ± 9.90 a
		oxi1	126.45 ± 70.81 b	472.54 ± 29.86 a	203.86 ± 6.82 ab	251.45 ± 17.91 a
	72 h	WT	220.22 ± 10.33 b	771.33 ± 132.53 a	169.89 ± 22.83 c	397.00 ± 1.77 a
		oxi1	285.36 ± 11.87 b	914.35 ± 39.83 a	183.57 ± 12.71 c	304.82 ± 20.47 b
G6PDH	24 h	WT	105.96 ± 7.61 a	136.36 ± 10.97 a	60.76 ± 16.62 b	115.95 ± 11.28 a
		oxi1	71.49 ± 31.76 a	146.31 ± 11.57 a	98.95 ± 5.17 ab	116.66 ± 6.56 a
	72 h	WT	95.06 ± 6.34 b	168.55 ± 18.84 a	73.75 ± 27.27 ab	118.88 ± 3.88 a
		oxi1	111.51 ± 12.88 b	183.75 ± 9.71 a	67.87 ± 6.44 b	102.71 ± 6.03 ab

Table 7.8 – Transcript levels in roots of three-week-old *A. thaliana* wild-type (WT) and *oxi1* knockout (*oxi1*) plants (accession Col-0) exposed to 5 µM $CdSO_4$ for 24 or 72 h. Values are the mean normalized expression relative to the non-exposed genotype (set at 1.00) ± S.E. of at least three biological replicates, each containing roots of at least one individual plant. Resolution values are mean inverse normalization factors relative to the non-exposed genotype, indicating the stability of the selected reference genes. Statistically significant (P<0.05) Cd-induced changes in expression relative to the non-exposed genotype are indicated by color (■ = upregulation; ■ = downregulation). Statistically significant (P<0.05) differences between genotypes are indicated by asterisks (within time point) and printed in bold. Abbreviations: *UPOX: upregulated by oxidative stress; Defensin-like: protein member of the defensin-like (DEFL) family; AT1G19020: unknown protein; AT1G05340: unknown protein; TIR-class: Toll-Interleukin-Resistance (TIR) domain family protein; LOX: lipoxygenase; GSH2: glutathione synthetase 2; FSD1: Fe superoxide dismutase 1; CSD: Cu/Zn superoxide dismutase; pri-miR398: primary microRNA 398; OXI1: oxidative signal inducible 1; MPK: mitogen-activated protein kinase; ZAT12: zinc finger of Arabidopsis thaliana 12; WRKY: WRKY DNA-binding protein; ERF1: ethylene response factor 1.*

24 h		Col-0	72 h	
WT	***oxi1***		**WT**	***oxi1***
0.97 ± 0.07	1.01 ± 0.06	Resolution	0.99 ± 0.04	1.10 ± 0.09
Genes encoding oxidative stress hallmark proteins				
4.16 ± 0.70	**2.13 ± 0.24 ***	*UPOX*	1.46 ± 0.10	1.95 ± 0.02
31.98 ± 20.93	4.80 ± 0.94	*Defensin-like*	**98.57 ± 33.57**	**17.38 ± 3.29 ***
6.39 ± 0.65	5.74 ± 1.26	*AT1G19020*	4.50 ± 0.11	3.48 ± 1.06
1.19 ± 0.13	1.00 ± 0.13	*AT1G05340*	1.34 ± 0.09	0.91 ± 0.15
7.39 ± 0.58	**3.5 ± 0.75 ***	*TIR-class*	**7.29 ± 1.44**	**2.64 ± 0.60 ***
Gene encoding ROS-producing enzyme				
6.62 ± 1.98	9.17 ± 0.73	*LOX1*	4.82 ± 0.80	3.12 ± 0.29
Genes encoding antioxidative enzymes				
1.49 ± 0.20	1.96 ± 0.22	*GSH2*	0.90 ± 0.22	0.74 ± 0.09
5.32 ± 0.25	**25.16 ± 2.76 ***	*FSD1*	**31.74 ± 10.61**	**18.02 ± 0.81 ***
0.96 ± 0.10	0.68 ± 0.04	*CSD1*	0.40 ± 0.01	0.49 ± 0.02
0.86 ± 0.05	0.72 ± 0.12	*CSD2*	0.52 ± 0.05	0.52 ± 0.02
Primary microRNA transcripts				
0.93 ± 0.09	**11.99 ± 1.86 ***	*pri-miR398a*	**6.42 ± 1.00**	**3.51 ± 0.80 ***
2.96 ± 0.17	3.74 ± 0.02	*pri-miR398b*	4.49 ± 0.29	3.33 ± 0.56
Genes encoding protein kinases				
1.98 ± 0.13	ND	*OXI1*	1.57 ± 0.17	ND
2.41 ± 0.16	3.03 ± 0.17	*MPK3*	2.08 ± 0.16	1.83 ± 0.21
1.27 ± 0.08	1.21 ± 0.04	*MPK6*	0.99 ± 0.02	0.87 ± 0.09

Table 7.8 – Transcript levels in roots of three-week-old *A. thaliana* wild-type (WT) and *oxi1* knockout (*oxi1*) plants (accession Col-0) exposed to 5 µM $CdSO_4$ for 24 or 72 h. Continuation.

24 h		Col-0	72 h	
WT	***oxi1***		**WT**	***oxi1***
0.97 ± 0.07	1.01 ± 0.06	Resolution	0.99 ± 0.04	1.10 ± 0.09
Genes encoding transcription factors				
2.67 ± 0.16	1.34 ± 0.32	*ZAT12*	3.27 ± 0.49	1.15 ± 0.49
1.59 ± 0.18	**0.82 ± 0.08 ***	*WRKY29*	1.49 ± 0.14	1.10 ± 0.16
4.40 ± 0.25	5.27 ± 0.55	*WRKY33*	3.16 ± 0.12	2.81 ± 0.65
Gene encoding protein involved in ethylene signaling				
134.2 ± 7.40	180.84 ± 28.75	*ERF1*	**8.72 ± 1.43**	**6.88 ± 1.35 ***

Table 7.9 – Transcript levels in roots of three-week-old *A. thaliana* wild-type (WT) and *oxi1* knockout (*oxi1*) plants (accession Ws) exposed to 5 µM $CdSO_4$ for 24 and 72 h. Values are the mean normalized expression relative to the non-exposed genotype (set at 1.00) ± S.E. of at least three biological replicates, each containing roots of at least one individual plant. Resolution values are mean inverse normalization factors relative to the non-exposed genotype, indicating the stability of the selected reference genes. Statistically significant (P<0.05) Cd-induced changes in expression relative to the non-exposed genotype are indicated by color (= upregulation; = downregulation). Statistically significant (P<0.05) differences between genotypes are indicated by asterisks (within time point) and printed in bold. Abbreviations: see Table 7.8.

24 h		Ws	72 h	
WT	***oxi1***		**WT**	***oxi1***
1.32 ± 0.20	0.95 ± 0.04	Resolution	0.70 ± 0.07	1.12 ± 0.09
Genes encoding oxidative stress hallmark proteins				
4.89 ± 0.01	9.98 ± 4.72	*UPOX*	4.73 ± 1.08	3.25 ± 0.86
6.38 ± 1.00	5.21 ± 1.30	*Defensin-like*	129.32 ± 26.57	54.28 ± 18.48
7.47 ± 0.93	7.49 ± 0.21	*AT1G19020*	**10.54 ± 0.54**	**4.71 ± 0.87 ***
1.32 ± 0.26	**2.75 ± 0.25 ***	*AT1G05340*	**5.15 ± 0.22**	**2.56 ± 0.28 ***
4.24 ± 0.16	5.00 ± 1.21	*TIR-class*	14.48 ± 2.02	10.31 ± 0.50
Gene encoding ROS-producing enzyme				
3.26 ± 0.38	3.60 ± 0.85	*LOX1*	8.92 ± 2.23	9.71 ± 0.55
Genes encoding antioxidative enzymes				
1.36 ± 0.12	1.07 ± 0.02	*GSH2*	0.92 ± 0.09	1.69 ± 0.38
105.08 ± 13.96	98.89 ± 44.29	*FSD1*	**4.85 ± 0.38**	**17.79 ± 2.03 ***
1.07 ± 0.09	1.03 ± 0.16	*CSD1*	0.69 ± 0.02	0.59 ± 0.04
0.96 ± 0.04	0.74 ± 0.11	*CSD2*	**0.73 ± 0.05**	**0.54 ± 0.04 ***
Primary microRNA transcripts				
4.05 ± 0.55	4.23 ± 0.17	*pri-miR398a*	0.15 ± 0.04	0.19 ± 0.03
2.89 ± 0.15	2.90 ± 0.37	*pri-miR398b*	1.88 ± 0.28	3.44 ± 0.39
Genes encoding protein kinases				
2.57 ± 0.46	ND	*OXI1*	3.03 ± 0.87	ND
2.39 ± 0.19	2.34 ± 0.15	*MPK3*	**2.39 ± 0.22**	**1.81 ± 0.04 ***
1.14 ± 0.05	0.98 ± 0.06	*MPK6*	0.90 ± 0.05	0.91 ± 0.10
Genes encoding transcription factors				
2.02 ± 0.41	1.91 ± 0.37	*ZAT12*	**4.61 ± 0.23**	**1.91 ± 0.25 ***
1.95 ± 0.13	1.58 ± 0.29	*WRKY29*	2.58 ± 0.08	1.94 ± 0.21
4.78 ± 0.49	5.55 ± 0.93	*WRKY33*	3.88 ± 0.40	3.10 ± 0.30
Gene encoding protein involved in ethylene signaling				
40.13 ± 4.29	77.02 ± 26.13	*ERF1*	46.54 ± 9.19	40.10 ± 11.57

Table 7.10 – Transcript levels in leaves of three-week-old *A. thaliana* wild-type (WT) and *oxi1* knockout (*oxi1*) plants (accession Col-0) exposed to 5 µM $CdSO_4$ for 24 or 72 h. Values are the mean normalized expression relative to the non-exposed genotype (set at 1.00) ± S.E. of at least three biological replicates, each containing rosettes of at least one individual plant. Resolution values are mean inverse normalization factors relative to the non-exposed genotype, indicating the stability of the selected reference genes. Statistically significant (P<0.05) Cd-induced changes in expression relative to the non-exposed genotype are indicated by color (= upregulation; = downregulation). Statistically significant (P<0.05) differences between genotypes are indicated by asterisks (within time point) and printed in bold. Abbreviations: see Table 7.8.

24 h		Col-0	72 h	
WT	***oxi1***		**WT**	***oxi1***
1.61 ± 0.13	1.25 ± 0.24	Resolution	0.74 ± 0.06	0.78 ± 0.05
Genes encoding oxidative stress hallmark proteins				
5.93 ± 1.16	6.26 ± 0.05	*UPOX*	6.27 ± 2.19	10.20 ± 1.67
27.80 ± 4.70	32.27 ± 0.96	*Defensin-like*	46.09 ± 17.38	34.48 ± 3.78
129.71 ± 43.01	77.68 ± 2.77	*AT1G19020*	9.28 ± 4.87	35.77 ± 4.24
77.41 ± 36.40	53.31 ± 5.79	*AT1G05340*	30.25 ± 15.94	40.35 ± 5.01
231.62 ± 80.13	139.96 ± 4.65	*TIR-class*	**9.90 ± 4.53**	**33.63 ± 3.78 ***
Genes encoding ROS-producing enzymes				
1.99 ± 0.37	2.28 ± 0.20	*LOX1*	1.90 ± 0.18	1.89 ± 0.12
9.42 ± 2.21	11.48 ± 0.27	*LOX2*	2.30 ± 0.50	2.84 ± 0.14
Genes encoding antioxidative enzymes				
2.13 ± 0.50	4.03 ± 0.94	*GSH2*	1.10 ± 0.37	1.85 ± 0.21
4.83 ± 1.14	2.95 ± 0.52	*FSD1*	**0.85 ± 0.15**	**4.89 ± 0.30 ***
1.40 ± 0.23	1.42 ± 0.20	*CSD1*	0.85 ± 0.02	0.64 ± 0.09
0.61 ± 0.17	0.30 ± 0.04	*CSD2*	0.22 ± 0.01	0.20 ± 0.03

Table 7.10 – Transcript levels in leaves of three-week-old *A. thaliana* wild-type (WT) and *oxi1* knockout (*oxi1*) plants (accession Col-0) exposed to 5 µM $CdSO_4$ for 24 or 72 h. Continuation.

24 h		Col-0	72 h	
WT	***oxi1***		**WT**	***oxi1***
1.61 ± 0.13	1.25 ± 0.24	Resolution	0.74 ± 0.06	0.78 ± 0.05
Primary microRNA transcripts				
2330.58 ± 267.36	**990.17 ± 185.34 ***	*pri-miR398a*	**13.67 ± 0.86**	**76.52 ± 9.68 ***
7.51 ± 0.39	4.05 ± 0.70	*pri-miR398b*	1.72 ± 0.15	3.39 ± 0.31
Genes encoding protein kinases				
272.11 ± 75.02	ND	*OXI1*	62.59 ± 36.07	ND
5.83 ± 1.49	4.86 ± 0.26	*MPK3*	2.24 ± 0.34	3.47 ± 0.25
2.28 ± 0.51	2.38 ± 0.06	*MPK6*	1.40 ± 0.06	1.46 ± 0.11
Genes encoding transcription factors				
78.56 ± 29.24	88.10 ± 2.71	*ZAT12*	**4.39 ± 2.53**	**25.62 ± 2.69 ***
1.02 ± 0.07	1.10 ± 0.20	*WRKY29*	2.80 ± 0.33	1.93 ± 0.05
41.42 ± 13.28	31.88 ± 2.30	*WRKY33*	7.69 ± 3.75	6.62 ± 1.38
Gene encoding protein involved in ethylene signaling				
767.03 ± 165.52	**175.99 ± 16.96 ***	*ERF1*	**10.18 ± 3.26**	**55.56 ± 8.07 ***

Table 7.11 – Transcript levels in leaves of three-week-old *A. thaliana* wild-type (WT) and *oxi1* knockout (*oxi1*) plants (accession Ws) exposed to 5 µM $CdSO_4$ for 24 and 72 h. Values are the mean normalized expression relative to the non-exposed genotype (set at 1.00) ± S.E. of at least three biological replicates, each containing rosettes of at least one individual plant. Resolution values are mean inverse normalization factors relative to the non-exposed genotype, indicating the stability of the selected reference genes. Statistically significant (P<0.05) Cd-induced changes in expression relative to the non-exposed genotype are indicated by color (= upregulation; = downregulation). Statistically significant (P<0.05) differences between genotypes are indicated by asterisks (within time point) and printed in bold. Abbreviations: see Table 7.8.

24 h		Ws	72 h	
WT	***oxi1***		**WT**	***oxi1***
1.07 ± 0.09	1.20 ± 0.09	Resolution	1.01 ± 0.07	0.85 ± 0.07
Genes encoding oxidative stress hallmark proteins				
2.21 ± 0.19	2.40 ± 0.75	*UPOX*	2.21 ± 0.32	2.01 ± 0.15
6.81 ± 0.60	5.12 ± 1.21	*Defensin-like*	8.93 ± 2.33	7.23 ± 3.41
56.87 ± 15.44	23.36 ± 12.87	*AT1G19020*	3.58 ± 0.06	3.59 ± 1.33
7.82 ± 2.30	4.84 ± 1.17	*AT1G05340*	4.14 ± 1.55	7.29 ± 3.11
422.48 ± 106.43	147.2 ± 80.10	*TIR-class*	8.84 ± 1.00	11.97 ± 5.94
Genes encoding ROS-producing enzymes				
1.27 ± 0.04	1.49 ± 0.12	*LOX1*	**1.11 ± 0.11**	**2.04 ± 0.18 ***
2.24 ± 0.08	2.07 ± 0.07	*LOX2*	1.95 ± 0.51	1.72 ± 0.23
Genes encoding antioxidative enzymes				
1.04 ± 0.07	1.15 ± 0.14	*GSH2*	1.29 ± 0.15	1.18 ± 0.08
1.92 ± 0.60	3.03 ± 0.69	*FSD1*	0.55 ± 0.28	0.65 ± 0.23
1.25 ± 0.14	0.92 ± 0.01	*CSD1*	0.67 ± 0.06	0.46 ± 0.08
0.80 ± 0.08	0.82 ± 0.06	*CSD2*	0.45 ± 0.22	0.17 ± 0.03
Primary microRNA transcripts				
645.33 ± 140.21	532.96 ± 183.43	*pri-miR398a*	6.62 ± 2.01	2.07 ± 0.91
5.00 ± 0.48	**10.2 ± 1.05 ***	*pri-miR398b*	**2.05 ± 0.10**	**4.52 ± 0.78 ***
Genes encoding protein kinases				
38.74 ± 1.32	ND	*OXI1*	5.94 ± 1.96	ND
5.35 ± 0.61	4.08 ± 1.63	*MPK3*	2.34 ± 0.38	2.36 ± 0.27
1.48 ± 0.12	1.33 ± 0.16	*MPK6*	1.11 ± 0.09	1.10 ± 0.06

Table 7.11 – Transcript levels in leaves of three-week-old *A. thaliana* wild-type (WT) and *oxi1* knockout (*oxi1*) plants (accession Ws) exposed to 5 µM $CdSO_4$ for 24 and 72 h. Continuation.

24 h		Ws	72 h	
WT	***oxi1***		**WT**	***oxi1***
1.07 ± 0.09	1.20 ± 0.09	Resolution	1.01 ± 0.07	0.85 ± 0.07
Genes encoding transcription factors				
8.83 ± 2.18	4.25 ± 1.78	*ZAT12*	1.79 ± 0.64	3.25 ± 0.79
0.93 ± 0.03	1.04 ± 0.21	*WRKY29*	1.53 ± 0.32	0.78 ± 0.26
18.64 ± 5.94	14.76 ± 7.64	*WRKY33*	3.72 ± 0.38	2.81 ± 0.82
Gene encoding protein involved in ethylene signaling				
243.55 ± 42.6	109.81 ± 53.36	*ERF1*	12.04 ± 2.67	7.28 ± 1.73

7.3 Discussion

Cadmium is one of the most widespread toxic non-essential elements. Although not redox-active, Cd indirectly induces ROS production in plant cells by interfering with diverse cellular processes such as photosynthesis and respiration (Keunen *et al*., 2011b). This results in an oxidative imbalance and culminates in oxidative stress-related responses. These oxidative stress responses are dependent on the transduction of the extracellular Cd stimulus through signaling pathways known to involve mitogen-activated protein kinase (MAPK) phosphorylation cascades (Liu *et al*., 2010; Opdenakker *et al*., 2012a; Smeets *et al*., 2013; Smékalová *et al*., 2014). Several authors suggested that these signal transduction pathways are initiated by ROS and mediated by the protein kinase OXIDATIVE-SIGNAL INDUCIBLE 1 (OXI1) protein kinase (Opdenakker *et al*., 2012a; Rentel *et al*., 2004; Smeets *et al*., 2013). To further understand the role of OXI1 during Cd stress, we investigated Cd-induced responses in wild types and *oxi1* knockout mutants of two different *Arabidopsis thaliana* accessions, Columbia (Col-0) and Wassilewskija (Ws), as our previous studies revealed accession-specific life strategies in relation to oxidative stress signaling as a response to Cd exposure (Chapter 4 and 5).

Root and rosette average weights of Col-0 plants were always significantly higher in *oxi1* knockout mutants than in WT plants grown in non-exposed conditions (Figure 7.1), whereas a significantly lower average rosette weight was observed after 72 h in Ws *oxi1* mutants as compared to its wild types (Figure 7.1). These results suggest that OXI1 is essential for normal plant growth. Since Rentel *et al*. (2004) observed a greater proportion of shorter root hairs in *oxi1* than in Ws WT plants, the observed effects to plant growth in this accession can (at least partly) result from the higher number of deficient root hairs in Ws *oxi1* plants, which ultimately affects the absorption of water and nutrients. Even though exposure to Cd decreased root and rosette weights in both accessions, genotype-related rosette weight differences were only observed in Col-0 plants but not in Ws plants (Figure 7.1, Table 7.1). In Col-0 plants, the average rosette weight was already affected after 24 h of exposure to Cd in WT plants, while rosette weight of *oxi1* plants significantly increased relatively to non-exposed plants at the same time point. Moreover, exposure to Cd for 72 h

only affected the weight of rosettes of Col-0 WT plants (Figure 7.1), as well as significantly inhibited root and rosette growth in Col-0 WT plants but not in Col-0 *oxi1* mutants (Table 7.1). Together, these growth-related parameters suggest that, within this experimental timeframe, Col-0 *oxi1* mutants are less sensitive to Cd than Col-0 wild types. In addition, the overall upregulation of the oxidative stress hallmark genes (Gadjev *et al*., 2006) indicates that exposure to Cd induces oxidative stress in Col-0 and Ws plants (Table 7.8-7.11). Nonetheless, a genotype-specific expression pattern is apparent in roots of Col-0 plants as these hallmark genes were generally less upregulated in *oxi1* mutants than in WT plants (Table 7.8). These results indicate that Cd induced different oxidative stress levels in both Col-0 genotypes, reinforcing our suggestion that Col-0 *oxi1* plants are less sensitive to Cd than their WT counterparts.

The concentration of Cd increased in roots and leaves of plants exposed to Cd (Table 7.2). While no significant differences were observed between wild types and *oxi1* mutants of Ws background, the Cd concentration was lower in leaves of Col-0 *oxi1* than of Col-0 WT plants after 72 h. Nevertheless, the Cd translocation factors were similar in both Col-0 genotypes at this time point (Figure 7.2). In fact, the translocation factors of Cd only differed between the genotypes of both accessions after the initial exposure time of 24 h. In Col-0 plants, the Cd translocation factor was significantly higher in *oxi1* mutants than in the wild types (Figure 7.2). The opposite genotype-related pattern was observed in Ws plants (Figure 7.2). These results indicate that, in both accessions, the *oxi1* mutation led to alterations to the initial root-to-shoot translocation of Cd. Previously, it was discussed that the differences in Cd translocation observed between Col-0 and Ws WT plants derived from accession-specific HEAVY METAL ATPase (HMA) responses (Chapter 5). In particular, *HMA3* encodes for a truncated non-functional HMA3 protein in Col-0 plants (Hussain *et al*., 2004; Morel *et al*., 2009), which leads to *HMA4* overexpression when these plants are exposed to Cd (Park *et al*., 2012). In turn, this results in more Cd translocated to the shoots of Col-0 plants, which Park *et al*. (2012) associated to an increased sensitivity to Cd as compared to Ws plants. Therefore, the apparent lower sensitivity of Col-0 *oxi1* plants to Cd might be related to lower Cd concentrations in their aerial parts (Table 7.2) as a result of alterations to normal Cd transport mechanisms arising from knocking out the *OXI1* gene.

A possible link between OXI1-mediated signaling and Cd transport should be explored in future research.

Since exposure to Cd has been shown to induce Cu deficiency-like responses mediated by the Cu homeostasis central regulator *SQUAMOSA* PROMOTER-BINDING PROTEIN-LIKE 7 (SPL7) (Gayomba *et al.*, 2013; Gielen *et al.*, 2016), these responses were also investigated in the Cd-exposed WT and *oxi1* knockout plants of both accessions. Interestingly, Gayomba *et al*. (2013) observed that exposure to Cd promoted Cu accumulation in the roots which, together with SPL7-mediated Cu remobilization and reallocation, resulted in decreased Cd sensitivity in *A. thaliana* (accession Col-0). However, this does not seem to be determining the decreased Cd sensitivity in Col-0 *oxi1* plants. A similar increase in root Cu concentrations was observed after exposure to Cd in all conditions except Col-0 *oxi1* plants exposed for 24 h, in which the Cu concentration was not significantly different from the non-exposed Col-0 *oxi1* plants, and resulted in a similar root-to-shoot Cu translocation factor in these plants at this time point (Table 7.3). Moreover, although it increased at 72 h, root Cu concentrations of Cd-exposed Col-0 *oxi1* mutants still remained lower than that of WT plants at the same time point (Table 7.3). These results coincide with Cd-induced SPL7-regulated Cu deficiency-like responses such as an upregulation of *FSD1* and downregulation of *CSD* genes (Table 7.8 and 7.10; Gielen *et al*., 2016). Therefore, our results suggest that, in Col-0 plants, the Cd-induced SPL7-mediated Cu deficiency-like responses involve OXI1 activity. However, a possible role for OXI1 in the activation of SPL7 by Cd should be further explored as it is clearly not solely linked to the total Cu concentrations. Copper homeostasis appears to have been equally affected in both Cd-exposed Ws genotypes (Table 7.3), but Cu deficiency-like responses, such as alterations to SOD activities (Table 7.6) and transcript levels (*FSD1* and *CSD1/2*; Table 7.9 and 7.11), were more affected in Ws *oxi1* mutants than in the wild types. Recently, Carrió-Seguí *et al*. (2015) proposed that, in addition to and independently of SPL7-mediated Cu-deficiency-like responses, COPT5-mediated Cu transport has an important role in basal Cd resistance in *A. thaliana.* Supported by the work of Smeets *et al*. (2013), these authors hypothesized that COPT5-mediated Cu remobilization from the vacuoles induces oxidative stress and triggers NADPH/RESPIRATORY BURST OXIDASE PROTEIN D (RBOHD)/ROS-

mediated OXI1 signaling pathway targeting *FSD1* and *miR398* gene expression which ultimately leads to Cd translocation and basal Cd resistance (Carrió-Seguí *et al*., 2015). Therefore, future investigations into Cu transport, chelation, and localization during Cd stress in *oxi1* mutants might reveal new functions for OXI1 and implications to Cd sensitivity.

In an attempt to identify new downstream targets of OXI1 during Cd stress, the transcript levels of signaling-related components were evaluated in WT and *oxi1* plants. For example, several MAPK components are known to be activated in *A. thaliana* after Cd exposure, often via ROS-induced OXI1 mediation (Liu *et al*., 2010; Opdenakker *et al*., 2012a; Rentel *et al*., 2004; Smeets *et al*., 2013; Smékalová *et al*., 2014). Smeets *et al*. (2013) hypothesized that the MAPK MPK4 is activated after Cd exposure and regulated by OXI1 after observing a Cd-induced *MPK4* upregulation in roots and leaves of Ws WT plants that was not present in *oxi1* knockout mutants. Liu *et al*. (2010) reported a Cd-induced ROS-mediated activation of MAPKs MPK3 and MPK6 in Col-0 plants, which genes were observed to be upregulated after exposure to Cd for 24 h by Opdenakker *et al*. (2012). In our study, *MPK3* was also upregulated in roots and leaves of Col-0 and Ws plants after exposure to Cd (Table 7.8-7.11). Although exposure to Cd increased the transcript levels of *OXI1*, no significant differential *MPK3* or *MPK6* regulation was observed between WT and *oxi1* plants (Table 7.8-7.11) which indicates that, when occurring, Cd-induced *MPK3/6* upregulation is not dependent on OXI1 activity. Highly conserved in eukaryotes, MAPKs cascades are major signaling modules that relay and amplify signals that ultimately result in cellular responses (Colcombet and Hirt, 2008; Jalmi and Sinha, 2015; Pitzschke *et al*., 2009; Smékalová *et al*., 2014; Taj *et al*., 2010). Downstream of MAPK cascades are often transcription factors that modulate gene expression in response to the signal perceived by the cell (Smékalová *et al*., 2014; Taj *et al*., 2010). For example, several WRKY proteins, such as WRKY22, WRKY25, WRKY29 and WRKY33, have been reported to respond to metal and/or oxidative stress in association with MAPK signaling (Opdenakker *et al*., 2012a, 2012b; Phukan *et al*., 2016; Smeets *et al*., 2013; Smékalová *et al*., 2014). Although Smeets *et al*. (2013) suggested WRKY25 as a downstream target of OXI1-mediated MAPK signaling during Cu stress, no WRKY protein has yet been associated with Cd-induced OXI1 activity. Indeed, *WRKY29*

and *WRKY33* were often upregulated after exposure to Cd, but no genotype-specific transcription pattern is observed between WT and *oxi1* plants (Table 7.8-7.11). Another transcription factor known to respond to abiotic stress conditions is the zinc-finger protein ZAT12 (Davletova *et al*., 2005). After clustering analysis, Opdenakker *et al*. (2012a) identified a gene cluster comprised of *RBOHD*, *OXI1* and *ZAT12* in Cd-exposed plants and hypothesized that the amplification of the ROS signal by ROS-producing RBOHD leads to OXI1-mediated signaling and gene regulation by ZAT12 in response to Cd stress. Our results support this hypothesis by validating ZAT12 as a downstream target of OXI1 in Cd-exposed roots. In both Col-0 (24 and 72 h; Table 7.8) and Ws plants (72 h; Table 7.9), the transcript levels of *ZAT12* were significantly increased in roots of Cd-exposed WT plants only. This tissue-specific response is not surprising considering that both *OXI1* (Anthony *et al*., 2004; Rentel *et al*., 2004) and *ZAT12* (Davletova *et al*., 2005) are particularly expressed in the roots, which are also the first organs to come into contact with and respond to the toxic Cd in the growth medium. However, a stronger increase in *ZAT12* gene expression at 72 h was observed in leaves of *oxi1* mutants as compared to WT plants in both Cd-exposed accessions. This suggests that, eventually, other signaling pathways bypass the lack of functional OXI1 to regulate *ZAT12* expression. In this regard, the interaction between stress-induced signaling and phytohormones, such as ethylene might play an important role. It is clear that ethylene is essential to properly regulate plant growth in response to metal stress (Keunen *et al*., 2016b; Schellingen *et al*., 2014, 2015b, 2015a; Smékalová *et al*., 2014). Although studies relating Cd-induced oxidative stress and ethylene signaling are scarce, Schellingen *et al*. (2015b) suggested a link between early oxidative stress signals and ethylene biosynthesis after exposure to Cd. In their model, these authors proposed that the Cd-induced ethylene response is mediated by OXI1 activity in leaves. This is also supported by the present study as the ethylene-responsive *ETHYLENE RESPONSE FACTOR 1 (ERF1)* was significantly more upregulated in leaves of Col-0 WT plants than in *oxi1* mutants after 24 h (Table 7.10). After exposure to Cd for 72h, *ERF1* was observed to be more upregulated in the Col-0 *oxi1* mutants than in the wild types after 72 h, which hints at the activation of OXI1-independent signaling pathways to bypass the loss of OXI1 activity and mediate later Cd-induced

phytohormone responses. Since ERF1 is a transcription factor activated by both ethylene and jasmonic acid (JA) signaling and plays a role in integrating these two signals to induce defense responses (Cheng *et al*., 2013; Lorenzo *et al*., 2003), JA signaling might become important when Cd-induced OXI1-mediated ethylene biosynthesis and signaling is disrupted. In Chapter 6, it was suggested that a mechanism mediated by the plant defense-associated and JA/ethylene-responsive PLANT DEFENSIN 1.2 is induced in leaves of Cu-exposed Col-0 *oxi1* mutants to bypass the impaired OXI1-dependent ERF1-activated phytohormone response. Therefore, the evaluation of other ethylene and JA-related signaling components is essential to reveal which (bypass) signal transduction mechanisms are at play during Cd stress.

In conclusion, OXI1 is essential for normal plant growth and its loss of function affects the responses of Col-0 and Ws plants to Cd. Interestingly, our results suggest that Col-0 *oxi1* mutant plants are less sensitive to Cd-induced oxidative stress than their WT counterparts. Since root-to-shoot translocation of Cd is affected in Col-0 *oxi1* mutants, a possible role for OXI1 in the regulation of Cd transportation mechanisms should be considered and further investigated in connection to the decrease in Cd sensitivity. Moreover, a function in the regulation of Cu transportation and remobilization should be explored as the Cd-induced SPL7-mediated Cu deficiency responses are differentially affected. Finally, the investigation of OXI1-signaling in relation to phytohormonal signaling pathways needs further attention to interconnect and unravel the signaling networks in plant responses to abiotic stress.

Supplemental Table 7.1 – Transcript levels in roots of three-week-old *A. thaliana* non-exposed wild-type (WT) and *oxi1* knockout (*oxi1*) plants (accession Col-0). Values are the mean normalized expression relative to the non-exposed WT plant (set at 1.00) ± S.E. of at least three biological replicates, each containing rosettes of at least one individual plant. Resolution values are mean inverse normalization factors relative to the non-exposed WT plant, indicating the stability of the selected reference genes. Statistically significant (P<0.05) differences between genotypes are indicated by asterisks and printed in bold. Abbreviations: see Table 7.8.

24 h		Col-0	72 h	
WT	***oxi1***		**WT**	***oxi1***
1.00 ± 0.07	1.04 ± 0.13	Resolution	1.00 ± 0.02	0.94 ± 0.11
Genes encoding oxidative stress hallmark proteins				
1.00 ± 0.09	1.21 ± 0.10	*UPOX*	1.00 ± 0.06	1.03 ± 0.15
1.00 ± 0.14	1.24 ± 0.51	*Defensin-like*	1.00 ± 0.12	1.32 ± 0.37
1.00 ± 0.16	0.79 ± 0.14	*AT1G19020*	1.00 ± 0.08	1.56 ± 0.61
1.00 ± 0.10	0.74 ± 0.10	*AT1G05340*	1.00 ± 0.23	1.06 ± 0.28
1.00 ± 0.19	0.89 ± 0.21	*TIR-class*	1.00 ± 0.10	1.87 ± 0.84
Gene encoding ROS-producing enzyme				
1.00 ± 0.08	0.92 ± 0.10	*LOX1*	1.00 ± 0.04	1.01 ± 0.21
Genes encoding antioxidative enzymes				
1.00 ± 0.09	0.85 ± 0.09	*GSH2*	1.00 ± 0.39	0.72 ± 0.12
1.00 ± 0.37	0.54 ± 0.13	*FSD1*	1.00 ± 0.33	2.42 ± 0.46
1.00 ± 0.07	1.16 ± 0.00	*CSD1*	1.00 ± 0.04	0.87 ± 0.11
1.00 ± 0.01	0.91 ± 0.07	*CSD2*	1.00 ± 0.17	1.15 ± 0.17
Primary microRNA transcripts				
1.00 ± 0.43	**0.15 ± 0.02 ***	*pri-miR398a*	1.00 ± 0.13	1.75 ± 0.56
1.00 ± 0.01	0.88 ± 0.05	*pri-miR398b*	1.00 ± 0.29	0.73 ± 0.11
Genes encoding protein kinases				
1.00 ± 0.14	ND	*OXI1*	1.00 ± 0.08	ND
1.00 ± 0.02	0.92 ± 0.05	*MPK3*	1.00 ± 0.07	1.20 ± 0.26
1.00 ± 0.10	1.06 ± 0.07	*MPK6*	1.00 ± 0.05	1.05 ± 0.15
Genes encoding transcription factors				
1.00 ± 0.33	1.64 ± 0.68	*ZAT12*	1.00 ± 0.05	3.47 ± 1.74
1.00 ± 0.15	1.17 ± 0.13	*WRKY29*	1.00 ± 0.11	1.26 ± 0.35
1.00 ± 0.04	0.89 ± 0.09	*WRKY33*	1.00 ± 0.06	1.21 ± 0.35
Gene encoding protein involved in ethylene signaling				
1.00 ± 0.35	1.04 ± 0.21	*ERF1*	1.00 ± 0.17	0.77 ± 0.05

Supplemental Table 7.2 – Transcript levels in roots of three-week-old *A. thaliana* non-exposed wild-type (WT) and *oxi1* knockout (*oxi1*) plants (accession Ws). Values are the mean normalized expression relative to the non-exposed WT plant (set at 1.00) ± S.E. of at least three biological replicates, each containing rosettes of at least one individual plant. Resolution values are mean inverse normalization factors relative to the non-exposed WT plant, indicating the stability of the selected reference genes. Statistically significant (P<0.05) differences between genotypes are indicated by asterisks and printed in bold. Abbreviations: see Table 7.8.

24 h		Ws	72 h	
WT	***oxi1***		**WT**	***oxi1***
1.00 ± 0.06	1.17 ± 0.06	Resolution	1.00 ± 0.16	0.75 ± 0.06
Genes encoding oxidative stress hallmark proteins				
1.00 ± 0.10	1.10 ± 0.09	*UPOX*	1.00 ± 0.20	0.97 ± 0.07
1.00 ± 0.22	1.08 ± 0.27	*Defensin-like*	1.00 ± 0.31	2.52 ± 1.61
1.00 ± 0.06	2.15 ± 0.47	*AT1G19020*	1.00 ± 0.19	1.95 ± 0.83
1.00 ± 0.18	0.70 ± 0.11	*AT1G05340*	1.00 ± 0.15	1.91 ± 0.47
1.00 ± 0.21	1.61 ± 0.04	*TIR-class*	1.00 ± 0.21	1.59 ± 0.53
Gene encoding ROS-producing enzyme				
1.00 ± 0.15	0.98 ± 0.09	*LOX1*	1.00 ± 0.15	0.98 ± 0.09
Genes encoding antioxidative enzymes				
1.00 ± 0.10	1.01 ± 0.06	*GSH2*	1.00 ± 0.20	1.15 ± 0.12
1.00 ± 0.31	1.08 ± 0.31	*FSD1*	1.00 ± 0.30	0.34 ± 0.19
1.00 ± 0.08	1.17 ± 0.04	*CSD1*	1.00 ± 0.09	1.14 ± 0.15
1.00 ± 0.06	1.11 ± 0.07	*CSD2*	1.00 ± 0.14	1.37 ± 0.16
Primary microRNA transcripts				
1.00 ± 0.19	0.77 ± 0.03	*pri-miR398a*	1.00 ± 0.32	0.84 ± 0.32
1.00 ± 0.09	1.00 ± 0.07	*pri-miR398b*	1.00 ± 0.26	0.60 ± 0.10
Genes encoding protein kinases				
1.00 ± 0.27	ND	*OXI1*	1.00 ± 0.11	ND
1.00 ± 0.13	1.55 ± 0.22	*MPK3*	1.00 ± 0.19	1.58 ± 0.39
1.00 ± 0.09	1.21 ± 0.05	*MPK6*	1.00 ± 0.05	1.06 ± 0.08
Genes encoding transcription factors				
1.00 ± 0.34	2.44 ± 0.83	*ZAT12*	1.00 ± 0.30	2.54 ± 1.19
1.00 ± 0.02	1.42 ± 0.17	*WRKY29*	1.00 ± 0.08	1.50 ± 0.27
1.00 ± 0.09	1.63 ± 0.35	*WRKY33*	1.00 ± 0.10	1.55 ± 0.50
Gene encoding protein involved in ethylene signaling				
1.00 ± 0.16	1.76 ± 0.37	*ERF1*	1.00 ± 0.19	1.48 ± 0.36

Supplemental Table 7.3 – Transcript levels in leaves of three-week-old *A. thaliana* non-exposed wild-type (WT) and *oxi1* knockout (*oxi1*) plants (accession Col-0). Values are the mean normalized expression relative to the non-exposed WT plant (set at 1.00) ± S.E. of at least three biological replicates, each containing rosettes of at least one individual plant. Resolution values are mean inverse normalization factors relative to the non-exposed WT plant, indicating the stability of the selected reference genes. Statistically significant (P<0.05) differences between genotypes are indicated by asterisks and printed in bold. Abbreviations: see Table 7.8.

24 h		Col-0	72 h	
WT	***oxi1***		**WT**	***oxi1***
1.00 ± 0.18	1.14 ± 0.20	Resolution	1.00 ± 0.11	1.05 ± 0.19
Genes encoding oxidative stress hallmark proteins				
1.00 ± 0.06	1.05 ± 0.07	*UPOX*	1.00 ± 0.14	1.52 ± 0.09
1.00 ± 0.13	1.53 ± 0.28	*Defensin-like*	1.00 ± 0.44	0.86 ± 0.19
1.00 ± 0.13	1.84 ± 0.34	*AT1G19020*	1.00 ± 0.34	0.41 ± 0.10
1.00 ± 0.14	1.28 ± 0.14	*AT1G05340*	1.00 ± 0.22	0.84 ± 0.01
1.00 ± 0.38	1.89 ± 0.59	*TIR-class*	1.00 ± 0.62	0.43 ± 0.23
Genes encoding ROS-producing enzymes				
1.00 ± 0.22	1.18 ± 0.10	*LOX1*	1.00 ± 0.12	1.05 ± 0.06
1.00 ± 0.17	1.21 ± 0.10	*LOX2*	1.00 ± 0.20	0.78 ± 0.09
Genes encoding antioxidative enzymes				
1.00 ± 0.23	0.83 ± 0.07	*GSH2*	1.00 ± 0.29	0.58 ± 0.04
1.00 ± 0.48	3.53 ± 1.67	*FSD1*	1.00 ± 0.54	0.21 ± 0.10
1.00 ± 0.16	1.01 ± 0.11	*CSD1*	1.00 ± 0.32	1.61 ± 0.03
1.00 ± 0.20	1.01 ± 0.13	*CSD2*	1.00 ± 0.40	1.36 ± 0.25
Primary microRNA transcripts				
1.00 ± 0.22	**2.56 ± 0.21 ***	*pri-miR398a*	1.00 ± 0.61	0.35 ± 0.12
1.00 ± 0.22	1.71 ± 0.50	*pri-miR398b*	1.00 ± 0.50	0.34 ± 0.13
Genes encoding protein kinases				
1.00 ± 0.19	ND	*OXI1*	1.00 ± 0.48	ND
1.00 ± 0.22	1.11 ± 0.05	*MPK3*	1.00 ± 0.25	0.63 ± 0.07
1.00 ± 0.08	0.96 ± 0.03	*MPK6*	1.00 ± 0.04	1.07 ± 0.05
Genes encoding transcription factors				
1.00 ± 0.57	1.14 ± 0.03	*ZAT12*	**1.00 ± 0.26**	**0.16 ± 0.02 ***
1.00 ± 0.23	0.89 ± 0.07	*WRKY29*	1.00 ± 0.22	1.61 ± 0.05
1.00 ± 0.25	1.51 ± 0.24	*WRKY33*	1.00 ± 0.32	0.73 ± 0.13
Gene encoding protein involved in ethylene signaling				
1.00 ± 0.22	**4.53 ± 1.36 ***	*ERF1*	1.00 ± 0.34	0.32 ± 0.08

Supplemental Table 7.4 – Transcript levels in leaves of three-week-old *A. thaliana* non-exposed wild-type (WT) and *oxi1* knockout (*oxi1*) plants (accession Ws). Values are the mean normalized expression relative to the non-exposed WT plant (set at 1.00) ± S.E. of at least three biological replicates, each containing rosettes of at least one individual plant. Resolution values are mean inverse normalization factors relative to the non-exposed WT plant, indicating the stability of the selected reference genes. Statistically significant (P<0.05) differences between genotypes are indicated by asterisks and printed in bold. Abbreviations: see Table 7.8.

24 h		Ws	72 h	
WT	***oxi1***		**WT**	***oxi1***
1.00 ± 0.09	1.44 ± 0.09	Resolution	1.00 ± 0.14	1.20 ± 0.12
Genes encoding oxidative stress hallmark proteins				
1.00 ± 0.11	1.09 ± 0.10	*UPOX*	1.00 ± 0.10	1.28 ± 0.19
1.00 ± 0.11	0.99 ± 0.12	*Defensin-like*	1.00 ± 0.18	1.19 ± 0.04
1.00 ± 0.07	**2.00 ± 0.27 ***	*AT1G19020*	**1.00 ± 0.12**	**0.48 ± 0.05 ***
1.00 ± 0.07	1.22 ± 0.19	*AT1G05340*	1.00 ± 0.07	0.79 ± 0.09
1.00 ± 0.16	1.28 ± 0.31	*TIR-class*	1.00 ± 0.32	0.43 ± 0.04
Genes encoding ROS-producing enzymes				
1.00 ± 0.13	1.16 ± 0.27	*LOX1*	1.00 ± 0.10	0.77 ± 0.10
1.00 ± 0.08	1.24 ± 0.28	*LOX2*	1.00 ± 0.08	0.96 ± 0.14
Genes encoding antioxidative enzymes				
1.00 ± 0.14	1.12 ± 0.08	*GSH2*	1.00 ± 0.11	0.80 ± 0.10
1.00 ± 0.37	0.61 ± 0.27	*FSD1*	1.00 ± 0.20	0.89 ± 0.49
1.00 ± 0.11	1.37 ± 0.21	*CSD1*	1.00 ± 0.19	1.20 ± 0.11
1.00 ± 0.02	1.12 ± 0.13	*CSD2*	1.00 ± 0.20	1.19 ± 0.02
Primary microRNA transcripts				
1.00 ± 0.04	0.98 ± 0.25	*pri-miR398a*	1.00 ± 0.27	1.89 ± 0.12
1.00 ± 0.23	0.87 ± 0.10	*pri-miR398b*	1.00 ± 0.19	0.65 ± 0.26
Genes encoding protein kinases				
1.00 ± 0.25	ND	*OXI1*	1.00 ± 0.08	ND
1.00 ± 0.04	1.34 ± 0.21	*MPK3*	1.00 ± 0.13	0.84 ± 0.12
1.00 ± 0.04	1.10 ± 0.08	*MPK6*	1.00 ± 0.04	0.91 ± 0.08
Genes encoding transcription factors				
1.00 ± 0.45	3.95 ± 1.87	*ZAT12*	**1.00 ± 0.23**	**0.15 ± 0.04 ***
1.00 ± 0.21	1.04 ± 0.20	*WRKY29*	1.00 ± 0.32	1.58 ± 0.26
1.00 ± 0.06	1.75 ± 0.17	*WRKY33*	1.00 ± 0.14	0.58 ± 0.09
Gene encoding protein involved in ethylene signaling				
1.00 ± 0.25	1.67 ± 0.48	*ERF1*	1.00 ± 0.19	0.67 ± 0.19

Supplemental Table 7.5 – List of primers used in quantitative real-time PCR. E-E-jn: Exon-Exon-junction. UTR: Untranslated region.

Locus	Annotation	Forward primer (5′ – 3′)	Reverse primer (5′ – 3′)	Exon location	Amplicon length (bp)	Primer Efficiency		
Reference genes								
AT2G28390	*SAND family*	AACTCTATGCAGCATTTGATCCACT	TGATTGCATATCTTTATCGCCATC	Exon 13	61	Roots	Col-0	89.21 %
							Ws	98.14 %
						Leaves	Col-0	100.95 %
							Ws	99.73 %
AT3G18780	*ACT2*	CTTGCACCAAGCAGCATGAA	CCGATCCAGACACTGTACTTCCTT	Exon 2	68	Roots	Col-0	81.49 %
							Ws	89.86 %
						Leaves	Col-0	96.05 %
							Ws	97.33 %
AT4G05320	*UBQ10*	GGCCTTGTATAATCCCTGATGAATAAG	AAAGAGATAACAGGAACGGAAACATAGT	3′ UTR	61	Roots	Col-0	100.44 %
							Ws	102.12 %
						Leaves	Col-0	103.37 %
							Ws	103.14 %
AT5G15710	*F-box protein*	TTTCGGCTGAGAGGTTCGAGT	GATTCCAAGACGTAAAGCAGATCAA	Exon 1	63	Roots	Col-0	90.39 %
							Ws	103.59 %
						Leaves	Col-0	99.48 %
							Ws	91.03%
AT5G60390	*EF1A*	TGAGCACGCTCTTCTTGCTTTCA	GGTGGTGGCATCCATCTTGTTACA	E1-E2-jn	76	Roots	Col-0	101.77 %
							Ws	105.74 %
						Leaves	Col-0	97.49 %
							Ws	101.62 %

Supplemental Table 7.5 – List of primers used in quantitative real-time PCR. Continuation.

Locus	Annotation	Forward primer (5′ – 3′)	Reverse primer (5′ – 3′)	Exon location	Amplicon length (bp)	Primer Efficiency		
Genes encoding oxidative stress hallmark proteins								
AT1G05340	Unknown	TCGGTAGCTCAGGGTAAAGTGG	CCAGGGCACAACAGCAACA	E2-E3-jn	91	Roots	Col-0	96.63 %
							Ws	101.14 %
						Leaves	Col-0	100.78 %
							Ws	77.20 %
AT1G19020	Unknown	GAAAATGGGACAAGGGTTAGACAAA	CCCAACGAAAACCAATAGCAGA	Exon 1	92	Roots	Col-0	96.35 %
							Ws	100.40 %
						Leaves	Col-0	102.94 %
							Ws	71.42 %
AT1G57630	*TIR-class*	ACTCAAACAGGCGATCAAAGGA	CACCAATTCGTCAAGACAACACC	Exon 1	91	Roots	Col-0	95.96 %
							Ws	89.74 %
						Leaves	Col-0	95.60 %
							Ws	102.66 %
AT2G21640	*UPOX*	GACTTGTTTCAAAAACACCATGGAC	CACTTCCTTAGCCTCAATTTGCTTC	E1-E2-jn	91	Roots	Col-0	91.21 %
							Ws	89.23 %
						Leaves	Col-0	110.30 %
							Ws	88.40 %
AT2G43510	*Defensin-like*	ATGGCAAAGGCTATCGTTTCC	CGTTACCTTGCGCTTCTATCTCC	E1-E2-jn	91	Roots	Col-0	91.16 %
							Ws	92.50 %
						Leaves	Col-0	114.14 %
							Ws	95.13 %

Supplemental Table 7.5 – List of primers used in quantitative real-time PCR. Continuation.

Locus	Annotation	Forward primer (5′ – 3′)	Reverse primer (5′ – 3′)	Exon location	Amplicon length (bp)	Primer Efficiency		
Genes encoding ROS-producing enzymes								
AT1G55020	*LOX1*	TTGGCTAAGGCTTTTGTCGG	GTGGCAATCACAAACGGTTC	Exon 6	101	Roots	Col-0	97.74 %
							Ws	92.69 %
						Leaves	Col-0	93.40 %
							Ws	95.17 %
AT3G45140	*LOX2*	TTTGCTCGCCAGACACTTG	GGGATCACCATAAACGGCC	E3-E4-jn	102	Leaves	Col-0	91.07 %
							Ws	95.51 %
Genes encoding antioxidative enzymes								
AT5G27380	*GSH2*	GGACTCGTCGTTGGTGACAA	TCTGGGAATGCAGTTGGTAGC	Exon 11	101	Roots	Col-0	91.24 %
							Ws	90.60 %
						Leaves	Col-0	95.30 %
							Ws	98.02 %
AT1G08830	*CSD1*	TCCATGCAGACCCTGATGAC	CCTGGAGACCAATGATGCC	Exon 5	102	Roots	Col-0	98.95 %
							Ws	92.77 %
						Leaves	Col-0	114.5 %
							Ws	85.93 %
AT2G28190	*CSD2*	GAGCCTTTGTGGTTCACGAG	CACACCACATGCCAATCTCC	Exon 6	101	Roots	Col-0	99.21 %
							Ws	94.02 %
						Leaves	Col-0	98.37 %
							Ws	105.29 %
AT4G25100	*FSD1*	CTCCCAATGCTGTGAATCCC	TGGTCTTCGGTTCTGGAAGTC	Exon 4	101	Roots	Col-0	94.84 %
							Ws	92.96 %
						Leaves	Col-0	94.81 %
							Ws	94.90 %

Supplemental Table 7.5 – List of primers used in quantitative real-time PCR. Continuation.

Locus	Annotation	Forward primer (5′ – 3′)	Reverse primer (5′ – 3′)	Exon location	Amplicon length (bp)	Primer Efficiency		
Primary microRNA transcripts								
AT2G03445	*pri-miRNA398a*	AGAAGAAGAGAAGAACAACAGGAGGTG	ATTAGTAAGGTGAAAAAATGG		156	Roots	Col-0	74.77 %
							Ws	88.43 %
						Leaves	Col-0	88.14 %
							Ws	102.96 %
AT5G14545	*pri-miRNA398b*	AGTAATCAACGGCTGTAATGACGCTAC	TGACCTGAGAACACATGAAAACGAGAG		67	Roots	Col-0	89.86 %
							Ws	88.63 %
						Leaves	Col-0	90.36 %
							Ws	83.82 %
Genes encoding protein kinases								
AT3G25250	*OXI1*	TAGAGGATCGAACCGGAAAG	GACCCTTGATTTCCTCAACG	Exon 2	149	Roots	Col-0	90.29 %
						Leaves		95.76 %
		TTCAATCGACTCGAGGTTTTG	AGCAAGCAATTTAGCGTCGT	Exon 1	90	Roots	Ws	92.59 %
						Leaves		100.35 %
AT3G45640	*MPK3*	GACGTTTGACCCCAACAGAA	TGGCTTTTGACAGATTGGCTC	E5-E6-jn	103	Roots	Col-0	99.15 %
							Ws	96.23 %
						Leaves	Col-0	95.50 %
							Ws	97.04 %
AT2G43790	*MPK6*	TAAGTTCCCGACAGTGCATCC	GATGGGCCAATGCGTCTAA	E5-E6-jn	100	Roots	Col-0	92.16 %
							Ws	92.51 %
						Leaves	Col-0	94.05 %
							Ws	100.87 %

Supplemental Table 7.5 – List of primers used in quantitative real-time PCR. Continuation.

Locus	Annotation	Forward primer (5′ – 3′)	Reverse primer (5′ – 3′)	Exon location	Amplicon length (bp)	Primer Efficiency		
Genes encoding transcription factors								
AT5G59820	*ZAT12*	GTGCGAGTCACAAGAAGCCTAACA	GCGACGACGTTTTCACCTTCTTCA	Exon 1	72	Roots	Col-0	91.52 %
							Ws	91.65 %
						Leaves	Col-0	98.00 %
							Ws	99.06 %
AT4G23550	*WRKY29*	CATGGGCGTGGCGTAAATA	TTGTTTTCTTGCCAAACACCC	E2-E3-jn	104	Roots	Col-0	92.34 %
							Ws	101.40 %
						Leaves	Col-0	103.48 %
							Ws	94.72 %
AT2G38470	*WRKY33*	TCATCGATTGTCAGCAGAGACG	CCATTCCCACCATTTGTTTCAT	E3-E4-jn	92	Roots	Col-0	97.52 %
							Ws	103.16 %
						Leaves	Col-0	89.92 %
							Ws	95.48 %
Gene encoding protein involved in ethylene signaling								
AT3G23240	*ERF1*	TCCTCGGCGATTCTCAATTTT	CAACCGGAGAACAACCATCCT	Exon 1	91	Roots	Col-0	98.47 %
							Ws	98.59 %
						Leaves	Col-0	98.47 %
							Ws	98.59 %

Supplemental Table 7.6 – Quantitative real-time PCR parameters according to the "Minimum Information for publication of Quantitative real-time PCR Experiments" (MIQE) guidelines derived from Bustin *et al.* (2009).

Sample/Template	
Source	Roots and leaves of *Arabidopsis thaliana* plants (accessions Col-0 and Ws) cultivated in hydroponics
Method of preservation	Liquid nitrogen
Storage time	Six weeks at – 70 °C
Handling	Frozen
Extraction method	Phenol-free Total RNA isolation: Ambion™ RNAqueous® Total RNA Isolation Kit * (Life Technologies, Waltham, MA, USA)
RNA: DNA-free	TURBO DNA-*free*™ Kit * (Life Technologies, Waltham, MA, USA) Design of intron-spanning primers whenever possible
Concentration	NanoDrop®: ND-1000 Spectrophotometer (Thermo Fisher Scientific, Inc., MA, USA)
Assay optimization and validation	
Accession number	Supplemental Table 7.5
Amplicon details	Exon location and amplicon size: Supplemental Table 7.5
Primer sequences	Supplemental Table 7.5
In silico	Primers were blasted using the BLAST tool at http://arabidopsis.org/
Empirical	Primer concentration: 300 nM (600 nM for *ERF1* measurements) Annealing temperature: 60 °C
Priming conditions	Combination of oligo(dT)-primers and random hexamers
PCR efficiency	Dilution series (slope, y-intercept and r^2; Supplemental Table 7.5)
Linear dynamic range	Samples are situated within the range of the efficiency curve
Reverse transcription – PCR	
Protocols	As stated in the Materials and Methods (Section 3.8)
Reagents	As stated in the Materials and Methods (Section 3.8)
No template control (NTC)	Cq and dissociation curve verification
Data analysis	
Specialist software	7500 Fast Real-Time PCR System (Applied Biosystems, Life Technologies, Belgium) Software v2.0.1
Statistical justification	At least three biological replicates Elimination of outliers after statistical validation using the Grubbs' test at significance level 0.05 (R version 3.3.1, package "outliers") Log transformation of the data One- and two-way ANOVA and the Tukey-Kramer post-hoc test to correct for multiple comparisons using R version 3.3.1
Normalization	Three stable reference genes selected using the GrayNorm algorithm (Remans *et al*., 2014): *AT2G28390, AT4G05320,* and *AT5G15710.*

* All procedures were performed according to the manufacturer's protocols.

CHAPTER 8

General discussion

Arabidopsis thaliana is an important model organism in plant biology. Whereas it might not be the perfect model for studies on crop plants, a fully sequenced genome as well as a large available collection of mutant lines and genomic resources have significantly contributed to the advancements in plant molecular genetics. Moreover, these genetic tools are complemented by an assortment of different *A. thaliana* natural accessions, the result of subcosmopolitan distribution of this species and habitat-specific selective pressures. Taken together, these resources are assets in stimuli-response experiments designed to evaluate plant responses to adverse environmental conditions, such as toxic metal concentrations.

While several metals are vital for normal plant development, high bioavailable metal concentrations often lead to toxicity responses and ultimately growth inhibition. For example, copper (Cu) is an essential micronutrient that in excess concentrations interferes with diverse cellular and metabolic processes. Due to its redox-active behavior, Cu directly catalyzes formation of ROS and thus induces oxidative stress. In parallel, exposure to non-essential and non-redox-active elements, such as cadmium (Cd), also affects several cellular processes but only indirectly induces oxidative stress by disrupting the normal antioxidative response mechanisms. Interestingly, exposure to Cd is also known to disturb Cu homeostasis, resulting in Cu deficiency-like responses which are also part of the Cd toxicity effects.

In this study, the ultimate objective was to investigate responses of *A. thaliana* plants to excess Cu and Cd using different genetic resources, *i.e.* different accessions and genotypes. First, by comparing the responses of two different natural accessions, Columbia (Col-0) and Wassilewskija (Ws), accession-specific responses are revealed (Chapters 4 and 5). Second, by using knockout mutants of the H_2O_2-responsive protein kinase OXIDATIVE SIGNAL-INDUCIBLE KINASE 1

(OXI1) in both natural accessions, metal-induced ROS signaling is explored and possible OXI1 downstream targets, functions and interactions are identified during Cu (Chapter 6) and Cd stress (Chapter 7). Using (1) the Cd-induced Cu deficiency-like responses at molecular level and (2) the *OXI1* knockout plants in both natural accessions, this provides an extra dimension to the existing research literature.

8.1 Ws plants are less sensitive to excess Cu and Cd than Col-0 plants, the reference genome

Several authors have described some accessions to be less sensitive to environment-induced impairment than others, and have explored the associated cellular, metabolic, and molecular response mechanisms. For example, Murphy and Taiz (1995a) reported Col-0 plants to be more sensitive to Cd than Ws plants. These authors also observed significant levels of inducible Cu tolerance in Ws and a low constitutive tolerance to Cu in Col-0 plants (Murphy and Taiz, 1995a), which was associated with a differential regulation of the Cu-chelating *METALLOTHIONEIN 2* (*MT2*) gene (Murphy and Taiz, 1995b) and different levels of potassium leakage (Murphy and Taiz, 1997). Schiavon *et al*. (2007) also described the Ws accession as less sensitive to Cu than Col-0, crediting this lower sensitivity of Ws plants to less Cu-induced nutrient deficiency, not to better metal exclusion. Park *et al*. (2012) observed Col-0 to be more sensitive to Cd than Ws and related it to distinctive inter-organ transport of elements in connection to differential expression and physiological function of the *HEAVY METAL ATPase* (*HMA*) transporter genes.

In agreement with these former studies, root (Chapter 4) and rosette (Chapter 5) growth results indicate that Ws plants are less sensitive to excess Cu and Cd than Col-0 plants. After exposure to excess Cu and Cd, root growth inhibition is less pronounced in Ws plants than in Col-0 plants (Table 4.1), which corresponded to lower metal concentrations in roots of Ws plants than of Col-0 plants (Table 4.2). Moreover, dry matter content (Figure 4.3) and cell wall residue levels (Figure 4.6) suggest that only roots of Cu-exposed Col-0 plants significantly suffered damage. At the leaf level, excess Cu resulted in the immediate inhibition of Col-0 rosette growth, which also coincided with a significantly higher Cu concentration in the leaves (Supplemental Table 5.1) and

a higher root-to-shoot Cu translocation factor (Figure 5.2A), whereas rosettes of Ws plants were only significantly affected after prolonged Cu exposure (Figure 5.1).

8.2 Col-0 and Ws plants favor different life strategies under physiological conditions

Our results (Chapter 5) suggest that Col-0 and Ws plants employ different life strategies, which were probably forged by the environmental cues in their native habitats, Germany and Belarus respectively. Under non-exposed conditions, hierarchical clustering of gene expression data of leaves from Col-0 and Ws plants revealed two gene clusters with differential expression patterns (Figure 5.3): (1) hallmark genes for oxidative stress or associated to the MAPK and ethylene signaling pathways were more expressed in Col-0 plants as compared to Ws plants, while (2) genes involved in Cu homeostasis, such as *COPT2*, *MT1a* and *MT1c* (Table 5.3), were more expressed in Ws plants as compared to Col-0 plants. This indicates that Col-0 plants invest in detoxification responses related to oxidative stress signaling and antioxidative defense mechanisms, whereas Ws plants primarily invest in a constitutively efficient metal homeostasis.

8.3 Accession-specific life strategies underlie the responses of Col-0 and Ws plants to excess Cu and Cd

Our results suggest that the different life strategies favored by Col-0 and Ws plants clearly affect their response to metal exposure (Chapter 5).

Due to their constitutively efficient metal homeostasis, Ws plants appear to better maintain Cu homeostasis than Col-0 plants, which results in these plants being less sensitive to excess Cu and Cd. Modulating Cu uptake is essential to maintain Cu homeostasis. Therefore, the significant downregulation of the transcript levels of the plasma membrane Cu transporters *COPT1, COPT2,* and *COPT5* in roots of Cu-exposed Ws plants, but only of *COPT2* in roots of Col-0 plants (Table 4.4), indicates that the Ws accession rapidly attempts to lower the amounts of Cu transported into the cells to avoid Cu toxicity. In addition, Cu concentrations were higher in roots of Col-0 plants than of Ws plants. As a result, a higher root-to-shoot translocation factor of Cu (Figure 5.2A) and higher

Cu concentrations were observed in leaves of Col-0 plants than of Ws after exposure to excess Cu for 24 h (Supplemental Table 5.1). Complementary to the Cu uptake and distribution, the cellular Cu homeostasis was maintained via the strong upregulation of the metallothionein *MT2b* gene in roots of Ws plants (Table 4.4), which has been associated to a higher Cu tolerance (Murphy and Taiz, 1995b).

Earlier studies in our research group demonstrated that exposure to Cd induces Cu deficiency-like responses (Gielen *et al*., 2016, 2017), which can be defined by an increase in Cu uptake and reallocation of intracellular Cu to essential cupro-proteins (Gielen *et al*., 2016; Yamasaki *et al*., 2007, 2008, 2009). Even though Cu concentrations increased in roots of both accessions exposed to Cd, they were lower in Ws than in Col-0 plants (Table 4.2) and the translocation factor was less affected in Ws than in Col-0 plants (Figure 5.2A). This indicates that Ws plants possess a constitutively more efficient metal homeostasis, which constitutes the primary defense strategy of these plants. Moreover, the continuous upregulation of *COPT5* together with restored *COPT1* expression levels at 72 h (Table 4.5) suggests that the roots of Ws plants react more efficiently and better remobilize the intracellular Cu supplies in response to Cd-induced Cu deficiency. In order to free and reallocate Cu to essential proteins, Cu-containing enzymes are replaced by other functionally equivalent enzymes in Cu deficiency conditions (Abdel-Ghany *et al*., 2005; Benatti *et al*., 2014; Garcia-Molina *et al*., 2013; Yamasaki *et al*., 2008). In connection with this, *CSD1* and *CSD2* (Cu/Zn-SOD isozyme) transcript levels were downregulated, while *FSD1* (iron isozyme) transcript levels were upregulated in roots of plants exposed to Cd (Table 4.5). However, the expression of *FSD1* was significantly more upregulated in roots of Cd-exposed Ws than in those of Col-0 plants after 24 h (Table 4.5), which suggests that Ws plants are able to rapidly counteract Cd-induced Cu deficiency-like responses.

The ability to efficiently counterbalance Cd-induced alterations to Cu homeostasis is further evidenced by lignification, which depends on proper Cu homeostasis (Printz *et al*., 2016), only being preserved in Ws plants. After Cd exposure, lignin levels were maintained in roots of Ws plants in association with an increased SPOD activity, but not in Col-0 plants (Figure 4.5 and 4.7).

Moreover, the transcript levels of *MT2b*, which encodes a protein that acts as a storage mechanism to provide Cu as a cofactor for laccases catalyzing lignification of the cell wall (Guo *et al*., 2003), were downregulated in roots of Col-0 plants and upregulated in those of Ws plants (Table 4.5). Together, these data suggest that cell wall dynamics, and hence the binding properties of the cell wall and its role in Cd detoxification, might be significant underlying mechanisms that further explain the improved Cd tolerance in Ws in comparison to Col-0 plants.

After exposure to excess Cu and Cd, Col-0 plants favor the activation of detoxification responses, related to oxidative stress signaling and antioxidative defense mechanisms (Chapter 5). As such, a more pronounced Cd-induced oxidative stress response was observed in leaves of Cd-exposed Col-0 plants than of Ws plants, as indicated by an overall higher upregulation of the oxidative stress hallmark and lipoxygenase genes (Table 5.5). Moreover, the significant upregulation of *GSH2* (Table 5.5) and the increased GSH concentration (Table 5.2) in leaves of Cd-exposed Col-0 plants points towards phytochelatin production and hence increased Cd-chelating capacities. Considering that Schellingen *et al.* (2015a) described ethylene to be involved in regulating GSH levels during the early Cd-induced oxidative challenge, the strong and concurrent upregulation of ethylene-responsive *ERF1* and ROS signaling-related genes *OXI1*, *MPK3*, *MPK6,* and *WRKY33* (Table 5.5) suggests that MAPK/ethylene signaling might be regulating this GSH metabolism response in leaves of Col-0 plants. Interestingly, the parallel upregulation of *ERF1* and *OXI1* in response to excess Cu (Figure 5.4) suggests that these two signaling-related molecules also interact in leaves of Col-0 plants, but a possible role in regulating a Cu-induced GSH response is not revealed and needs further investigation.

8.4 OXI1 loss-of-function affects Col-0 and Ws responses to excess Cu and Cd

The protein kinase OXI1 plays a central role in the ROS signal transduction pathway by linking ROS production to downstream responses under metal stress (Opdenakker *et al*., 2012b; Smeets *et al*., 2013). Although Col-0 plants favor the activation of detoxification responses involving oxidative stress signaling after exposure to excess Cu and Cd (Chapter 5), the loss of OXI1

function resulted in Col-0 *oxi1* mutants being less sensitive to both Cu- (Chapter 5) and Cd-induced (Chapter 6) oxidative stress than the wild types (within the experimental timeframe).

In excess Cu conditions, a diminished Cu-induced growth inhibition in Col-0 *oxi1* mutants than in WT plants, which was particularly significant for the leaves of Cu-exposed plants after 24 h (Table 6.1), supports that these plants are less sensitive to Cu exposure. This might arise from less Cu being accumulated in roots of Col-0 *oxi1* plants than of Ws (Table 6.2), possibly related to alterations to normal root hair development, which requires OXI1 activity as observed by Rentel *et al*. (2004) in Ws plants. Moreover, the lack of a functional OXI1 protein interferes with Cu-induced stress mechanisms, resulting in an overall earlier stimulation and higher increase in the activities of NAD(P)H-producing enzymes (Table 6.3 and 6.4). More specifically, exposure to Cu resulted in increased ICDH and G6PDH activities solely in *oxi1* plants or in an accelerated rise in GR, GPOD, SPOD and ME activities in *oxi1* plants at 24 h, whereas this was only observed after 72 h in WT plants (Table 6.3 and 6.4). Together with a delayed and diminished Cu-induced ROS-mediated lipid peroxidation in roots (Figure 6.3), as well as lower H_2O_2 concentrations (Figure 6.4) and transcript levels of oxidative stress hallmark genes in leaves of *oxi1* mutants as compared to WT plants, these results suggest that the lack of a functional OXI1 protein interferes with Cu-induced stress mechanisms in Col-0 plants and culminates in decreased sensitivity to excess Cu in Col-0 *oxi1* mutants.

After exposure to Cd, genotype-specific plant growth responses, which were only observed in Col-0 plants but not in Ws plants (Figure 7.1, Table 7.1), suggest that, within this experimental timeframe, Col-0 *oxi1* mutants are also less sensitive to Cd than their WT counterparts. In fact, while the average rosette weight was already affected after 24 h of exposure to Cd in WT plants, rosette weight of *oxi1* plants significantly increased relatively to non-exposed plants at the same time point (Figure 7.1). Moreover, in Col-0 WT plants only, exposure to Cd for 72 h led to significant inhibitions of root and rosette growth (Table 7.1), which affected rosette weight (Figure 7.1). These differences in Cd sensitivity are also illustrated by lower upregulations of oxidative stress hallmark

genes in Col-0 *oxi1* mutants than in the wild types (Table 7.8-7.11). This implies that the absence of OXI1 activity results in genotype-specific Cd-induced oxidative stress levels.

8.5 Responses of *oxi1* plants hint at new functions for OXI1 protein kinase during Cu and Cd stress

Gene knockout is a powerful reverse genetics tool that allows to gain knowledge about gene functions. In this study, by investigating *oxi1* knockout mutants in excess Cu and Cd conditions, we proposed to identify new functions for the OXI1 protein kinase in metal stress situations. In this regard, our results suggest that the protein kinase OXI1 is involved in the early regulation of metal transport under excess Cu and Cd stress. After metal exposure, the root-to-shoot translocation factors of Cu and Cd were significantly higher in *oxi1* mutants than in WT plants (Figure 6.2, 7.2, and 7.3). As such, the Cu concentrations were similar in non- and Cd-exposed Col-0 *oxi1* plants after 24 h (Table 7.3), resulting in similar root-to-shoot Cu translocation factors (Figure 7.3), whereas this was already affected in WT plants. Together with the simultaneous upregulation of *FSD1* and downregulation of *CSD* genes (Table 7.8 and 7.9), these data suggest that OXI1 might also be involved in the regulation of Cd-induced SPL7-mediated Cu deficiency-like responses in Col-0 plants.

Rentel *et al*. (2004) suggested that OXI1 is essential for H_2O_2-mediated signaling in *A. thaliana*. After sensing the ROS signal, OXI1 is known to initiate a MAPK signaling cascade, which then leads to the phosphorylation of a wide range of substrates (Colcombet and Hirt, 2008; Pitzschke and Hirt, 2006; Rodriguez *et al*., 2010). Rentel *et al*. (2004) also identified the MAPKs MPK3 and MPK6 as downstream elements of this OXI1-initiated signal transduction pathway. The concurrent upregulation of *OXI1* and *MPK3* in leaves of Col-0 WT plants and the significantly lower upregulation of *MPK3* gene in *oxi1* mutants after Cu exposure (Table 6.7) confirm earlier reports that MPK3 is involved in Cu-induced oxidative stress signaling and is modulated upstream by OXI1 (Opdenakker *et al*., 2012a). During Cd stress, however, *MPK3/6* upregulation is not dependent on OXI1 activity (Table 7.8-7.11). Instead, our results endorse the transcription factor ZAT12 as a downstream target of OXI1 in Cd-exposed roots (Table 7.8 and 7.9). Nevertheless, the stronger Cd-induced upregulation of

ZAT12 in leaves of *oxi1* mutants as compared to WT plants after 72 h (Table 7.10 and 7.11) allude to the activation of OXI1-independent signaling pathways to eventually bypass the absence of OXI1-regulated *ZAT12* expression. This is supported by more elevated transcript levels of ethylene-responsive *ERF1* in the Col-0 *oxi1* mutants than in WT plants after exposure to Cd (Table 7.10). Nevertheless, in agreement with the Cd-induced OXI1-mediated early ethylene response model proposed by Schellingen *et al*. (2015b), *ERF1* was significantly more upregulated in leaves of Col-0 WT plants than in *oxi1* mutants after 24 h (Table 7.10). Since ERF1 integrates both ethylene and jasmonic acid (JA) signals to induce defense responses (Cheng *et al*., 2013; Lorenzo *et al*., 2003), it should be investigated whether JA signaling might be involved in circumventing disruptions to Cd-induced phytohormonal responses in *oxi1* mutants. This is also relevant during Cu stress as indicated by the interchanged expression of the ethylene/jasmonic acid-responsive genes *ERF1* and *PDF1.2* in leaves of Cu-exposed *oxi1* mutants as compared to WT plants (Table 6.7). This illustrates the crosstalk between different signaling pathways (Keunen *et al*., 2016b) and indicates that OXI1 is involved in Cu-induced phytohormone signaling in WT plants.

8.6 Perspectives

This study provides an insight into the responses of *A. thaliana* plants to excess Cu and Cd in two different natural accessions and genotypes. Since these responses are very complex and involve diverse cellular and molecular processes, this study focused on investigating aspects and response mechanisms well established in our research group (Cuypers *et al*., 2011; Gielen *et al*., 2016, 2017, Jozefczak *et al*., 2014, 2015, Keunen *et al*., 2011b, 2013, 2015, 2016a; Loix *et al*., 2017; Opdenakker *et al*., 2012a; Schellingen *et al*., 2014, 2015b; Smeets *et al*., 2013). As such, this study is a mere glimpse into interesting accession-specific Cu- and Cd-induced responses in the experimental timeframe and it is but the starting point to understand the molecular mechanisms underlying the observed differences in sensitivity. Therefore, as indicated by our results, future experiments should mainly focus on: (1) accession-specific responses to excess Cu and Cd; (2) Cu homeostasis

mechanisms during both Cu and Cd stress; and (3) the interplay between ROS production, OXI1 signaling, and hormone signaling.

Ultimately, a whole genome approach is necessary to fully capture the details underlying the accession-specific responses to excess Cu and Cd. To that purpose, complex (and expensive) experimental setups such as genome-wide association studies and RNA-sequencing can be performed in the future. Alternatively, several bioinformatics tools have been developed in the aftermath of the "1001 Genomes Project" (Weigel and Mott, 2009), and made available in the last few years. These resources allow the study genotype–phenotype relationships in natural accessions (Seren *et al*., 2017; Togninalli *et al*., 2018) to reveal new lines of research and new experimental objectives.

An comprehensive study of the functions and localizations of Cu transporters and metal-binding proteins is important to elucidate the Cu homeostasis mechanisms during both Cu and Cd stress. To that purpose, the evaluation of the Cu- and Cd-induced responses in available knockout mutants of these components is possible. Immunofluorescence protein labeling experiments will reveal the cellular localization of these transporter and metal-binding proteins. This can be complemented by evaluating time- and tissue-specific gene expression through promoter activity determination using GUS reporter systems. The integration of these results will provide an overview of the mechanisms involved in maintaining Cu homeostasis during metal stress.

Evaluating ROS and hormone production in Cu- and Cd-exposed *oxi1* mutants will shed light on the interplay between ROS production, OXI1 signaling, and hormone signaling. In addition, experimenting with knockout mutants of other OXI1 signaling-related components or even with double mutants of hormone and ROS signaling components might reveal new insights and new lines of research.

Finally, a long term experiment is necessary to consolidate and confirm the results. This is particularly relevant in relation to the accession-specific and genotype-related metal sensitivities, in order to determine if Col-0 *oxi1* plants continue to be less sensitive to excess Cu and Cd than Ws *oxi1* mutants or if the accession-specific life strategies offset these genotype-related effects over time.

REFERENCES

Abdel-Ghany, S. E., Müller-Moulé, P., Niyogi, K. K., Pilon, M., and Shikanai, T. (2005). Two P-type ATPases are required for copper delivery in *Arabidopsis thaliana* chloroplasts. *The Plant Cell* **17**, 1233–51. doi:10.1105/tpc.104.030452.

Alonso-Blanco, C., Andrade, J., Becker, C., Bemm, F., Bergelson, J., Borgwardt, K. M., *et al*. (2016). 1,135 Genomes reveal the global pattern of polymorphism in *Arabidopsis thaliana*. *Cell* **166**, 481–491. doi:10.1016/j.cell.2016.05.063.

Alscher, R. G. (2002). Role of superoxide dismutases (SODs) in controlling oxidative stress in plants. *Journal of Experimental Botany* **53**, 1331–1341. doi:10.1093/jexbot/53.372.1331.

An, G., Watson, B. D., and Chiang, C. C. (1986). Transformation of tobacco, tomato, potato, and *Arabidopsis thaliana* using a binary Ti vector system. *Plant Physiology* **81**, 301–305. doi:10.1104/pp.81.1.301.

Andrés-Colás, N., Sancenón, V., Rodríguez-Navarro, S., Mayo, S., Thiele, D. J., Ecker, J. R., *et al*. (2006). The *Arabidopsis* heavy metal P-type ATPase HMA5 interacts with metallochaperones and functions in copper detoxification of roots. *Plant Journal* **45**, 225–236. doi:10.1111/j.1365-313X.2005.02601.x.

Anthony, R. G., Henriques, R., Helfer, A., Meszaros, T., Rios, G., Testerink, C., *et al*. (2004). A protein kinase target of a PDK1 signalling pathway is involved in root hair growth in Arabidopsis. *EMBO Journal* **23**, 572–581. doi:10.1038/sj.emboj.7600068.

Anthony, R. G., Khan, S., Costa, J., Pais, M. S., and Bögre, L. (2006). The Arabidopsis protein kinase PTI1-2 is activated by convergent phosphatidic acid and oxidative stress signaling pathways downstream of PDK1 and OXI1. *The Journal of Biological Chemistry* **281**, 37536–46. doi:10.1074/jbc.M607341200.

Arabidopsis Biological Resource Center (1991). Available at: https://abrc.osu.edu/.

Asai, T., Tena, G., Plotnikova, J., Willmann, M. R., Chiu, W.-L., Gomez-Gomez, L., *et al*. (2002). MAP kinase signalling cascade in *Arabidopsis* innate immunity. *Nature* **415**, 977–983. doi:10.1038/415977a.

Bailey-Serres, J., and Mittler, R. (2006). The roles of reactive oxygen species in plant cells. *Plant Physiology* **141**, 311. doi:10.1104/pp.104.900191.

Barah, P., Jayavelu, N. D., Mundy, J., and Bones, A. M. (2013a). Genome scale transcriptional response diversity among ten ecotypes of *Arabidopsis thaliana* during heat stress. *Frontiers in Plant Science* **4**, 532. doi:10.3389/fpls.2013.00532.

Barah, P., Jayavelu, N., Rasmussen, S., Nielsen, H., Mundy, J., and Bones, A. M. (2013b). Genome-scale cold stress response regulatory networks in ten *Arabidopsis thaliana* ecotypes. *BMC Genomics* **14**, 722. doi:10.1186/1471-2164-14-722.

Baxter, I., Brazelton, J. N., Yu, D., Huang, Y. S., Lahner, B., Yakubova, E., *et al*. (2010). A coastal cline in sodium accumulation in *Arabidopsis thaliana* is driven by natural variation of the sodium transporter AtHKT1;1. *PLoS Genetics* **6**, e1001193. doi:10.1371/journal.pgen.1001193.

Beck, J. B., Schmuths, H., and Schaal, B. A. (2007). Native range genetic variation in *Arabidopsis thaliana* is strongly geographically structured and reflects Pleistocene glacial dynamics. *Molecular Ecology* **17**, 902–915. doi:10.1111/j.1365-294X.2007.03615.x.

Beemster, G. T. S., De Vusser, K., De Tavernier, E., De Bock, K., and Inzé, D. (2002). Variation in growth rate between *Arabidopsis* ecotypes is correlated with cell division and A-type cyclin-dependent kinase activity. *Plant Physiology* **129**, 854–864. doi:10.1104/pp.002923.

Benatti, M. R., Yookongkaew, N., Meetam, M., Guo, W. J., Punyasuk, N., Abuqamar, S., *et al*. (2014). Metallothionein deficiency impacts copper accumulation and redistribution in leaves and seeds of *Arabidopsis*. *New Phytologist* **202**, 940–951. doi:10.1111/nph.12718.

Benavides, M. P., Gallego, S. M., and Tomaro, M. L. (2005). Cadmium toxicity in plants. *Brazilian Journal of Plant Physiology* **17**, 21–34. doi:10.1590/S1677-04202005000100003.

Bergmeyer, H. U., Gawehn, K., and Grassi, M. (1974). 'Enzymes as biochemical reagents', in Bergmeyer, H. U. (ed.) *Methods of Enzymatic Analysis*. New York: Academic Press, pp. 425–522.

Bernal, M., Ramiro, M. V., Cases, R., Picorel, R., and Yruela, I. (2006). Excess copper effect on growth, chloroplast ultrastructure, oxygen-evolution activity and chlorophyll fluorescence in *Glycine max* cell suspensions. *Physiologia Plantarum* **127**, 312–325. doi:10.1111/j.1399-3054.2006.00641.x.

Bochicchio, R., Sofo, A., Terzano, R., Gattullo, C. E., Amato, M., and Scopa, A. (2015). Root architecture and morphometric analysis of *Arabidopsis thaliana* grown in Cd/Cu/Zn-gradient agar dishes: A new screening technique for studying plant response to metals. *Plant Physiology and Biochemistry* **91**, 20–27. doi:10.1016/j.plaphy.2015.03.010.

Boucher, N., and Carpentier, R. (1999). Hg^{2+}, Cu^{2+}, and Pb^{2+}-induced changes in Photosystem II photochemical yield and energy storage in isolated thylakoid membranes: A study using simultaneous fluorescence and photoacoustic measurements. *Photosynthesis Research* **59**, 167–174. doi:10.1023/a:1006194621553.

Burkhead, J. L., Gogolin Reynolds, K. A., Abdel-Ghany, S. E., Cohu, C. M., and Pilon, M. (2009). Copper homeostasis. *New Phytologist* **182**, 799–816. doi:10.1111/j.1469-8137.2009.02846.x.

Bustin, S. A., Benes, V., Garson, J. A., Hellemans, J., Huggett, J., Kubista, M., *et al*. (2009). The MIQE guidelines: Minimum information for publication of quantitative real-time PCR experiments. *Clinical Chemistry* **55**, 611–622. doi:10.1373/clinchem.2008.112797.

Cao, J., Schneeberger, K., Ossowski, S., Günther, T., Bender, S., Fitz, J., *et al*. (2011). Whole-genome sequencing of multiple *Arabidopsis thaliana* populations. *Nature Genetics* **43**, 956–63. doi:10.1038/ng.911.

Carrió-Seguí, A., Garcia-Molina, A., Sanz, A., and Peñarrubia, L. (2015). Defective copper transport in the *copt5* mutant affects cadmium tolerance. *Plant and Cell Physiology* **56**, 442–454. doi:10.1093/pcp/pcu180.

Chao, D. Y., Silva, A., Baxter, I., Huang, Y. S., Nordborg, M., Danku, J., *et al*. (2012). Genome-wide association studies identify heavy metal ATPase3 as the primary determinant of natural variation in leaf cadmium in *Arabidopsis thaliana*. *PLoS Genetics* **8**. doi:10.1371/journal.pgen.1002923.

Cheeseman, J. M. (2007). Hydrogen peroxide and plant stress: A challenging relationship. *Plant Stress* **1**, 4–15.

Cheng, M.-C., Liao, P.-M., Kuo, W.-W., and Lin, T.-P. (2013). The *Arabidopsis* ETHYLENE RESPONSE FACTOR1 regulates abiotic stress-responsive gene expression by binding to different cis-acting elements in response to different stress signals. *Plant Physiology* **162**, 1566–82. doi:10.1104/pp.113.221911.

Chevalier, F., Martin, O., Rofidal, V., Devauchelle, A.-D., Barteau, S., Sommerer, N., *et al*. (2004). Proteomic investigation of natural variation between *Arabidopsis* ecotypes. *Proteomics* **4**, 1372–1381. doi:10.1002/pmic.200300750.

Chmielowska-Bak, J., Gzyl, J., Rucinska-Sobkowiak, R., Arasimowicz-Jelonek, M., and Deckert, J. (2014). The new insights into cadmium sensing. *Frontiers in Plant Science* 5, 1–13. doi:10.3389/fpls.2014.00245.

Cho, U. H., and Seo, N. H. (2005). Oxidative stress in *Arabidopsis thaliana* exposed to cadmium is due to hydrogen peroxide accumulation. *Plant Science* **168**, 113–120. doi:10.1016/j.plantsci.2004.07.021.

Cho, Y. H., and Yoo, S. D. (2009). Emerging complexity of ethylene signal transduction. *Journal of Plant Biology* **52**, 283–288. doi:10.1007/s12374-009-9038-6.

Cobbett, C., and Goldsbrough, P. (2002). Phytochelatins and metallothioneins: Roles in heavy metal detoxification and homeostasis. *Annual Review of Plant Biology* **53**, 159–182. doi:10.1146/annurev.arplant.53.100301.135154.

Cobbett, C. S. (2000). Phytochelatins and their roles in heavy metal detoxification. *Plant Physiology* **123**, 825–832. doi:10.1104/pp.123.3.825.

Colcombet, J., and Hirt, H. (2008). *Arabidopsis* MAPKs: a complex signalling network involved in multiple biological processes. *Biochemical Journal* **413**, 217–226. doi:10.1042/bj20080625.

Connolly, E. L. (2002). Expression of the IRT1 metal transporter is controlled by metals at the levels of transcript and protein accumulation. *The Plant Cell* **14**, 1347–1357. doi:10.1105/tpc.001263.

Cuypers, A., Hendrix, S., Amaral dos Reis, R., De Smet, S., Deckers, J., Gielen, H., *et al*. (2016). Hydrogen peroxide, signaling in disguise during metal phytotoxicity. *Frontiers in Plant Science* **7**, 470. doi:10.3389/fpls.2016.00470.

Cuypers, A., Keunen, E., Bohler, S., Jozefczak, M., Opdenakker, K., Gielen, H., *et al*. (2012). 'Cadmium and copper stress induce a cellular oxidative challenge leading to damage versus signalling', in Gupta, D. K. and Sandalio, L. M. (eds.) *Metal Toxicity in Plants: Perception, Signaling and Remediation*. Heidelberg: Springer, pp. 65–90. doi:10.1007/978-3-642-22081-4_4.

Cuypers, A., Plusquin, M., Remans, T., Jozefczak, M., Keunen, E., Gielen, H., *et al*. (2010). Cadmium stress: an oxidative challenge. *Biometals* **23**, 927–940. doi:10.1007/s10534-010-9329-x.

Cuypers, A., Smeets, K., Ruytinx, J., Opdenakker, K., Keunen, E., Remans, T., *et al*. (2011). The cellular redox state as a modulator in cadmium and copper responses in *Arabidopsis thaliana* seedlings. *Journal of Plant Physiology* **168**, 309–316. doi:10.1016/j.jplph.2010.07.010.

Cuypers, A., Vangronsveld, J., and Clijsters, H. (2002). Peroxidases in roots and primary leaves of *Phaseolus vulgaris*. Copper and zinc phytotoxicity: a comparison. *Journal of Plant Physiology* **159**, 869–876. doi: 10.1078/0176-1617-00676.

Dąbrowska, G., Mierek-Adamska, A., and Goc, A. (2012). Plant metallothioneins: Putative functions identified by promoter analysis in silico. *Acta Biologica Cracoviensia Series Botanica* **54**, 109–120. doi:10.2478/v10182-012-0030-y.

DalCorso, G., Manara, A., and Furini, A. (2013). An overview of heavy metal challenge in plants: from roots to shoots. *Metallomics* **5**, 1117. doi:10.1039/c3mt00038a.

Davletova, S., Schlauch, K., Coutu, J., and Mittler, R. (2005). The zinc-finger protein ZAT12 plays a central role in reactive oxygen and abiotic stress signaling in *Arabidopsis*. *Plant Physiology* **139**, 847–856. doi:10.1104/pp.105.068254.

de Mendiburu, F. (2016). agricolae: Statistical procedures for agricultural research. Available at: https://cran.r-project.org/package=agricolae.

Degenkolbe, T., Giavalisco, P., Zuther, E., Seiwert, B., Hincha, D. K., and Willmitzer, L. (2012). Differential remodeling of the lipidome during cold acclimation in natural accessions of *Arabidopsis thaliana*. *The Plant Journal* **72**, 972–982. doi:10.1111/tpj.12007.

Dhindsa, R. S., Plumb-dhindsa, P., and Thorpe, T. A. (1981). Leaf senescence: Correlated with increased levels of membrane permeability and lipid peroxidation, and decreased levels of superoxide dismutase and catalase. *Journal of Experimental Botany* **32**, 93–101. doi:10.1093/jxb/32.1.93.

Drazkiewicz, M., Skorzynska-Polit, E., and Krupa, Z. (2003). Response of the ascorbate-glutathione cycle to excess copper in *Arabidopsis thaliana* (L.). *Plant Science* **164**, 195–202. doi: 10.1016/S0168-9452(02)00383-7.

Drążkiewicz, M., Skórzyńska-Polit, E., and Krupa, Z. (2004). Copper-induced oxidative stress and antioxidant defence in *Arabidopsis thaliana*. *Biometals* **17**, 379–387. doi:10.1023/B:BIOM.0000029417.18154.22.

Droppa, M., and Horváth, G. (1990). The role of copper in photosynthesis. *Critical Reviews in Plant Sciences* **9**, 111–123. doi:10.1080/07352689009382284.

Fajardo, C., Costa, G., Nande, M., Botías, P., García-Cantalejo, J., and Martín, M. (2018). Pb, Cd, and Zn soil contamination: Monitoring functional and structural impacts on the microbiome. *Applied Soil Ecology*. doi:10.1016/j.apsoil.2018.10.022.

Fernandes, J. C., and Henriques, F. S. (1991). Biochemical, physiological, and structural effects of excess copper in plants. *Botanical Review* **57**, 246–273. doi: 10.1007/BF02858564

Festa, R. A., and Thiele, D. J. (2011). Copper: An essential metal in biology. *Current Biology* **21**, R877–R883. doi:10.1016/J.CUB.2011.09.040.

Fischer, S., Spielau, T., and Clemens, S. (2017). Natural variation in *Arabidopsis thaliana* Cd responses and the detection of quantitative trait loci affecting Cd tolerance. *Scientific Reports* **7**, 3693. doi:10.1038/s41598-017-03540-z.

Fox, J., and Weisberg, S. (2011). *A {R} Companion to Applied Regression*. 2nd edn. Thousand Oaks: Sage.

Foyer, C. H., and Noctor, G. (2011). Ascorbate and glutathione: The heart of the redox hub. *Plant Physiology* **155**, 2–18. doi:10.1104/pp.110.167569.

Gadjev, I., Vanderauwera, S., Gechev, T. S., Laloi, C., Minkov, I. N., Shulaev, V., *et al*. (2006). Transcriptomic footprints disclose specificity of reactive oxygen species signaling in *Arabidopsis*. *Plant Physiology* **141**, 436–445.
doi:10.1104/pp.106.078717.

Gan, X., Stegle, O., Behr, J., Steffen, J. G., Drewe, P., Hildebrand, K. L., *et al*. (2011). Multiple reference genomes and transcriptomes for *Arabidopsis thaliana*. *Nature* **477**, 419–423.
doi:10.1038/nature10414.

Garcia-Molina, A., Andrés-Colás, N., Perea-García, A., del Valle-Tascón, S., Peñarrubia, L., and Puig, S. (2011). The intracellular *Arabidopsis* COPT5 transport protein is required for photosynthetic electron transport under severe copper deficiency. *The Plant Journal* **65**, 848–860.
doi:10.1111/j.1365-313X.2010.04472.x.

Garcia-Molina, A., Andrés-Colás, N., Perea-García, A., Neumann, U., Dodani, S. C., Huijser, P., *et al*. (2013). The *Arabidopsis* COPT6 transport protein functions in copper distribution under copper-deficient conditions. *Plant and Cell Physiology* **54**, 1378–1390.
doi:10.1093/pcp/pct088.

Gayomba, S. R., Jung, H., Yan, J., Danku, J., Rutzke, M. A., Bernal, M., *et al*. (2013). The CTR/COPT-dependent copper uptake and SPL7-dependent copper deficiency responses are required for basal cadmium tolerance in *A. thaliana*. *Metallomics* **5**, 1262–75.
doi:10.1039/c3mt00111c.

Gechev, T. S., Van Breusegem, F., Stone, J. M., Denev, I., and Laloi, C. (2006). Reactive oxygen species as signals that modulate plant stress responses and programmed cell death. *Bioessays* **28**, 1091–1101.
doi:10.1002/bies.20493.

Geebelen, W., Sappin-Didier, V., Ruttens, A., Carleer, R., Yperman, J., Bongué-Boma, K., *et al*. (2006). Evaluation of cyclonic ash, commercial Na-silicates, lime and phosphoric acid for metal immobilisation purposes in contaminated soils in Flanders (Belgium). *Environmental Pollution* **144**, 32–39.
doi:10.1016/J.ENVPOL.2006.01.013.

Gielen, H., Remans, T., Vangronsveld, J., and Cuypers, A. (2016). Toxicity responses of Cu and Cd: the involvement of miRNAs and the transcription factor SPL7. *BMC Plant Biology* **16**, 145.
doi:10.1186/s12870-016-0830-4.

Gielen, H., Vangronsveld, J., and Cuypers, A. (2017). Cd-induced Cu deficiency responses in *Arabidopsis thaliana*: are phytochelatins involved? *Plant Cell and Environment* **40**, 390–400.
doi:10.1111/pce.12876.

Gross, E. L. (1993). Plastocyanin: Structure and function. *Photosynthesis Research* **37**, 103–116. doi:10.1007/BF02187469.

Gross, G. G. (2008). From lignins to tannins: Forty years of enzyme studies on the biosynthesis of phenolic compounds. *Phytochemistry* **69**, 3018–3031. doi:10.1016/j.phytochem.2007.04.031.

Guo, W.-J. J., Bundithya, W., and Goldsbrough, P. B. (2003). Characterization of the *Arabidopsis* metallothionein gene family: tissue-specific expression and induction during senescence and in response to copper. *New Phytologist* **159**, 369–381. doi:10.1046/j.1469-8137.2003.00813.x.

Guo, W.-J., Meetam, M., and Goldsbrough, P. B. (2008). Examining the specific contributions of individual *Arabidopsis* metallothioneins to copper distribution and metal tolerance. *Plant Physiology* **146**, 1697–706. doi:10.1104/pp.108.115782.

Gupta, H., Cuypers, A., Vangronsveld, J., and Clijsters, H. (1999). Copper affects the enzymes of the ascorbate-glutathione cycle and its related metabolites in the roots of *Phaseolus vulgaris*. *Physiologia Plantarum* **106**, 262–267. doi: 10.1034/j.1399-3054.1999.106302.x.

Harir, Y., and Mittler, R. (2009). "The ROS Signaling Network of Cells," in *Reactive Oxygen Species in Plant Signaling*, ed. L. A. P. A. DelRio, 165–174. doi:10.1007/978-3-642-00390-5_10.

Hernández, L. E., Carpena-Ruiz, R., Gárate, A., Hernandez, L. E., Carpena-Ruiz, R., and Garate, A. (1996). Alterations in the mineral nutrition of pea seedlings exposed to cadmium. *Journal of Plant Nutrition* **19**, 1581–1598. doi:10.1080/01904169609365223.

Hoffmann, M. H. (2002). Biogeography of *Arabidopsis thaliana* (L.) Heynh. (Brassicaceae). *Journal of Biogeography* **29**, 125–134. doi:10.1046/j.1365-2699.2002.00647.x.

Huang, P.-Y., Catinot, J., and Zimmerli, L. (2016). Ethylene response factors in *Arabidopsis* immunity. *Journal of Experimental Botany* **67**, 1231–1241. doi:10.1093/jxb/erv518.

Hussain, D., Haydon, M. J., Wang, Y., Wong, E., Sherson, S. M., Young, J., *et al*. (2004). P-type ATPase heavy metal transporters with roles in essential zinc homeostasis in *Arabidopsis*. *The Plant Cell* **16**, 1327–39. doi:10.1105/tpc.020487.

Imberty, A., Goldberg, R., and Catesson, A. M. (1984). Tetramethylbenzidine and p-phenylenediamine-pyrocatechol for peroxidase histochemistry and biochemistry: Two new, non-carcinogenic chromogens for investigating lignification process. *Plant Science Letters* **35**, 103–108. doi:10.1016/0304-4211(84)90182-2.

Iqbal, N., Khan, N. A., Ferrante, A., Trivellini, A., Francini, A., and Khan, M. I. R. (2017). Ethylene role in plant growth, development and senescence: Interaction with other phytohormones. *Frontiers in Plant Science* **8**, 475. doi:10.3389/fpls.2017.00475.

Jalmi, S. K., and Sinha, A. K. (2015). ROS mediated MAPK signaling in abiotic and biotic stress- striking similarities and differences. *Frontiers in Plant Science* **6**, 769. doi:10.3389/fpls.2015.00769.

Jin, C.-W., Mao, Q.-Q., Luo, B.-F., Lin, X.-Y., and Du, S.-T. (2013). Mutation of *mpk6* enhances cadmium tolerance in *Arabidopsis plants* by alleviating oxidative stress. *Plant and Soil* **371**, 387–396. doi:10.1007/s11104-013-1699-8.

Jozefczak, M., Bohler, S., Schat, H., Horemans, N., Guisez, Y., Remans, T., *et al*. (2015). Both the concentration and redox state of glutathione and ascorbate influence the sensitivity of *Arabidopsis* to cadmium. *Annals of Botany* **116**, 601–612. doi:10.1093/aob/mcv075.

Jozefczak, M., Keunen, E., Schat, H., Bliek, M., Hernández, L. E., Carleer, R., *et al*. (2014). Differential response of *Arabidopsis* leaves and roots to cadmium: Glutathione-related chelating capacity vs antioxidant capacity. *Plant Physiology and Biochemistry* **83**, 1–9. doi:10.1016/j.plaphy.2014.07.001.

Jung, H. Il, Gayomba, S. R., Rutzke, M. A., Craft, E., Kochian, L. V., and Vatamaniuk, O. K. (2012). COPT6 is a plasma membrane transporter that functions in copper homeostasis in *Arabidopsis* and is a novel target of SQUAMOSA promoter-binding protein-like 7. *Journal of Biological Chemistry* **287**, 33252–33267. doi:10.1074/jbc.M112.397810.

Kawakatsu, T., Huang, S.-S. C., Jupe, F., Sasaki, E., Schmitz, R. J., Urich, M. A., *et al*. (2016). Epigenomic diversity in a global collection of *Arabidopsis thaliana* accessions. *Cell* **166**, 492–505. doi:10.1016/j.cell.2016.06.044.

Keunen, E., Florez-Sarasa, I., Obata, T., Jozefczak, M., Remans, T., Vangronsveld, J., *et al*. (2016a). Metabolic responses of *Arabidopsis thaliana* roots and leaves to sublethal cadmium exposure are differentially influenced by ALTERNATIVE OXIDASE1a. *Environmental and Experimental Botany* **124**, 64–78.
doi:10.1016/j.envexpbot.2015.11.015.

Keunen, E., Jozefczak, M., Remans, T., Vangronsveld, J., and Cuypers, A. (2013). Alternative respiration as a primary defence during cadmium-induced mitochondrial oxidative challenge in *Arabidopsis thaliana*. *Environmental and Experimental Botany* **91**, 63–73.
doi:10.1016/j.envexpbot.2013.02.008.

Keunen, E., Remans, T., Bohler, S., Vangronsveld, J., and Cuypers, A. (2011a). Metal-induced oxidative stress and plant mitochondria. *International Journal of Molecular Sciences* **12**, 6894–6918.
doi:10.3390/ijms12106894.

Keunen, E., Schellingen, K., Van Der Straeten, D., Remans, T., Colpaert, J., Vangronsveld, J., *et al*. (2015). ALTERNATIVE OXIDASE1a modulates the oxidative challenge during moderate Cd exposure in *Arabidopsis thaliana* leaves. *Journal of Experimental Botany* **66**, 2967–2977.
doi:10.1093/jxb/erv035.

Keunen, E., Schellingen, K., Vangronsveld, J., and Cuypers, A. (2016b). Ethylene and metal stress: Small molecule, big impact. *Frontiers in Plant Science* **7**, 23.
doi:10.3389/fpls.2016.00023.

Keunen, E., Truyens, S., Bruckers, L., Remans, T., Vangronsveld, J., and Cuypers, A. (2011b). Survival of Cd-exposed *Arabidopsis thaliana*: Are these plants reproductively challenged? *Plant Physiology and Biochemistry* **49**, 1084–1091.
doi:10.1016/j.plaphy.2011.07.013.

Kim, J., Chang, C., and Tucker, M. L. (2015). To grow old: regulatory role of ethylene and jasmonic acid in senescence. *Frontiers in plant science* **6**, 20.
doi:10.3389/fpls.2015.00020.

Klaumann, S., Nickolaus, S. D., Fürst, S. H., Starck, S., Schneider, S., Ekkehard Neuhaus, H., *et al*. (2011). The tonoplast copper transporter COPT5 acts as an exporter and is required for interorgan allocation of copper in *Arabidopsis thaliana*. *New Phytologist* **192**, 393–404.
doi:10.1111/j.1469-8137.2011.03798.x.

Kobayashi, Y., Kuroda, K., Kimura, K. K., Southron-Francis, J. L. J., Furuzawa, A., Kimura, K. K., *et al*. (2008). Amino acid polymorphisms in strictly conserved domains of a P-type ATPase HMA5 are involved in the mechanism of copper tolerance variation in *Arabidopsis*. *Plant Physiology* **148**, 969–980.
doi:10.1104/pp.108.119933.

Koch, M. A., Haubold, B., and Mitchell-Olds, T. (2000). Comparative evolutionary analysis of chalcone synthase and alcohol dehydrogenase loci in *Arabidopsis*, *Arabis*, and related genera (Brassicaceae). *Molecular Biology and Evolution* **17**, 1483–1498.
doi:10.1093/oxfordjournals.molbev.a026248.

Koornneef, M., and Meinke, D. (2010). The development of *Arabidopsis* as a model plant. *The Plant Journal* **61**, 909–921.
doi:10.1111/j.1365-313X.2009.04086.x.

Koornneef, M., and Scheres, B. (2001). '*Arabidopsis thaliana* as an experimental organism', in *eLS.* John Wiley & Sons, Ltd.
doi:10.1002/9780470015902.a0002031.pub2.

Kuśnierczyk, A., Winge, P., Midelfart, H., Armbruster, W. S., Rossiter, J. T., and Bones, A. M. (2007). Transcriptional responses of *Arabidopsis thaliana* ecotypes with different glucosinolate profiles after attack by polyphagous *Myzus persicae* and oligophagous *Brevicoryne brassicae*. *Journal of Experimental Botany* **58**, 2537–2552.
doi:10.1093/jxb/erm043.

Laibach, F. (1943). Arabidopsis thaliana (L.) HEYNH. als Objekt fur genetische und entwicklungsphysiologische Untersuchungen. *Bot. Arch.* **44**, 439–455.

Leopold, I., Gunther, D., Schmidt, J., and Neumann, D. (1999). Phytochelatins and heavy metal tolerance. *Phytochemistry* **50**, 1323–1328.
doi:10.1016/S0031-9422(98)00347-1.

Lequeux, H., Hermans, C., Lutts, S., and Verbruggen, N. (2010). Response to copper excess in *Arabidopsis thaliana*: Impact on the root system architecture, hormone distribution, lignin accumulation and mineral profile. *Plant Physiology and Biochemistry* **48**, 673–682.
doi:http://dx.doi.org/10.1016/j.plaphy.2010.05.005.

Lešková, A., Giehl, R. F. H., Hartmann, A., Fargašová, A., and von Wirén, N. (2017). Heavy metals induce iron deficiency responses at different hierarchic and regulatory levels. *Plant Physiology* **174**, 1648–1668.
doi:10.1104/pp.16.01916.

Leutwiler, L. S., Hough-Evans, B. R., and Meyerowitz, E. M. (1984). The DNA of *Arabidopsis thaliana*. *MGG Molecular & General Genetics* **194**, 15–23.
doi:10.1007/BF00383491.

Li, G. J., Meng, X. Z., Wang, R. G., Mao, G. H., Han, L., Liu, Y. D., *et al*. (2012). Dual-level regulation of ACC synthase activity by MPK3/MPK6 cascade and its downstream WRKY transcription factor during ethylene induction in *Arabidopsis*. *PLoS Genetics* **8**, e1002767.
doi:10.1371/journal.pgen.1002767.

Liu, X.-M., Kim, K. E., Kim, K.-C., Nguyen, X. C., Han, H. J., Jung, M. S., *et al*. (2010). Cadmium activates *Arabidopsis* MPK3 and MPK6 via accumulation of reactive oxygen species. *Phytochemistry* **71**, 614–618.
doi:10.1016/j.phytochem.2010.01.005.

Loix, C., Huybrechts, M., Vangronsveld, J., Gielen, M., Keunen, E., and Cuypers, A. (2017). Reciprocal interactions between cadmium-induced cell wall responses and oxidative stress in plants. *Frontiers in Plant Science* **8**, 1867.
doi:10.3389/fpls.2017.01867.

Long, Q., Rabanal, F. A., Meng, D., Huber, C. D., Farlow, A., Platzer, A., *et al*. (2013). Massive genomic variation and strong selection in *Arabidopsis thaliana* lines from Sweden. *Nature Genetics* **45**, 884–890.
doi:10.1038/ng.2678.

Lorenzo, O., Piqueras, R., Sánchez-Serrano, J. J., and Solano, R. (2003). ETHYLENE RESPONSE FACTOR1 integrates signals from ethylene and jasmonate pathways in plant defense. *The Plant Cell* **15**, 165–78.
doi:10.1105/TPC.007468.

Loscos, J., Naya, L., Ramos, J., Clemente, M. R., Matamoros, M. A., and Becana, M. (2006). A reassessment of substrate specificity and activation of phytochelatin synthases from model plants by physiologically relevant metals. *Plant Physiology* **140**, 1213–1221.
doi:10.1104/pp.105.073635.

Lux, A., Martinka, M., Vaculík, M., and White, P. J. (2011). Root responses to cadmium in the rhizosphere: A review. *Journal of Experimental Botany* **62**, 21–37.
doi:10.1093/jxb/erq281.

Maitani, T., Kubota, H., Sato, K., and Yamada, T. (1996). The composition of metals bound to class III metallothionein (phytochelatin and its desglycyl peptide) induced by various metals in root cultures of *Rubia tinctorum*. *Plant physiology* **110**, 1145–1150.
doi:10.1104/PP.110.4.1145.

Marschner, H. (2012). *Marschner's Mineral Nutrition of Higher Plants*. 3rd edn. Edited by Petra Marschner. New York: Academic Press. doi:10.1017/S001447971100130X.

McCord, J. M., and Fridovich, I. (1969). Superoxide dismutase. An enzymic function for erythrocuprein (hemocuprein). *Journal of Biological Chemistry* **244**, 6049–6055. doi:10.1016/0003-2697(69)90079-7.

Meyerowitz, E. M. (2001). Prehistory and history of *Arabidopsis* research. *Plant Physiology* **125**, 15–19. doi:10.1104/pp.125.1.15.

Miller, A. F. (2004). Superoxide dismutases: active sites that save, but a protein that kills. *Current Opinion in Chemical Biology* **8**, 162–168. doi:10.1016/j.cbpa.2004.02.011.

Miller, G., Shulaev, V., and Mittler, R. (2008). Reactive oxygen signaling and abiotic stress. *Physiologia Plantarum* **133**, 481–489. doi:10.1111/j.1399-3054.2008.01090.x.

Mittler, R. (2002). Oxidative stress, antioxidants and stress tolerance. *Trends in Plant Science* **7**, 405–410. doi: 10.1016/S1360-1385(02)02312-9

Mittler, R., Vanderauwera, S., Gollery, M., Breusegem, F. Van, and Van Breusegem, F. (2004). Reactive oxygen gene network of plants. *Trends in Plant Science* **9**, 490–498. doi:10.1016/j.tplants.2004.08.009.

Mittler, R., Vanderauwera, S., Suzuki, N., Miller, G., Tognetti, V. B., Vandepoele, K., *et al*. (2011). ROS signaling: the new wave? *Trends in Plant Science* **16**, 300–309. doi:10.1016/j.tplants.2011.03.007.

Moller, I. M., Jensen, P. E., and Hansson, A. (2007). Oxidative modifications to cellular components in plants. *Annual Review of Plant Biology* **58**, 459–481. doi:10.1146/annurev.arplant.58.032806.103946.

Morel, M., Crouzet, J., Gravot, A., Auroy, P., Leonhardt, N., Vavasseur, A., *et al*. (2009). AtHMA3, a P1B-ATPase allowing Cd/Zn/Co/Pb vacuolar storage in Arabidopsis. *Plant Physiology* **149**, 894–904. doi:10.1104/pp.108.130294.

Mourato, M. P., Reis, R., and Martins, L. L. (2012). 'Characterization of plant antioxidative system in response to abiotic stresses: A focus on heavy metal toxicity', in Montanaro, G. and Dichio, B. (eds.) *Advances in Selected Plant Physiology Aspects*. Rijeka: InTech, 23–44.

Müller, M., and Munné-Bosch, S. (2015). Ethylene response factors: A key regulatory hub in hormone and stress signaling. *Plant Physiology* **169**, 32–41.
doi:10.1104/pp.15.00677.

Murphy, A., and Taiz, L. (1995a). A new vertical mesh transfer technique for metal-tolerance studies in *Arabidopsis* (ecotypic variation and copper-sensitive mutants). *Plant Physiology* **108**, 29–38.
doi:108/1/29 [pii].

Murphy, A., and Taiz, L. (1995b). Comparison of metallothionein gene expression and nonprotein thiols in ten *Arabidopsis* ecotypes. Correlation with copper tolerance. *Plant Physiology* **109**, 945–54.
doi:10.1104/pp.109.3.945.

Murphy, A., and Taiz, L. (1997). Correlation between potassium efflux and copper sensitivity in 10 *Arabidopsis* ecotypes. *New Phytologist* **136**, 211–222.
doi:10.1046/j.1469-8137.1997.00738.x.

Nakagami, H., Pitzschke, A., and Hirt, H. (2005). Emerging MAP kinase pathways in plant stress signalling. *Trends in Plant Science* **10**, 339–346.
doi:10.1016/j.tplants.2005.05.009.

Neill, S. J., Desikan, R., Clarke, A., Hurst, R. D., and Hancock, J. T. (2002). Hydrogen peroxide and nitric oxide as signalling molecules in plants. *Journal of Experimental Botany* **53**, 1237–1247.
doi:10.1093/jexbot/53.372.1237.

Nelson, D. L., and Cox, M. M. (2008). *Lehninger Principles of Biochemistry*. 5th edn. New York: W. H. Freeman and Company.

Nigam, R., Srivastava, S., Prakash, S., and Srivastava, M. M. (2001). Cadmium mobilisation and plant availability - The impact of organic acids commonly exuded from roots. *Plant and Soil* **230**, 107–113.
doi:10.1023/A:1004865811529.

Nogueira, I. (1986). "*Arabidopsis* (L.) Heynh.," in *Flora Iberica*, eds. S. Castroviejo, J. Paiva, and I. Nogueira (Madrid: Real Jardín Botánico C. S. I. C.), 39–41.

Opdenakker, K., Remans, T., Keunen, E., Vangronsveld, J., and Cuypers, A. (2012a). Exposure of *Arabidopsis thaliana* to Cd or Cu excess leads to oxidative stress mediated alterations in MAPKinase transcript levels. *Environmental and Experimental Botany* **83**, 53–61.
doi:10.1016/j.envexpbot.2012.04.003.

Opdenakker, K., Remans, T., Vangronsveld, J., and Cuypers, A. (2012b). Mitogen-activated protein (MAP) kinases in plant metal stress: regulation and responses in comparison to other biotic and abiotic stresses. *International Journal of Molecular Sciences* **13**, 7828–7853. doi:10.3390/ijms13067828.

Ossowski, S., Schneeberger, K., Clark, R. M., Lanz, C., Warthmann, N., and Weigel, D. (2008). Sequencing of natural strains of *Arabidopsis thaliana* with short reads. *Genome research* **18**, 2024–33. doi:10.1101/gr.080200.108.

Park, W., Han, K.-H., and Ahn, S.-J. (2012). Differences in root-to-shoot Cd and Zn translocation and by HMA3 and 4 could influence chlorophyll and anthocyanin content in *Arabidopsis* Ws and Col-0 ecotypes under excess metals. *Soil Science and Plant Nutrition* **58**, 334–348. doi:10.1080/00380768.2012.684643.

Parmar, P., Kumari, N., and Sharma, V. (2013). Structural and functional alterations in photosynthetic apparatus of plants under cadmium stress. *Botanical Studies* **54**, 1–6. doi:10.1186/1999-3110-54-45.

Passardi, F., Dobias, J., Valério, L., Guimil, S., Penel, C., and Dunand, C. (2007). Morphological and physiological traits of three major *Arabidopsis thaliana* accessions. *Journal of Plant Physiology* **164**, 980–92. doi:10.1016/j.jplph.2006.06.008.

Penninckx, I. A. M. A., Thomma, B. P. H. J., Buchala, A., Métraux, J.-P., and Broekaert, W. F. (1998). Concomitant activation of jasmonate and ethylene response pathways is required for induction of a plant defensin gene in *Arabidopsis*. *The Plant Cell* **10**, 2103–2113. doi:10.1105/tpc.10.12.2103.

Pérez-Pérez, J. M., Serrano-Cartagena, J., Micol, J. L., Manuel Pérez-Pérez, J., Serrano-Cartagena, J., and Micol, J. L. (2002). Genetic analysis of natural variations in the architecture of *Arabidopsis thaliana* vegetative leaves. *Genetics* **162**, 893–915. doi:10.1104/pp.006536.

Perfus-Barbeoch, L., Leonhardt, N., Vavasseur, A., and Forestier, C. (2002). Heavy metal toxicity: Cadmium permeates through calcium channels and disturbs the plant water status. *Plant Journal* **32**, 539–548. doi:10.1046/j.1365-313X.2002.01442.x.

Petricka, J. J., Winter, C. M., and Benfey, P. N. (2012). Control of *Arabidopsis* root development. *Annual Review of Plant Biology* **63**, 563–590. doi:10.1146/annurev-arplant-042811-105501.

Phukan, U. J., Jeena, G. S., and Shukla, R. K. (2016). WRKY transcription factors: Molecular regulation and stress responses in plants. *Frontiers in Plant Science* **7**, 760.
doi:10.3389/fpls.2016.00760.

Pitzschke, A., and Hirt, H. (2006). Mitogen-activated protein kinases and reactive oxygen species signaling in plants. *Plant Physiology* **141**, 351–6.
doi:10.1104/pp.106.079160.

Pitzschke, A., Schikora, A., and Hirt, H. (2009). MAPK cascade signalling networks in plant defence. *Current Opinion in Plant Biology* **12**, 421–426.
doi:10.1016/j.pbi.2009.06.008.

Printz, B., Lutts, S., Hausman, J.-F., and Sergeant, K. (2016). Copper trafficking in plants and its implication on cell wall dynamics. *Frontiers in Plant Science* **7**, 601.
doi:10.3389/fpls.2016.00601.

Puig, S. (2014). Function and regulation of the plant COPT family of high-affinity copper transport proteins. *Advances in Botany* **2014**, 1–9.
doi:10.1155/2014/476917.

Puig, S., Andrés-Colás, N., García-Molina, A., and Peñarrubia, L. (2007). Copper and iron homeostasis in *Arabidopsis*: responses to metal deficiencies, interactions and biotechnological applications. *Plant, Cell & Environment* **30**, 271–290.
doi:10.1111/j.1365-3040.2007.01642.x.

Queval, G., and Noctor, G. (2007). A plate reader method for the measurement of NAD, NADP, glutathione, and ascorbate in tissue extracts: Application to redox profiling during *Arabidopsis* rosette development. *Analytical Biochemistry* **363**, 58–69.
doi:10.1016/j.ab.2007.01.005.

R Core Team (2016). R: A language and environment for statistical computing.
Available at: https://www.r-project.org/.

Rehrig, E. M., Appel, H. M., Jones, A. D., and Schultz, J. C. (2014). Roles for jasmonate- and ethylene-induced transcription factors in the ability of *Arabidopsis* to respond differentially to damage caused by two insect herbivores. *Frontiers in Plant Science* **5**, 407.
doi:10.3389/fpls.2014.00407.

Remans, T., Keunen, E., Bex, G. J., Smeets, K., Vangronsveld, J., and Cuypers, A. (2014). Reliable gene expression analysis by reverse transcription-quantitative PCR: reporting and minimizing the uncertainty in data accuracy. *The Plant Cell* **26**, 3829–37.
doi:10.1105/tpc.114.130641.

Remans, T., Smeets, K., Opdenakker, K., Mathijsen, D., Vangronsveld, J., and Cuypers, A. (2008). Normalisation of real-time RT-PCR gene expression measurements in *Arabidopsis thaliana* exposed to increased metal concentrations. *Planta* **227**, 1343–1349. doi:10.1007/s00425-008-0706-4.

Rentel, M. C., Lecourieux, D., Ouaked, F., Usher, S. L., Petersen, L., Okamoto, H., *et al*. (2004). OXI1 kinase is necessary for oxidative burst-mediated signalling in *Arabidopsis*. *Nature* **427**, 858–861. doi:10.1038/nature02353.

Rhee, S. Y. (2003). The Arabidopsis Information Resource (TAIR): a model organism database providing a centralized, curated gateway to *Arabidopsis* biology, research materials and community. *Nucleic Acids Research* **31**, 224–228. doi:10.1093/nar/gkg076.

Rizhsky, L., Davletova, S., Liang, H., and Mittler, R. (2004). The zinc finger protein ZAT12 is required for cytosolic ascorbate peroxidase 1 expression during oxidative stress in *Arabidopsis*. *Journal of Biological Chemistry* **279**, 11736–11743. doi:10.1074/JBC.M313350200.

Rodriguez, M. C. S., Petersen, M., and Mundy, J. (2010). Mitogen-activated protein kinase signaling in plants. *Annual Review of Plant Biology* **61**, 621–649. doi:10.1146/annurev-arplant-042809-112252.

RStudio Team (2015). RStudio: Integrated development for R. Available at: http://www.rstudio.com/.

Sancenón, V., Puig, S., Mira, H., Thiele, D. J., and Penarrubia, L. (2003). Identification of a copper transporter family in *Arabidopsis thaliana*. *Plant Molecular Biology* **51**, 577–587. doi:10.1023/A:1022345507112.

Sanità di Toppi, L., and Gabbrielli, R. (1999). Response to cadmium in higher plants. *Environmental and Experimental Botany* **41**, 105–130. doi: 10.1016/S0098-8472(98)00058-6.

Schellingen, K., Straeten, D. Van Der, Vandenbussche, F., Prinsen, E., Remans, T., Vangronsveld, J., *et al*. (2014). Cadmium-induced ethylene production and responses in *Arabidopsis thaliana* rely on ACS2 and ACS6 gene expression. *BMC Plant Biology* **14**, 1–14. doi: 10.1186/s12870-014-0214-6.

Schellingen, K., Van Der Straeten, D., Remans, T., Loix, C., Vangronsveld, J., and Cuypers, A. (2015a). Ethylene biosynthesis is involved in the early oxidative challenge induced by moderate Cd exposure in *Arabidopsis thaliana*. *Environmental and Experimental Botany* **117**, 1–11.
doi:10.1016/j.envexpbot.2015.04.005.

Schellingen, K., Van Der Straeten, D., Remans, T., Vangronsveld, J., Keunen, E., and Cuypers, A. (2015b). Ethylene signalling is mediating the early cadmium-induced oxidative challenge in *Arabidopsis thaliana*. *Plant Science* **239**, 137–146.
doi:10.1016/j.plantsci.2015.07.015.

Scheres, B., Benfey, P., and Dolan, L. (2002). Root Development. *The Arabidopsis Book* 1, e0101.
doi:10.1199/tab.0101.

Schiavon, M., Zhang, L. H., Abdel-Ghany, S. E., Pilon, M., Malagoli, M., and Pilon-Smits, E. A. H. (2007). Variation in copper tolerance in *Arabidopsis thaliana* accessions Columbia, Landsberg *erecta* and Wassilewskija. *Physiologia Plantarum* **129**, 342–350.
doi:10.1111/j.1399-3054.2006.00809.x.

Schiefelbein, J. W., and Somerville, C. (1990). Genetic control of root hair development in *Arabidopsis thaliana*. *The Plant Cell* **2**, 235–243.
doi:10.1105/tpc.2.3.235.

Schmitz, R. J., Schultz, M. D., Urich, M. A., Nery, J. R., Pelizzola, M., Libiger, O., *et al*. (2013). Patterns of population epigenomic diversity. *Nature* **495**, 193–198.
doi:10.1038/nature11968.

Schneeberger, K., Ossowski, S., Ott, F., Klein, J. D., Wang, X., Lanz, C., *et al*. (2011). Reference-guided assembly of four diverse *Arabidopsis thaliana* genomes. *Proceedings of the National Academy of Sciences* **108**, 10249–10254.
doi:10.1073/pnas.1107739108.

Semane, B., Cuypers, A., Smeets, K., Van Belleghem, F., Horemans, N., Schat, H., *et al*. (2007). Cadmium responses in *Arabidopsis thaliana*: glutathione metabolism and antioxidative defence system. *Physiologia Plantarum* **129**, 519–528.
doi:10.1111/j.1399-3054.2006.00822.x.

Seren, Ü., Grimm, D., Fitz, J., Weigel, D., Nordborg, M., Borgwardt, K., *et al*. (2017). AraPheno: a public database for *Arabidopsis thaliana* phenotypes. *Nucleic Acids Research* **45**, D1054–D1059.
doi:10.1093/nar/gkw986.

Sharbel, T. F., Haubold, B., and Mitchell-Olds, T. (2000). Genetic isolation by distance in *Arabidopsis thaliana*: biogeography and postglacial colonization of Europe. *Molecular Ecology* **9**, 2109–2118. doi:10.1046/j.1365-294X.2000.01122.x.

Shoala, T., Edwards, M. G., Knight, M. R., and Gatehouse, A. M. R. (2018). OXI1 kinase plays a key role in resistance of *Arabidopsis* towards aphids (*Myzus persicae*). *Transgenic Research* **27**, 355–366. doi:10.1007/s11248-018-0078-x.

Shulaev, V., Cortes, D., Miller, G., and Mittler, R. (2008). Metabolomics for plant stress response. *Physiologia Plantarum* **132**, 199–208. doi:10.1111/j.1399-3054.2007.01025.x.

Shumbe, L., Chevalier, A., Legeret, B., Taconnat, L., Monnet, F., and Havaux, M. (2016). Singlet oxygen-induced cell death in *Arabidopsis* under high-light stress is controlled by OXI1 kinase. *Plant Physiology* **170**, 1757–71. doi:10.1104/pp.15.01546.

Smeets, K., Cuypers, A., Lambrechts, A., Semane, B., Hoet, P., Van Laere, A., *et al*. (2005). Induction of oxidative stress and antioxidative mechanisms in *Phaseolus vulgaris* after Cd application. *Plant Physiology and Biochemistry* **43**, 437–444. doi:10.1016/j.plaphy.2005.03.007.

Smeets, K., Opdenakker, K., Remans, T., Forzani, C., Hirt, H., Vangronsveld, J., *et al*. (2013). The role of the kinase OXI1 in cadmium- and copper-induced molecular responses in *Arabidopsis thaliana*. *Plant, Cell & Environment* **36**, 1228–1238. doi:10.1111/pce.12056.

Smeets, K., Opdenakker, K., Remans, T., Van Sanden, S., Van Belleghem, F., Semane, B., *et al*. (2009). Oxidative stress-related responses at transcriptional and enzymatic levels after exposure to Cd or Cu in a multipollution context. *Journal of Plant Physiology* **166**, 1982–1992. doi:10.1016/j.jplph.2009.06.014.

Smeets, K., Ruytinx, J., Semane, B., Van Belleghem, F., Remans, T., Van Sanden, S., *et al*. (2008a). Cadmium-induced transcriptional and enzymatic alterations related to oxidative stress. *Environmental and Experimental Botany* **63**, 1–8. doi:10.1016/j.envexpbot.2007.10.028.

Smeets, K., Ruytinx, J., Van Belleghem, F., Semane, B., Lin, D., Vangronsveld, J., *et al*. (2008b). Critical evaluation and statistical validation of a hydroponic culture system for *Arabidopsis thaliana*. *Plant Physiology and Biochemistry* **46**, 212–218. doi:10.1016/j.plaphy.2007.09.014.

Smékalová, V., Doskočilová, A., Komis, G., and Samaj, J. (2014). Crosstalk between secondary messengers, hormones and MAPK modules during abiotic stress signalling in plants. *Biotechnology Advances* **32**, 2–11.
doi:10.1016/j.biotechadv.2013.07.009.

Somerville, C., and Koornneef, M. (2002). A fortunate choice: the history of *Arabidopsis* as a model plant. *Nature Reviews Genetics* **3**, 883–889.
doi:10.1038/nrg927.

Suzuki, N., Koussevitzky, S., Mittler, R., and Miller, G. (2012). ROS and redox signalling in the response of plants to abiotic stress. *Plant Cell and Environment* **35**, 259–270.
doi:10.1111/j.1365-3040.2011.02336.x.

Szymanowska-Pułka, J., and Szymanowska-Pulka, J. (2013). Form matters: morphological aspects of lateral root development. *Annals of Botany* **112**, 1643–54.
doi:10.1093/aob/mct231.

Taj, G., Agarwal, P., Grant, M., and Kumar, A. (2010). MAPK machinery in plants: recognition and response to different stresses through multiple signal transduction pathways. *Plant Signaling & Behavior* **5**, 1370–8.
doi:10.4161/PSB.5.11.13020.

Takahashi, F., Yoshida, R., Ichimura, K., Mizoguchi, T., Seo, S., Yonezawa, M., *et al*. (2007). The mitogen-activated protein kinase cascade MKK3–MPK6 is an important part of the jasmonate signal transduction pathway in *Arabidopsis*. *The Plant Cell* **19**, 805–818.
doi:10.1105/tpc.106.046581.

Tena, G., Boudsocq, M., and Sheen, J. (2011). Protein kinase signaling networks in plant innate immunity. *Current Opinion in Plant Biology* **14**, 519–529.
doi:10.1016/j.pbi.2011.05.006.

The Arabidopsis Genome Initiative (2000). Analysis of the genome sequence of the flowering plant *Arabidopsis thaliana*. *Nature* **408**, 796–815.
doi:10.1038/35048692.

The Nottingham Arabidopsis Stock Centre (NASC) (1991).
Available at: http://arabidopsis.info/.

Thomine, S., Wang, R., Ward, J. M., Crawford, N. M., and Schroeder, J. I. (2000). Cadmium and iron transport by members of a plant metal transporter family in *Arabidopsis* with homology to Nramp genes. *Proceedings of the National Academy of Sciences* **97**, 4991–4996.
doi:10.1073/pnas.97.9.4991.

Togninalli, M., Seren, Ü., Meng, D., Fitz, J., Nordborg, M., Weigel, D., *et al*. (2018). The AraGWAS Catalog: a curated and standardized *Arabidopsis thaliana* GWAS catalog. *Nucleic Acids Research* **46**, D1150–D1156.
doi:10.1093/nar/gkx954.

Tsukaya, H. (2013). Leaf Development. *The Arabidopsis Book* **11**, e0163.
doi:10.1199/tab.0163.

Van Acker, R., Vanholme, R., Storme, V., Mortimer, J. C., Dupree, P., and Boerjan, W. (2013). Lignin biosynthesis perturbations affect secondary cell wall composition and saccharification yield in *Arabidopsis thaliana*. *Biotechnology for Biofuels* **6**, 46.
doi:10.1186/1754-6834-6-46.

Van Breusegem, F., and Dat, J. F. (2006). Reactive oxygen species in plant cell death. *Plant Physiology* **141**, 384–390.
doi:10.1104/pp.106.078295.384.

Vangronsveld, J., Colpaert, J. V., and Van Tichelen, K. K. (1996). Reclamation of a bare industrial area contaminated by non-ferrous metals: Physico-chemical and biological evaluation of the durability of soil treatment and revegetation. *Environmental Pollution* **94**, 131–140.
doi:10.1016/S0269-7491(96)00082-6.

Vangronsveld, J., Herzig, R., Weyens, N., Boulet, J., Adriaensen, K., Ruttens, A., *et al*. (2009). Phytoremediation of contaminated soils and groundwater: lessons from the field. *Environmental Science and Pollution Research* **16**, 765–794.
doi:10.1007/s11356-009-0213-6.

Vangronsveld, J., Van Assche, F., and Clijsters, H. (1995). Reclamation of a bare industrial area contaminated by non-ferrous metals: In situ metal immobilization and revegetation. *Environmental Pollution* **87**, 51–59.
doi:10.1016/S0269-7491(99)80007-4.

Vanholme, R., Demedts, B., Morreel, K., Ralph, J., and Boerjan, W. (2010). Lignin biosynthesis and structure. *Plant Physiology* **153**, 895–905.
doi:10.1104/pp.110.155119.

Verbruggen, N., Hermans, C., and Schat, H. (2009). Mechanisms to cope with arsenic or cadmium excess in plants. *Current Opinion in Plant Biology* **12**, 364–372.
doi:10.1016/j.pbi.2009.05.001.

Wang, Y., Yang, L., Zheng, Z., Grumet, R., Loescher, W., Zhu, J.-K., *et al*. (2013). Transcriptomic and physiological variations of three *Arabidopsis* ecotypes in response to salt stress. *PLoS ONE* **8**, e69036.
doi:10.1371/journal.pone.0069036.

Weigel, D. (2012). Natural variation in *Arabidopsis*: from molecular genetics to ecological genomics. *Plant Physiology* **158**, 2–22. doi:10.1104/pp.111.189845.

Weigel, D., and Mott, R. (2009). The 1001 genomes project for *Arabidopsis thaliana*. *Genome biology* **10**, 107. doi:10.1186/gb-2009-10-5-107.

Wong, C. K. E., and Cobbett, C. S. (2009). HMA P-type ATPases are the major mechanism for root-to-shoot Cd translocation in *Arabidopsis thaliana*. *New Phytologist* **181**, 71–78. doi:10.1111/j.1469-8137.2008.02638.x.

Yamasaki, H., Abdel-Ghany, S. E., Cohu, C. M., Kobayashi, Y., Shikanai, T., and Pilon, M. (2007). Regulation of copper homeostasis by micro-RNA in *Arabidopsis*. *Journal of Biological Chemistry* **282**, 16369–16378. doi:10.1074/jbc.M700138200.

Yamasaki, H., Hayashi, M., Fukazawa, M., Kobayashi, Y., and Shikanai, T. (2009). SQUAMOSA promoter binding protein-like7 is a central regulator for copper homeostasis in *Arabidopsis*. *The Plant Cell* **21**, 347–361. doi:10.1105/tpc.108.060137.

Yamasaki, H., Pilon, M., and Shikanai, T. (2008). How do plants respond to copper deficiency? *Plant Signaling & Behavior* **3**, 231–232. doi:10.4161/psb.3.4.5094.

Yruela, I. (2005). Copper in plants. *Brazilian Journal of Plant Physiology* **17**, 145–156. doi:10.1590/S1677-04202005000100012.

Yruela, I. (2009). Copper in plants: acquisition, transport and interactions. *Functional Plant Biology* **36**, 409–430. doi:10.1071/fp08288.

Yruela, I., Alfonso, M., Baron, M., and Picorel, R. (2000). Copper effect on the protein composition of photosystem II. *Physiologia Plantarum* **110**, 551–557. doi:10.1034/j.1399-3054.2000.1100419.x.

SCIENTIFIC OUTPUT

International journals

Amaral dos Reis, R., Keunen, E., Mourato, M. P., Martins, L. L., Vangronsveld, J. and Cuypers, A. (2018). Accession-specific life strategies affect responses in leaves of *Arabidopsis thaliana* plants exposed to excess Cu and Cd. *Journal of Plant Physiology* **223**: 37-46. doi:10.1016/j.jplph.2018.01.008

Cuypers, A., Hendrix, S., Amaral dos Reis, R., De Smet, S., Deckers, J., Gielen, H., Jozefczak, M., Loix, C., Vercampt, H., Vangronsveld, J., and Keunen, E. (2016). Hydrogen peroxide, signaling in disguise during metal phytotoxicity. *Frontiers in Plant Science* **7**: 470. doi:10.3389/fpls.2016.00470.

Moreira, I., Mourato, M., Reis, R., Martins, L. (2015). Oxidative stress induced by cadmium and copper in *Brassica rapa* leaves: Indicators of stress, oxidative damage, and antioxidant mechanisms. *Communications in Soil Science and Plant Analysis* **46**(19): 2475-2489. doi: 10.1080/00103624.2015.1085554

Martins, L., Mourato, M., Baptista, S., Reis, R., Carvalheiro, F., Almeida, A., Fevereiro, P., and Cuypers, A. (2014). Response to oxidative stress induced by cadmium and copper in tobacco plants (*Nicotiana tabacum*) engineered with the trehalose-6-phosphate synthase gene (AtTPS1). *Acta Physiologiae Plantarum* **36**(3): 755-765. doi: 10.1007/s11738-013-1453-0

Fernández, R., Bertrand, A., Reis, R., Mourato, M., Martins, L., and González, A. (2013). Growth and physiological responses to cadmium stress of two populations of *Dittrichia viscosa* (L.) Greuter. *Journal of Hazardous Materials* **244–245**: 555-562. doi:10.1016/j.jhazmat.2012.10.044

Book chapters

Martins, L. L., Reis, R., Moreira, I., Pinto, F., Sales, J. and Mourato, M. (2013). 'Antioxidative response of plants to oxidative stress induced by cadmium', in Hasanuzzaman, M. and Fujita, M. (eds.) *Cadmium: characteristics, sources of exposure, health and environmental effects*., Nova Science Pub Inc., pp. 87-112.

Mourato, M., Reis, R. and Martins, L. L. (2012). 'Characterization of plant antioxidative system in response to abiotic stress: a focus on heavy metal toxicity', in Montanaro, G. and Dichio, B. (eds.) *Advances in selected plant physiology aspects*, InTech, pp. 23-44.

Abstracts

Reis, R. A., Keunen, E., Mourato, M. P., Vangronsveld, J. and Cuypers, A. (2016). Natural accessions in *Arabidopsis thaliana*: tools to unravel metal-induced stress responses? EPSO/FESPB 2016 Congress. Prague, Czech Republic. June 26-30, 2016. Abstract of poster presentation.

Reis, R. A., Keunen, E., Mourato, M. P., Vangronsveld, J. and Cuypers, A. (2015). Copper-induced oxidative stress responses in two *Arabidopsis thaliana* natural accessions. Plant Growth, Nutrition & Environment Interaction II. Vienna, Austria. June 25—26, 2015. Abstract of poster presentation.

Fernández, R., Bertrand, A., Reis, R., Mourato, M. P., Martins L. L., Sánchez-Tamés, R. and González, A. (2012). Antioxidant response to Cd of two populations of *Dittrichia viscosa*. 9th International Phytotechnology Society Conference. Hasselt, Belgium. September 11-14, 2012. Abstract of poster presentation.

Moreira, I. N., Reis, R. A., Martins, L. L. and Mourato, M. P. (2012). Antioxidative response of *Brassica rapa* L. to oxidative stress induced by cadmium and copper. Plant Abiotic Stress Tolerance II. Vienna, Austria. February 22-25, 2012. Abstract of poster presentation.

Pinto, F. R., Reis, R. A., Mourato, M. P. and Martins, L. L. (2012). Abiotic stress response induced by cadmium in spinach plants. Plant Abiotic Stress Tolerance II. Vienna, Austria. February 22-25, 2012. Abstract of poster presentation.

Martins, L. L., Mourato, M., Reis, R., Gonçalves, K. and Esquível, G. (2011). Intracellular mechanisms involved in plant tolerance strategies against heavy metal toxicity. Plant Abiotic Stress Tolerance Mechanisms, Water and Global Agriculture. Keystone, Colorado, USA. January 17-22, 2011. Abstract of poster presentation.